Supporting Information

Unraveling Organoboron/Nickel Ion-Pair Interactions *via* Benchtop-Stable Carbyl Iminopyridyl Ni^{II} Complexes for Olefin Polymerization

Hasaan S. Rauf[1], Yu-Sheng Liu[1], Surya Pratap S. Solanki[2], Eric Deydier[3], Rinaldo Poli[3,4*], Lars C. Grabow[2*], and Eva Harth[1*]

[1] Center of Excellence in Polymer Chemistry, Department of Chemistry, University of Houston, Houston, Texas 77204, United States.

[2] William A. Brookshire Department of Chemical and Biomolecular Engineering & Texas Center for Superconductivity (TcSUH), University of Houston, Texas 77204, United States.

[3] CNRS, LCC (Laboratoire de Chimie de Coordination), UPS, INPT, Université de Toulouse, 205 route de Narbonne, 31077 Toulouse, Cedex 4, France.

[4] Institut Universitaire de France, 1, rue Descartes, 75231 Paris, France.

E-mail: rinaldo.poli@lcc-toulouse.fr; grabow@uh.edu; harth@uh.edu.

Table of Contents

1. General Information

All manipulations of air- and water-sensitive compounds were carried out under an inert atmosphere using glovebox, Schlenk, high vacuum techniques unless otherwise noted.

1.1 Materials

Ethylene (Polymer Grade) was purchased from Matheson and used as received. Bis(1,5-cyclooctadiene)nickel ($Ni(COD)_2$, 98+%), bis(triphenylphosphino)(*o*-tolyl)chloronickel(II) ($(PPh_3)_2Ni(o\text{-}tol)Cl$, 99%), and tris(pentafluorophenyl)borane ($B(C_6F_5)_3$, 97%) were purchased from Strem Chemicals and used as received. Sodium tetrakis[3,5-bis(trifluoromethyl)phenyl]borate (NaBArF, 97%) was purchased from Matrix Scientific and purified according to literature methods before use.[1] Silver tetrakis[3,5-bis(trifluoromethyl)phenyl]borate (AgBArF) was prepared according to published procedure and purified by recrystallized from toluene/pentane, then filtered and dried under vacuum for 1 hour to obtain a white solid.[2] Dichloromethane (DCM), pentane, diethyl ether and toluene were purified *via* an Inert PureSolv MD5 Purification System. Diphenylmethanol (99%), *p*-toluidine (99%), calcium hydride powder (≥90%), 2-chlorotoluene (99%), 2,6-diisopropylaniline (97%), 2-acetylpyridine (≥99%), 2-benzoylpyridine (≥99%), triethylsilane (97%), chloroform (anhydrous, contains amylenes as stabilizer, ≥99%), n-butyllithium solution (1.6 M in hexanes), ethyl formate (97%), diethylaluminum chloride solution (1.0 M in hexanes), and MMAO-12 (7 wt% aluminum in toluene) were purchased from Sigma-Aldrich. *p*-Toluenesulfonic acid monohydrate (>98%), 5-bromo-m-xylene (>98%), and zinc chloride (>98%) were purchased from TCI. Dibenzosuberone (97%), and Sodium borohydride (95%) were purchased from Thermo Scientific Chemicals. Triethoxyvinylsilane (>97%), methyl acrylate (>99%), and vinyl acetate (>99%) were purchased from Sigma Aldrich, dried over CaH_2, distilled

under vacuum, and degassed immediately before use. 2,6-Bis(diphenylmethyl)-4-methylbenzenamine was synthesized according to literature.[3] 2,6-Bis(bis(3,5-dimethylphenyl)methyl)-4-methylaniline was synthesized according to literature.[4] 2,6-Bis(10,11-dihydro-5H-dibenzo[a,d][7]annulen-5-yl)-4-methylaniline was synthesized according to literature.[5]

1.2 Instrumentation

Nuclear Magnetic Resonance (NMR) – ^{1}H and ^{13}C NMR were acquired on a JEOL JNM-ECA 400 (400 MHz), JNM-ECZ400S (400 MHz), or ECA-600 (600 MHz). NMR spectrometer equipped with 5 mm broad-band probes. Chemical shifts are measured relative to residual solvent peaks as an internal standard set to δ 7.26 and δ 77.16 (chloroform-d1 ($CDCl_3$)), δ 5.32 and δ 53.84 (dichloromethane-d_2 (CD_2Cl_2)), and δ 6.00 and δ 73.78 (1,1,2,2-tetrachloroethane-d_2 ($C_2D_2Cl_4$,)) for ^{1}H and ^{13}C, respectively. Quantitative ^{13}C NMR spectra of polymers were recorded on the ECA-600 (600 MHz) at 125 °C, in $C_2D_2Cl_4$ with $Cr(acac)_3$ as a relaxation agent (0.05 M).

Gel Permeation Chromatography (GPC) – GPC was performed using a Tosoh EcoSEC HLC-8321 GPC/HT System equipped with an autosampler, three TSKgel GMHhr-H(S) HT2 columns, built-in dual flow refractive index (RI) detector, and viscometer. GPC analyses were carried out in HPLC grade 1,2,4-trichlorobenzene with a flow rate of 1.0 mL/min at 160 °C calibrated with polystyrene standards.

Differential Scanning Calorimetry (DSC) – DSC was conducted on a TA Instruments DSC 2500 System. The samples were heated from 25 °C to 180 °C, cooled to −90 °C, and then heated to 180 °C at a rate of 10 °C/minute. DSC data was obtained from the second heating cycles.

Elemental analysis - Elemental analysis was performed by Atlantic Microlab, lnc. Carbon, hydrogen, and nitrogen analyses are performed on automatic analyzers which utilize a technique based on a modification of the classical Pregl and Dumas methods. These analyzers are comprised of the following makes and models: Perkin-Elmer Model 2400 Series II Autoanalyzers and Carlo Erba Model 1108 Analyzers. Flash or static combustion, depending on the type of instrument, takes place at approximately 1400 °C in an oxygen atmosphere. Quantitative combustion is achieved by passing the mixture of gases over oxidizing agents comprised of copper oxide, EA1000 (chromium and nickel oxide mixture) and tungstic anhydride, and then over copper, which is maintained at 650 °C, to remove excess oxygen and to reduce the oxides of nitrogen to nitrogen. In the case of the Perkin Elmer 2400 series instruments and the Carlo Erba 1108 instruments, the mixture is passed through a chromatographic column containing Perapak PQS which is maintained at approximately 60 °C – 80 °C, and the individual components are separated and eluted as N_2, CO_2, and H_2O. They are measured by a thermal conductivity detector whose signal feeds to a computer for data processing.

Electro Spray Ionization - Mass Spectrometry (ESI-MS): ESI-MS experiments were performed using a Thermo Scientific Q Exactive Focus. Sample was loop injected (10 µL) and methanol was used as a mobile phase at a flow rate of 600 µL/min. The Q Exactive Focus HESI source was operated in full MS in positive mode. The mass resolution was tuned to 70000 FWHM at m/z 200. The spray voltage was set to 3.5 kV for positive mode. The sheath gas and auxiliary gas flow rates were set to 40 and 10 arbitrary units, respectively. The transfer capillary temperature was held at 320 °C and the S-Lens RF level was set at 50 v. Exactive Series 2.11 /Xcalibur 4.2.47 software was used for data acquisition and processing.

1.3 Calculations

The branching of polymer and monomer incorporation was calculated according to proton NMR.

$$\underline{\text{Branching (per 1000C)}} = \frac{2*\mathrm{I}(\mathrm{CH_3})}{2*\mathrm{I}(\mathrm{CH_3})+3*\mathrm{I}(\mathrm{CH_2}+\mathrm{CH_3})} * 1000$$

Where CH_3 = Integral of CH_3 (0.75-0.95 ppm); CH_2+CH = Integral of CH_2 & CH (1.10-1.50 ppm).

$$\underline{\text{The VTEoS incorporation (mol\%)}} = \frac{4*\mathrm{I}(\mathrm{O}\mathit{CH_2}\mathrm{CH_3})}{6*\mathrm{I}(\mathrm{CH_2}+\mathrm{CH})+4*\mathrm{I}(\mathrm{CH_3})-5*\mathrm{I}(\mathrm{O}\mathit{CH_2}\mathrm{CH_3})} * 100$$

Where O*CH*$_2$$CH_3$ = Integral of O*CH*$_2$ on OEt group from PVTEoS (3.75-3.85 ppm); CH_2+CH = Integral of CH_2 & CH from PE and Integral of OCH_2*CH*$_3$ from PVTEoS (1.05-1.65 ppm); CH_3 = Integral of CH_3 (0.75-0.95 ppm)

$$\underline{\text{The MA incorporation (mol\%)}} = \frac{4*I(\mathrm{OCH_3})}{4*I(\mathrm{OCH_3})+2*I(\mathrm{CH_3})+3*I(\mathrm{CH_2}+\mathrm{CH_3})} * 100$$

Where OMe = Integral of OMe group from PMA (3.67-3.82 ppm); CH_3 = Integral of CH3 from PE (0.75-0.95 ppm); CH_2+CH = Integral of CH_2 & CH from PE (1.10-1.45 ppm).

$$\underline{\text{The VAc incorporation (mol\%)}} = \frac{4*\mathrm{I}(\mathrm{OCH_3})}{3*\mathrm{I}(\mathrm{CH_2}+\mathrm{CH})+2*\mathrm{I}(\mathrm{CH_3})-2*\mathrm{I}(\mathrm{OCH_3})} * 100$$

Where OCH_3 = Integral of OCH_3 group from PVAc (2.00-2.20 ppm); CH_3 = Integral of CH_3 from PE (0.75-0.95 ppm); CH_2+CH = Integral of CH_2 & CH from PE (1.10-1.45 ppm).

1.4 General Procedure for Polymerization Reactions

(a) Ethylene Homopolymerization – Borate Cocatalyst

A 300 mL Series 5521 Compact Bench Top Reactor System (Parr Instrument Company) was heated to 120 °C for at least 1 hour under vacuum and then cooled to the desired temperature. A heating control system or a chiller kept the reactor's temperature constant. Toluene was injected into the Parr reactor under positive ethylene flow and subsequently pressurized to 200 psi of ethylene and maintained for 10 minutes. The reactor was vented and repressurized to 200 psi of ethylene and

maintained for another 10 minutes. The reactor was then vented, and 5.0 mL of DCM solution of nickel catalyst and 5.0 mL DCM solution of borate cocatalyst were sequentially injected under ethylene flow. The reactor was sealed, pressurized to the desired ethylene pressure, and stirred for the given reaction time. The reactor was carefully vented and poured into a solution of 300 mL methanol and 0.1 mL triethylsilane. The polymer was filtered and dried under vacuum to reach a constant weight.

(b) Ethylene Homopolymerization – Borane Cocatalyst

A 300 mL Series 5521 Compact Bench Top Reactor System (Parr Instrument Company) was heated to 120 °C for at least 1 hour under vacuum and then cooled to the desired temperature. A heating control system or a chiller kept the reactor's temperature constant. A toluene solution of $B(C_6F_5)_3$ (10 eq.) was injected into the parr reactor under positive ethylene flow and subsequently pressurized to the 200 psi of ethylene and maintained for 10 minutes. The reactor was vented and repressurized to 200 psi of ethylene and maintained for another 10 minutes. The reactor was vented, and 5.0 mL of DCM solution of nickel catalyst was injected under ethylene flow. The reactor was sealed, pressurized to the desired ethylene pressure, and stirred for the given reaction time. The reactor was carefully vented and poured into a solution of 400 mL methanol and 0.1 mL triethylsilane. The polymer was filtered and dried under vacuum to reach a constant weight.

(c) Ethylene Homopolymerization – Organoaluminium Cocatalyst

A 300 mL Series 5521 Compact Bench Top Reactor System (Parr Instrument Company) was heated to 120 °C for at least 1 hour under vacuum and then cooled to the desired temperature. A heating control system or a chiller kept the reactor's temperature constant. Toluene was injected into the parr reactor under positive ethylene flow and subsequently pressurized to the 200 psi of ethylene and maintained for 10 minutes. The reactor was vented and repressurized to 200 psi of ethylene

and maintained for another 10 minutes. The reactor was vented, and 5.0 mL of DCM solution of nickel catalyst was injected under ethylene flow followed by the organoaluminium cocatalyst. The reactor was sealed, pressurized to the desired ethylene pressure, and stirred for the given reaction time. The reactor was carefully vented and poured into a solution of 400 mL acidic methanol. The polymer was filtered and dried under vacuum to reach a constant weight.

(d) Ethylene/polar monomer Copolymerization – Borate Cocatalyst

A 300 mL Series 5521 Compact Bench Top Reactor System (Parr Instrument Company) was heated to 120 °C for at least 1 hour under vacuum and then cooled to the desired temperature. A heating control system or a chiller kept the reactor's temperature constant. Toluene was injected into the Parr reactor under positive ethylene flow and subsequently pressurized to 200 psi of ethylene and maintained for 10 minutes. The reactor was vented and repressurized to 200 psi of ethylene and maintained for another 10 minutes. The reactor was then vented, and the monomer was injected followed by 5.0 mL of DCM solution of nickel catalyst and 5.0 mL DCM solution of borate cocatalyst under ethylene flow. The reactor was sealed, pressurized to the desired ethylene pressure, and stirred for the given reaction time. The reactor was carefully vented, and the reaction solution was concentrated down. The polymer was washed with methanol and dried under vacuum to reach a constant weight.

2. Ethylene Polymerization Studies

Table S1. Ethylene polymerization of C2-C7 at varying reaction temperatures[a]

Entry	Catalyst	Temp (°C)	Time (min)	Yield (g)	Productivity (kg mol^{-1} $_{Ni}$·h)	TOF (10^3)(h^{-1})	Branches /1000C[b]	M_n[c] (kg mol^{-1})	$Đ$[c]	T_m[d] (°C)
1[e]	**C2**	0	120	1.1	110	3.9	12	36.2	1.62	121.7
2[e]	**C2**	60	60	1.2	240	8.6	94	1.5	1.64	3.3
3	**C3**	0	30	0.5	100	3.8	11	49.0	1.58	119.8

4	**C3**	60	10	3.1	1860	66.4	82	1.7	1.86	15.8
5	**C4**	0	120	0.7	35	1.3	18	164.6	1.81	113.8
6	**C4**	60	60	0.8	80	2.9	104	5.6	1.76	31.7
7	**C5**	0	30	0.9	180	6.4	10	71.7	1.73	121.3
8	**C5**	60	10	2.6	1560	55.7	86	3.9	1.71	19.6
9	**C6**	0	120	1.4	70	2.5	25	206.7	1.60	112.0
10	**C6**	60	30	1.3	260	9.3	65	7.3	1.85	32.3
11	**C7**	60	10	2.0	1200	42.8	77	36.1	1.69	24.1

Conditions: [a]10 μmol of Ni catalyst, 10 equivalents of $B(C_6F_5)_3$, 400 psi ethylene, 45 mL of toluene. [b]Determined by ^1H NMR in D_2-tetrachloroethane at 125 °C. [c]Determined by GPC in 1,2,4-trichlorobenzene at 160 °C using polystyrene calibration. [d]Determined by differential scanning calorimetry. [e]5 μmol of Ni.

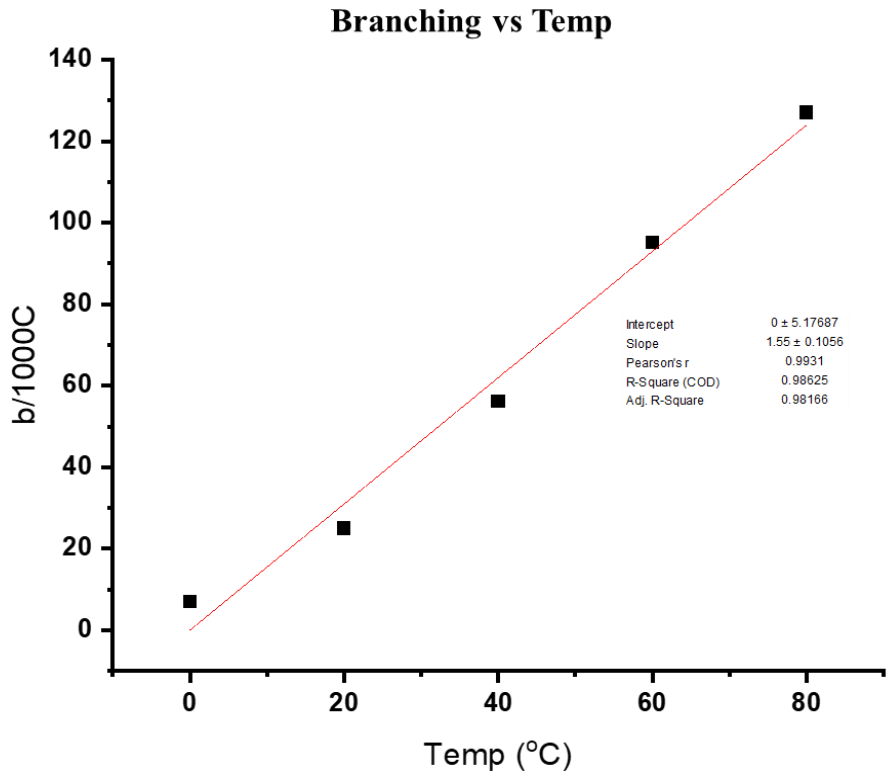

Figure S1: Branching number compared to reaction temperature. Branching data from C1 ethylene polymerization (Table 3, entries 1-5).

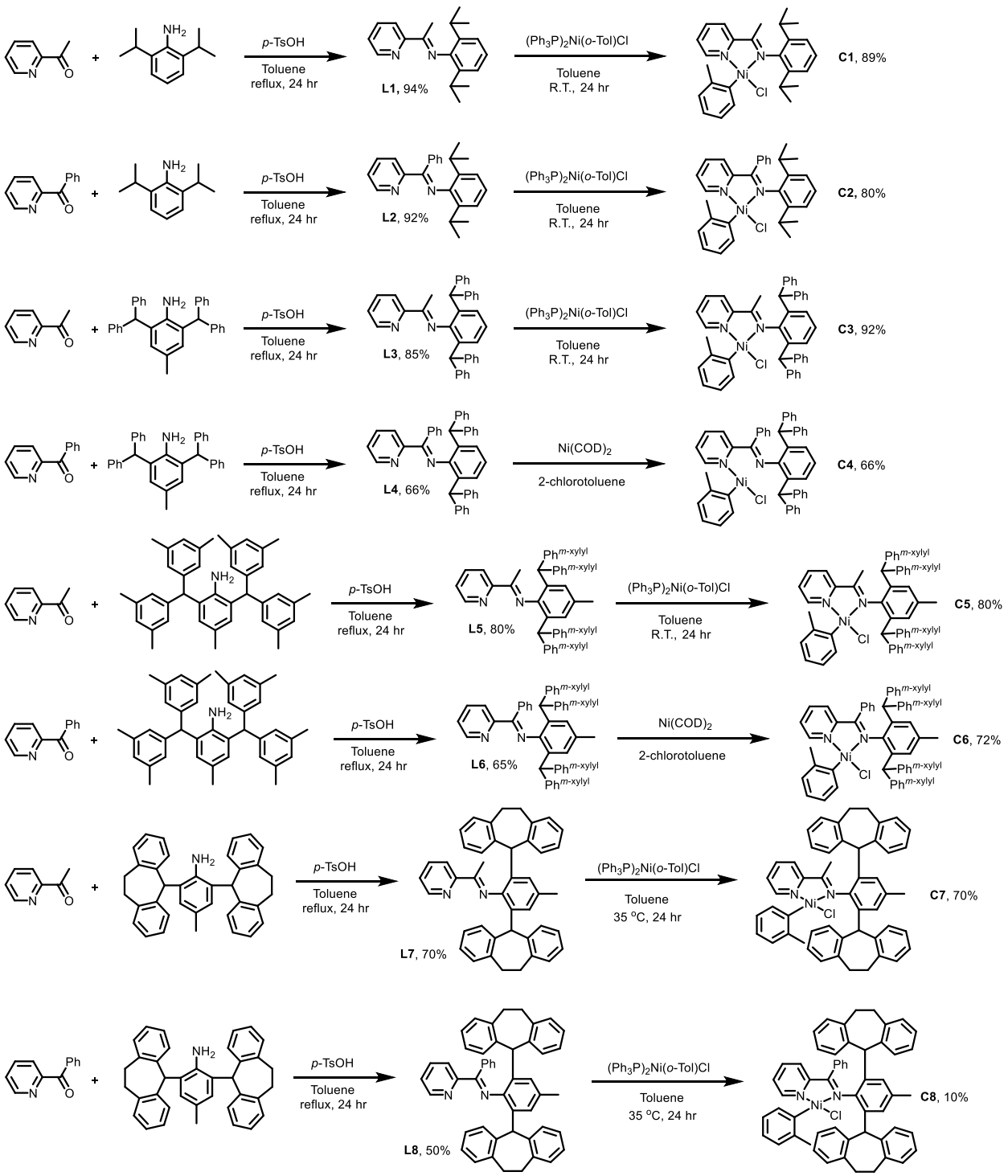

Figure S2: Full synthetic route for the synthesis of iminopyridyl Ni^{II} complexes **C1**-**C8**.

3. Synthesis and Characterization of Complexes

3.1 Synthesis Procedure of Ligands and Complexes

Synthesis of *N*-(2,6-diisopropylphenyl)-1-(pyridin-2-yl)ethan-1-imine (L1):

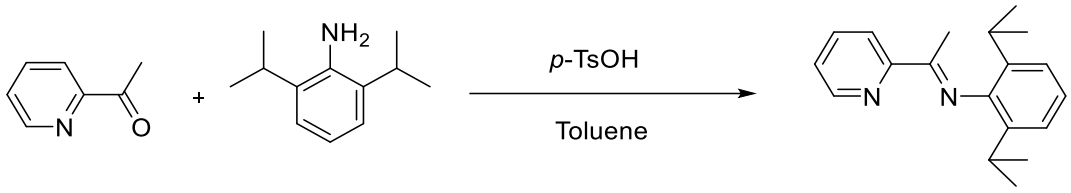

A dried 100 mL round-bottomed flask was charged with 2-acetylpyridine (3.39 g, 28 mmol), 25 mL toluene, and a catalytic amount of *p*-toluenesulfonic acid. 2,6-diisopropylaniline (3.90 g, 22 mmol) was slowly injected into the solution and the reaction mixture was refluxed for 6 hours. The crude product was filtered, dissolved in 50 mL of DCM, washed twice with 50 mL water, and dried with $MgSO_4$. After filtration and solvent evaporation, the ligand was recrystallized from methanol as bright yellow solid. Yield: 5.80 g, 94.1%. ^{1}H NMR (400 MHz, CD_2Cl_2) δ = 8.66 (d, J = 4.8 Hz, 1H), 8.35 (d, J = 8.0 Hz, 1H), 7.84 (t, J = 8.0 Hz, 1H), 7.41 (t, J = 7.5 Hz, 1H), 7.17 (s, 1H), 7.15 (s, 1H), 7.10 – 7.05 (m, 1H,), 2.73 (m, 2H), 2.18 (s, 3H), 1.13 (t, 12H, J = 6.9 Hz). The NMR spectra agreed well with the reported literature.[6]

Synthesis of [*N*-(2,6-diisopropylphenyl)-1-(pyridin-2-yl)ethan-1-imine]·Ni(*o*-tol)Cl (C1):

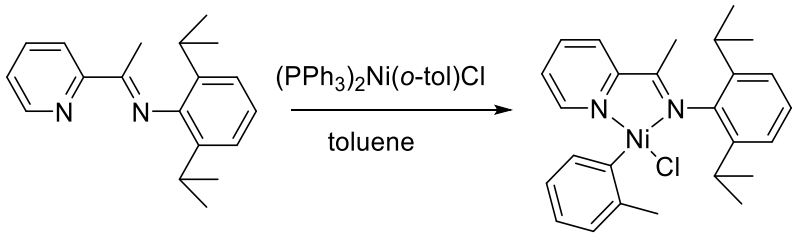

A dried 100 mL round-bottomed flask filled with nitrogen was added $(PPh_3)_2$Ni(*o*-tol)Cl (500 mg, 0.7 mmol) and **L1** (216 mg, 0.77 mmol). Toluene (20 mL) was injected to the reaction and stirring

at room temperature. The purple suspensions were formed after stirring for 16 hours. 10 mL of pentane was added to the reaction, and the precipitate was filtered and collected. The catalyst was dissolved in DCM and filtered through celite. The filtrate was concentrated, and the resulting product was purified *via* recrystallization from DCM and pentane. The purple solids were then filtered and dried under vacuum. Yield: 290 mg, 89.3%. ^{1}H NMR (400 MHz, CD_2Cl_2) δ = 7.98 (t, J = 7.8 Hz, 1H), 7.69 (d, J = 7.8 Hz, 1H), 7.49 (d, J = 8.0 Hz, 1H), 7.41 (dd, J = 7.1, 2.1 Hz, 1H), 7.33 – 7.16 (m, 4H), 6.84 – 6.72 (m, 3H), 3.44 (m, 1H), 3.27 (m, 1H), 2.98 (s, 3H), 2.05 (s, 3H), 1.50 (dd, J = 6.8, 4.0 Hz, 6H), 1.16 (dd, J = 6.9, 2.0 Hz, 6H). ^{13}C NMR (150 MHz, CD_2Cl_2) δ = 70.14 (N=*C*Me), 156.60, 151.68, 141.99, 140.00, 137.56, 135.08, 128.79, 127.56, 126.98, 124.68, 123.38, 122.85, 29.27 (*C*H_3), 29.21 (*C*H_3), 24.97 (*C*H_3), 24.04 (*C*H_3), 23.87 (*C*H_3), 18.06 (*C*H_3). Anal. Calcd. for $C_{26}H_{31}ClN_2Ni$: C, 67.06; H, 6.71; N, 6.02; Found: C, 67.12; H, 6.76; N, 5.94.

Synthesis of *N*-(2,6-diisopropylphenyl)-1-phenyl-1-(pyridin-2-yl)methanimine (L2):

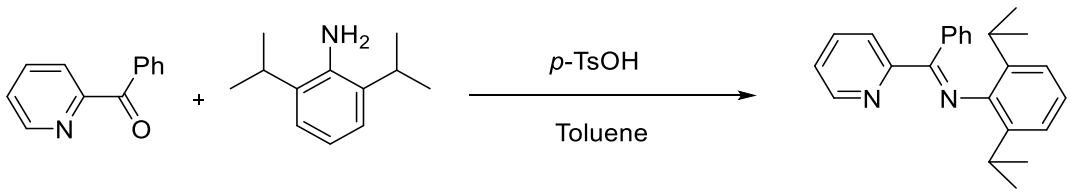

Ligand **L2** was synthesized in a similar manner as **L1** but using 2-benzoylpyridine (3.66 g, 20 mmol) as the precursor. Isolated as bright yellow powder. Yield: 6.31 g, 92.2%. ^{1}H NMR (400 MHz, CD_2Cl_2) δ = 8.59 (dd, J = 18.4, 4.9 Hz, 1H), 8.30 (d, J = 7.9 Hz, 0.5H), 7.89 (t, 0.5H), 7.76 (d, J = 7.6 Hz, 1H), 7.54 – 7.46 (m, 1H), 7.45 – 7.38 (m, 1H), 7.30 – 7.15 (m, 2H), 7.11 – 6.89 (m, 4H), 3.01 – 2.80 (m, 2H), 1.12 (d, J = 6.8 Hz, 6H), 0.99 (d, J = 6.8 Hz, 3H), 0.94 (d, J = .1 Hz, 3H). The NMR spectra agreed well with the reported literature.[7]

Synthesis of [*N*-(2,6-diisopropylphenyl)-1-phenyl-1-(pyridin-2-yl)methanimine]·Ni(*o*-tol)Cl (C2):

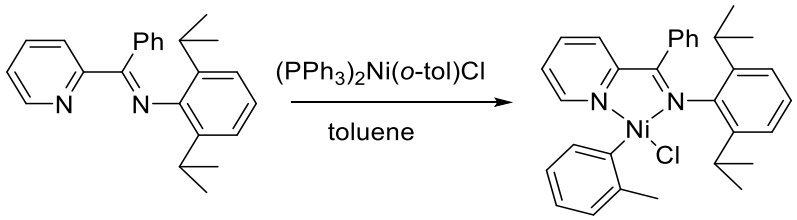

A dried 100 mL round-bottomed flask filled with nitrogen was added $(PPh_3)_2Ni(o\text{-tol})Cl$ (500 mg, 0.7 mmol) and **L2** (264 mg, 0.77 mmol). Toluene (50 mL) was injected to the reaction and stirring at room temperature. The purple suspension was formed after stirring for 16 hours. 10 mL of pentane was added to the reaction, and the precipitate was filtered and collected. The catalyst was dissolved in DCM and filtered through celite. The filtrate was concentrated, and the resulting product was purified *via* recrystallization from DCM and pentane. The dark purple solids were then filtered and dried under vacuum. Yield: 296 mg, 80.1%. ^{1}H NMR (400 MHz, CD_2Cl_2) δ = 7.86 (t, J = 7.8 Hz, 1H), 7.59 (d, J = 5.6 Hz, 1H), 7.48 – 7.37 (m, 2H), 7.33 (t, J = 7.6 Hz, 4H), 7.18 – 7.11 (m, 3H), 7.04 (t, J = 6.5 Hz, 2H), 6.86 – 6.75 (m, 3H), 3.49 – 3.38 (m, 1H), 3.37 – 3.26 (m, 1H), 3.02 (s, 3H), 1.62 – 1.54 (m, 6H), 0.97 (dd, 6H, J = 11.3, 6.8 Hz). ^{13}C NMR (150 MHz, CD_2Cl_2) δ = 169.24 (N=*C*Me), 156.56, 151.97, 151.40, 141.90, 141.79, 140.14, 139.98, 135.38, 131.81, 130.83, 129.02, 128.75, 128.58, 128.05, 127.73, 126.97, 123.40, 123.22, 122.97, 29.24 (*C*H$_3$), 24.99 (*C*H$_3$), 23.40 (*C*H$_3$), 23.20 (*C*H$_3$). Anal. Calcd. for $C_{31}H_{33}ClN_2Ni$: C, 70.55; H, 6.30; N, 5.31; Found: C, 70.42; H, 6.27; N, 5.25.

Synthesis of *N*-(2,6-dibenzhydryl-4-methylphenyl)-1-(pyridin-2-yl)ethan-1-imine (L3):

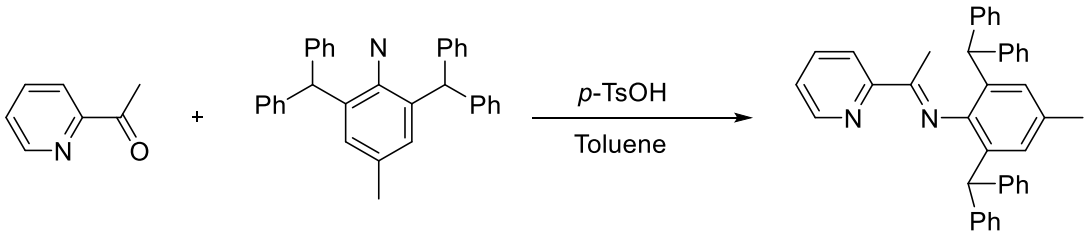

2-Acetylpyridine (0.61 g, 5 mmol), 2,6-bis(diphenylmethyl)-4-methylbenzenamine (2.21 g, 5 mmol), and catalytic amount of *p*-toluenesulfonic acid monohydrate were added to a 100 mL round-bottomed flask. Toluene (50 mL) was injected to the reaction and refluxed overnight. After cool to room temperature, solvent was removed by vacuum. The resulting product was isolated *via* recrystallization from DCM and methanol. The pale-yellow solid was filtered and dried under vacuum. Alternatively, the product can be purified by flash column (DCM/hexanes = 7:3). Yield: 2.3 g, 85.3%. ^{1}H NMR (400 MHz, $CDCl_3$): δ 8.58 (d, *J* = 4.4 Hz, 1H), 8.02 (d, *J* = 8.4 Hz, 1H), 7.71 (td, *J* = 8, 2 Hz, 1H), 7.33 (m, 1H), 7.25-7.11 (m, 12H), 6.98-7.05 (m, 8H), 6.68 (s, 2H), 5.26 (s, 2H, C*H*Ar$_2$), 2.17 (s, 3H, C*H*$_3$), 1.04 (s, 3H, C*H*$_3$). The NMR spectra agreed well with the reported literature.[8]

Synthesis of [*N*-(2,6-dibenzhydryl-4-methylphenyl)-1-(pyridin-2-yl)ethan-1-imine]·Ni(*o*-tol)Cl (C3):

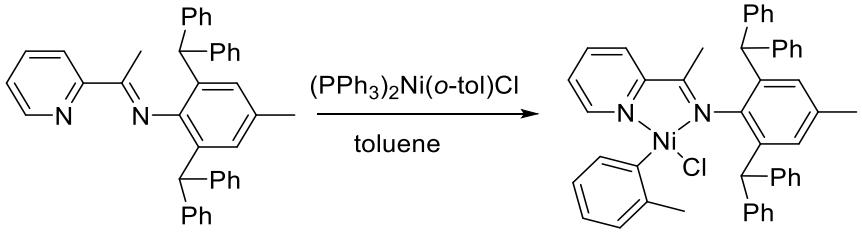

A dried 100 mL round-bottomed flask filled with nitrogen was added $(PPh_3)_2$Ni(*o*-tol)Cl (340.7 mg, 0.48 mmol) and **L3** (271.4 mg, 0.5 mmol). Toluene (10 mL) was injected to the reaction and stirring at room temperature. The red suspensions were formed after stirring for 16 hours. 5 mL of pentane was added to the reaction, and the precipitate was filtered and collected. The catalyst was dissolved in DCM and filtered through celite. The filtrate was concentrated, and the resulting product was purified *via* recrystallization from DCM and pentane. The dark red solids were then filtered and dried under vacuum. Yield: 320 mg, 91.6%. ^{1}H NMR (400 MHz, CD_2Cl_2): δ 7.83 (t, *J* = 8 Hz, 1H), 7.61 (d, *J* = 7.2 Hz, 1H), 7.54 (d, *J* = 6 Hz, 1H), 7.43-7.35 (m, 4H), 7.32-7.24 (m,

5H), 7.22-7.18 (m, 2H), 7.17-7.08 (m, 10H), 6.90-6.80 (m, 4H), 6.67 (s, 2H), 6.64 (s, 1H), 6.39 (s, 1H), 3.15 (s, 3H, C*H*$_3$), 2.17 (s, 3H, C*H*$_3$), -0.27 (s, 3H, C*H*$_3$). ^{13}C NMR (150 MHz, CD_2Cl_2): δ 173.69 (N=*C*Me), 155.90, 151.80, 151.72, 143.99, 143.94, 142.12, 141.80, 141.69, 137.98, 136.84, 136.67, 135.70, 135.56, 130.57, 130.44, 130.00, 129.93, 128.99, 128.96, 128.89, 128.86, 128.77, 128.50, 128.44, 127.81, 126.95, 126.90, 126.59, 126.57, 124.16, 123.73, 123.16, 53.04 (*C*HPh$_2$), 52.94 (*C*HPh$_2$), 26.05 (*C*H$_3$), 21.56 (*C*H$_3$), 16.46 (*C*H$_3$). Anal. Calcd for $C_{47}H_{41}ClN_2Ni$: C, 77.54; H, 5.68; N, 3.85. Found: C, 77.19; H, 5.66; N, 3.87.

Synthesis of *N*-(2,6-dibenzhydryl-4-methylphenyl)-1-phenyl-1-(pyridin-2-yl)methanimine (L4):

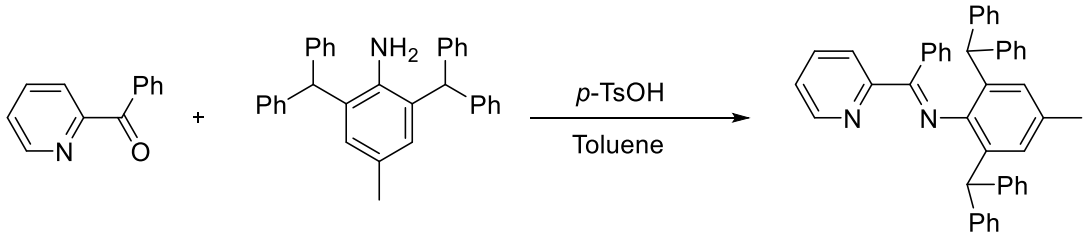

Ligand **L4** was synthesized in a similar manner as **L3** but using 2-benzoylpyridine (0.92 g, 5 mmol) as the ketone precursor. Isolated as bright yellow powder. Yield: 2.0 g, 66.1%.^{1}H NMR (400 MHz, $CDCl_3$): δ 8.53 (d, 1H), 7.65-6.95 (m, 23H), 6.85-6.47 (m, 7H), 5.53 (s, 1H, C*H*Ar$_2$), 5.24 (s, 1H, C*H*Ar$_2$), 2.13 (s, 3H, C*H*$_3$). The NMR spectra agreed well with the reported literature.[9]

Synthesis of [*N*-(2,6-dibenzhydryl-4-methylphenyl)-1-phenyl-1-(pyridin-2-yl)methanimine]·Ni(*o*-tol)Cl (C4):

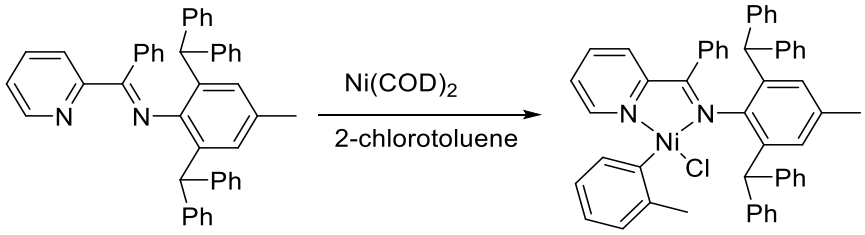

A flame-dried 100 mL round-bottomed flask filled with nitrogen was added $Ni(COD)_2$ (137.5 mg, 0.5 mmol) and **L4** (302.4 mg, 0.5 mmol). 2-chlorotoluene (4 mL) was injected to the reaction and stirred at room temperature. The purple suspensions were formed after stirring for 16 hours. The reaction was diluted with DCM and then filtered through celite. The filtrate was concentrated, and the resulting product was purified by recrystallization from chloroform and pentane. The purple solids were then filtered and dried under vacuum. Yield: 260 mg, 65.8%. ^{1}H NMR (400 MHz, CD_2Cl_2): δ 7.81 (t, *J* = 7.5 Hz, 1H), 7.66 (d, *J* = 5.5 Hz, 1H), 7.55-7.44 (m, 5H), 7.36-7.28 (m, 3H), 7.27-7.14 (m, 4H), 7.10 (t, *J* = 7.5 Hz, 1H), 7.03-6.65 (m, 20H), 6.30 (s, 1H, C*H*Ar_2), 6.06 (s, 1H, C*H*Ar_2), 3.02 (s, 3H, C*H*$_3$), 2.16 (s, 3H, C*H*$_3$). ^{13}C NMR (150 MHz, $CDCl_3$): δ 207.22, 169.64, 151.64, 151.05, 144.01, 143.49, 142.15, 141.82, 141.45, 136.33, 136.22, 135.40, 135.14, 131.09, 130.55, 130.27, 130.01, 129.81, 129.55, 128.66, 128.44, 128.26, 128.20, 128.02, 127.67, 126.41, 126.20, 126.02, 123.67, 123.10, 53.59 (*C*HPh_2), 52.34 (*C*HPh_2), 31.10, 25.51 (*C*H$_3$), 21.77 (*C*H$_3$). Anal. Calcd for $C_{52}H_{43}ClN_2Ni$: C, 79.05; H, 5.49; N, 3.55. Found: C, 78.88; H, 5.52; N, 3.51.

Synthesis of *N*-(2,6-bis(bis(3,5-dimethylphenyl)methyl)-4-methylphenyl)-1-(pyridine-2-yl)ethan-1-imine (L5):

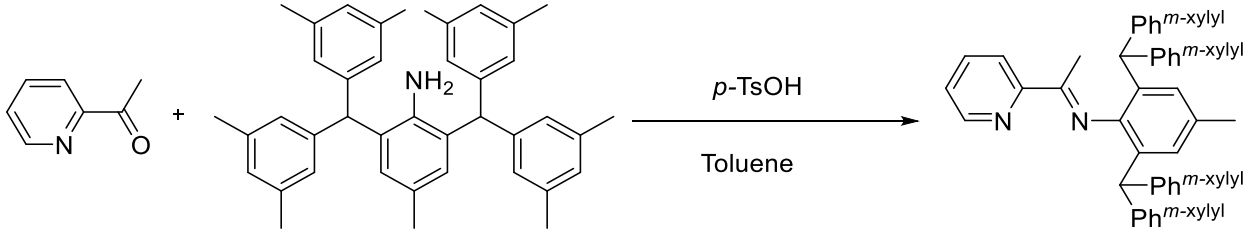

Ligand **L5** was synthesized in a similar manner as **L3** but using 2,6-bis(bis(3,5-dimethylphenyl)methyl)-4-methylaniline (2.75 g, 5 mmol) as the aniline precursor. Isolated as pale-yellow powder. Yield: 2.62 g, 80.0%. ^{1}H NMR (400 MHz, CD_2Cl_2): δ 8.56 (d, *J* = 4.8 Hz, 1H), 8.06 (d, *J* = 7.9 Hz, 1H), 7.76 (t, *J* = 8 Hz, 1H), 7.34 (t, *J* = 5.4Hz, 1H), 6.82 (s, 2H), 6.77 (s,

2H), 6.70 (s, 2H), 6.67 (s, 4H), 6.60 (s, 4H), 5.03 (s, 2H, CH_2Ar_2), 2.21 (s, 12H), 2.19 (s, 3H), 2.12 (s, 12H), 1.12 (s, 3H). The NMR spectra agreed well with the reported literature.[10]

Synthesis of [*N*-(2,6-bis(bis(3,5-dimethylphenyl)methyl)-4-methylphenyl)-1-(pyridin-2-yl)ethan-1-imine]·Ni(*o*-tol)Cl (C5):

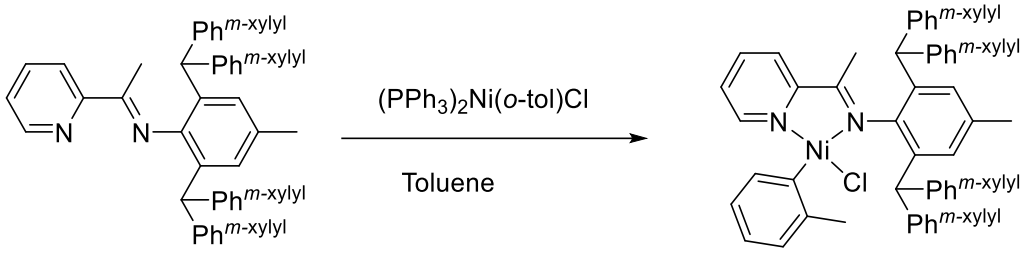

A dried 100 mL round-bottomed flask filled with nitrogen was added ($PPh_3)_2$Ni(*o*-tol)Cl (340.7 mg, 0.48 mmol) and **L5** (327.4 mg, 0.5 mmol). Toluene (10 mL) was injected to the reaction and stirring at room temperature. The red suspensions were formed after stirring for 16 hours. Pentane (5 mL) was added to the reaction and the precipitate was filtered and collected. The catalyst was dissolved in DCM and filtered through celite. The filtrate was concentrated, and the resulting product was purified *via* recrystallization from DCM and pentane. The dark red solids were then filtered and dried under vacuum. Yield: 336.5 mg, 80.1%. ^{1}H NMR (400 MHz, CD_2Cl_2): δ 7.84 (td, *J* = 7.7, 1.5 Hz, 1H), 7.67 – 7.64 (m, 1H), 7.55 – 7.52 (m, 1H), 7.26 (ddd, *J* = 7.4, 5.7, 1.4 Hz, 1H), 7.09 (s, 2H), 7.03 (s, 2H), 6.91–6.77 (m, 6H), 6.75 (s, 2H), 6.73 (s, 2H), 6.70 (s, 2H), 6.67 – 6.63 (m, 2H), 6.46 (s, 1H), 6.23 (s, 1H), 3.19 (s, 3H, CH_3), 2.24 (s, 12H), 2.19 (s, 3H, CH_3), 1.99 (s, 6H, CH_3), 1.99 (s, 6H, CH_3), -0.34 (s, 3H, CH_3). ^{13}C NMR (150 MHz, $CDCl_3$): δ 172.80, 155.77, 152.10, 151.33, 143.05, 143.02, 142.05, 142.00, 141.87, 141.38, 137.79, 137.54, 137.44, 136.51, 136.32, 136.05, 135.28, 135.01, 128.45, 128.37, 128.31, 128.09, 127.81, 127.76, 127.73, 127.63, 123.77, 123.10, 123.01, 77.37, 76.95, 52.89, 52.86, 25.77, 22.46, 21.88, 21.66, 21.64, 21.29, 16.09,

14.20. Anal. Calcd for $C_{55}H_{57}ClN_2Ni$: C, 78.62; H, 6.84; N, 3.33. Found: C, 78.61; H, 6.79; N, 3.31.

Synthesis of *N*-(2,6-bis(bis(3,5-dimethylphenyl)methyl)-4-methylphenyl)-1-phenyl-1-(pyridin-2-yl)methanimine (L6):

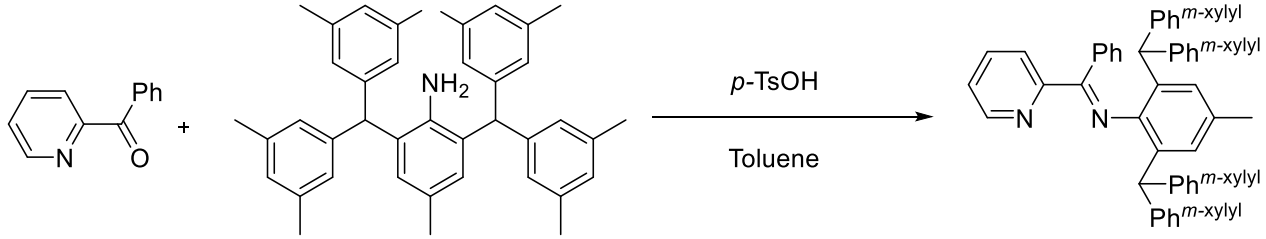

Ligand **L6** was synthesized in a similar manner as **L5** but using 2-benzoylpyridine (0.92 g, 5 mmol) as the ketone precursor. Isolated as bright yellow powder. Yield: 2.33 g, 65.0%. ^{1}H NMR (400 MHz, CD_2Cl_2): δ 8.56 (s, 0.5H), 8.48 (s, 0.5H), 7.71 (s, 0.5H), 7.48 – 7.10 (m, 6H), 6.90 – 6.53 (m, 11H), 6.38 (s, 2H), 6.28 (s, 2H), 5.94 (d, *J* = 5.3 Hz, 0.5H), 5.28 (s, 1H, C*H*Ar$_2$), 5.13 (s, 1H, C*H*Ar$_2$), 2.22 (s, 12H), 2.14 (s, 6H), 2.13 (s, 9H). ^{13}C NMR (150 MHz, CD_2Cl_2): δ 165.79, 158.20, 154.93, 149.64, 148.57, 145.46, 145.03, 143.90, 143.79, 143.09, 142.82, 140.11, 137.84, 136.43, 136.19, 135.68, 132.89, 132.49, 131.96, 130.42, 129.98, 129.76, 129.64, 128.70, 128.56, 128.10, 128.02, 127.76, 127.66, 124.56, 124.43, 123.88, 52.35, 52.07, 21.57, 21.51, 21.44. HRMS (ESI) m/z: $[M+H]^+$ Calcd for $C_{53}H_{53}N_2$: 717.4203; Found: 717.4183.

Synthesis of [*N*-(2,6-bis(bis(3,5-dimethylphenyl)methyl)-4-methylphenyl)-1-phenyl-1-(pyridin-2-yl)methanimine]·Ni(*o*-tol)Cl (C6):

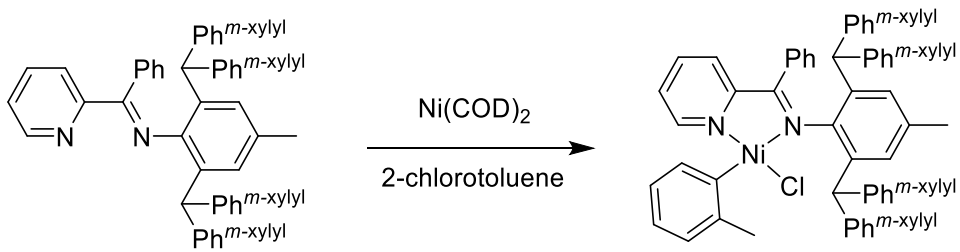

A flame-dried 100 mL round-bottomed flask filled with nitrogen was added $Ni(COD)_2$ (82.5 mg, 0.3 mmol) and **L6** (215.1 mg, 0.3 mmol). 2-chlorotoluene (4 mL) was injected to the reaction and stirred at room temperature. The purple suspensions were formed after stirring for 16 hours. The reaction was diluted with DCM and then filtered through celite. The filtrate was concentrated, and the resulting product was purified by recrystallization from chloroform and pentane. The purple solids were then filtered and dried under vacuum. Yield: 195 mg, 72%. ^{1}H NMR (400 MHz, $CDCl_3$): δ 7.73 (t, *J* = 7.7 Hz, 1H), 7.63 – 7.56 (m, 2H), 7.24 (s, 4H), 7.03 (t, *J* = 7.3 Hz, 1H), 6.94 – 6.64 (m, 11H), 6.62– 6.51 (m, 5H), 6.36 (s, 2H), 6.30 (s, 1H), 6.17 (s, 2H), 3.10 (s, 3H, C*H*$_3$), 2.23 (s, 6H), 2.21 (s, 6H), 2.18 (s, 3H), 2.00 (s, 6H), 1.98 (s, 6H). ^{13}C NMR (150 MHz, $CDCl_3$) δ 168.45, 158.20, 151.47, 143.83, 142.05, 141.83, 141.66, 141.49, 137.37, 137.21, 136.56, 136.01, 134.99, 134.70, 129.88, 129.48, 129.27, 128.80, 128.41, 128.09, 127.65, 127.01, 123.37, 122.97, 53.59, 52.23, 51.98, 25.57, 21.97, 21.59, 21.38. Anal. Calcd for $C_{60}H_{59}ClN_2Ni$: C, 79.87; H, 6.59; N, 3.10. Found: C, 79.60; H, 6.50; N, 3.10.

Synthesis of *N*-(2,6-bis(10,11-dihydro-5H-dibenzo[a,d][7]annulen-5-yl)-4-methylphenyl)-1-(pyridin-2-yl)ethan-1-imine (L7):

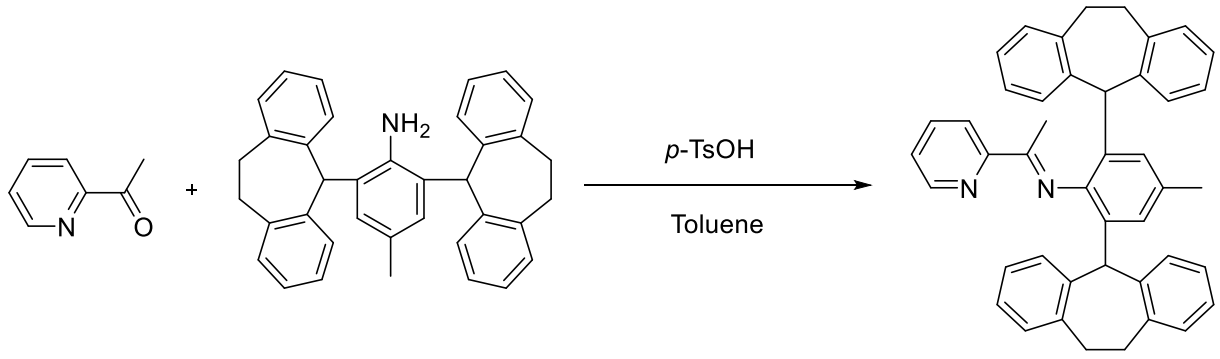

Ligand **L7** was synthesized in a similar manner as **L3** but using 2,6-bis(10,11-dihydro-5H-dibenzo[a,d][7]annulen-5-yl)-4-methylaniline (2.46 g, 5.0 mmol) as the aniline precursor. Isolated as pale-yellow powder. Yield: 2.1 g, 70.4%. ^{1}H NMR (400 MHz, CD_2Cl_2): δ 8.63 (d, *J* = 4.8 Hz,

1H), 8.15 (d, *J* = 8.0 Hz, 1H), 7.84 (t, *J* = 7.8 Hz, 1H), 7.46 – 7.40 (m, 1H), 7.12 – 6.98 (m, 8H), 6.89 – 6.81 (m, 6H), 6.73 (s, 2H), 6.67 – 6.60 (m, 2H), 4.87 (s, 2H, CH_2Ar_2), 3.53 – 3.36 (m, 4H), 2.78 – 2.63 (m, 4H), 2.13 (s, 3H, CH_3), 1.30 (s, 3H, CH_3). ^{13}C NMR (150 MHz, CD_2Cl_2): δ 170.23, 155.95, 148.68, 145.87, 141.06, 140.15, 140.10, 140.05, 136.15, 131.97, 131.95, 131.19, 130.89, 130.52, 130.27, 129.97, 127.18, 127.08, 126.18, 126.02, 125.16, 122.26, 56.44, 32.25, 31.85, 21.60, 16.56. HRMS (ESI) m/z: $[M+H]^+$ Calcd for $C_{44}H_{39}N_2$:595.3108; Found: 595.3093.

Synthesis of [*N*-(2,6-bis(10,11-dihydro-5H-dibenzo[a,d][7]annulen-5-yl)-4-methylphenyl)-1-(pyridin-2-yl)ethan-1-imine]·Ni(*o*-tol)Cl (C7):

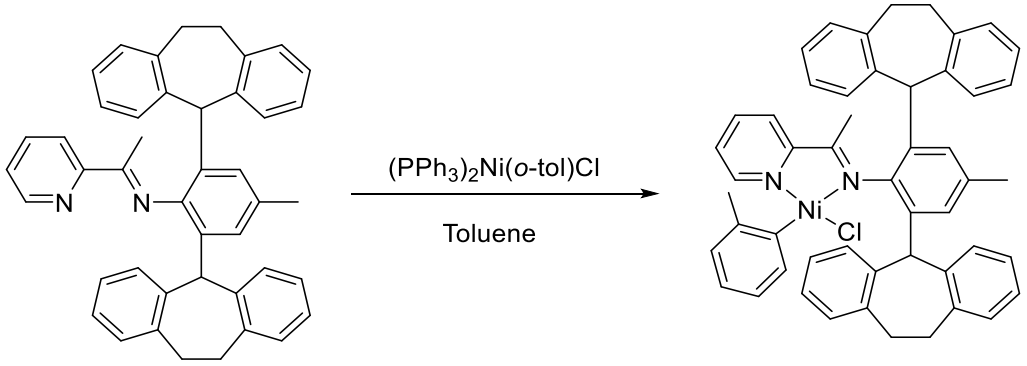

A dried 100 mL round-bottomed flask filled with nitrogen was added $(PPh_3)_2$Ni(*o*-tol)Cl (200 mg, 0.28 mmol) and **L7** (232 mg, 0.39 mmol). Toluene (15 mL) was injected to the reaction and stirring at 35 °C. The red suspensions were formed after stirring for 16 hours. 5 mL of pentane was added to the reaction and the precipitate was filtered and collected. The catalyst was dissolved in DCM and filtered through celite. The filtrate was concentrated, and the resulting product was purified *via* recrystallization from DCM and pentane. The dark red solids were then filtered and dried under vacuum. Yield: 164 mg, 75%. ^{1}H NMR (400 MHz, CD_2Cl_2): δ 7.84 (t, *J* = 7.6 Hz, 1 H), 7.79 (d, *J* = 6.9 Hz, 1H), 7.69 (d, *J* = 7.6 Hz, 1H), 7.60 (d, *J* = 5.5 Hz, 1H), 7.51 (d, *J* = 7.3 Hz, 1H), 7.46 (d, *J* = 6.8 Hz, 2H), 7.32 (t, *J* = 6.6 Hz, 1H), 7.20 – 7.06 (m, 6H), 7.00 – 6.85 (m, 7H), 6.80 – 6.72 (m, 3H), 6.37 – 6.27 (m, 3H), 6.23 (s, 1H), 3.87 – 3.70 (m, 2H), 3.43 (s, 1H), 3.39 (s,

1H), 3.29 (s, 3H), 3.05 – 2.93 (m, 2H), 2.55 – 2.44 (m, 2H), 2.13 (s, 3H), 0.05 (s, 3H). ^{13}C NMR (150 MHz, CD_2Cl_2): δ 175.52, 156.67, 152.35, 151.53, 142.65, 142.60, 142.34, 142.24, 141.95, 141.78, 139.07, 139.03, 138.83, 138.70, 137.54, 135.48, 134.59, 134.44, 133.93, 132.40, 132.32, 132.04, 131.73, 131.61, 130.46, 130.35, 129.32, 128.35, 127.98, 127.34, 127.30, 127.25, 126.99, 126.92, 126.10, 125.15, 123.62, 123.17, 56.71, 56.43, 33.81, 33.66, 30.40, 30.34, 25.92, 21.84, 15.91. Anal. Calcd for $C_{51}H_{45}ClN_2Ni$: C, 78.53; H, 5.81; N, 3.59. Found: C, 78.25; H, 5.72; N, 3.48.

Synthesis of *N*-(2,6-bis(10,11-dihydro-5H-dibenzo[a,d][7]annulen-5-yl)-4-methylphenyl)-1-phenyl-1-(pyridin-2-yl)methanimine (L8):

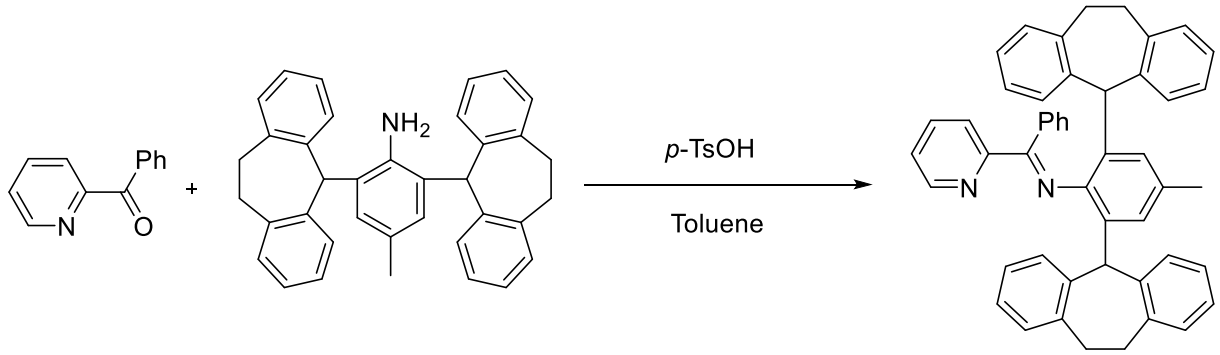

Ligand **L8** was synthesized in a similar manner as **L7** but using 2-benzoylpyridine (0.37g, 2.0 mmol) as the ketone precursor. A bright yellow powder was isolated as a mixture of E/Z isomers. Yield: 0.85 g, 65%. ^{1}H NMR (400 MHz, CD2Cl2): δ 8.74 (d, *J* = 2.2 Hz, 0.6H), 8.64 (d, *J* = 2.4 Hz, 0.4H), 7.88 – 7.80 (m, 0.7H), 7.58 – 7.50 (m, 0.5H), 7.47 – 7.18 (m, 5.6H), 7.17 – 7.06 (m, 5.2H), 7.05 – 6.80 (m, 8H), 6.67 (t, *J* = 7.2 Hz, 1H), 6.61 (s, 1H), 6.60 – 6.55 (m, 2H), 6.44 (s, 0.6H), 6.42 (s, 0.4H) 6.16 (d, *J* = 7.3 Hz, 0.6H), 5.93 (d, *J* = 7.8 Hz, 0.4H), 5.07 (s, 1H), 4.89 (s, 1H), 3.53 – 3.40 (m, 2H), 3.40 – 3.26 (m, 2H), 2.85 – 2.72 (m, 2H), 2.71 – 2.60 (m, 2H), 2.08 (s, 1.2H), 2.05 (s, 1.8H). ^{13}C NMR (150 MHz, CD_2Cl_2) δ 164.84, 164.60, 156.86, 154.99, 149.28, 148.12, 144.45, 144.02, 140.49, 140.40, 140.17, 139.98, 139.89, 139.82, 139.68, 139.48,

138.63, 135.96, 135.48, 132.03, 131.64, 131.61, 131.55, 131.38, 131.12, 130.60, 130.53, 130.51, 130.49, 130.29, 130.21, 130.09, 130.05, 129.81, 129.63, 129.45, 129.28, 127.54, 127.46, 126.93, 126.82, 126.77, 126.74, 125.98, 125.96, 125.86, 125.75, 125.17, 124.60, 123.73, 123.43, 55.39, 55.01, 32.18, 31.49, 31.46, 21.27, 21.25. HRMS (ESI) m/z: [M+H] + Calcd for $C_{49}H_{40}N_2$: 657.326 Found: 657.325.

Synthesis of [*N*-(2,6-bis(10,11-dihydro-5H-dibenzo[a,d][7]annulen-5-yl)-4-methylphenyl)-1-phenyl-1-(pyridin-2-yl)methanimine]·Ni(*o*-tol)Cl (C8):

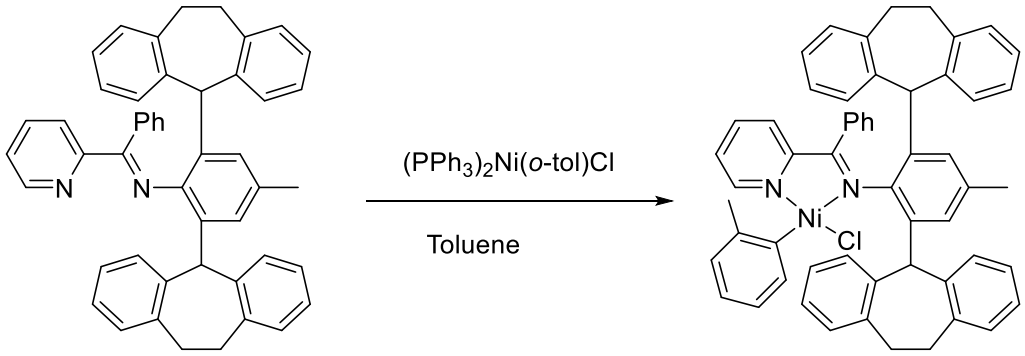

A dried 100 mL round-bottomed flask filled with nitrogen was added $(PPh_3)_2Ni$(*o*-tol)Cl (200 mg, 0.28 mmol) and **L8** (276 mg, 0.42 mmol). Toluene (20 mL) was injected into the round bottom and stirred at 40 °C for 3 days. 10 mL of pentane was added to the reaction and the precipitate was filtered and collected. The catalyst was dissolved in DCM and filtered through celite. The filtrate was concentrated, and the resulting product was purified *via* recrystallization from methylene chloride and pentane. The dark red solids were then filtered and dried under vacuum. X-Ray crystallography data confirmed the identity of the catalyst (Figure S139). Although crystals were successfully isolated for **C8**, ^{1}H, ^{13}C NMR, and elemental analysis of the crystals produced inconclusive data for further structure determination. Yield: 25 mg, 10.5%.

3.2 ^{1}H and ^{13}C NMR of Ligand and Complexes

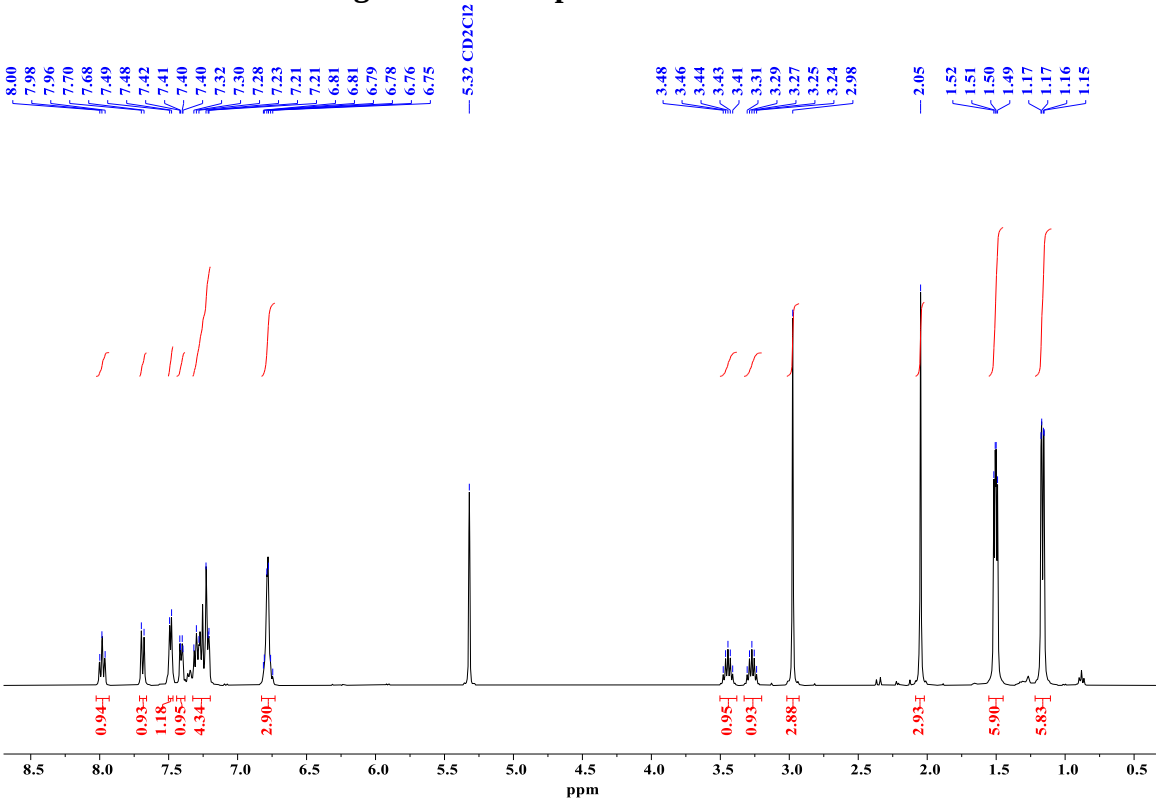

Figure S3. ^{1}H NMR Spectrum of **C1** in CD_2Cl_2, 400 MHz.

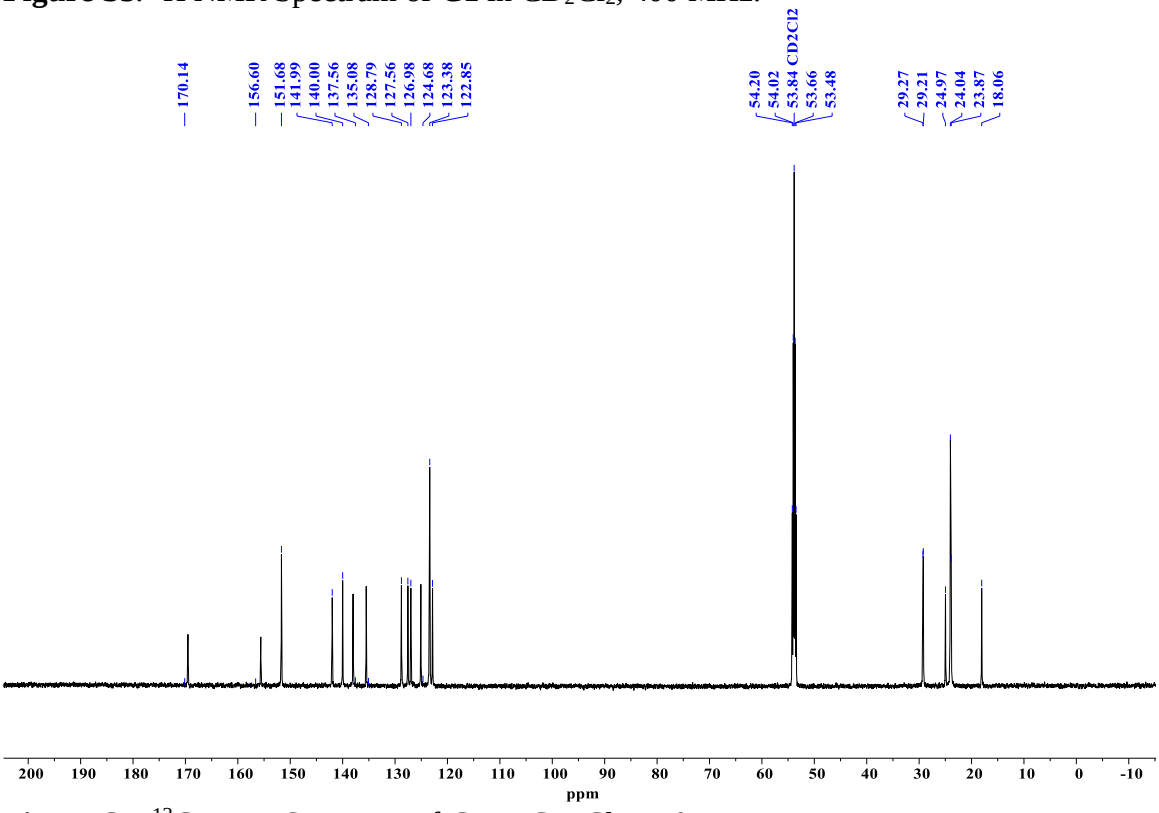

Figure S4. ^{13}C NMR Spectrum of **C1** in CD_2Cl_2, 150 MHz.

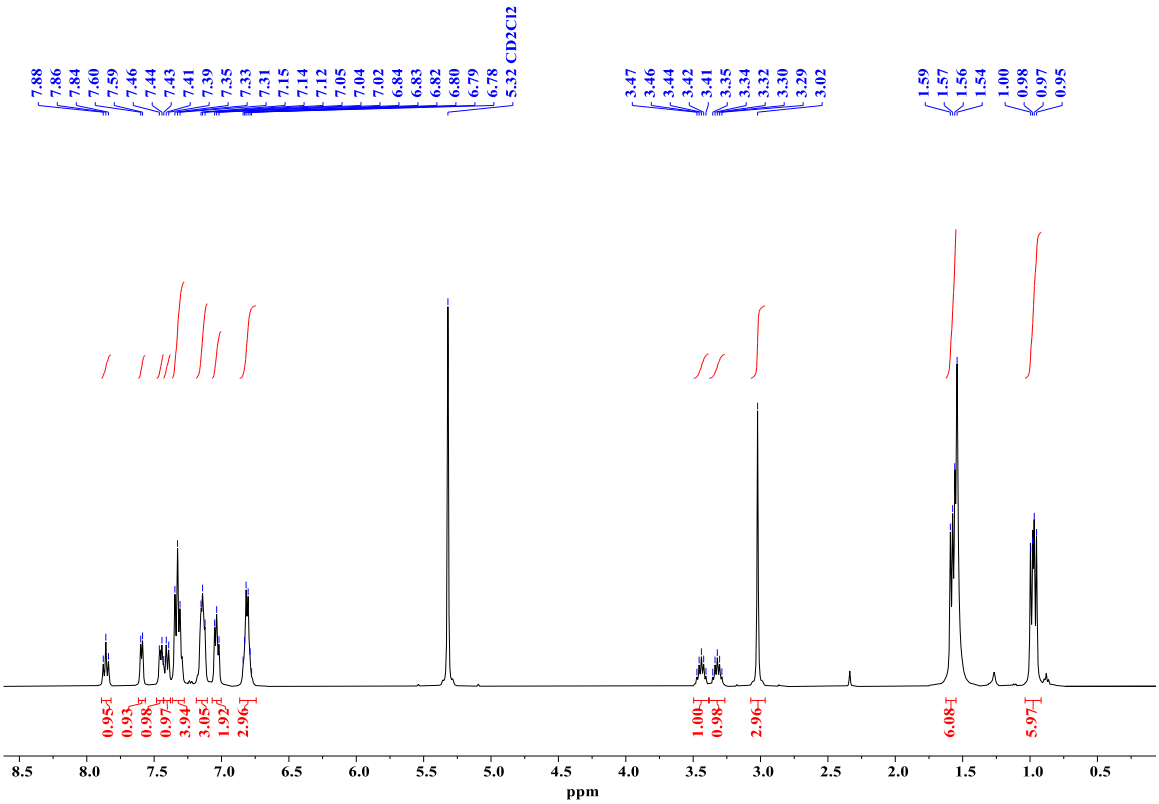

Figure S5. ^{1}H NMR Spectrum of **C2** in CD_2Cl_2, 400 MHz.

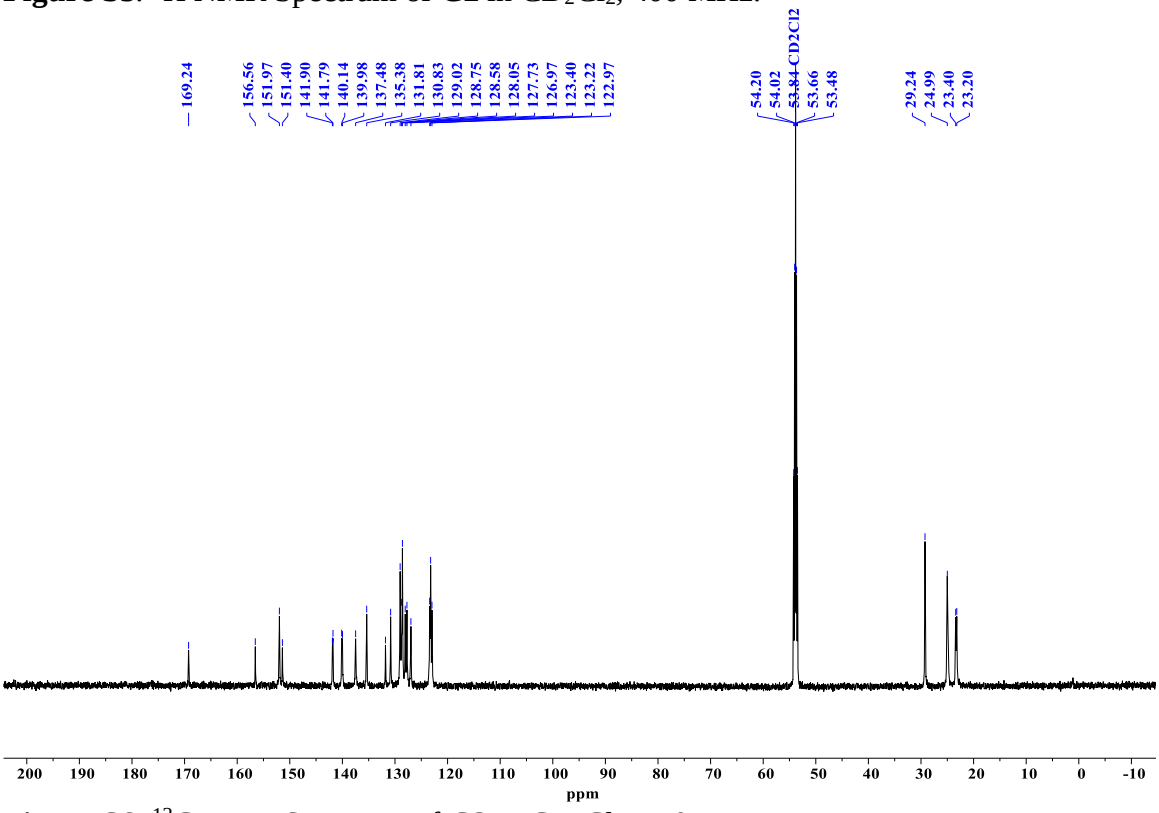

Figure S6. ^{13}C NMR Spectrum of **C2** in CD_2Cl_2, 150 MHz.

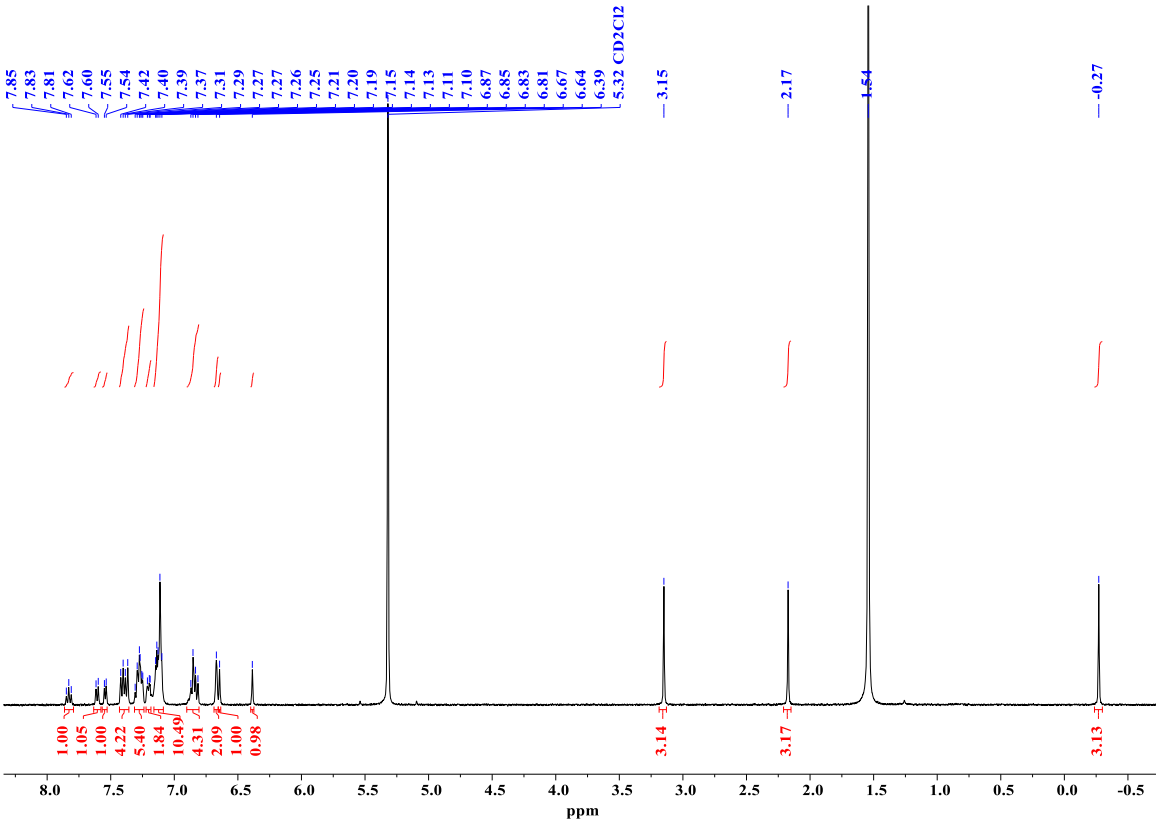

Figure S7. ^{1}H NMR Spectrum of **C3** in CD_2Cl_2, 400 MHz.

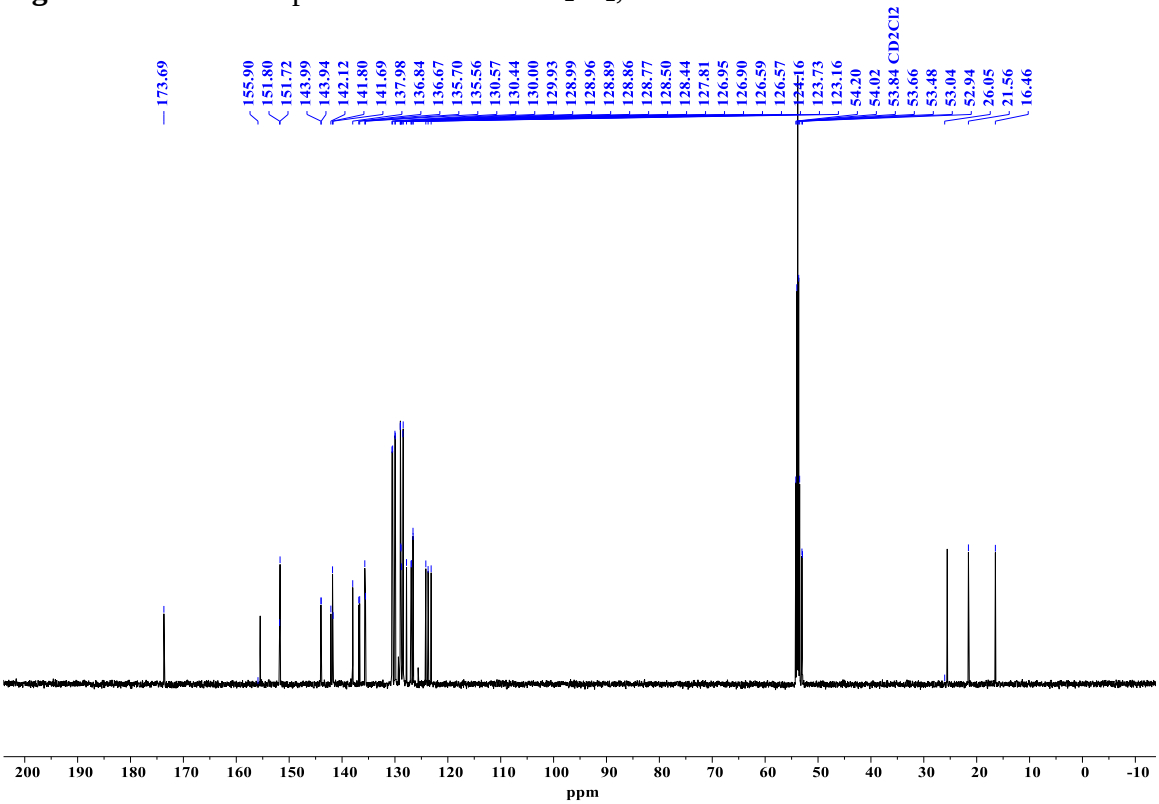

Figure S8. ^{13}C NMR Spectrum of **C3** in CD_2Cl_2, 150 MHz.

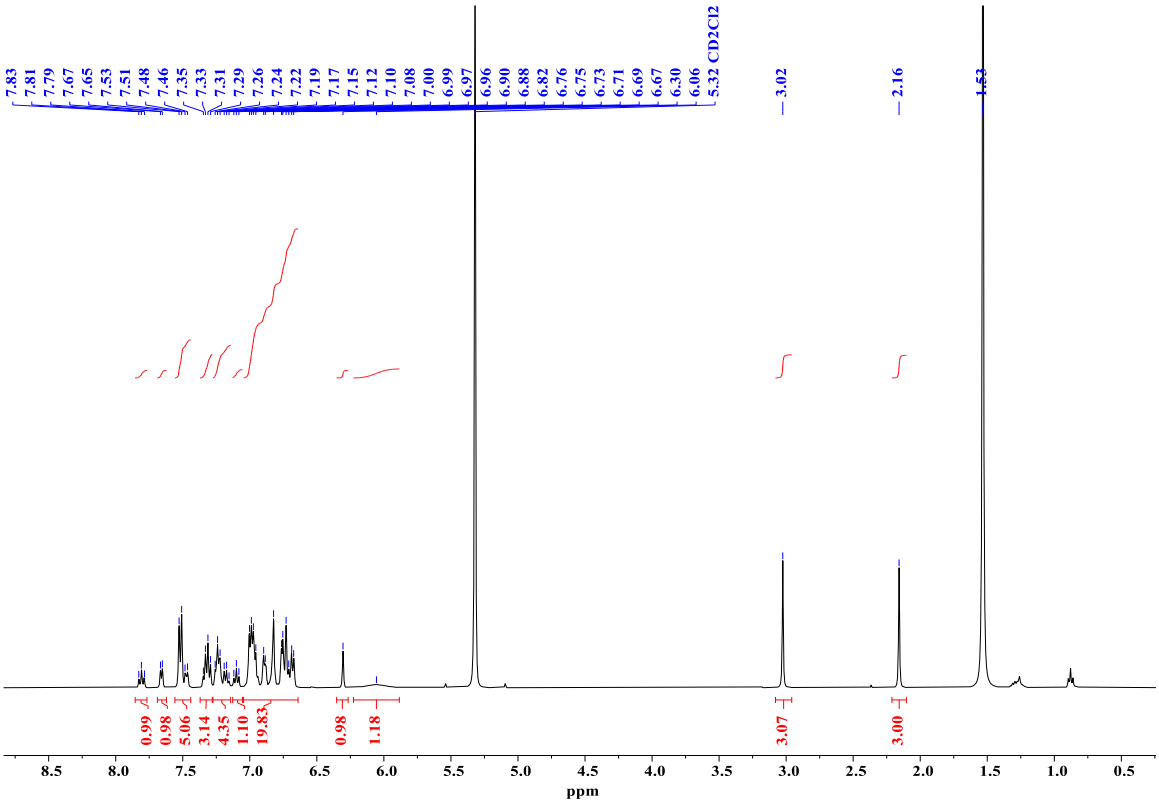

Figure S9. ^{1}H NMR Spectrum of **C4** in CD_2Cl_2, 400 MHz.

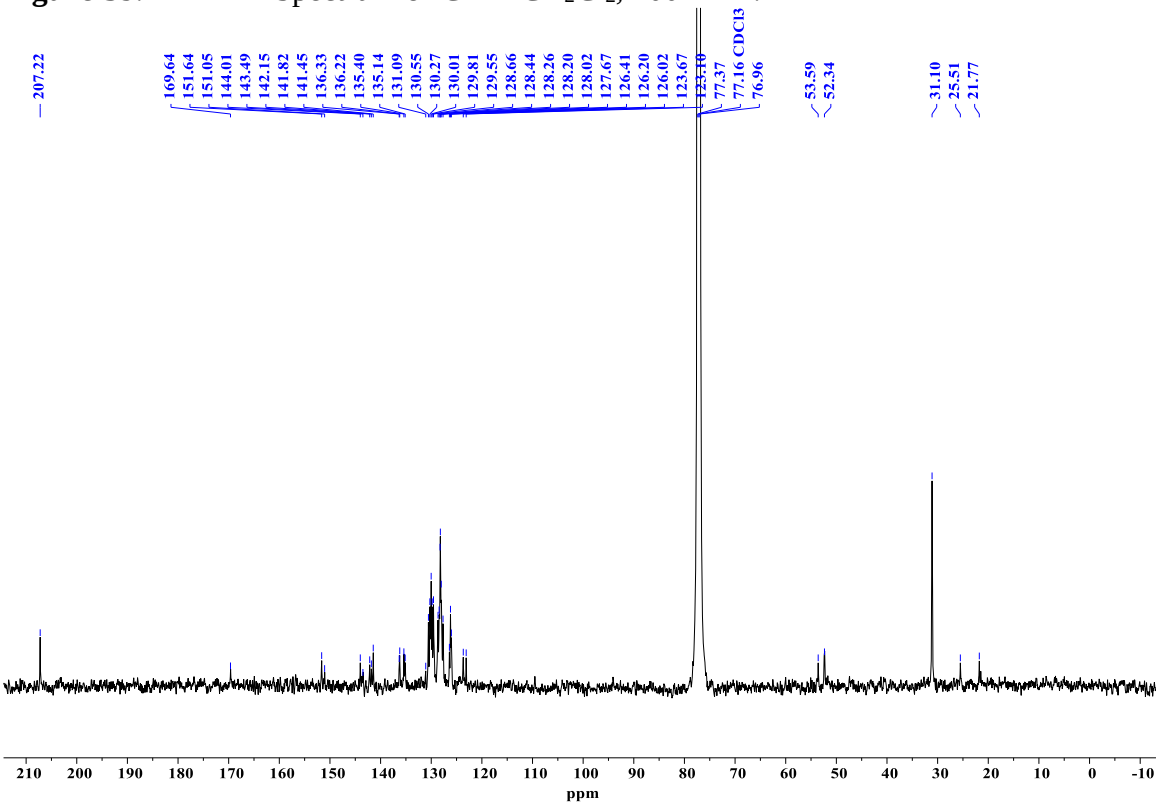

Figure S10. ^{13}C NMR Spectrum of **C4** in $CDCl_3$, 150 MHz.

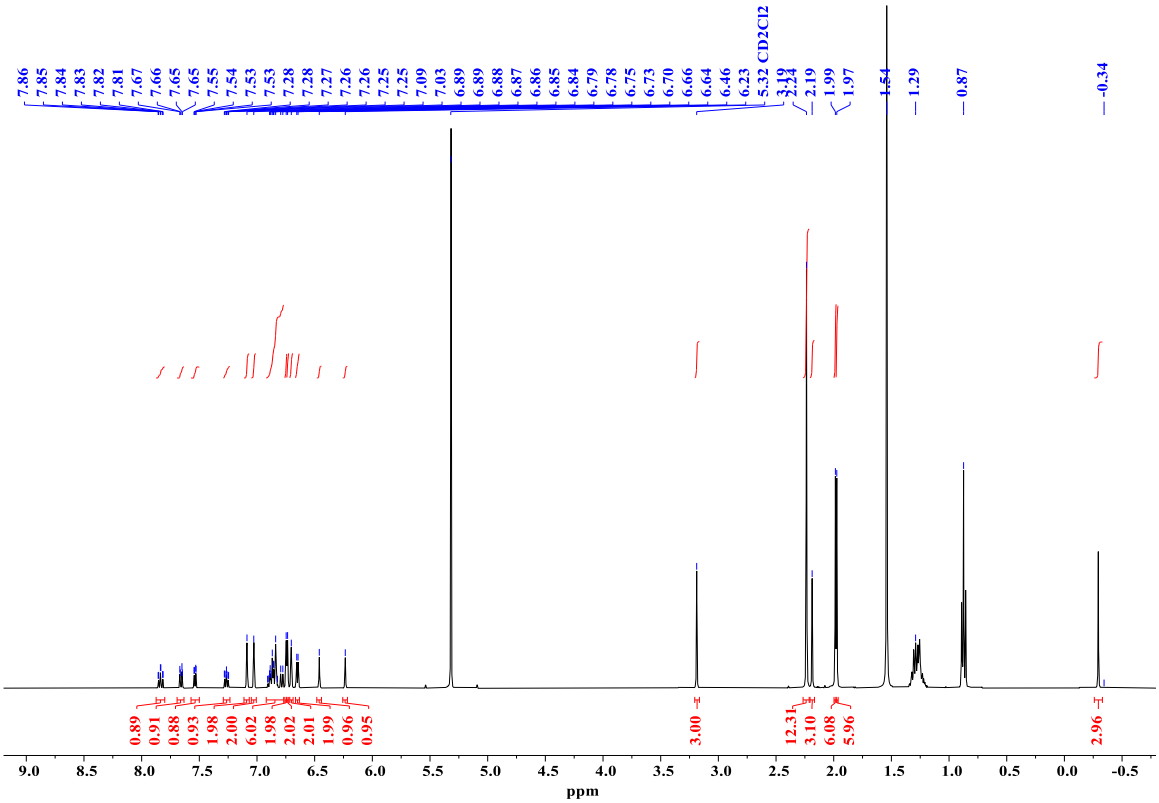

Figure S11. ^{1}H NMR Spectrum of **C5** in CD_2Cl_2, 400 MHz.

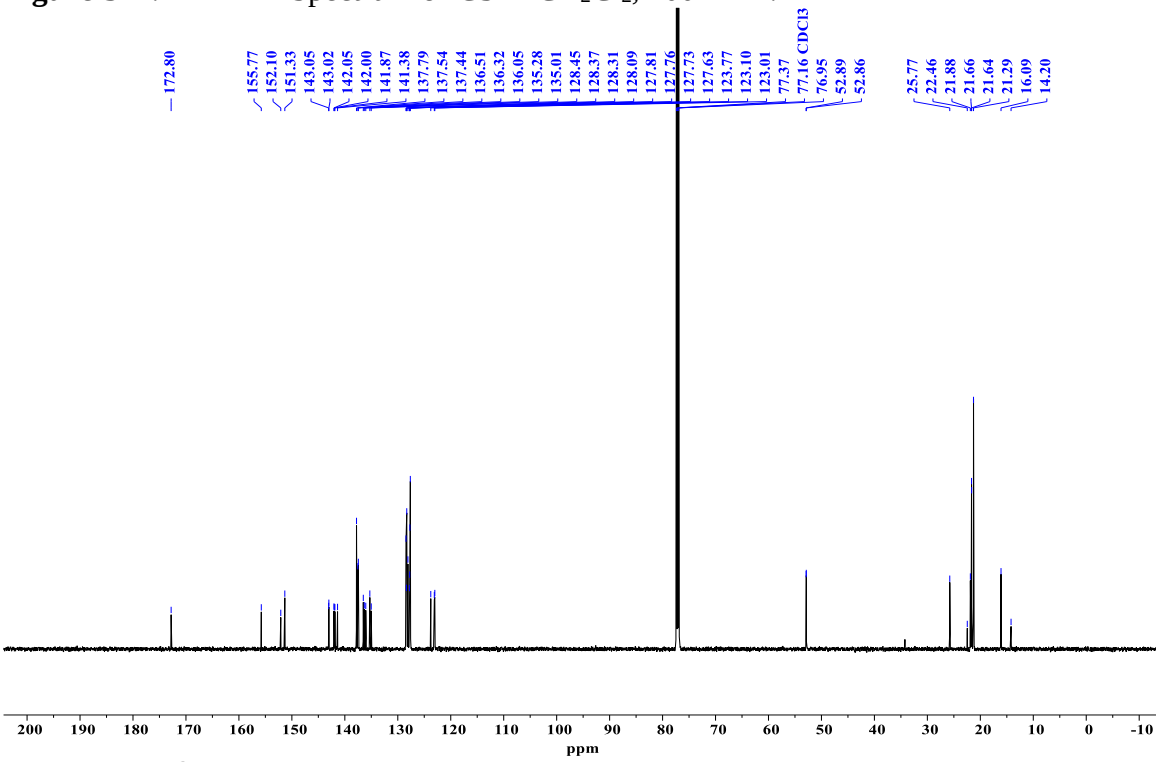

Figure S12. ^{13}C NMR Spectrum of **C5** in $CDCl_3$, 150 MHz.

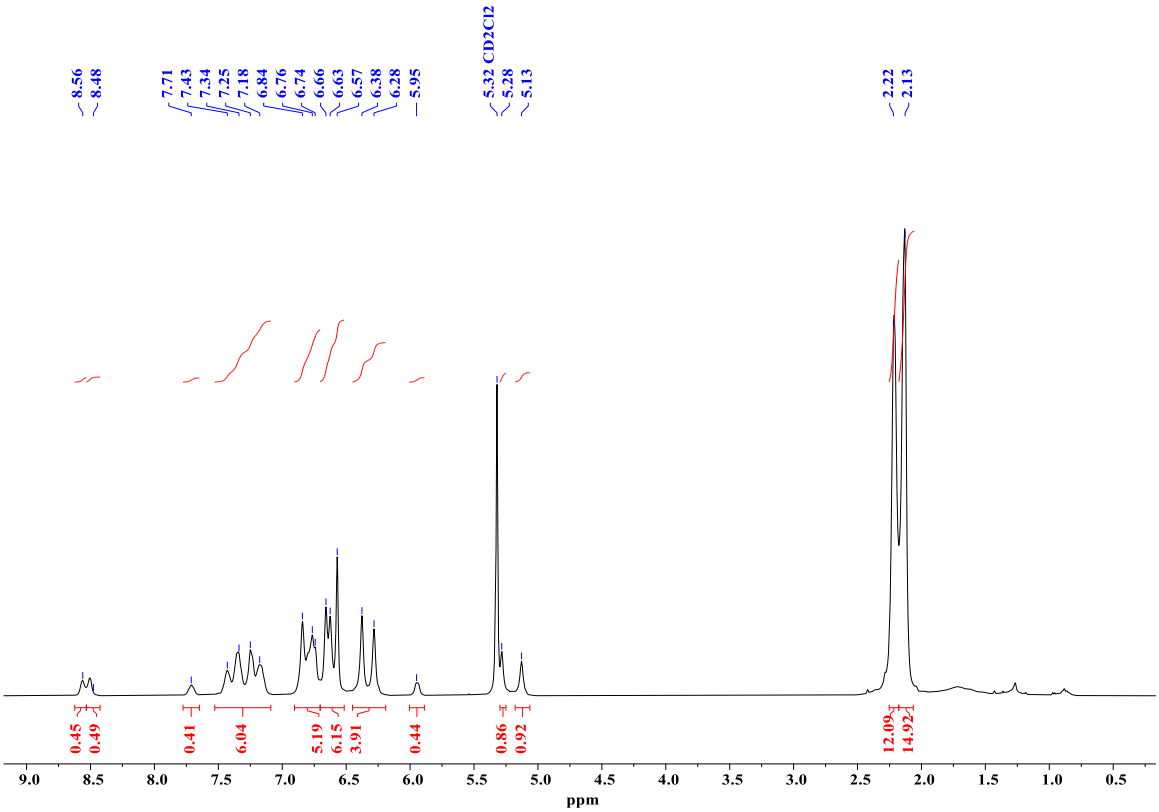

Figure S13. ^{1}H NMR Spectrum of **L6** in CD_2Cl_2, 400 MHz.

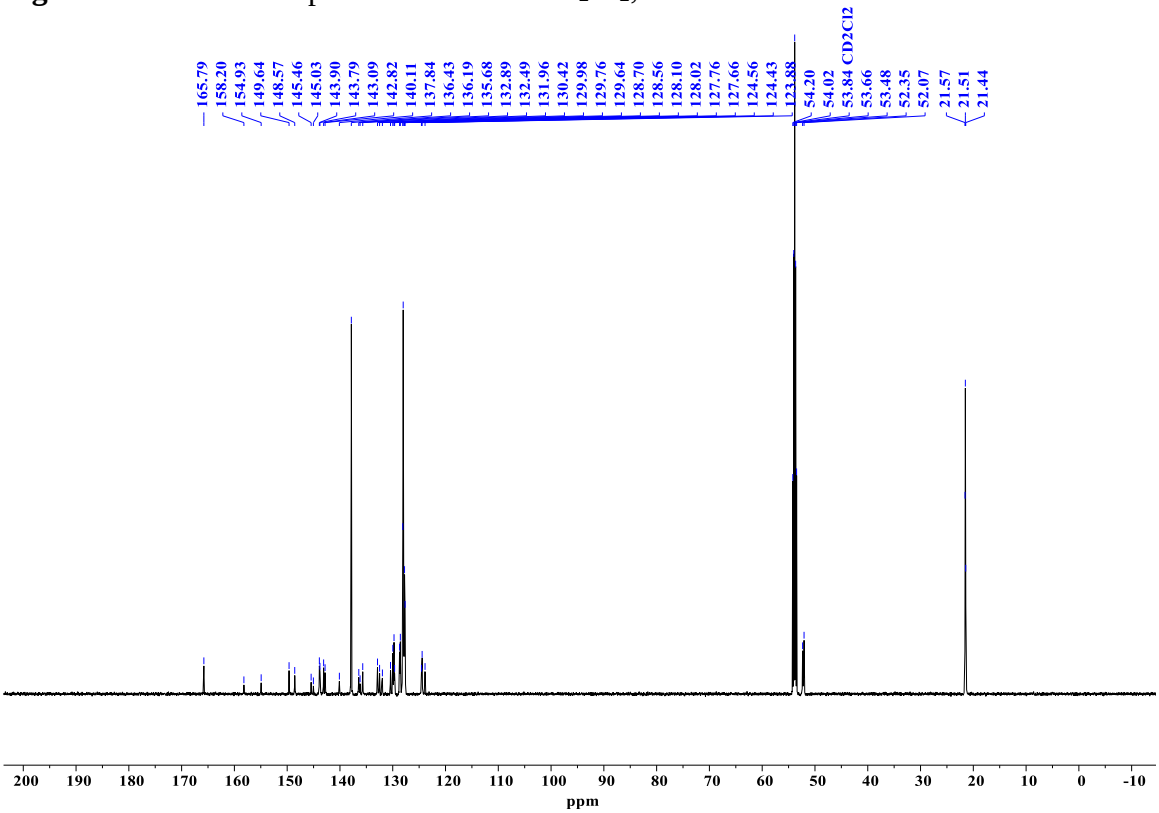

Figure S14. ^{13}C NMR Spectrum of **L6** in CD_2Cl_2, 150 MHz.

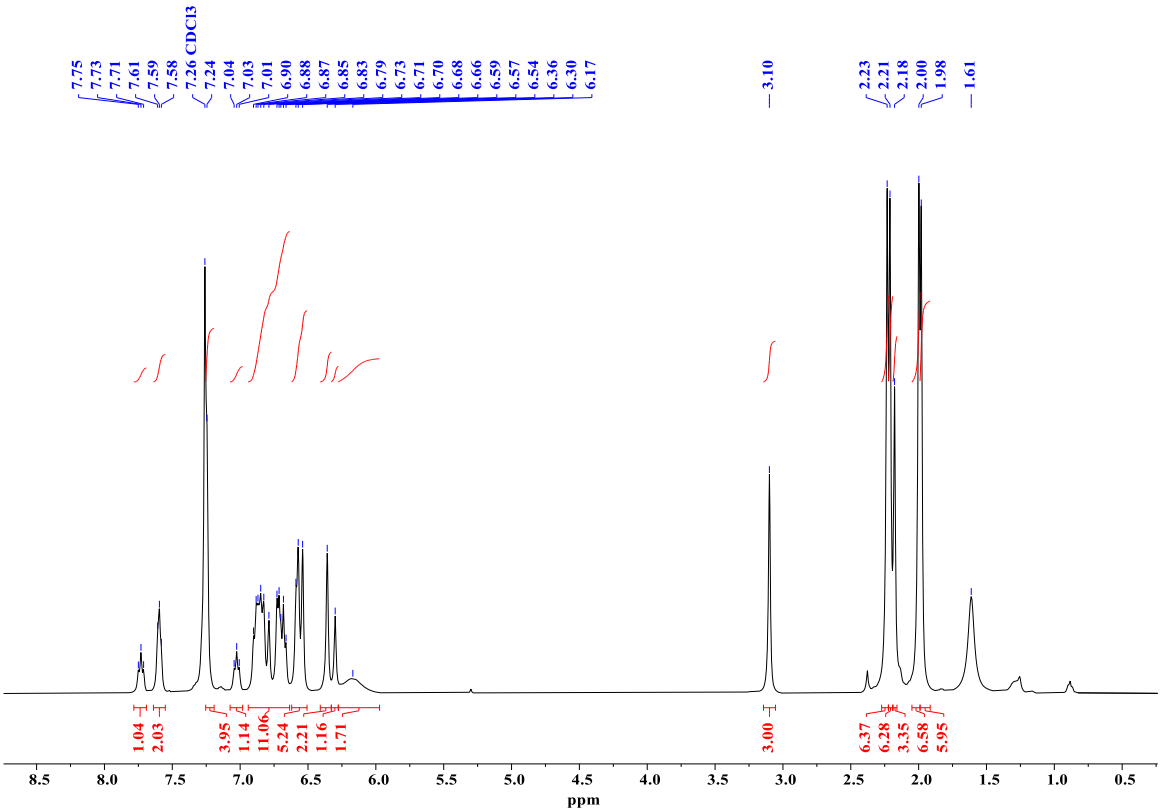

Figure S15. ^{1}H NMR Spectrum of **C6** in $CDCl_3$, 400 MHz.

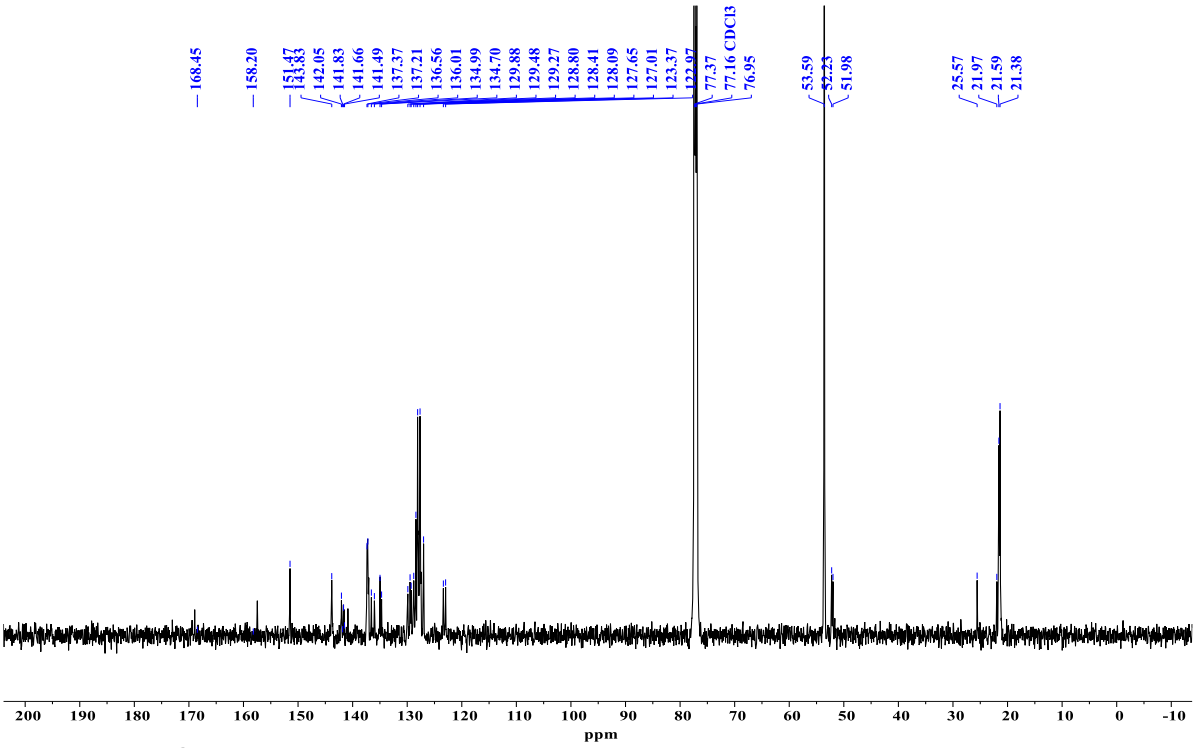

Figure S16. ^{13}C NMR Spectrum of **C6** in $CDCl_3$, 150 MHz.

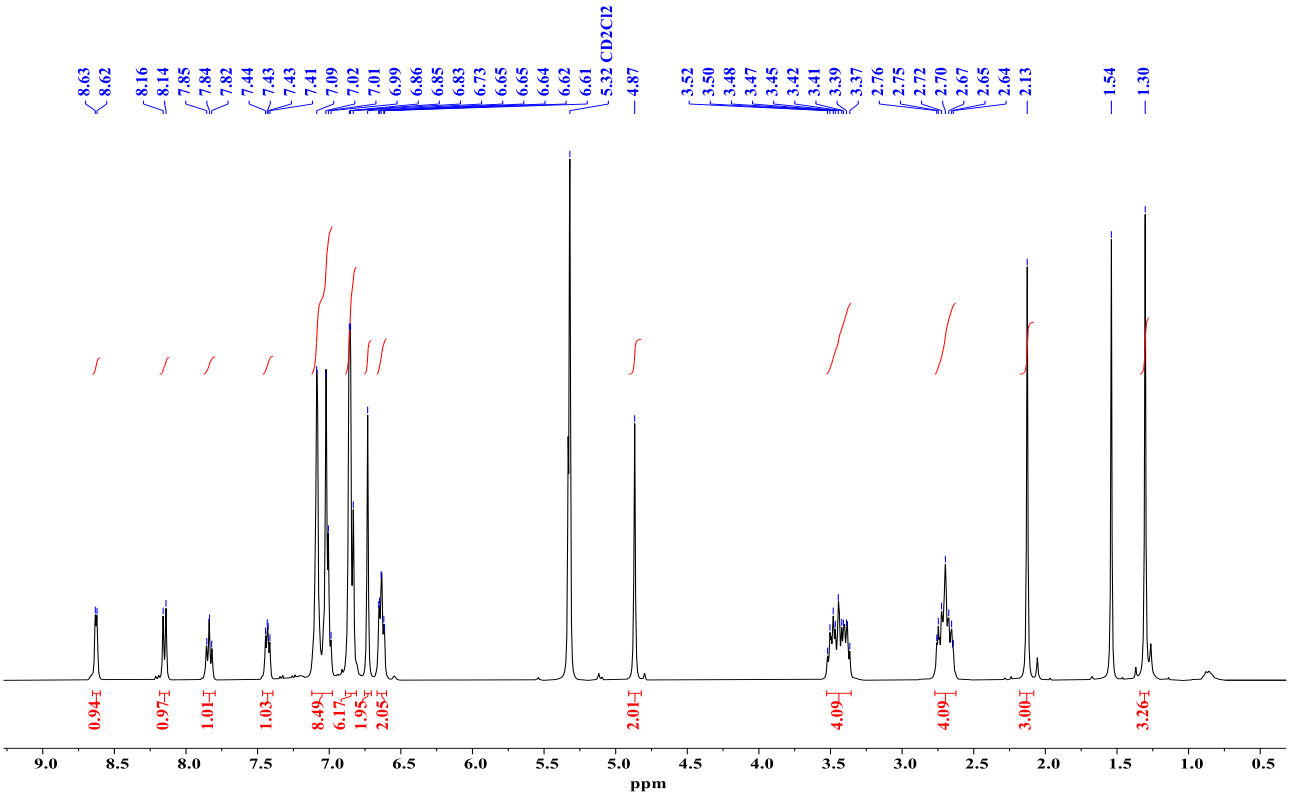

Figure S17. ^{1}H NMR Spectrum of **L7** in CD_2Cl_2, 400 MHz.

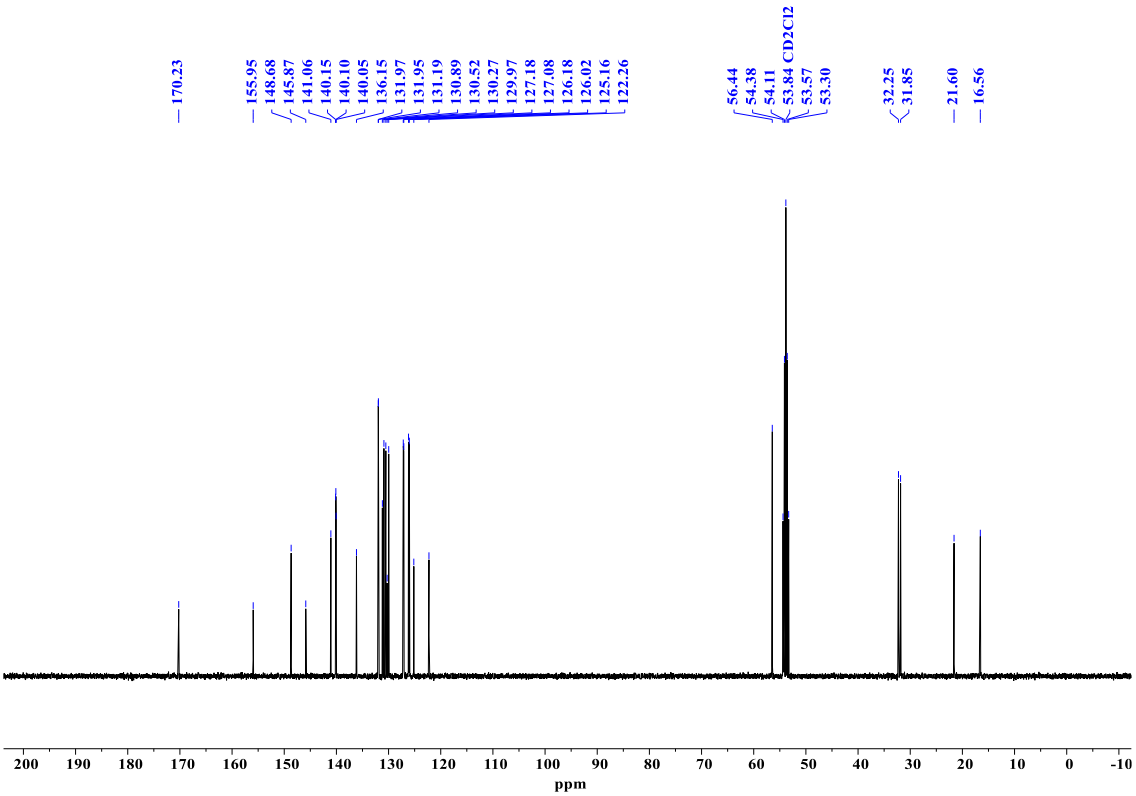

Figure S18. ^{13}C NMR Spectrum of **L7** in CD_2Cl_2, 150 MHz.

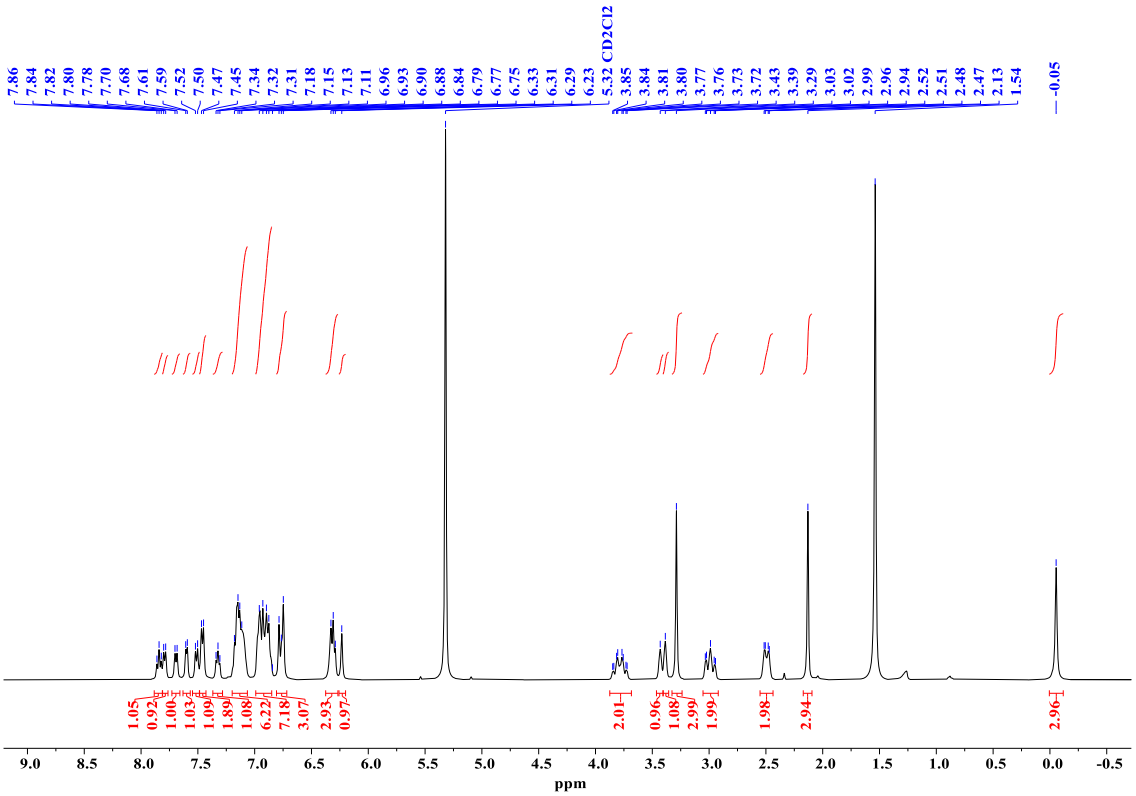

Figure S19. ^{1}H NMR Spectrum of **C7** in CD_2Cl_2, 400 MHz.

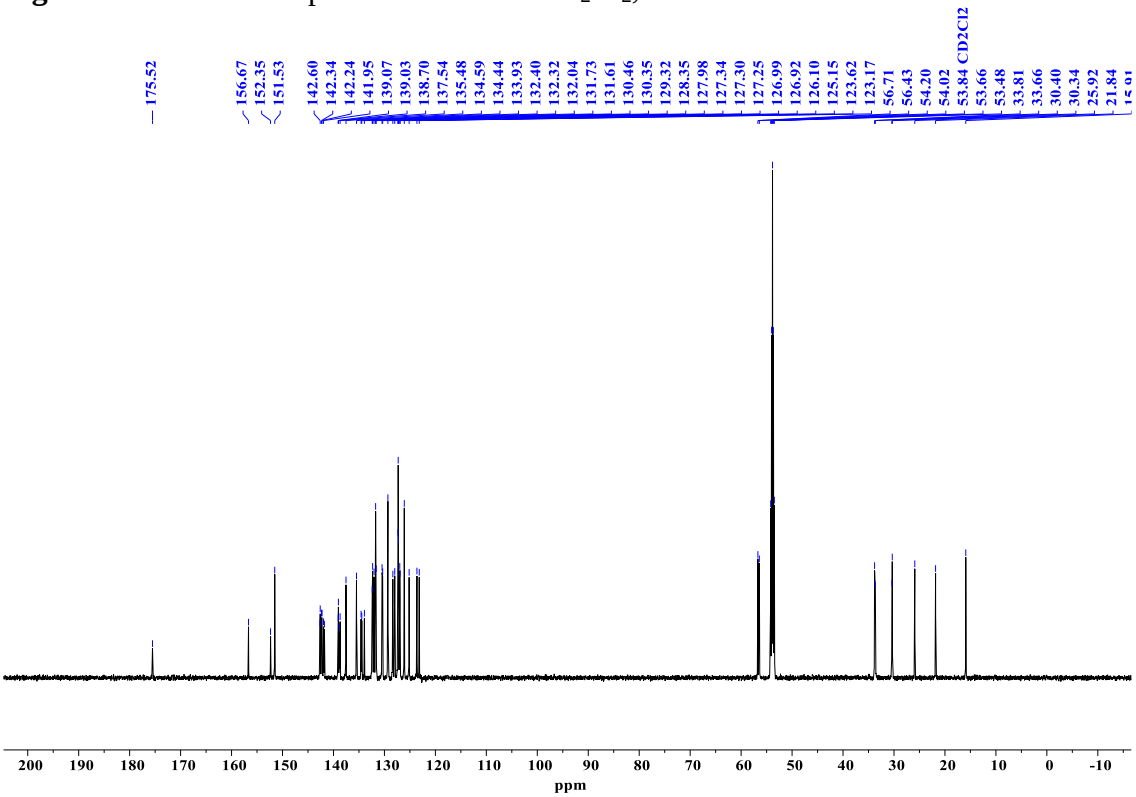

Figure S20. ^{13}C NMR Spectrum of **C7** in CD_2Cl_2, 150 MHz.

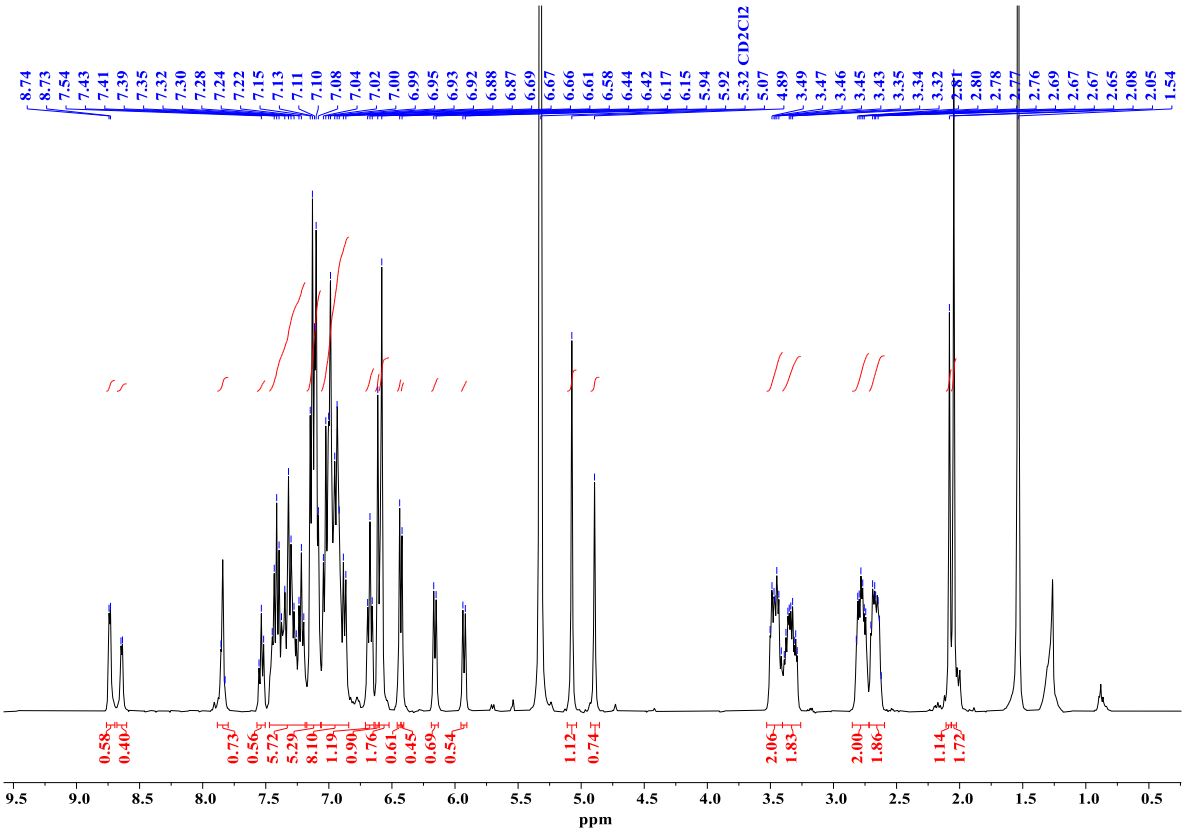

Figure S21. ^{1}H NMR Spectrum of **L8** in CD_2Cl_2, 400 MHz.

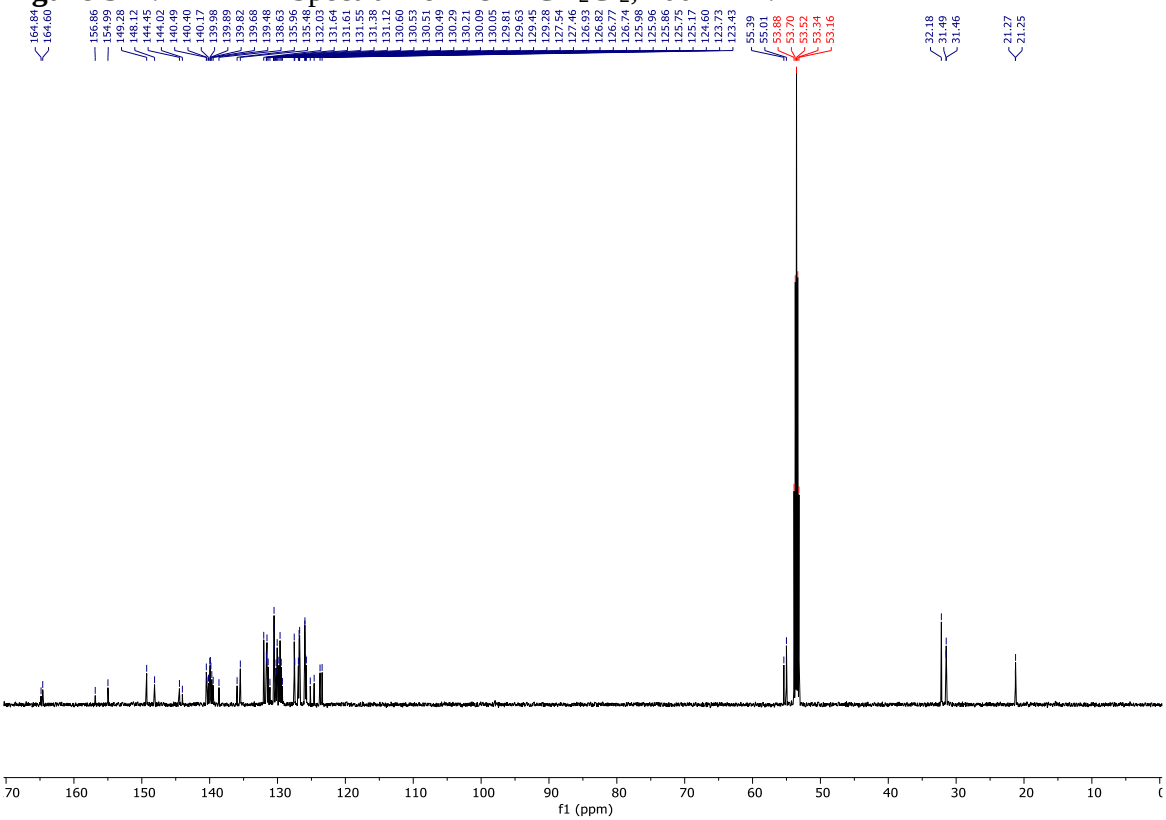

Figure S22. ^{13}C NMR Spectrum of **L8** in CD_2Cl_2, 150 MHz.

4. Characterization of Polymers

4.1 ^{1}H and ^{13}C NMR of Polymers

4.1.1 ^{1}H NMR of Polymers from Table 1

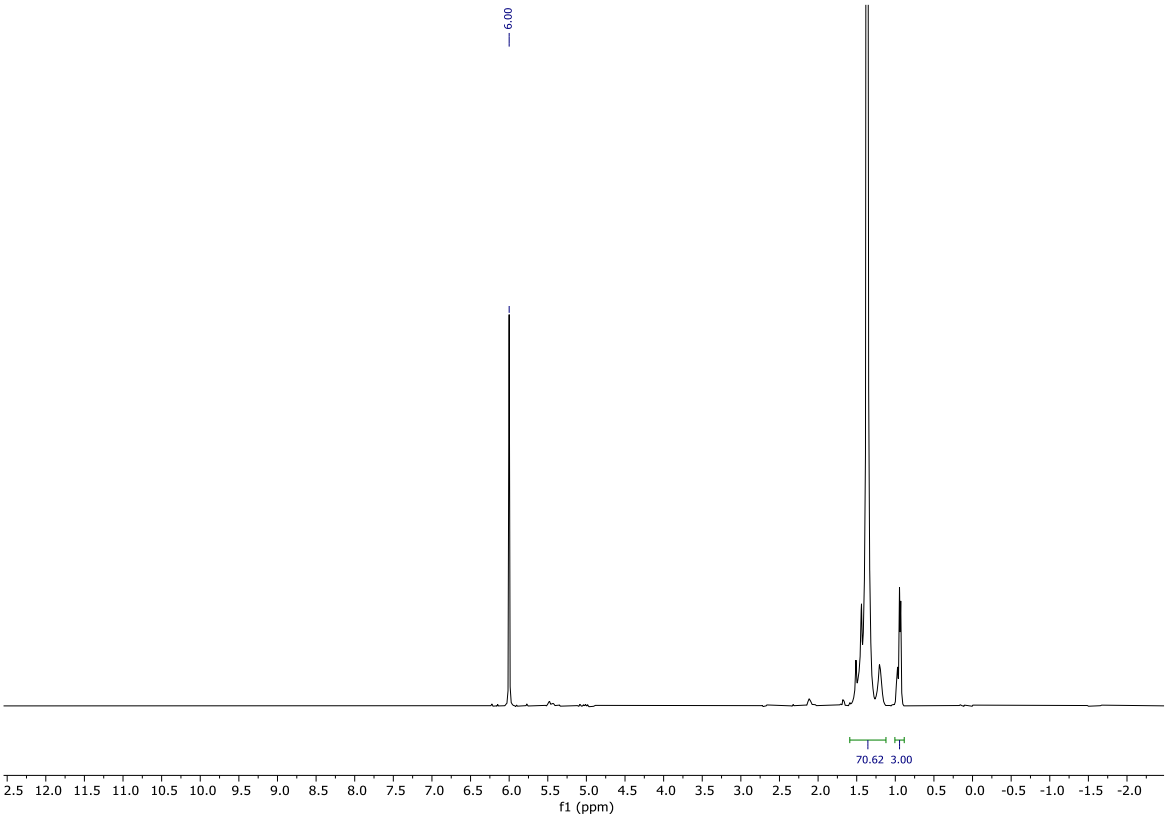

Figure S23. ^{1}H NMR Spectrum of polymer in entry 1, Table 1, 400 MHz (125 °C, $C_2D_2Cl_4$).

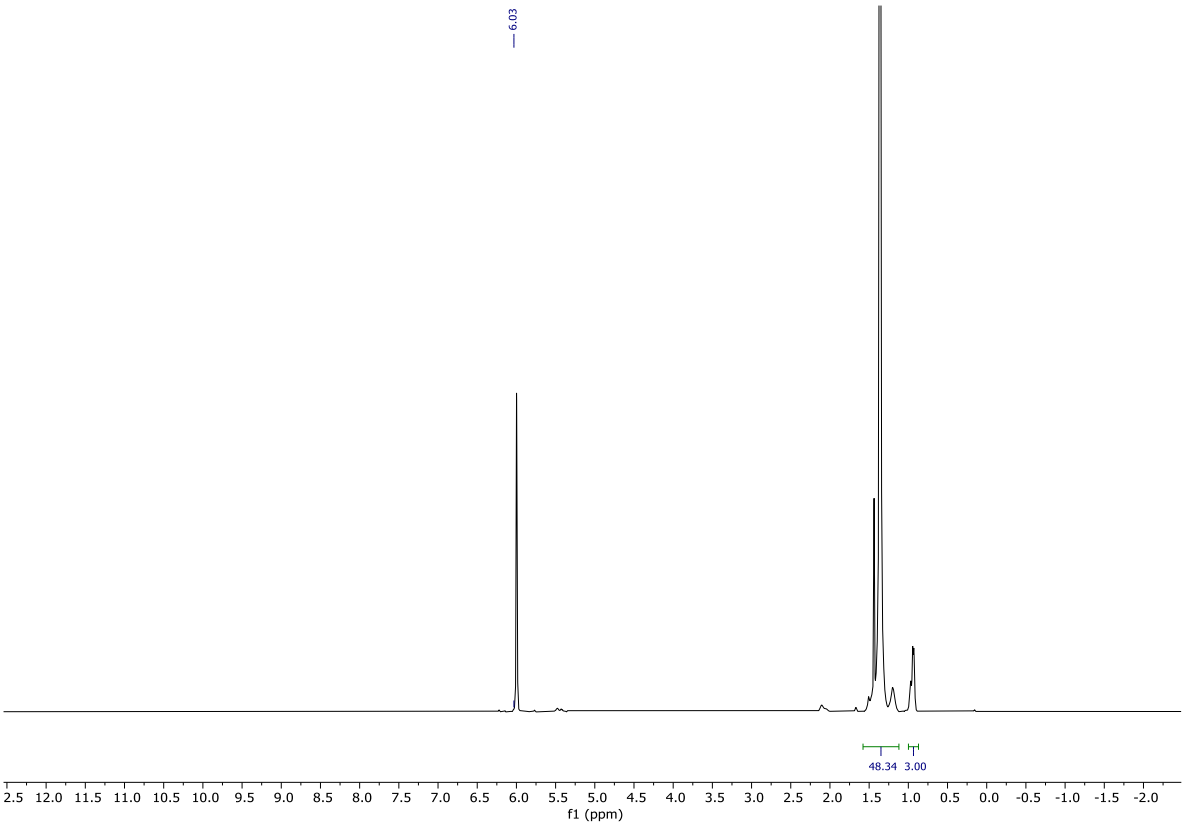

Figure S24. ^{1}H NMR Spectrum of polymer in entry 2, Table 1, 400 MHz (125 °C, $C_2D_2Cl_4$).

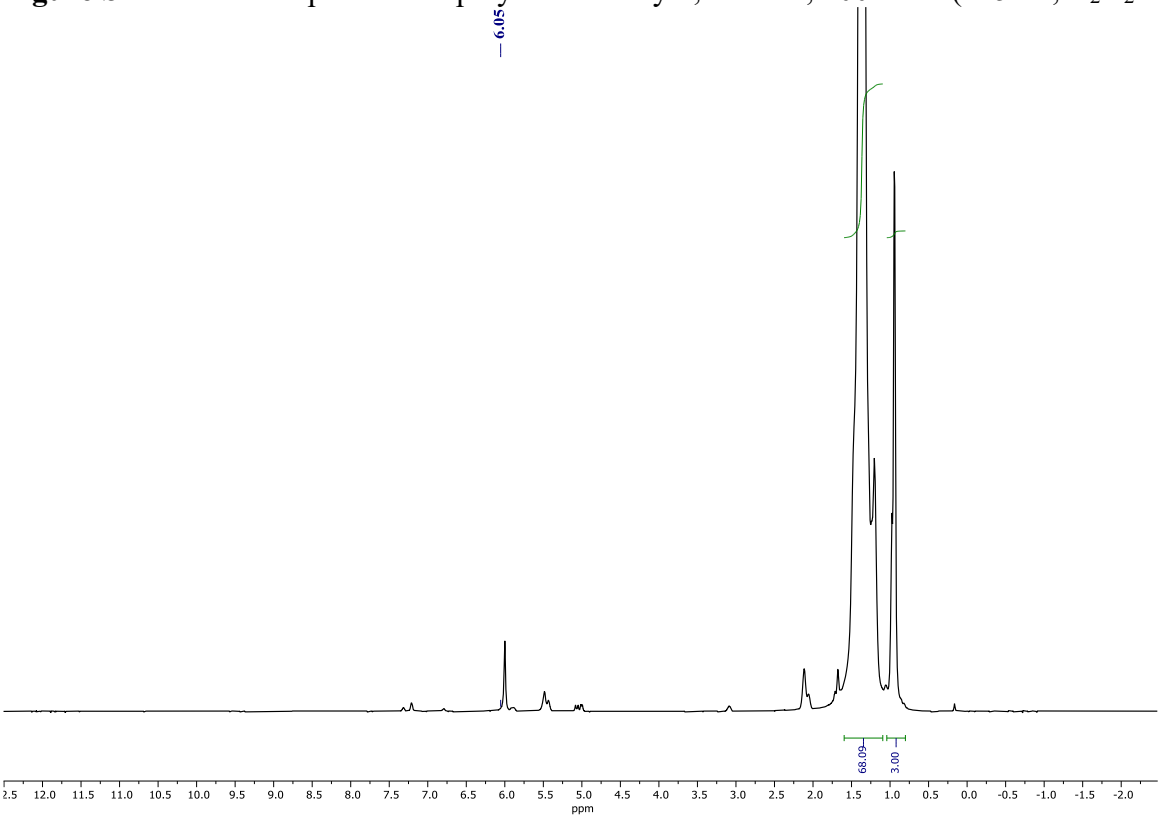

Figure S25. ^{1}H NMR Spectrum of polymer in entry 3, Table 1, 400 MHz (125 °C, $C_2D_2Cl_4$).

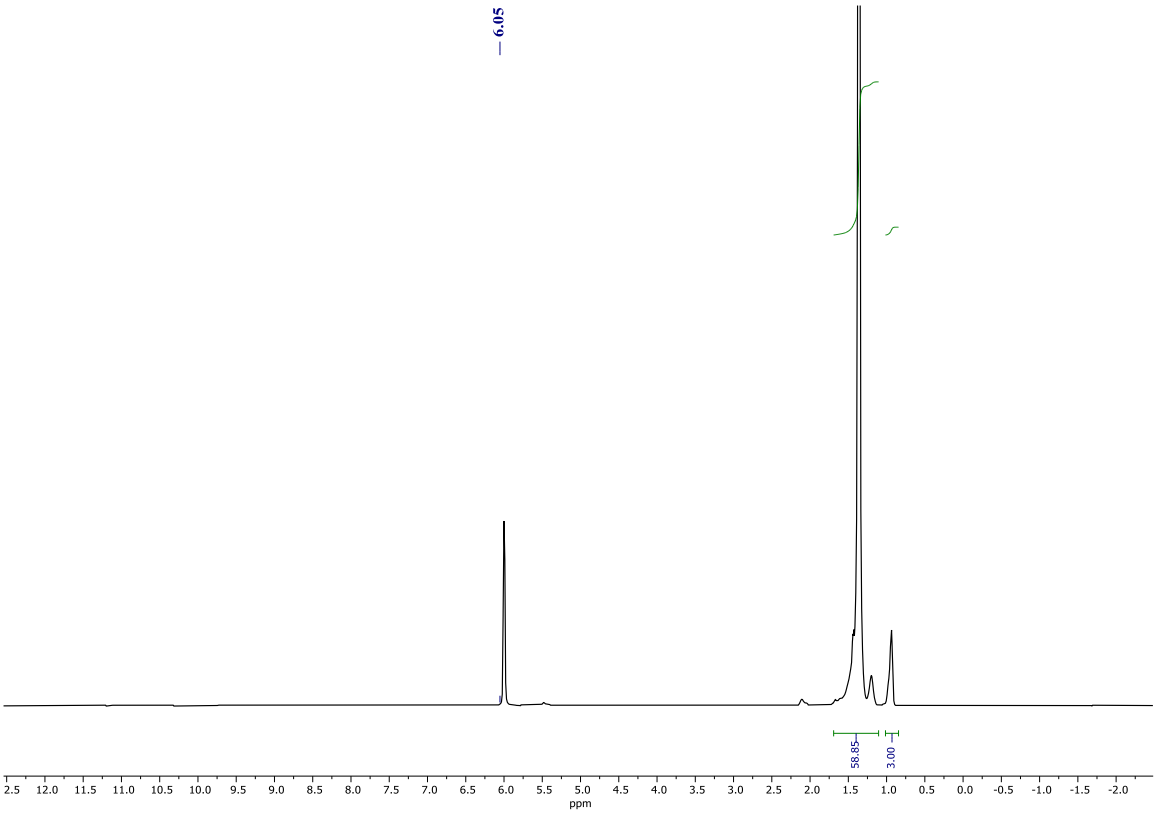

Figure S26. ^{1}H NMR Spectrum of polymer in entry 4, Table 1, 400 MHz (125 °C, $C_2D_2Cl_4$).

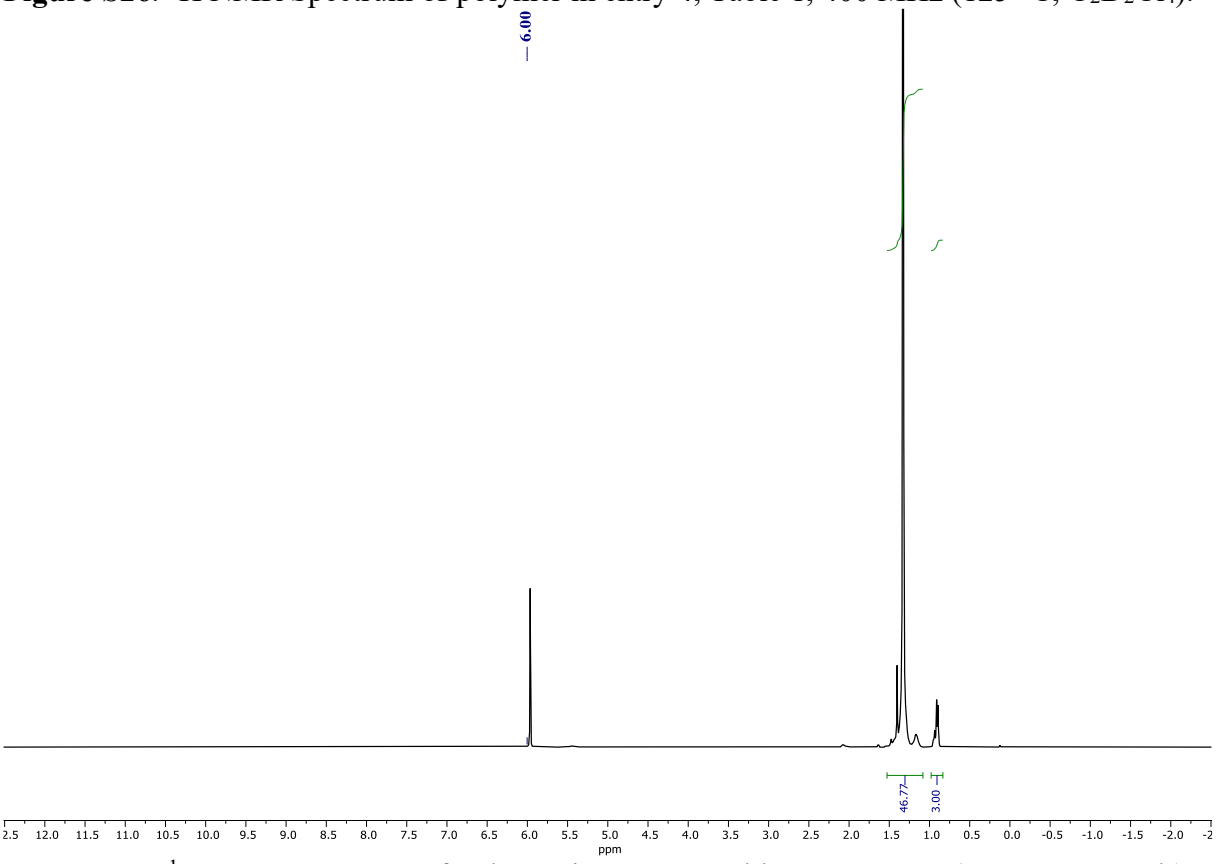

Figure S27. ^{1}H NMR Spectrum of polymer in entry 5, Table 1, 400 MHz (125 °C, $C_2D_2Cl_4$).

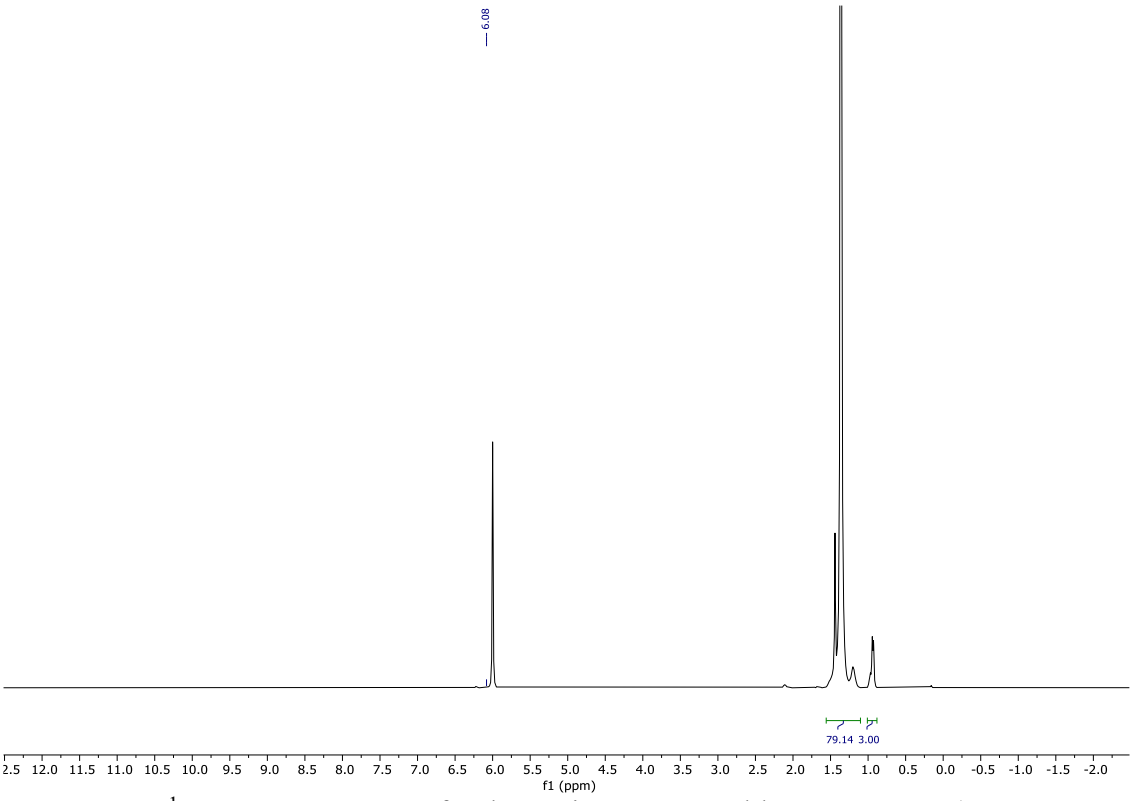

Figure S28. ^{1}H NMR Spectrum of polymer in entry 6, Table 1, 400 MHz (125 °C, $C_2D_2Cl_4$).

4.1.2 ^{1}H NMR of Polymers from Table 2

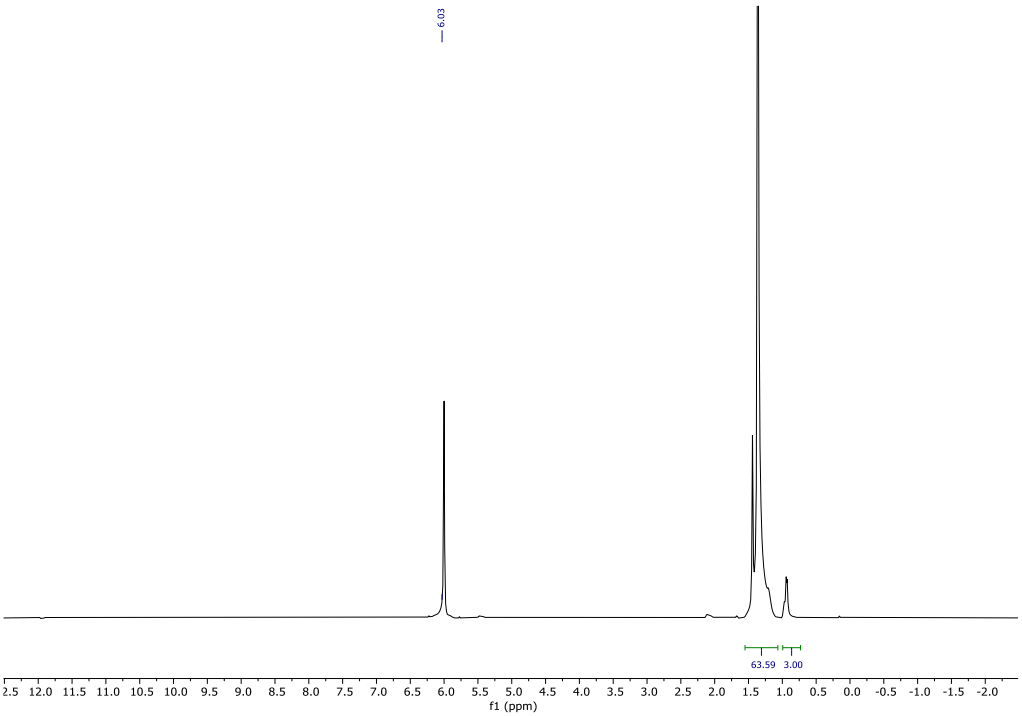

Figure S29. ^{1}H NMR Spectrum of polymer in entry 2, Table 2, 400 MHz (125 °C, $C_2D_2Cl_4$).

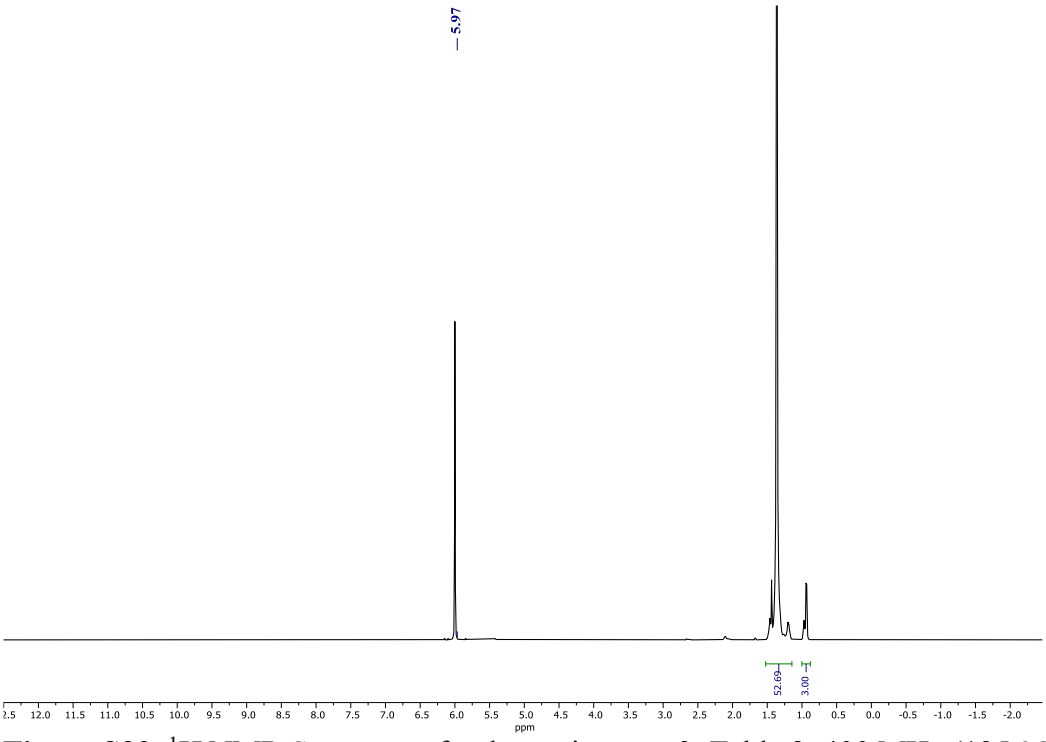

Figure S30. ^{1}H NMR Spectrum of polymer in entry 3, Table 2, 400 MHz (125 °C, $C_2D_2Cl_4$).

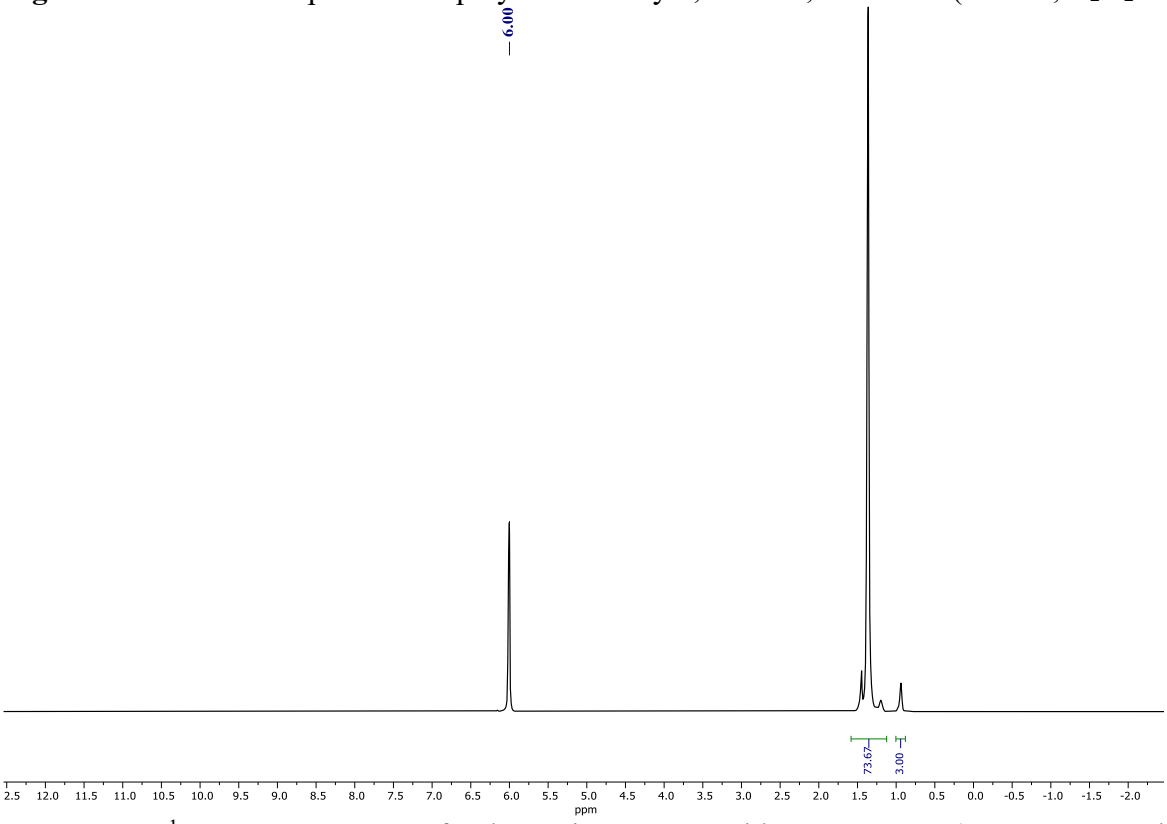

Figure S31. ^{1}H NMR Spectrum of polymer in entry 4, Table 2, 400 MHz (125 °C, $C_2D_2Cl_4$).

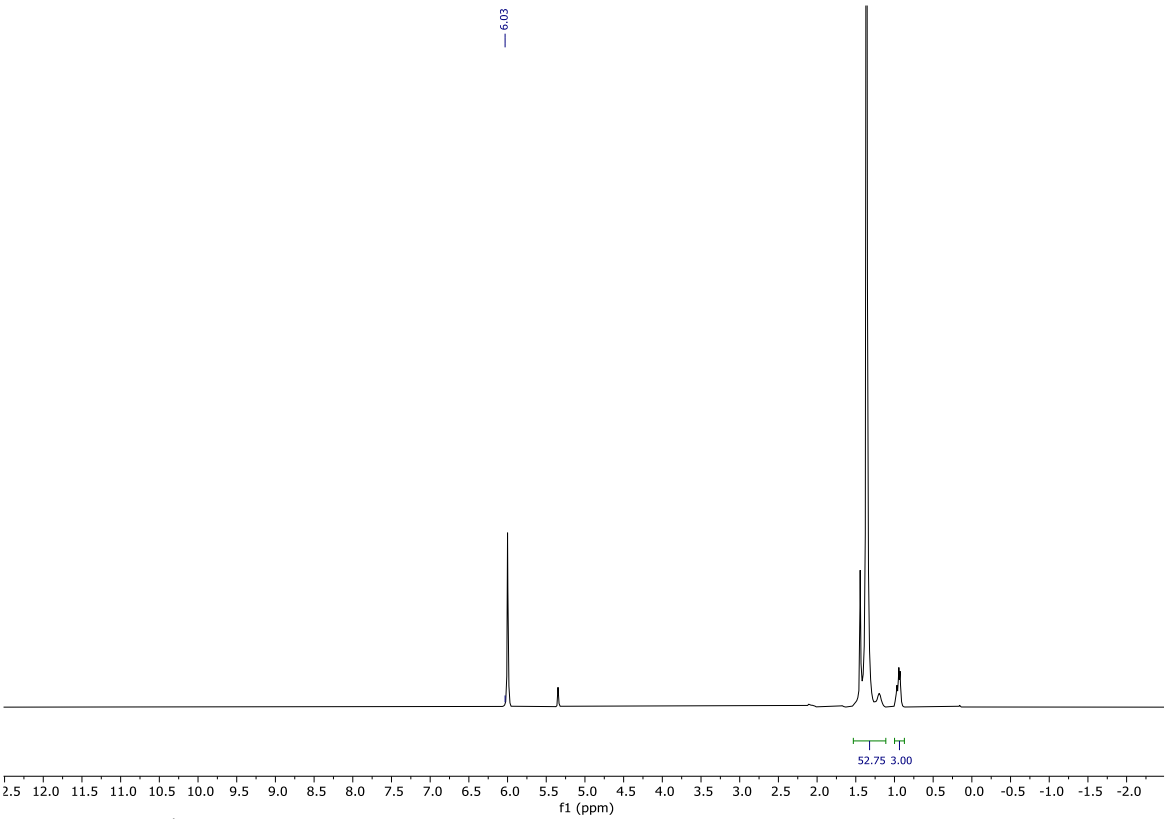

Figure S32. ^{1}H NMR Spectrum of polymer in entry 5, Table 2, 400 MHz (125 °C, $C_2D_2Cl_4$).

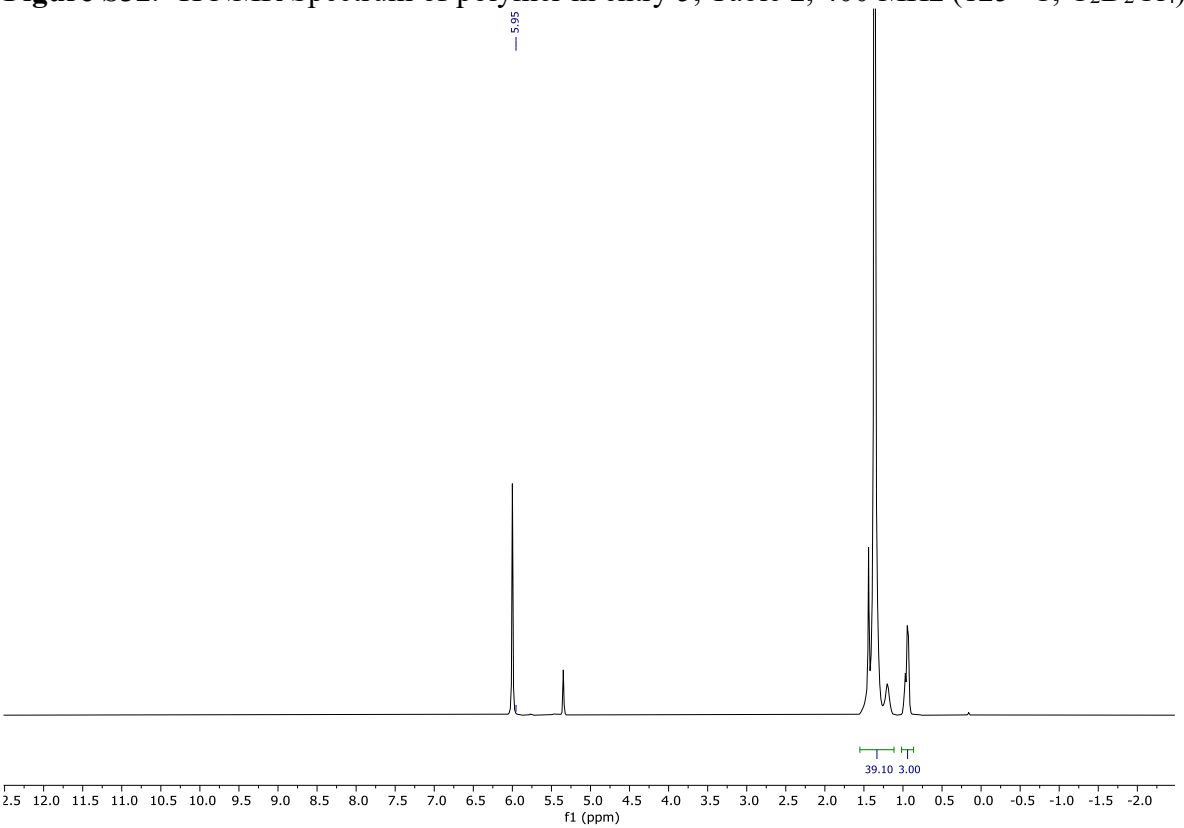

Figure S33. ^{1}H NMR Spectrum of polymer in entry 6, Table 2, 400 MHz (125 °C, $C_2D_2Cl_4$).

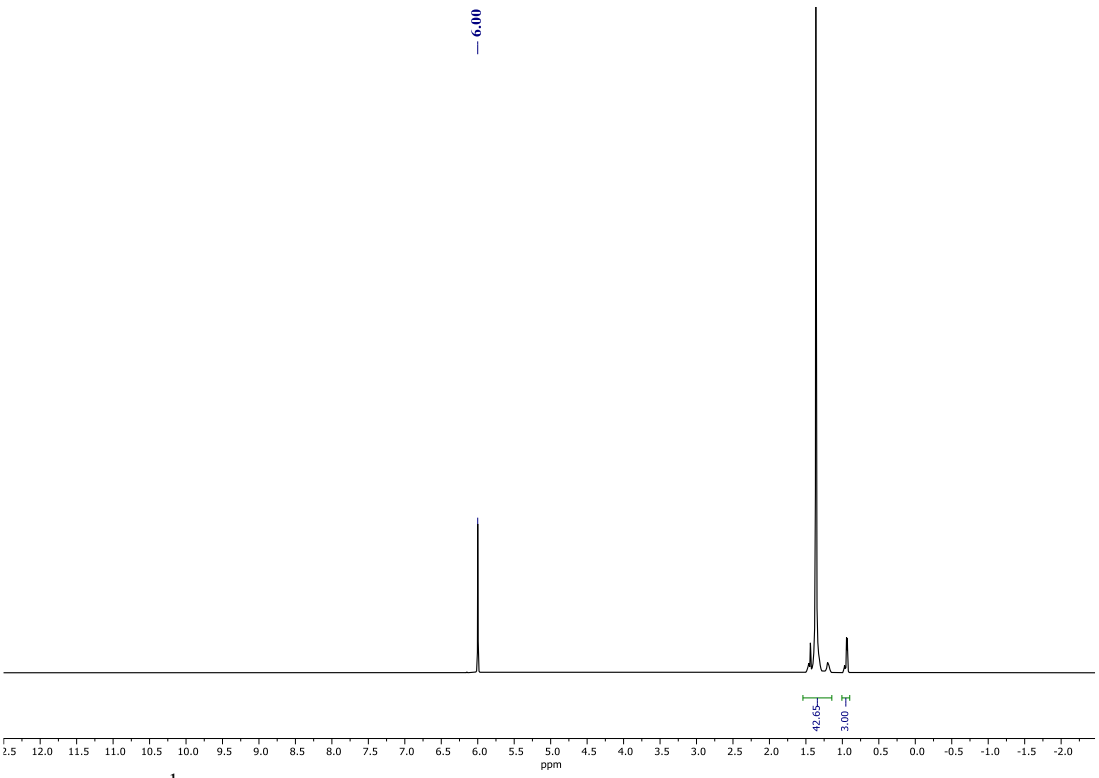

Figure S34. ^{1}H NMR Spectrum of polymer in entry 7, Table 2, 400 MHz (125 °C, $C_2D_2Cl_4$).

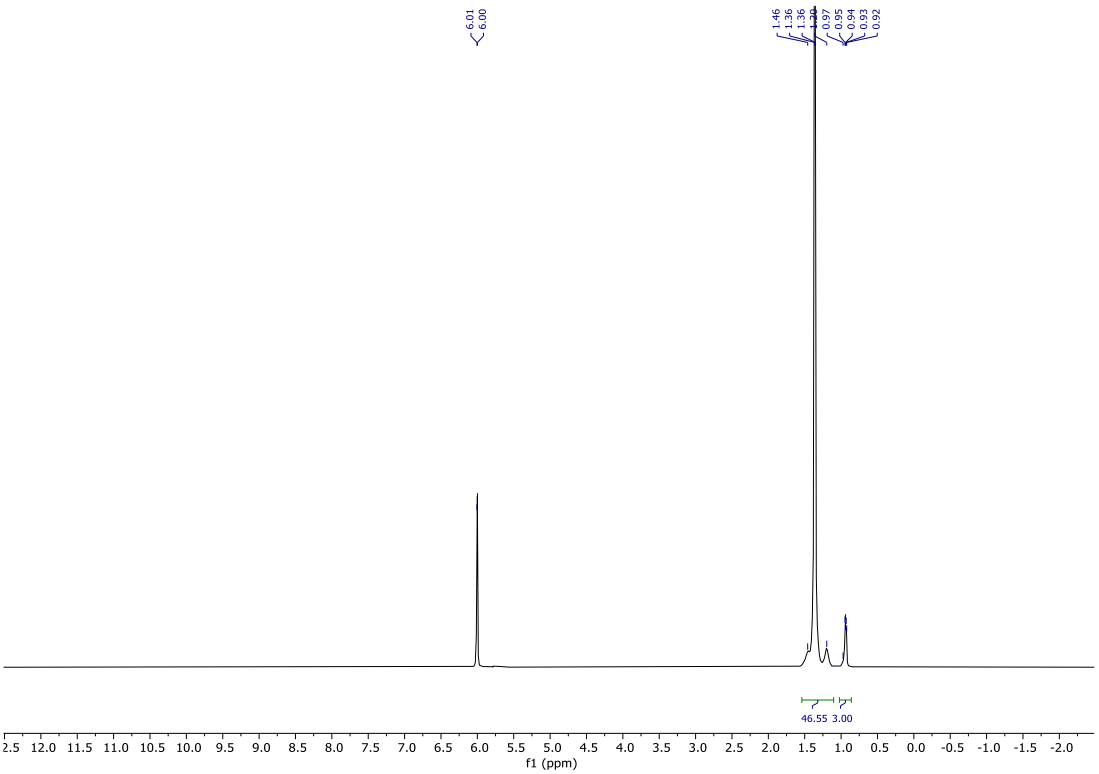

Figure S35. ^{1}H NMR Spectrum of polymer in entry 8, Table 2, 400 MHz (125 °C, $C_2D_2Cl_4$).

4.1.3 ^{1}H NMR of Polymers from Table 3

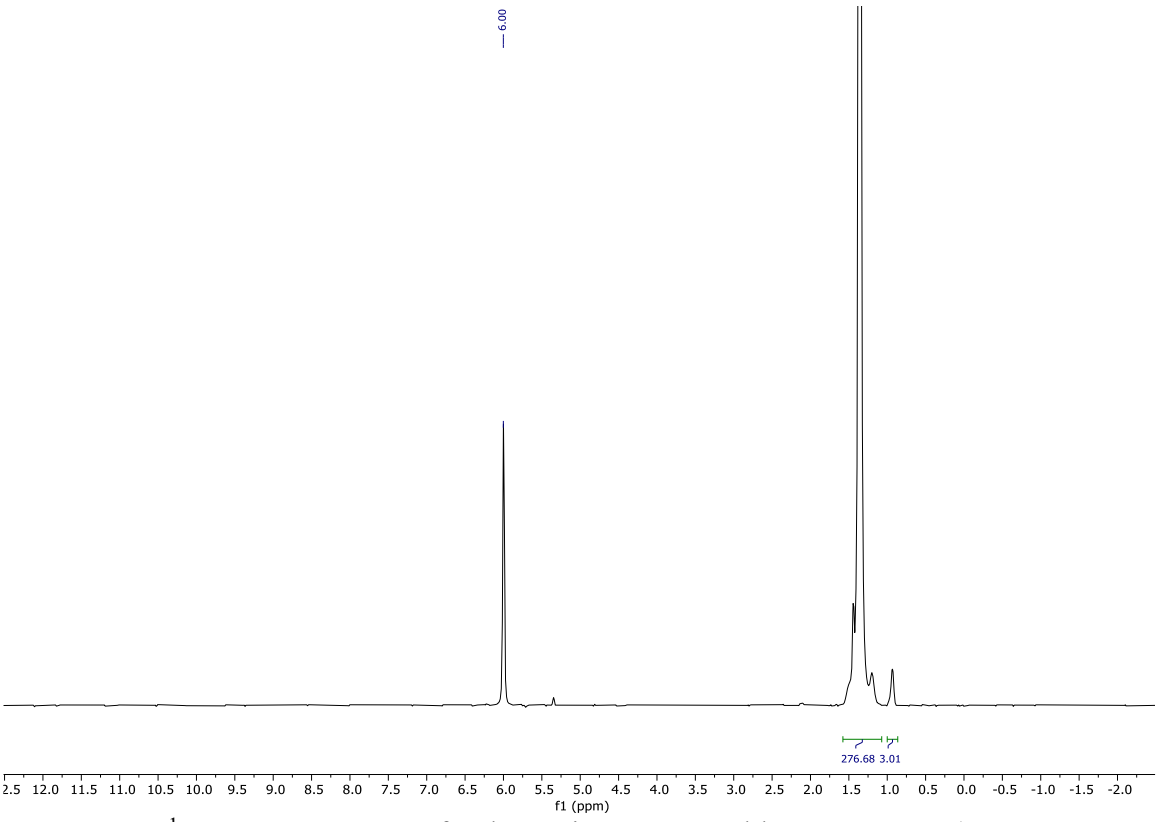

Figure S36. ^{1}H NMR Spectrum of polymer in entry 1, Table 3, 400 MHz (125 °C, $C_2D_2Cl_4$).

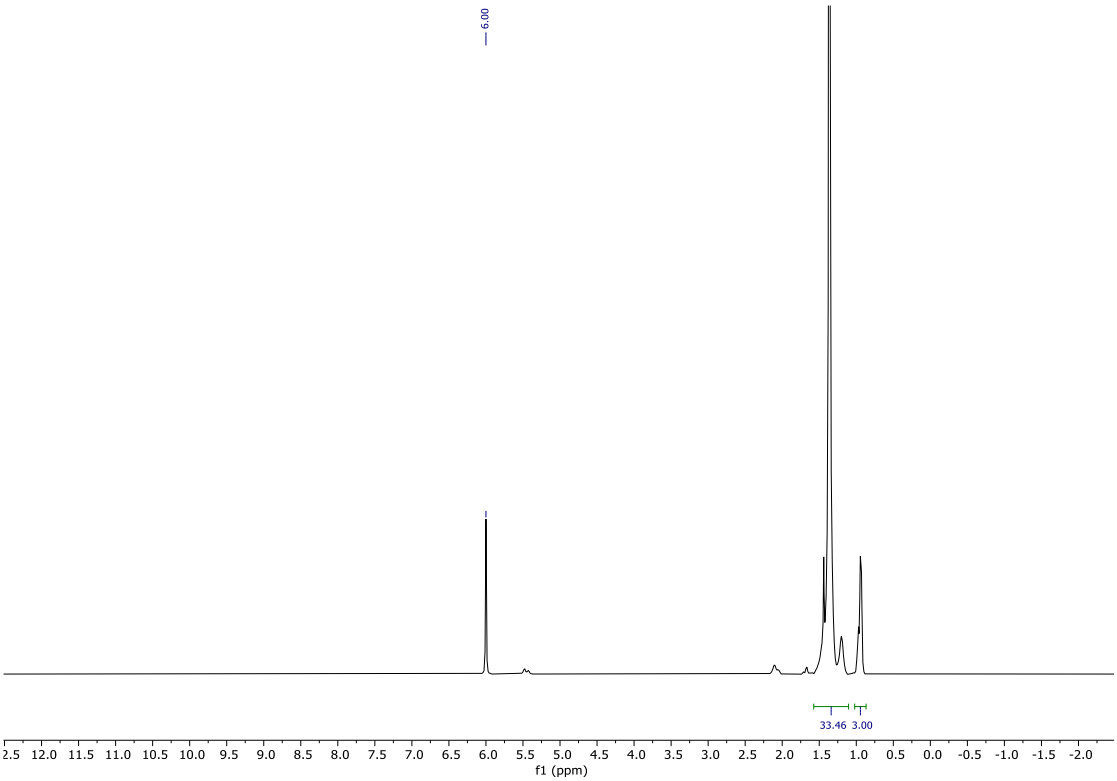

Figure S37. ^{1}H NMR Spectrum of polymer in entry 3, Table 3, 400 MHz (125 °C, $C_2D_2Cl_4$).

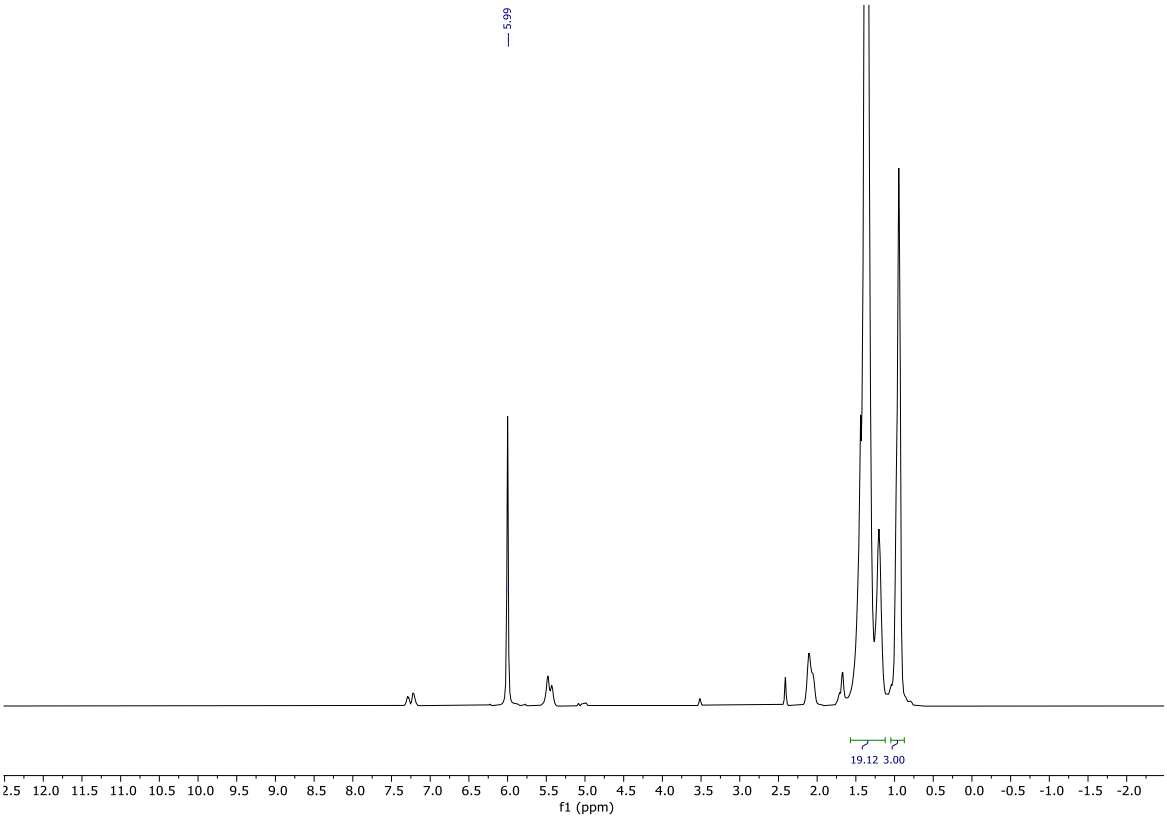

Figure S38. ^{1}H NMR Spectrum of polymer in entry 4, Table 3, 400 MHz (125 °C, $C_2D_2Cl_4$).

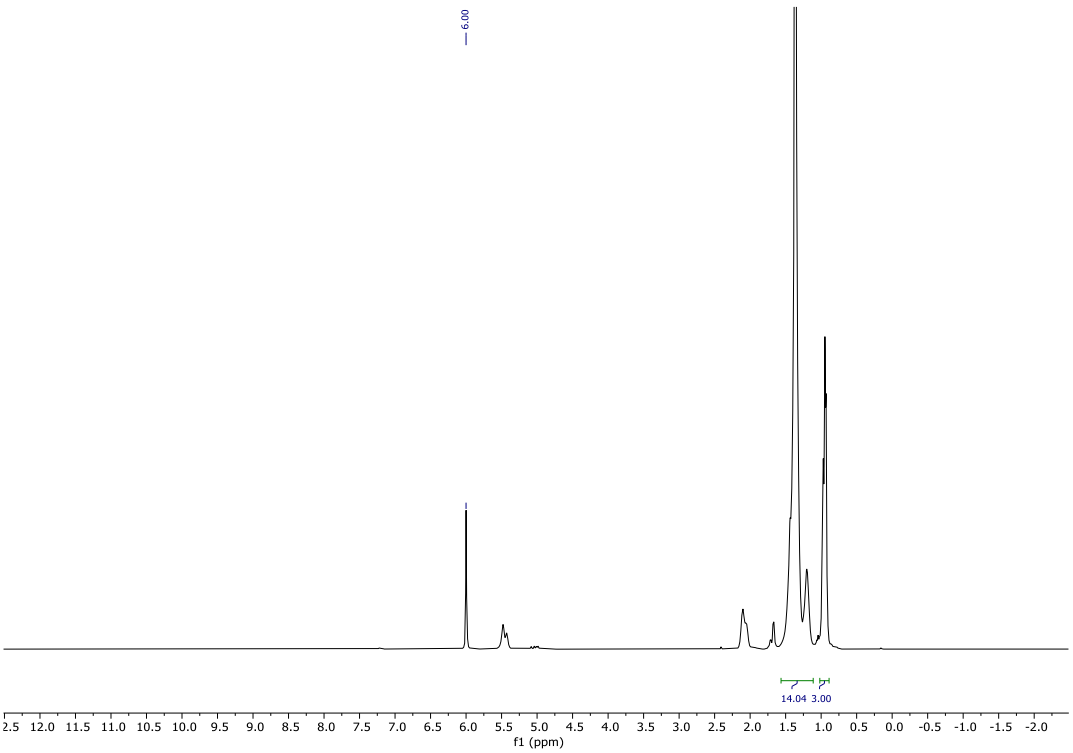

Figure S39. ^{1}H NMR Spectrum of polymer in entry 5, Table 3, 400 MHz (125 °C, $C_2D_2Cl_4$).

4.1.4 ^{1}H NMR of Polymers from Table 4

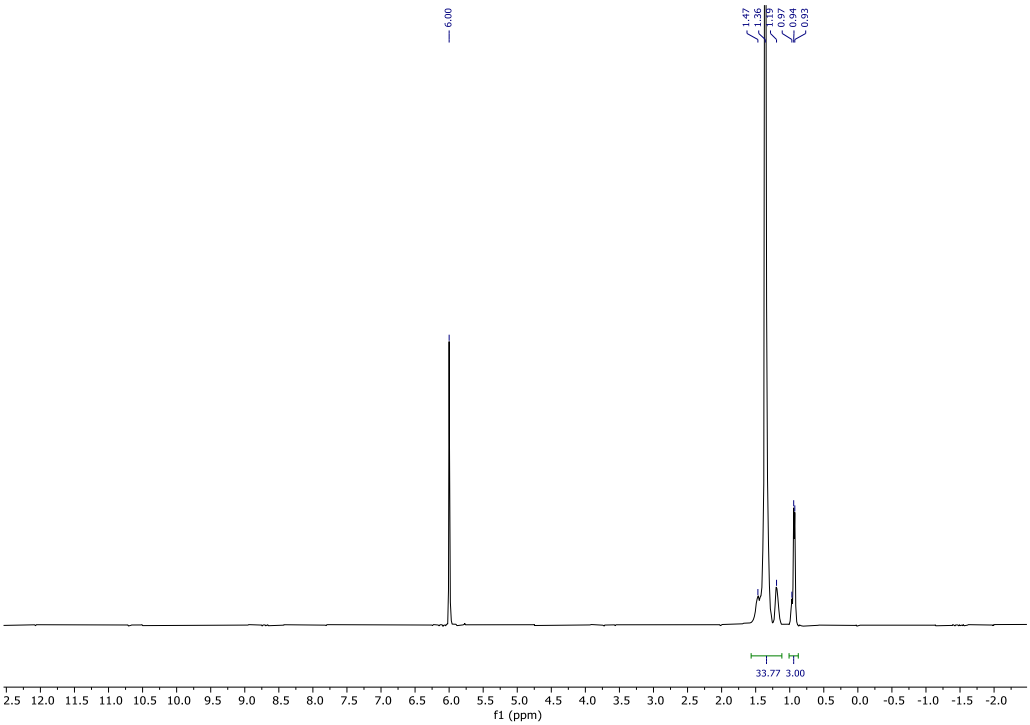

Figure S40. ^{1}H NMR Spectrum of polymer in entry 1, Table 4, 400 MHz (125 °C, $C_2D_2Cl_4$).

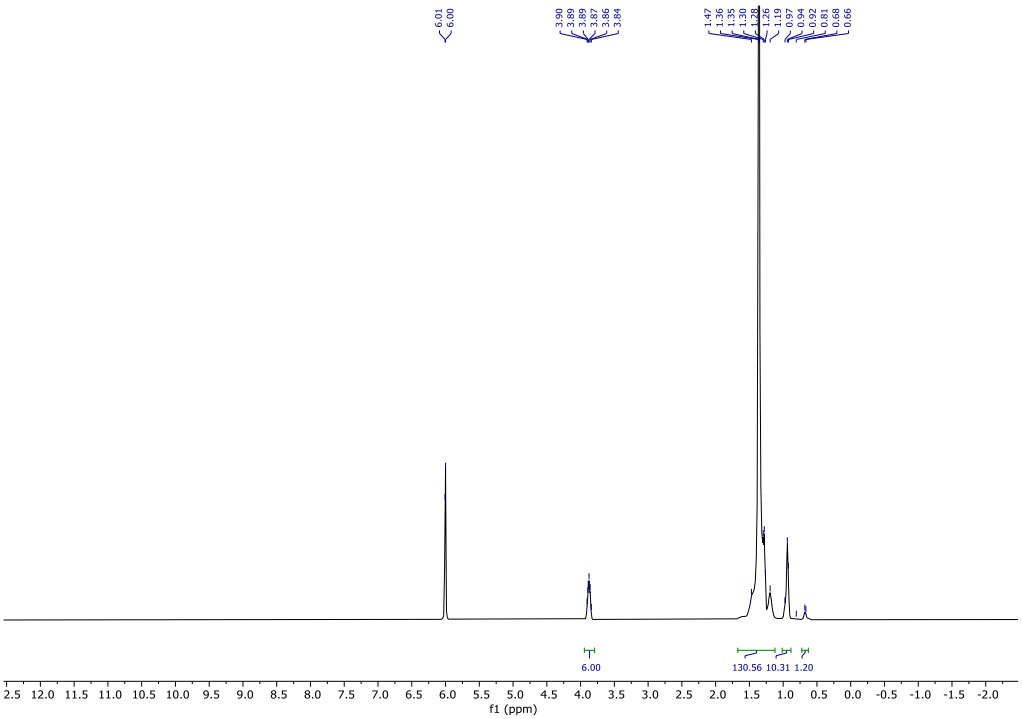

Figure S41. ^{1}H NMR Spectrum of polymer in entry 2, Table 4, 400 MHz (125 °C, $C_2D_2Cl_4$).

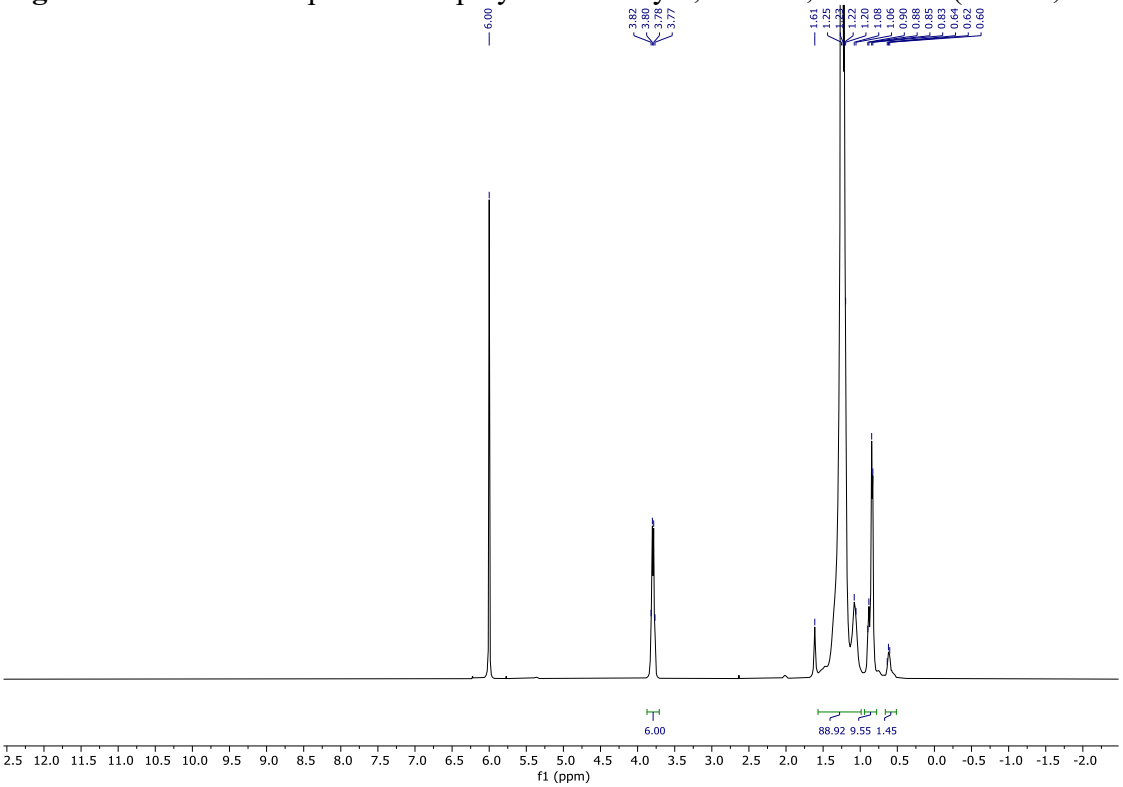

Figure S42. ^{1}H NMR Spectrum of polymer in entry 3, Table 4, 400 MHz (125 °C, $C_2D_2Cl_4$).

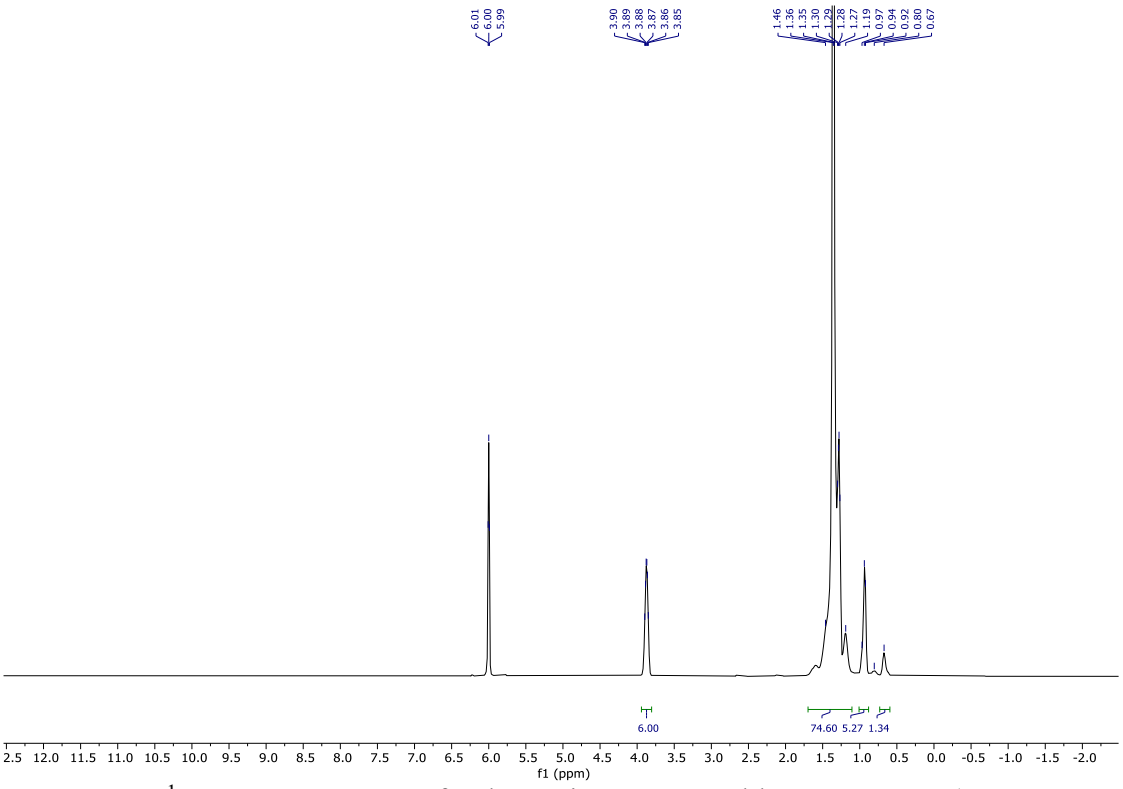

Figure S43. ^{1}H NMR Spectrum of polymer in entry 4, Table 4, 400 MHz (125 °C, $C_2D_2Cl_4$).

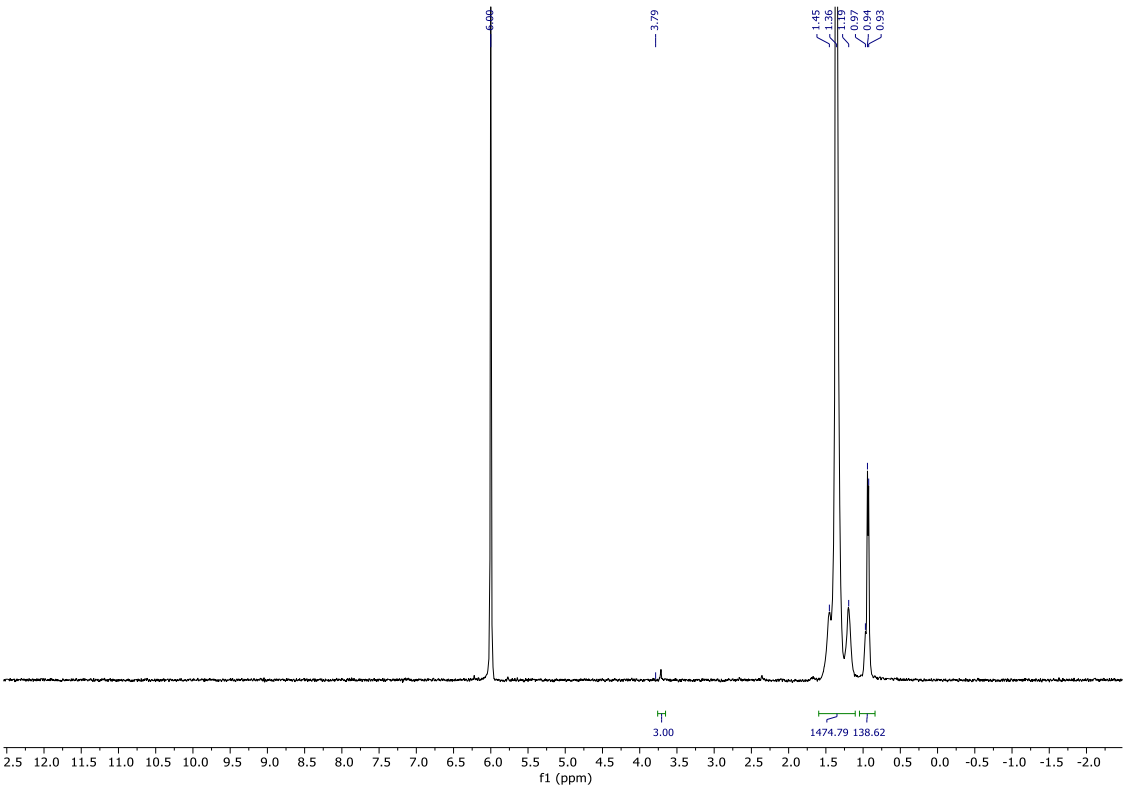

Figure S44. ^{1}H NMR Spectrum of polymer in entry 5, Table 4, 400 MHz (125 °C, $C_2D_2Cl_4$).

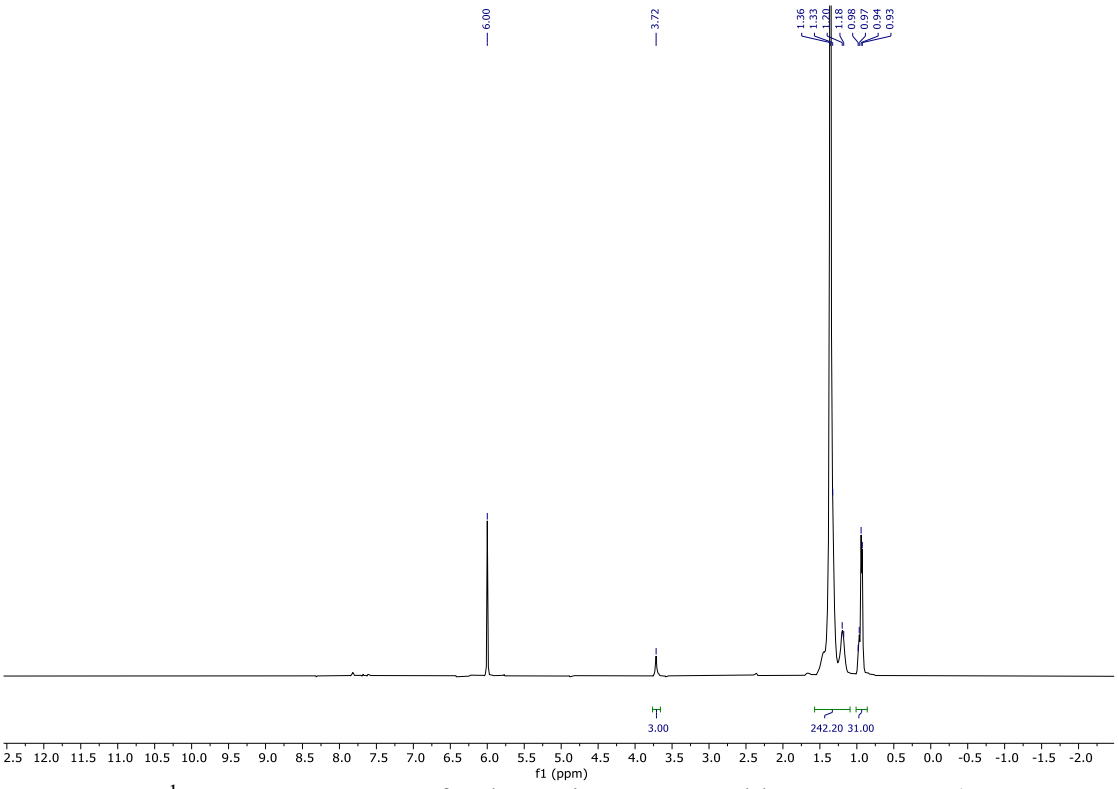

Figure S45. ^{1}H NMR Spectrum of polymer in entry 6, Table 4, 400 MHz (125 °C, $C_2D_2Cl_4$).

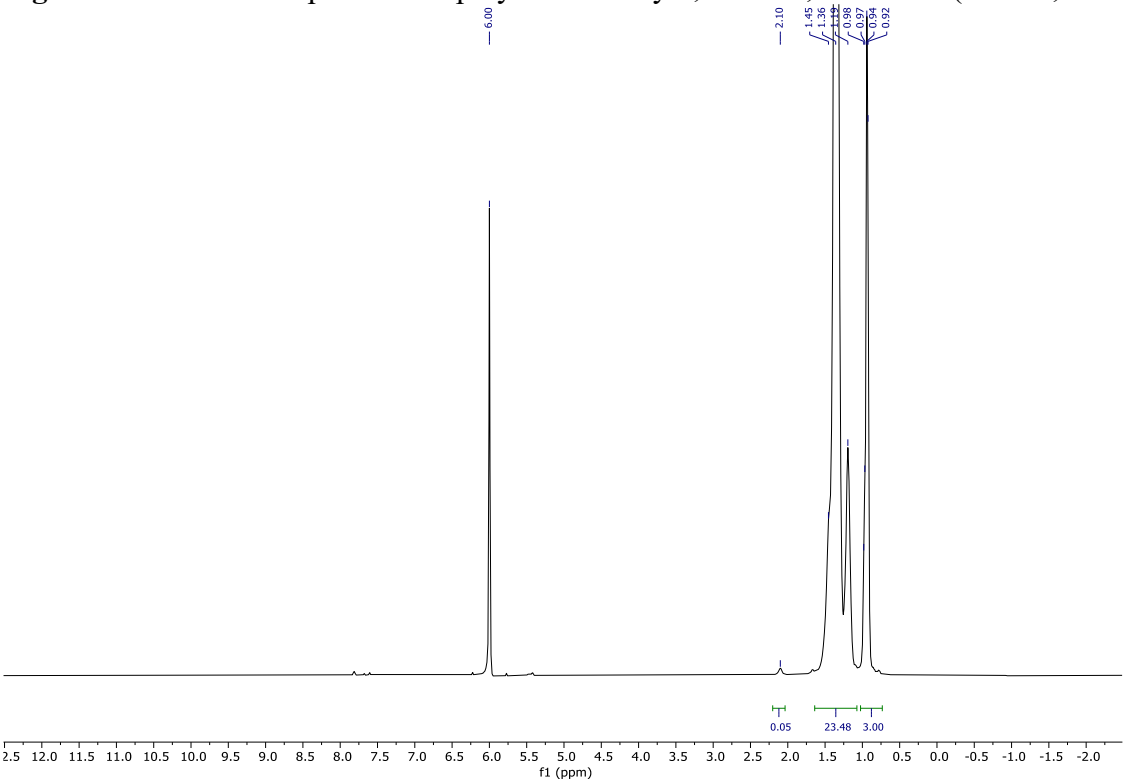

Figure S46. ^{1}H NMR Spectrum of polymer in entry 7, Table 4, 400 MHz (125 °C, $C_2D_2Cl_4$).

4.1.5 ^{1}H NMR of Polymers from Table S1

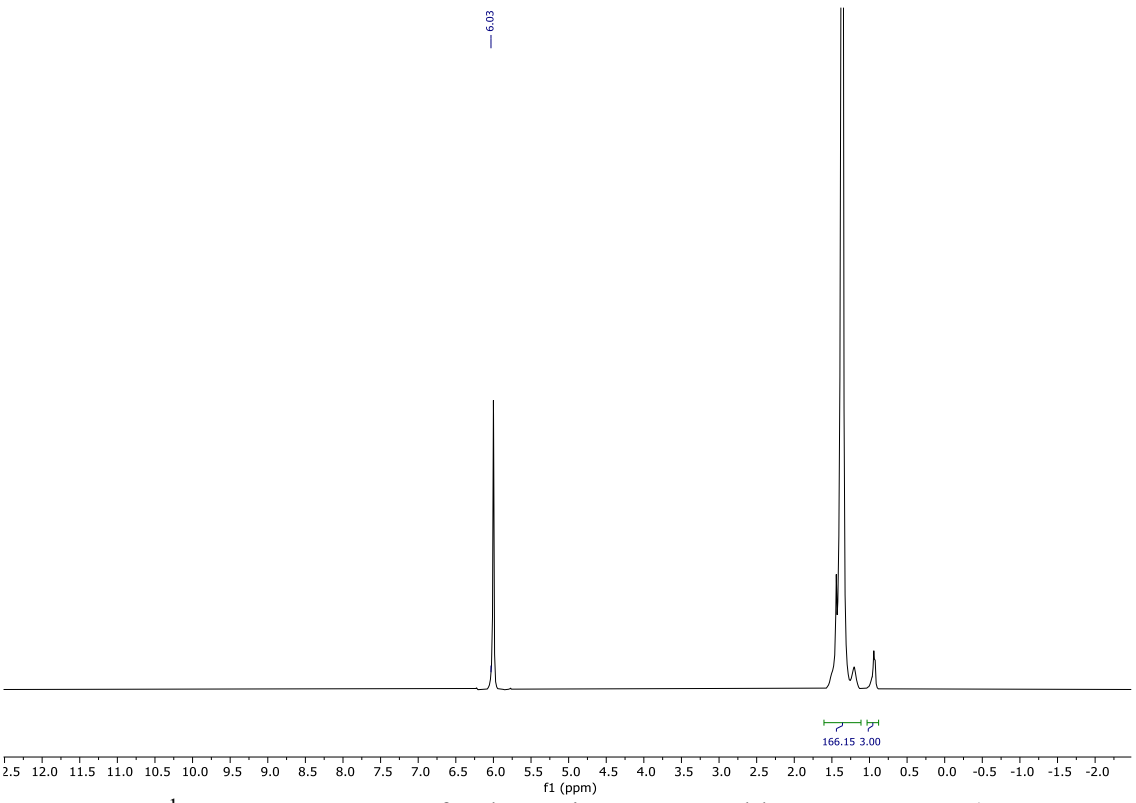

Figure S47. ^{1}H NMR Spectrum of polymer in entry 1, Table S1, 400 MHz (125 °C, $C_2D_2Cl_4$).

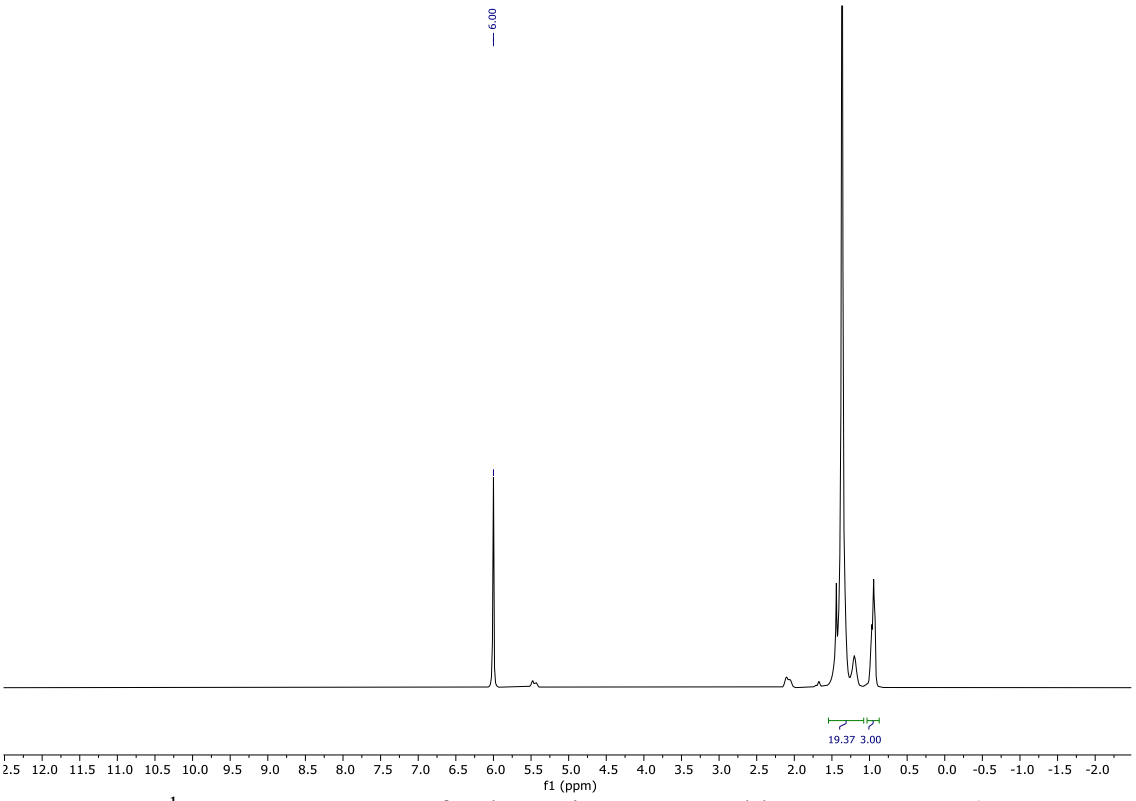

Figure S48. ^{1}H NMR Spectrum of polymer in entry 2, Table S1, 400 MHz (125 °C, $C_2D_2Cl_4$).

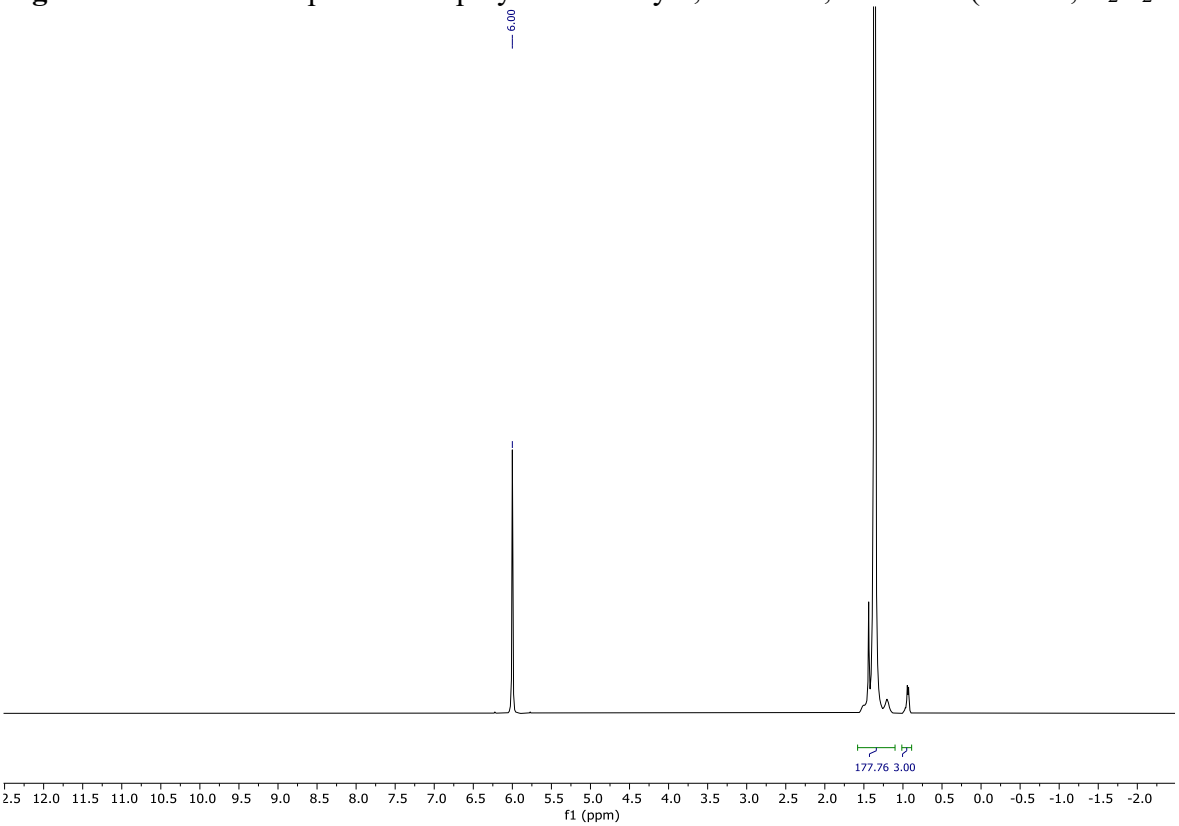

Figure S49. ^{1}H NMR Spectrum of polymer in entry 3, Table S1, 400 MHz (125 °C, $C_2D_2Cl_4$).

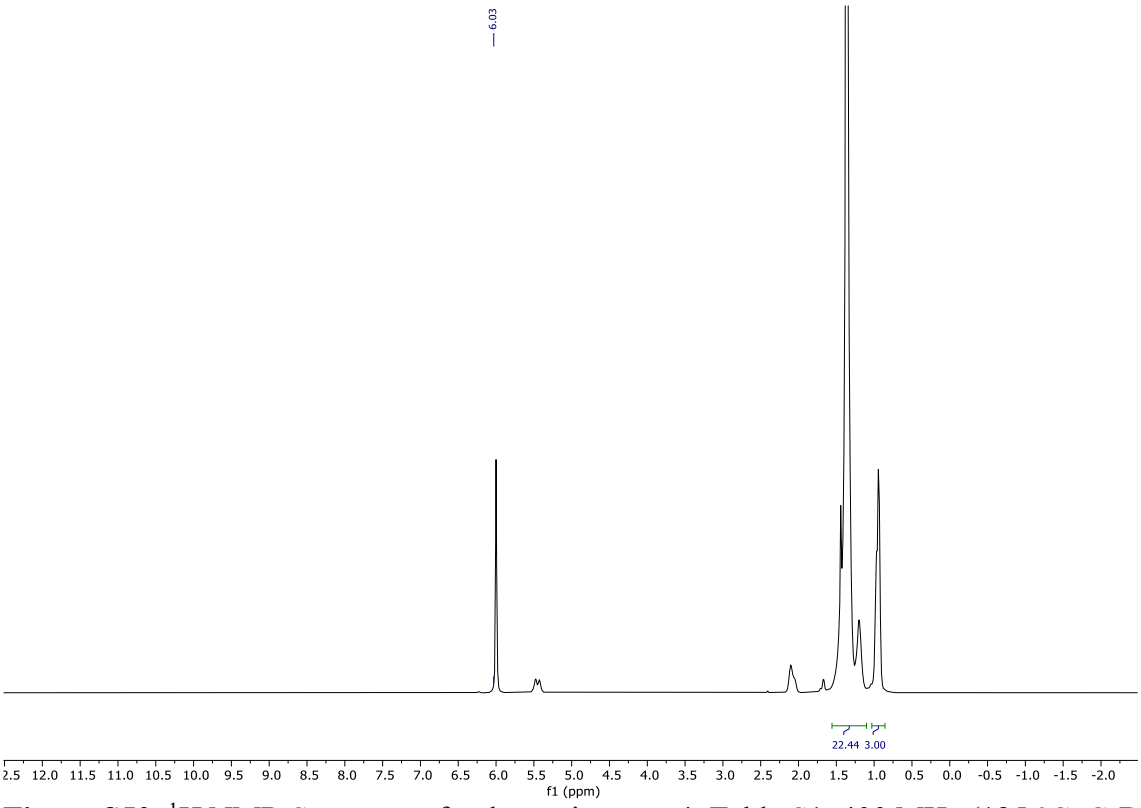

Figure S50. ^{1}H NMR Spectrum of polymer in entry 4, Table S1, 400 MHz (125 °C, $C_2D_2Cl_4$).

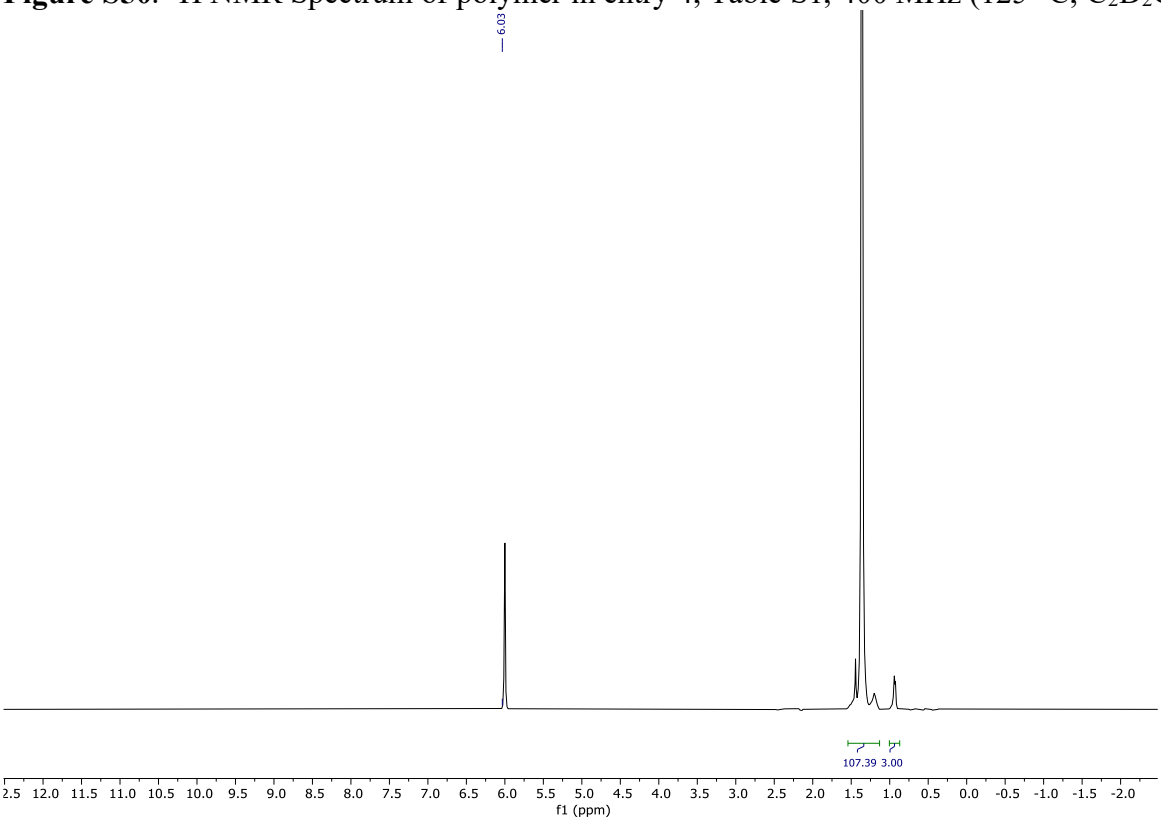

Figure S51. ^{1}H NMR Spectrum of polymer in entry 5, Table S1, 400 MHz (125 °C, $C_2D_2Cl_4$).

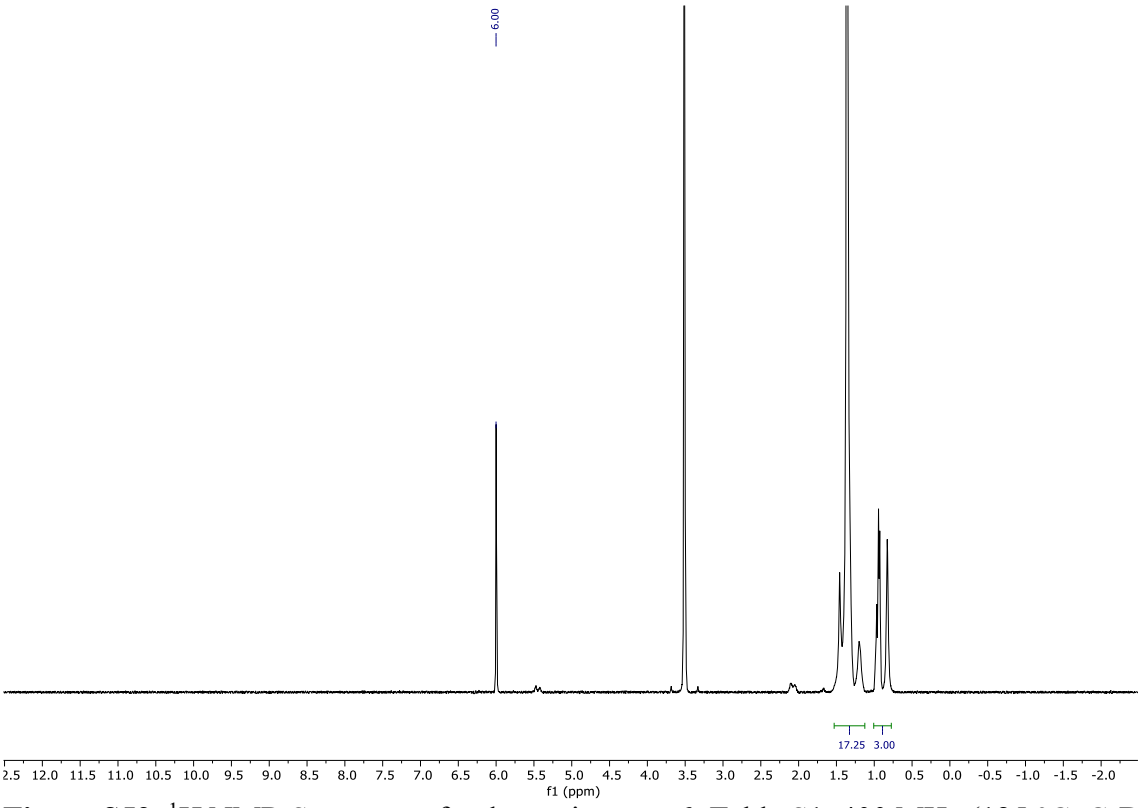

Figure S52. ^{1}H NMR Spectrum of polymer in entry 6, Table S1, 400 MHz (125 °C, $C_2D_2Cl_4$).

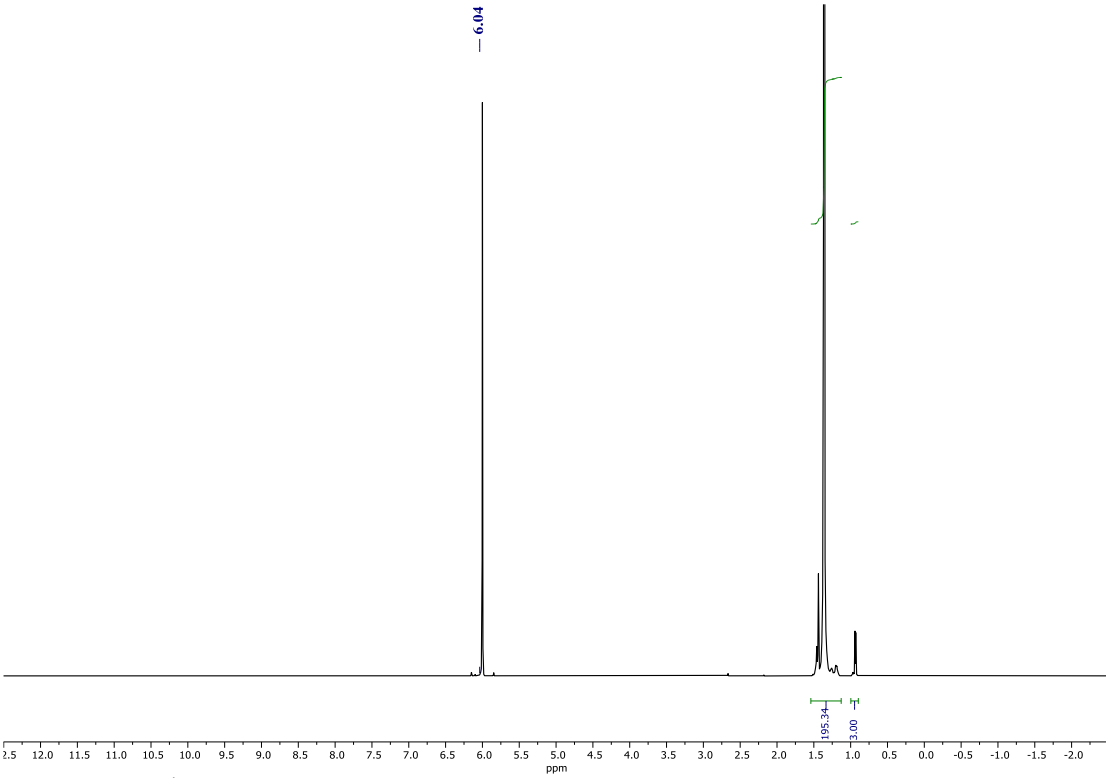

Figure S53. ^{1}H NMR Spectrum of polymer in entry 7, Table S1, 400 MHz (125 °C, $C_2D_2Cl_4$).

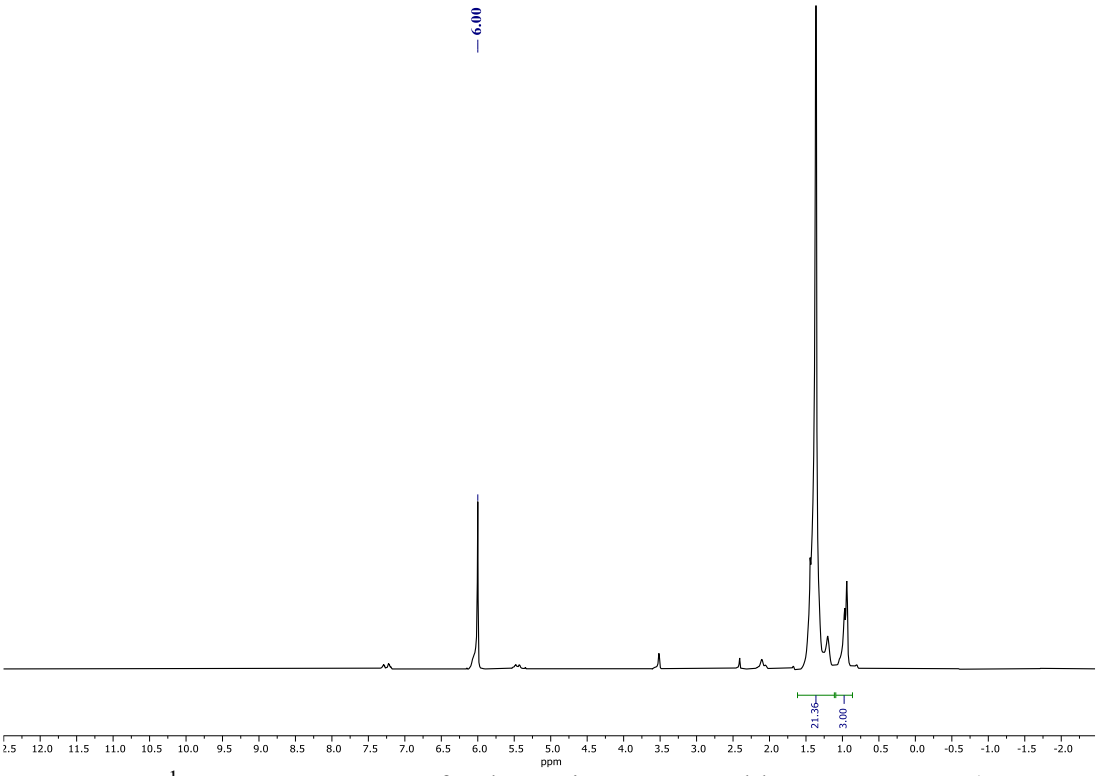

Figure S54. ^{1}H NMR Spectrum of polymer in entry 8, Table S1, 400 MHz (125 °C, $C_2D_2Cl_4$).

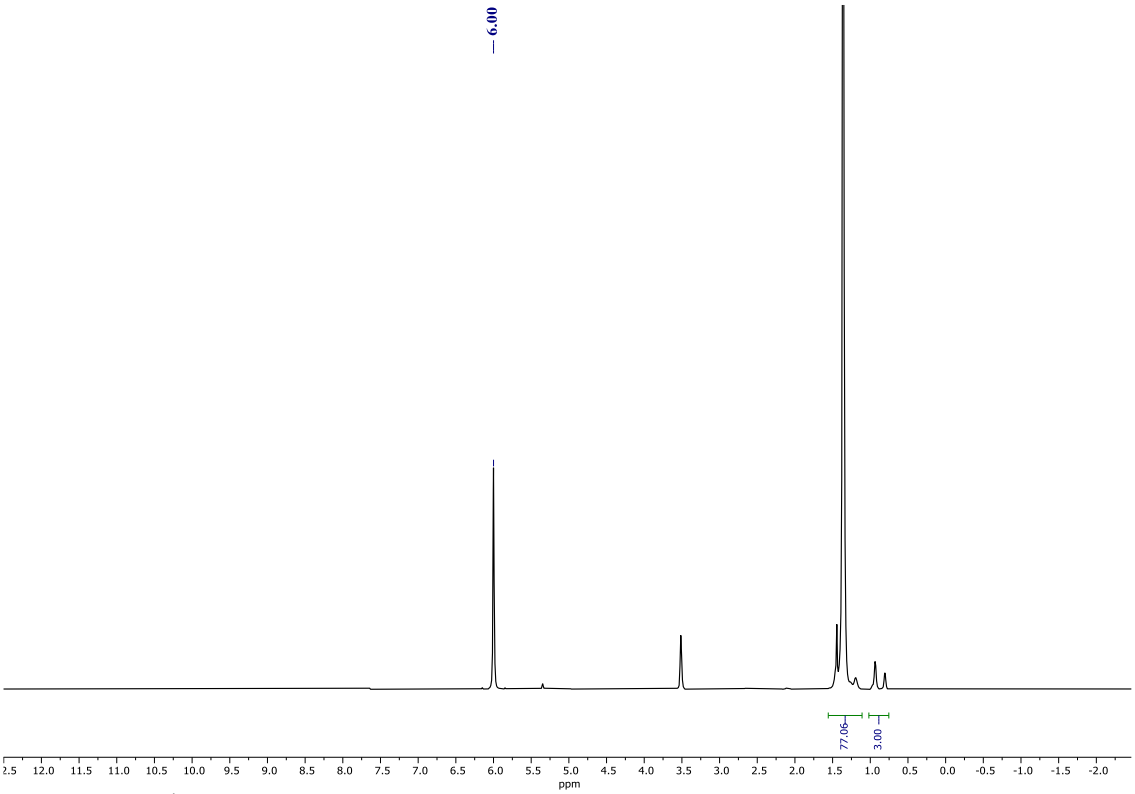

Figure S55. ^{1}H NMR Spectrum of polymer in entry 9, Table S1, 400 MHz (125 °C, $C_2D_2Cl_4$).

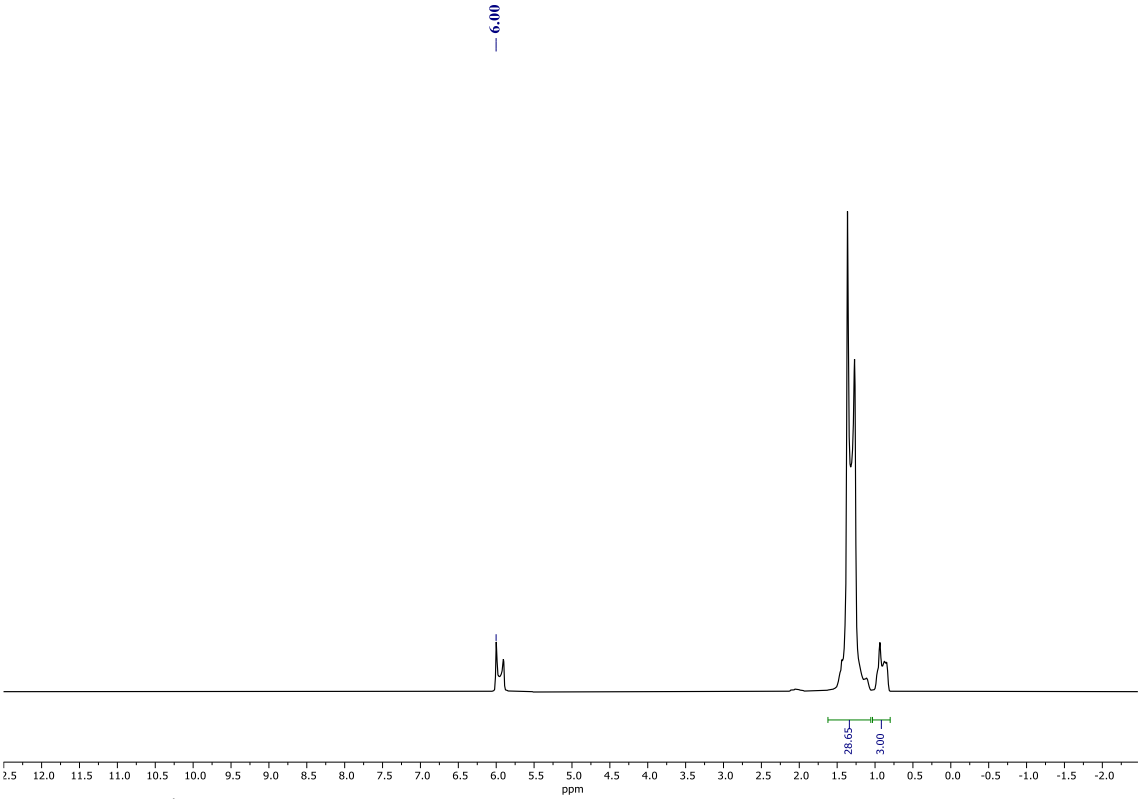

Figure S56. ^{1}H NMR Spectrum of polymer in entry 10, Table S1, 400 MHz (125 °C, $C_2D_2Cl_4$).

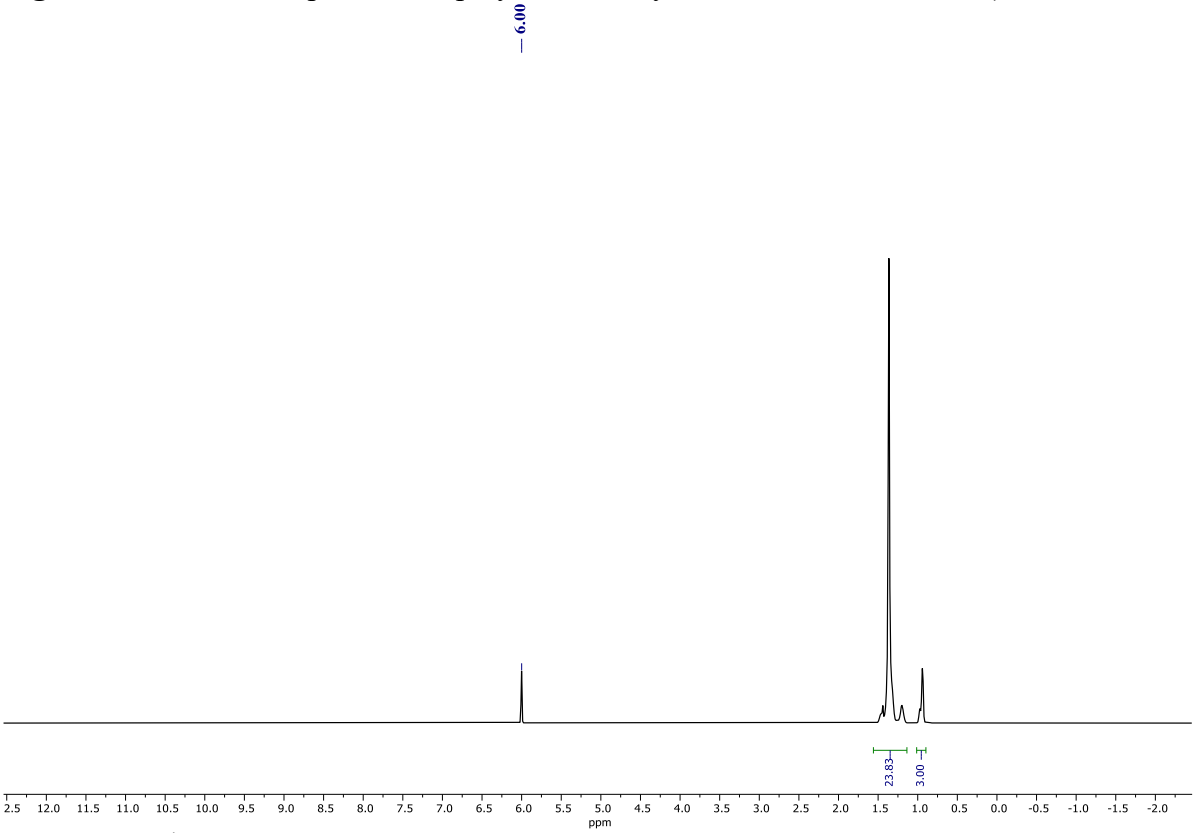

Figure S57. ^{1}H NMR Spectrum of polymer in entry 11, Table S1, 400 MHz (125 °C, $C_2D_2Cl_4$).

4.1.6 ^{13}C NMR of Polymers from Table 3

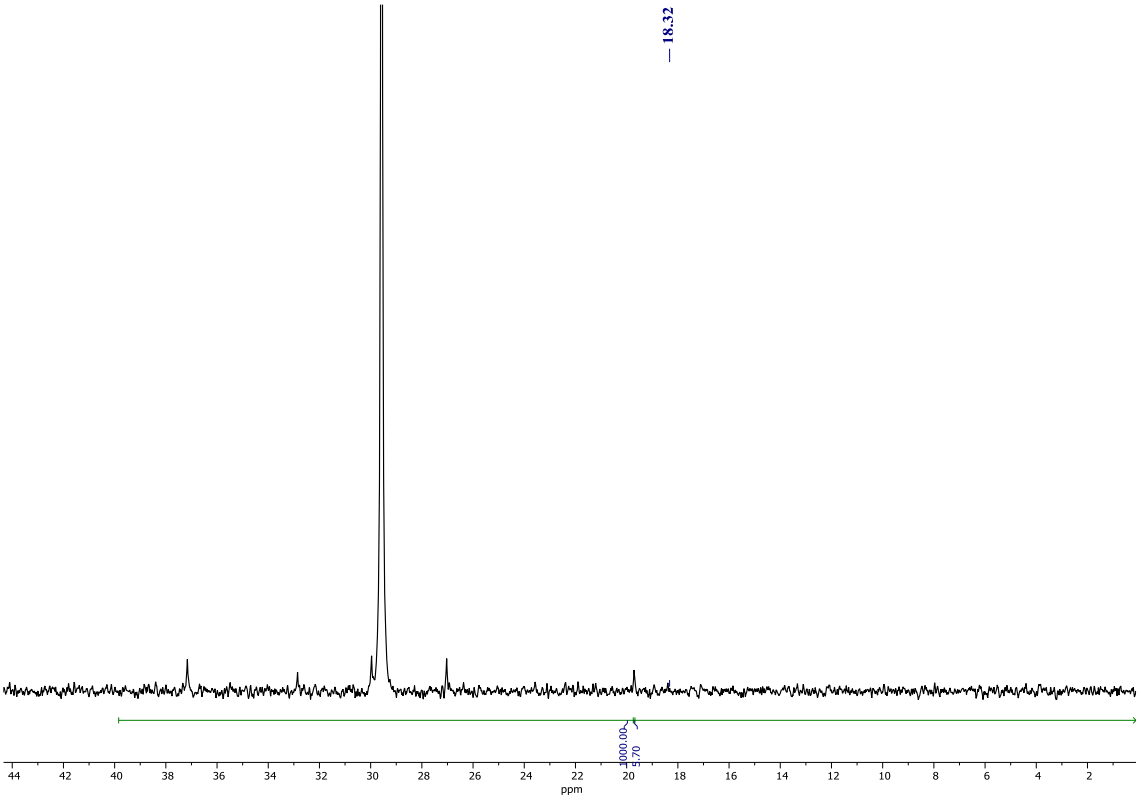

Figure S58. ^{13}C NMR Spectrum of polymer in entry 1, Table 3, 150 MHz (125 °C, $C_2D_2Cl_4$).

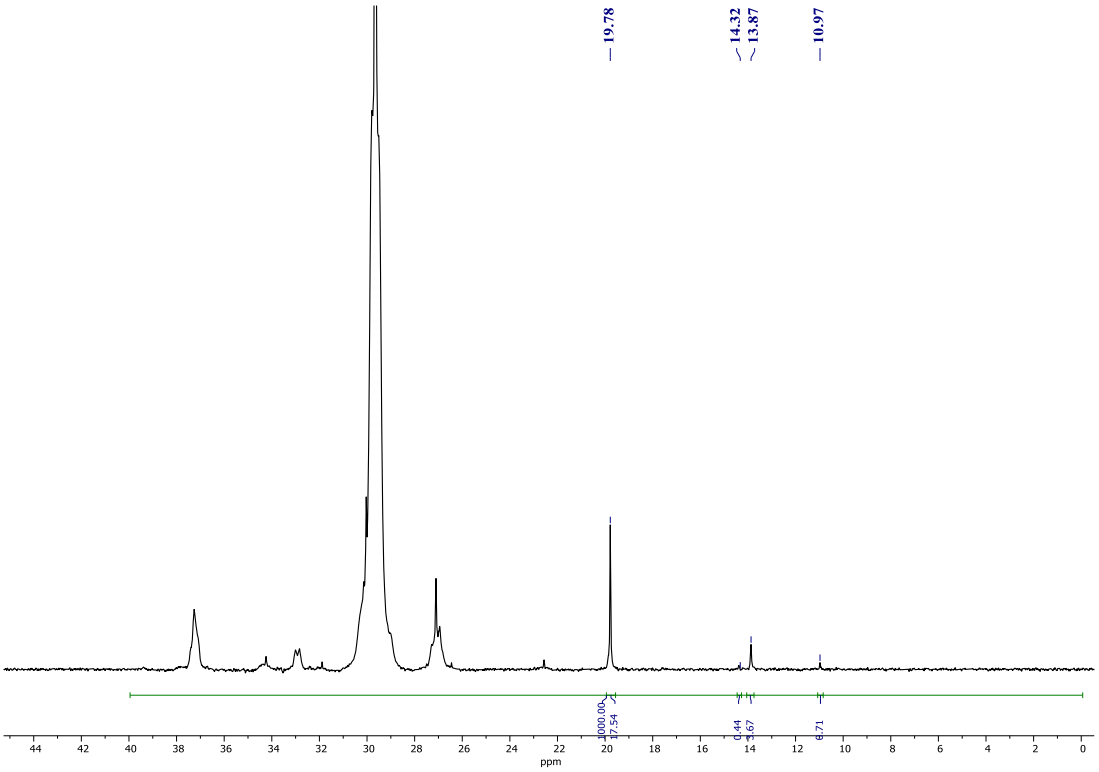

Figure S59. ^{13}C NMR Spectrum of polymer in entry 2, Table 3, 150 MHz (125 °C, $C_2D_2Cl_4$).

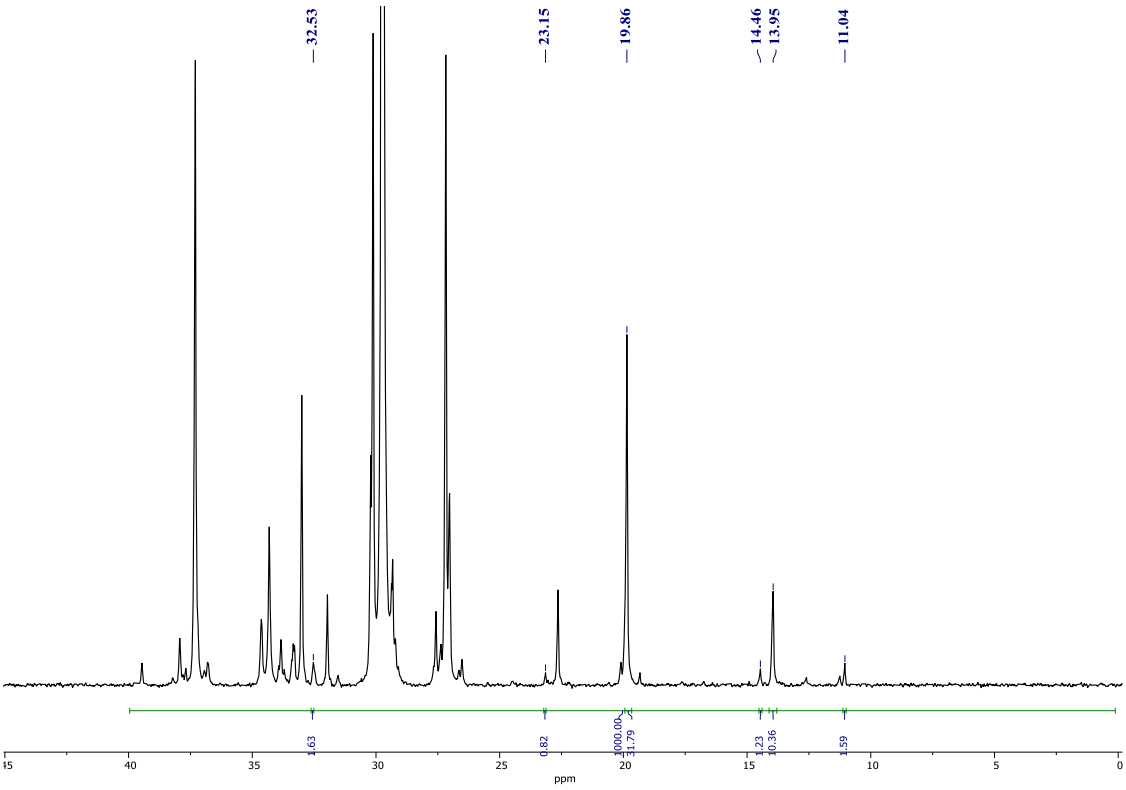

Figure S60. ^{13}C NMR Spectrum of polymer in entry 3, Table 3, 150 MHz (125 °C, $C_2D_2Cl_4$).

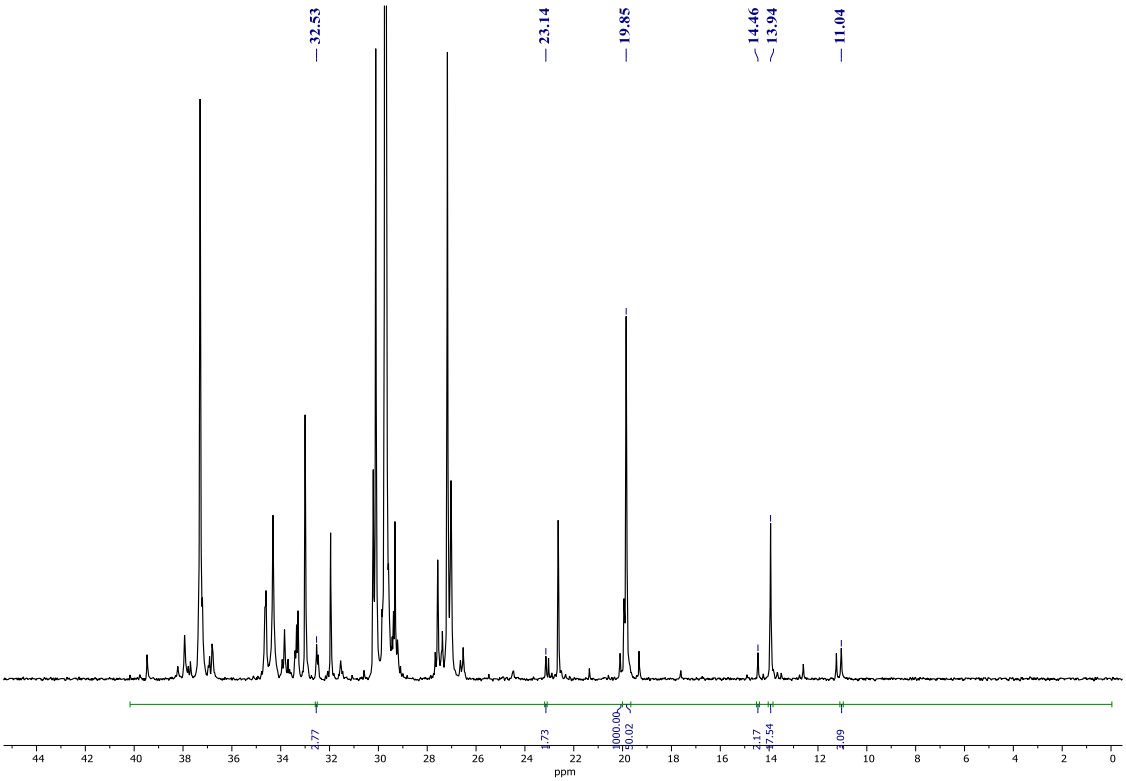

Figure S61. ^{13}C NMR Spectrum of polymer in entry 4, Table 3, 150 MHz (125 °C, $C_2D_2Cl_4$).

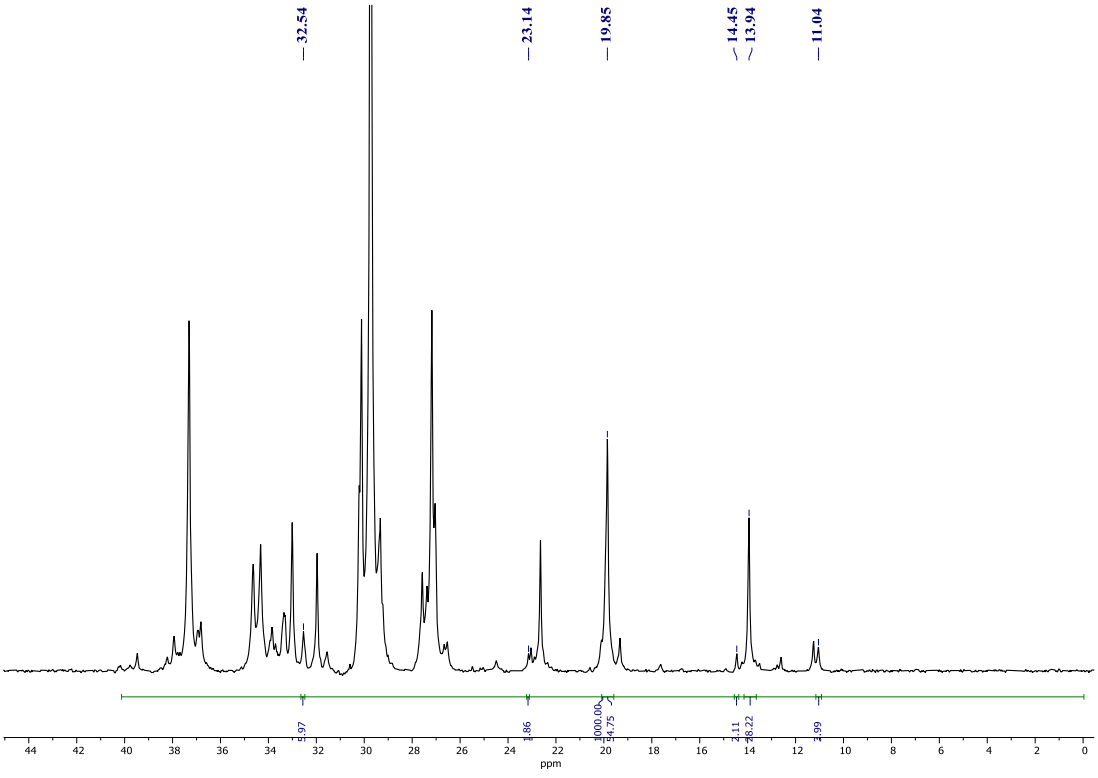

Figure S62. ^{13}C NMR Spectrum of polymer in entry 5, Table 3, 150 MHz (125 °C, $C_2D_2Cl_4$).

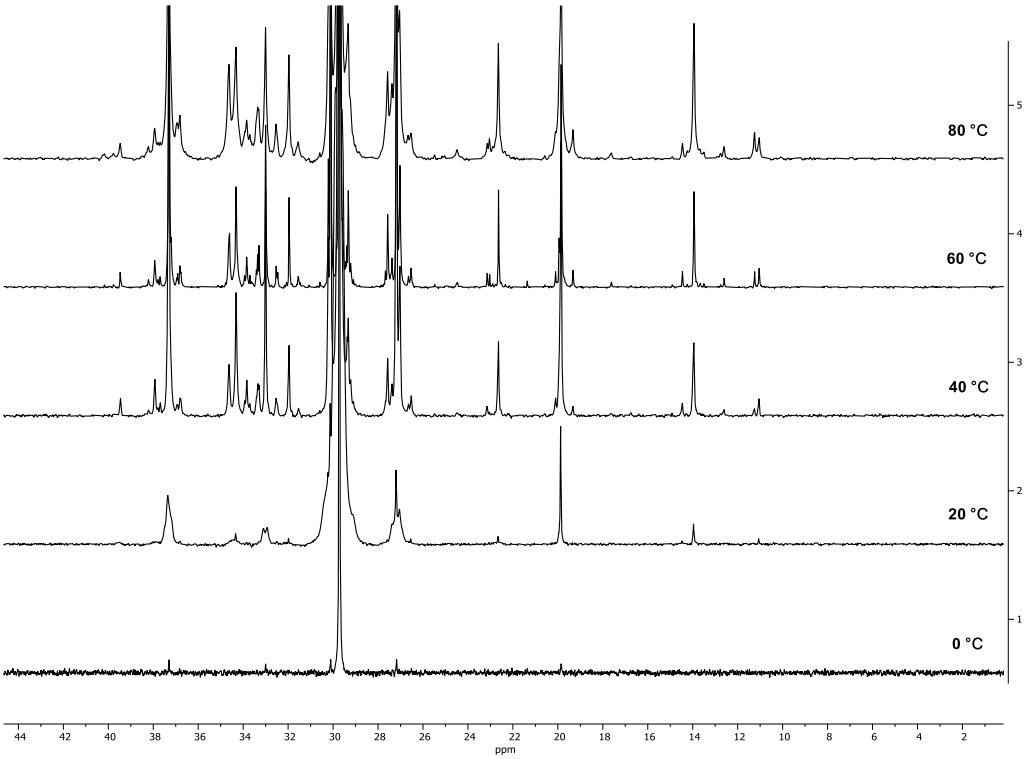

Figure S63. Stacked ^{13}C NMR Spectrum of polymer in entries 1-5, Table 3, 150 MHz (125 °C, $C_2D_2Cl_4$).

4.2 Gel Permeation Chromatography (GPC)

4.2.1 GPC Traces from Table 1

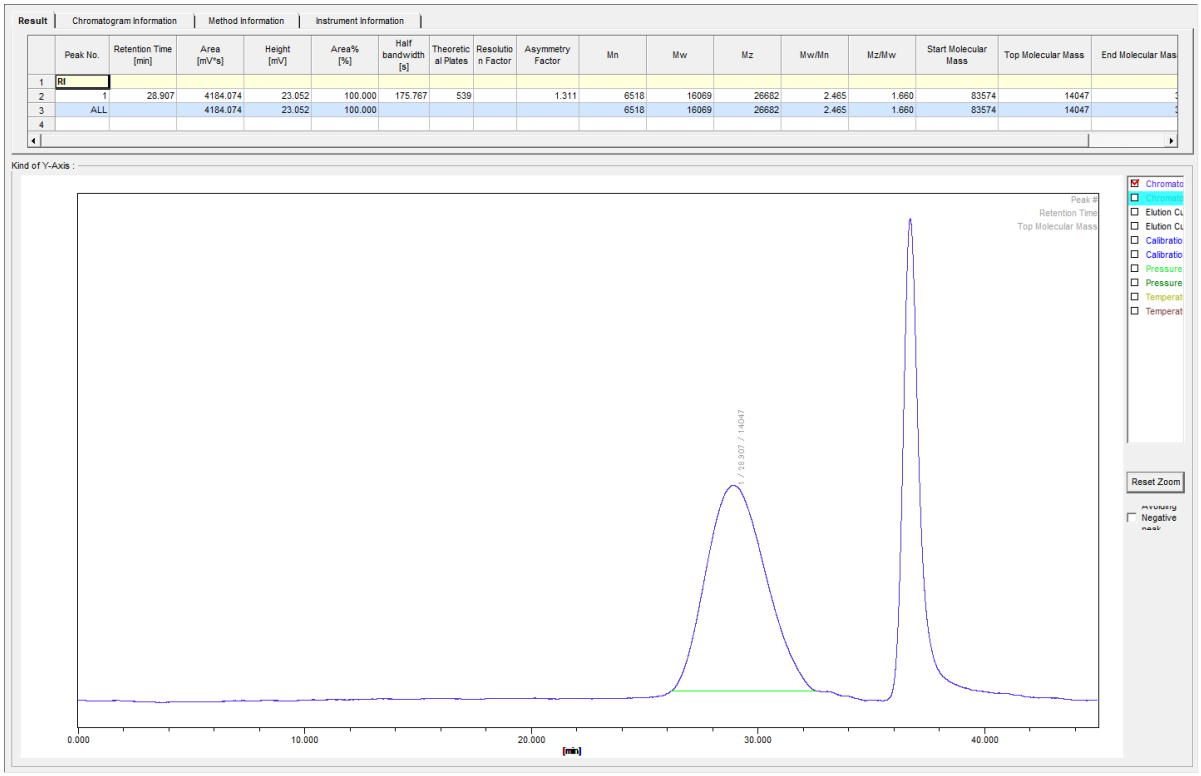

Figure S64. GPC of polymer in entry 1, Table 1.

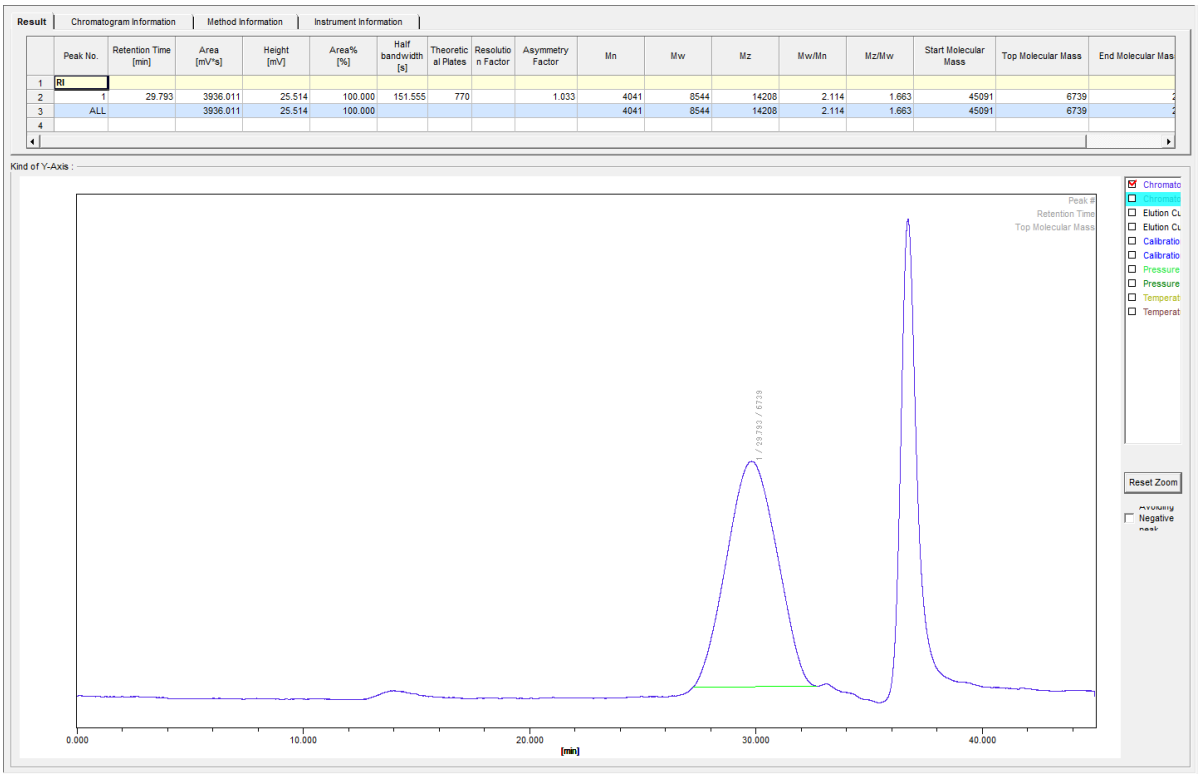

Figure S65. GPC of polymer in entry 2, Table 1.

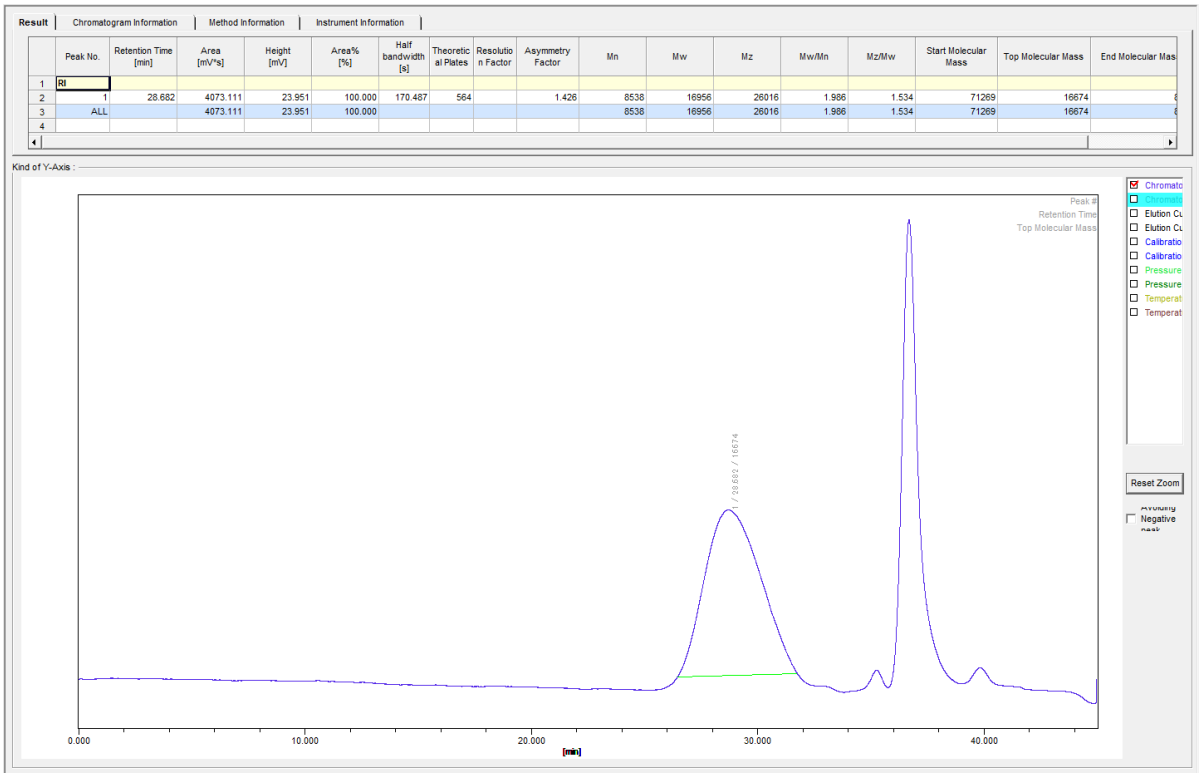

Figure S66. GPC of polymer in entry 3, Table 1.

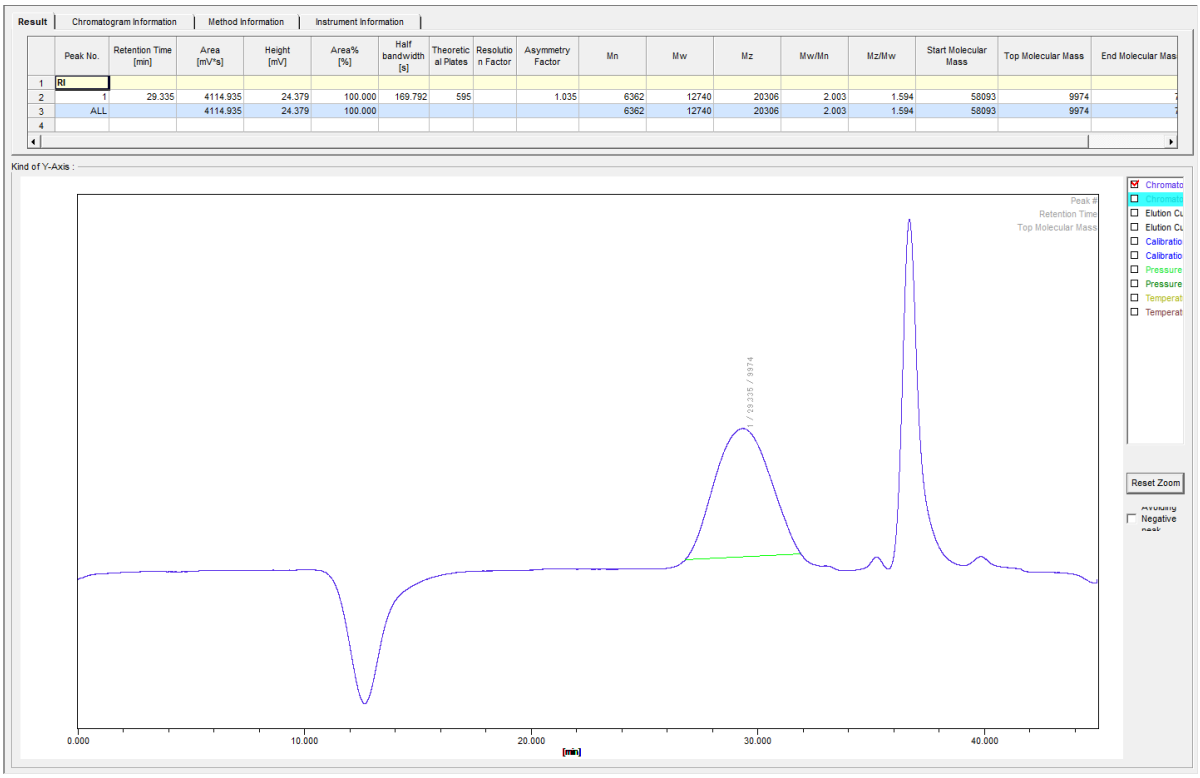

Figure S67. GPC of polymer in entry 4, Table 1.

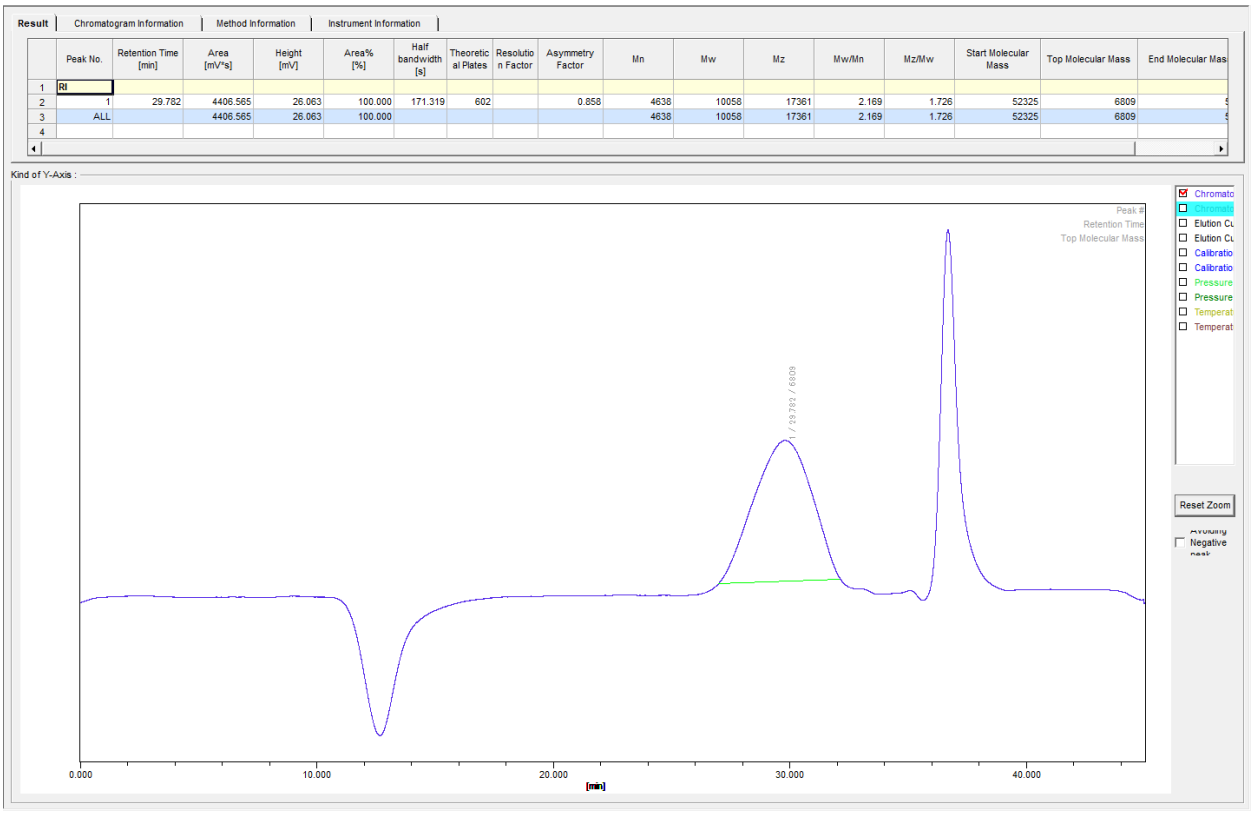

Figure S68. GPC of polymer in entry 5, Table 1.

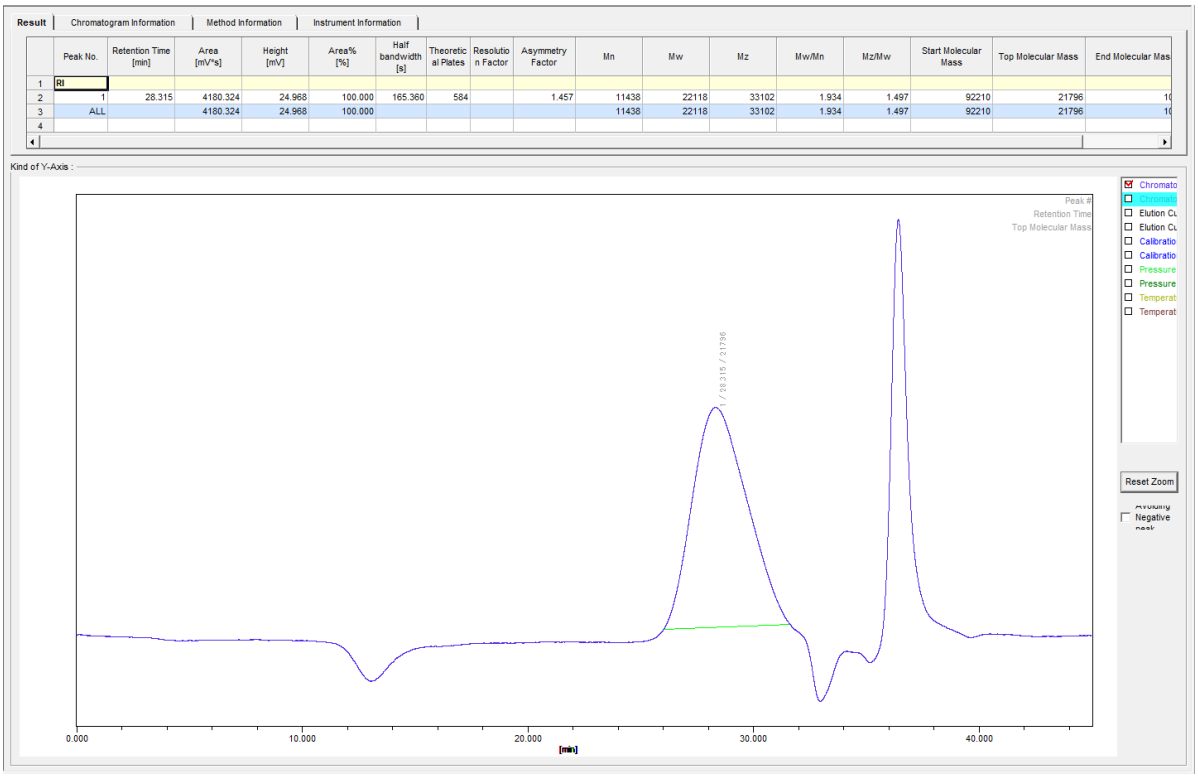

Figure S69. GPC of polymer in entry 6, Table 1.

4.2.2 GPC Traces from Table 2

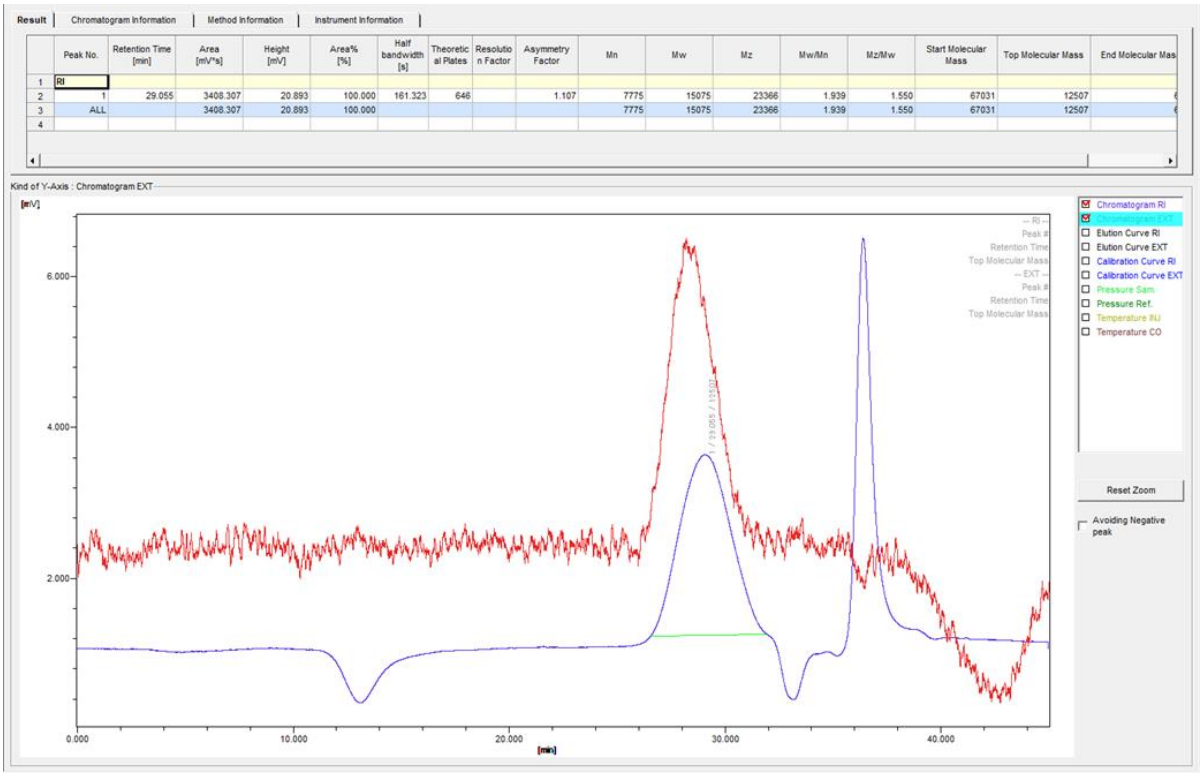

Figure S70. GPC of polymer in entry 2, Table 2.

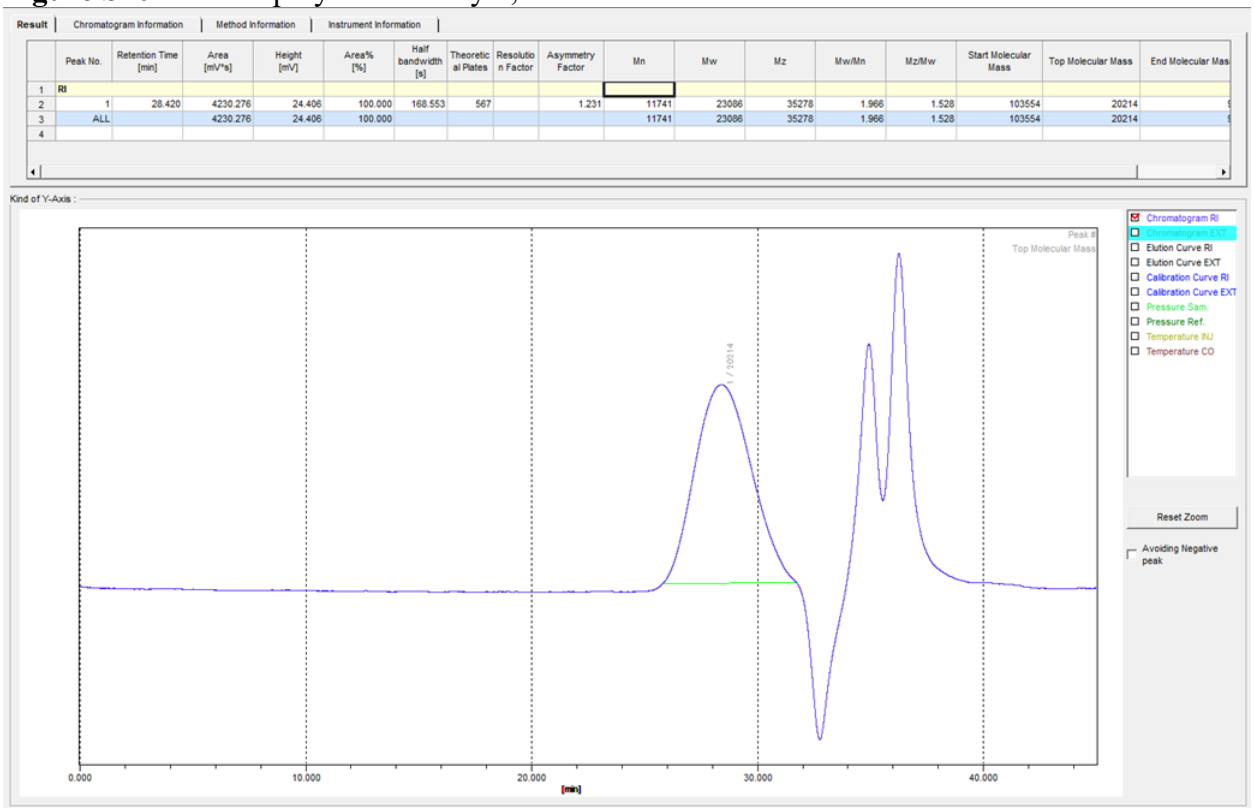

Figure S71. GPC of polymer in entry 3, Table 2.

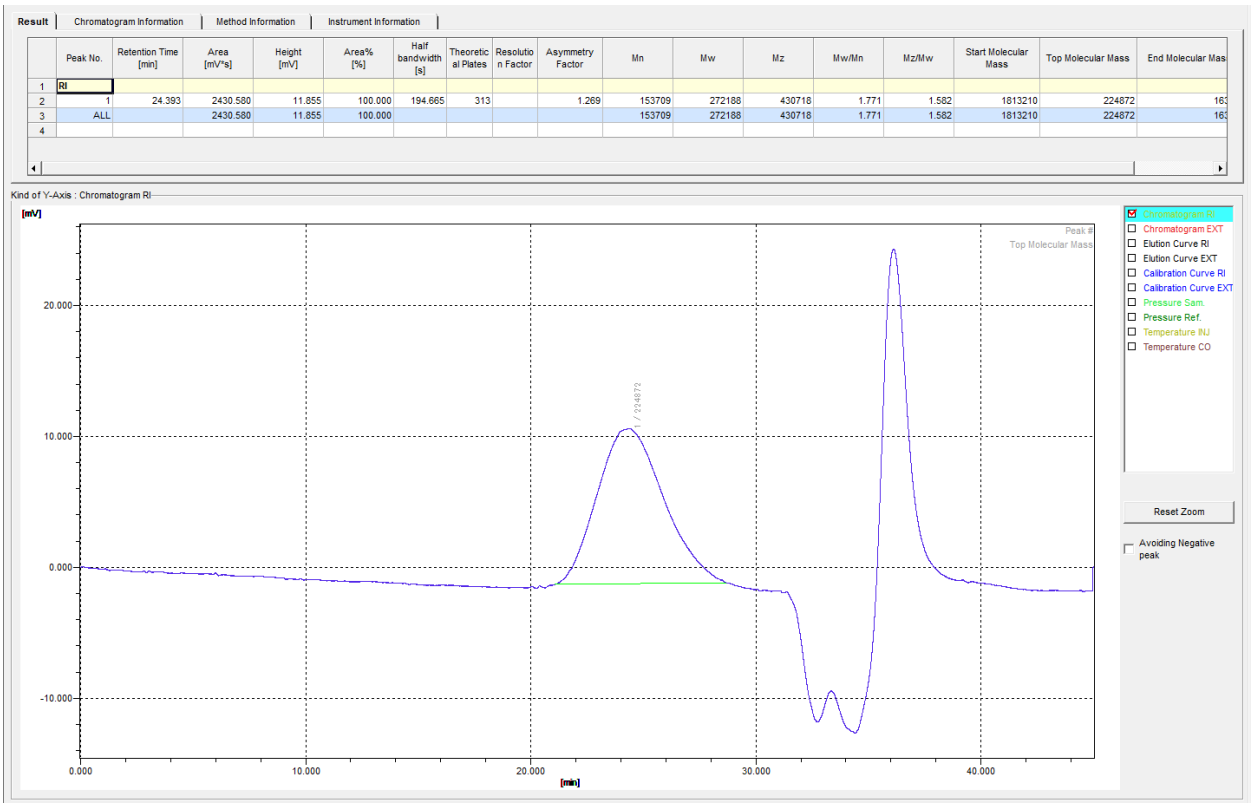

Figure S72. GPC of polymer in entry 4, Table 2.

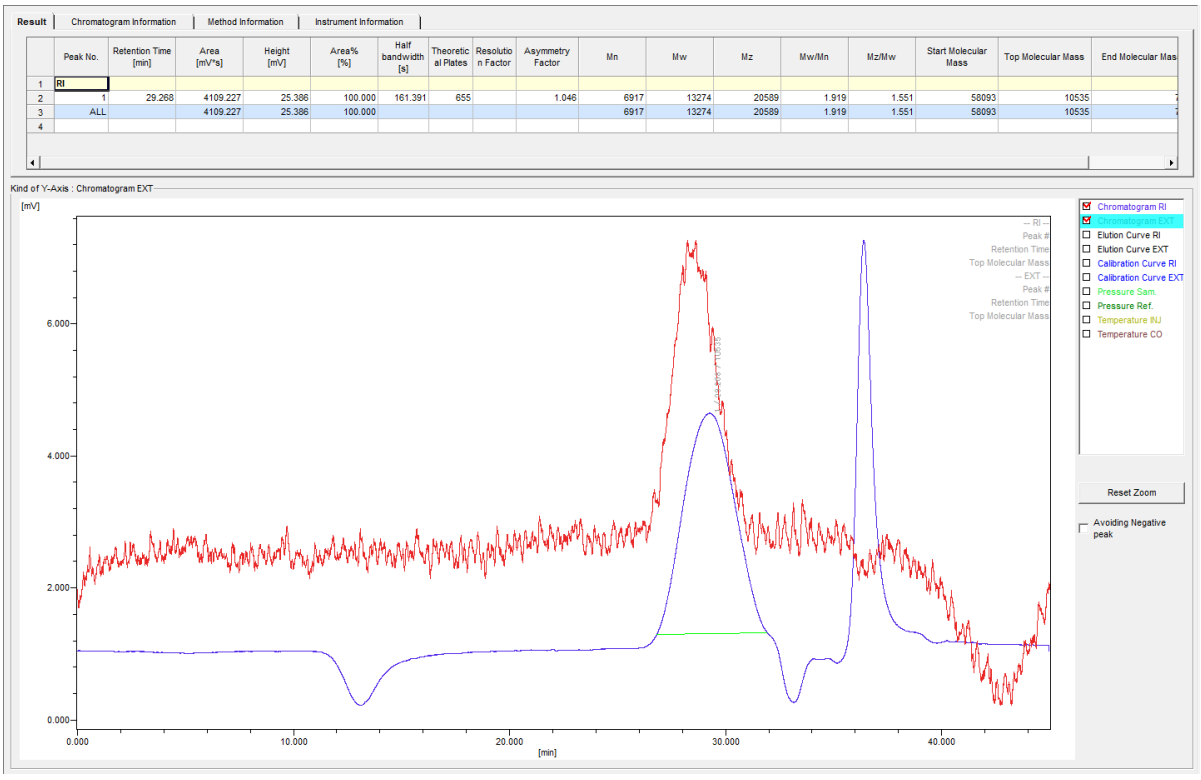

Figure S73. GPC of polymer in entry 5, Table 2.

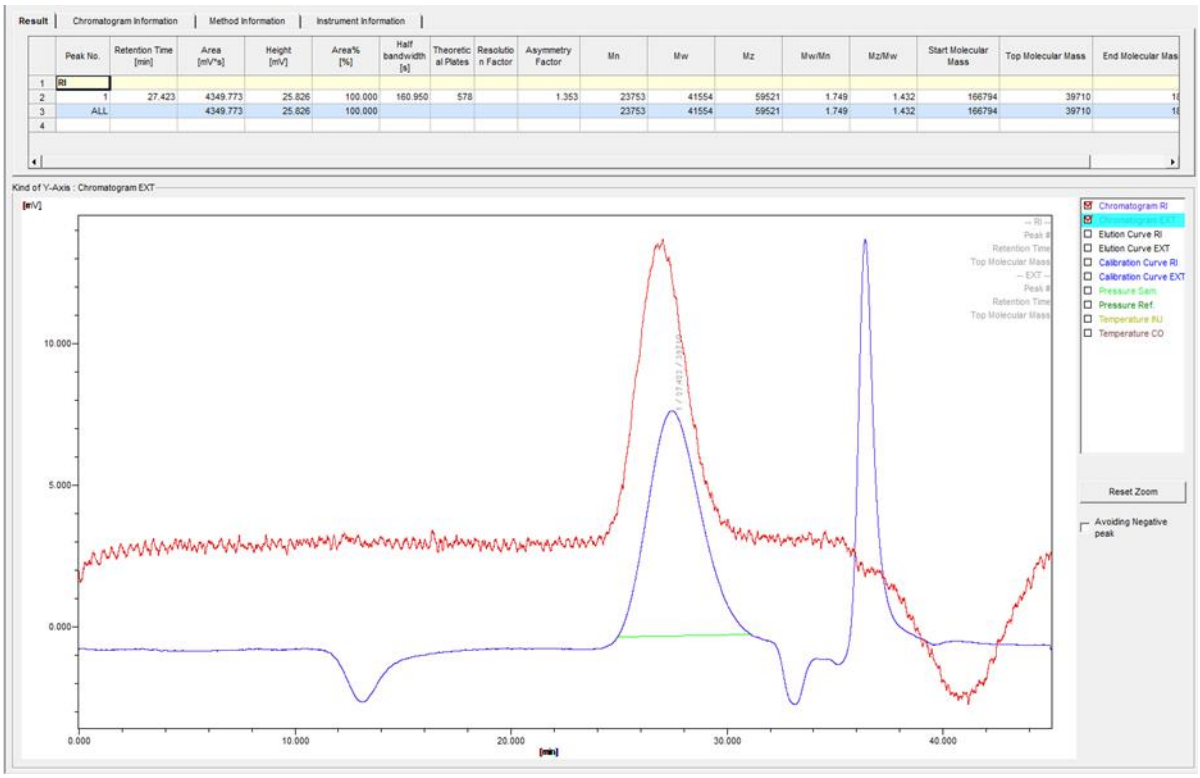

Figure S74. GPC of polymer in entry 6, Table 2.

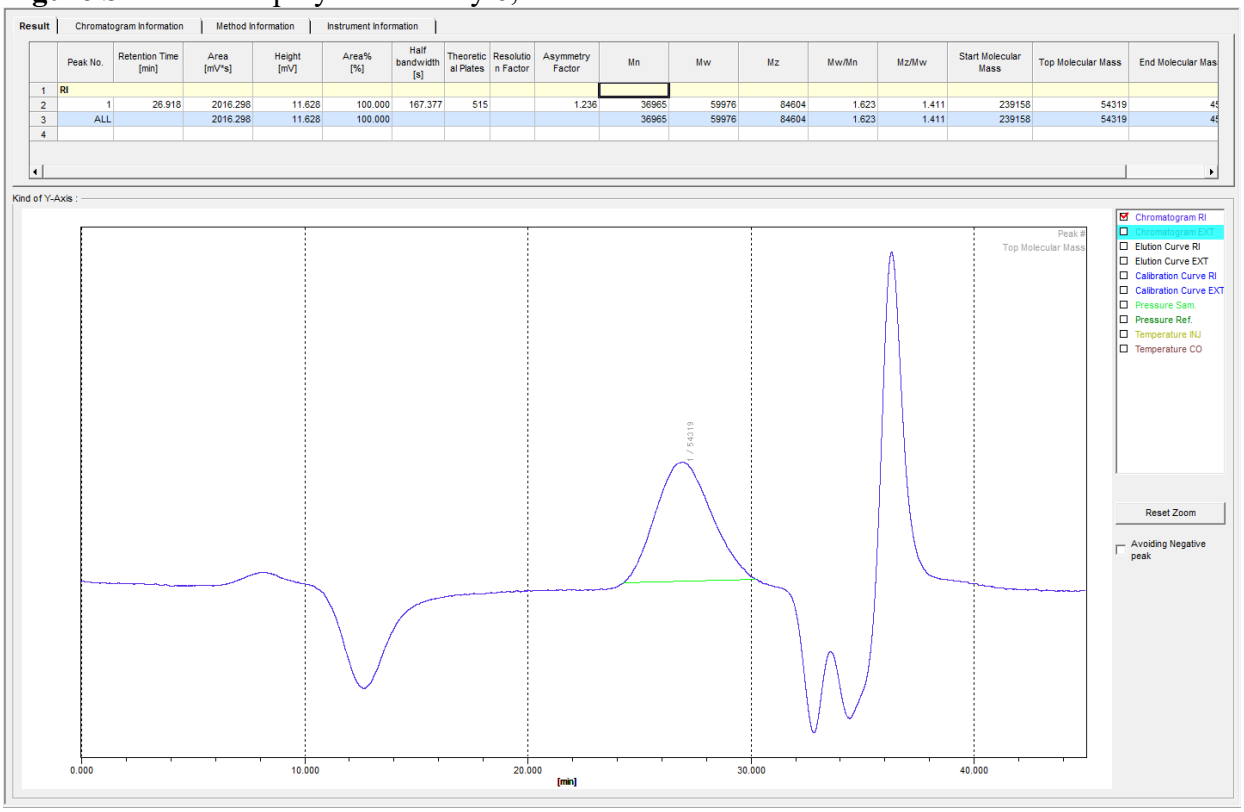

Figure S75. GPC of polymer in entry 7, Table 2.

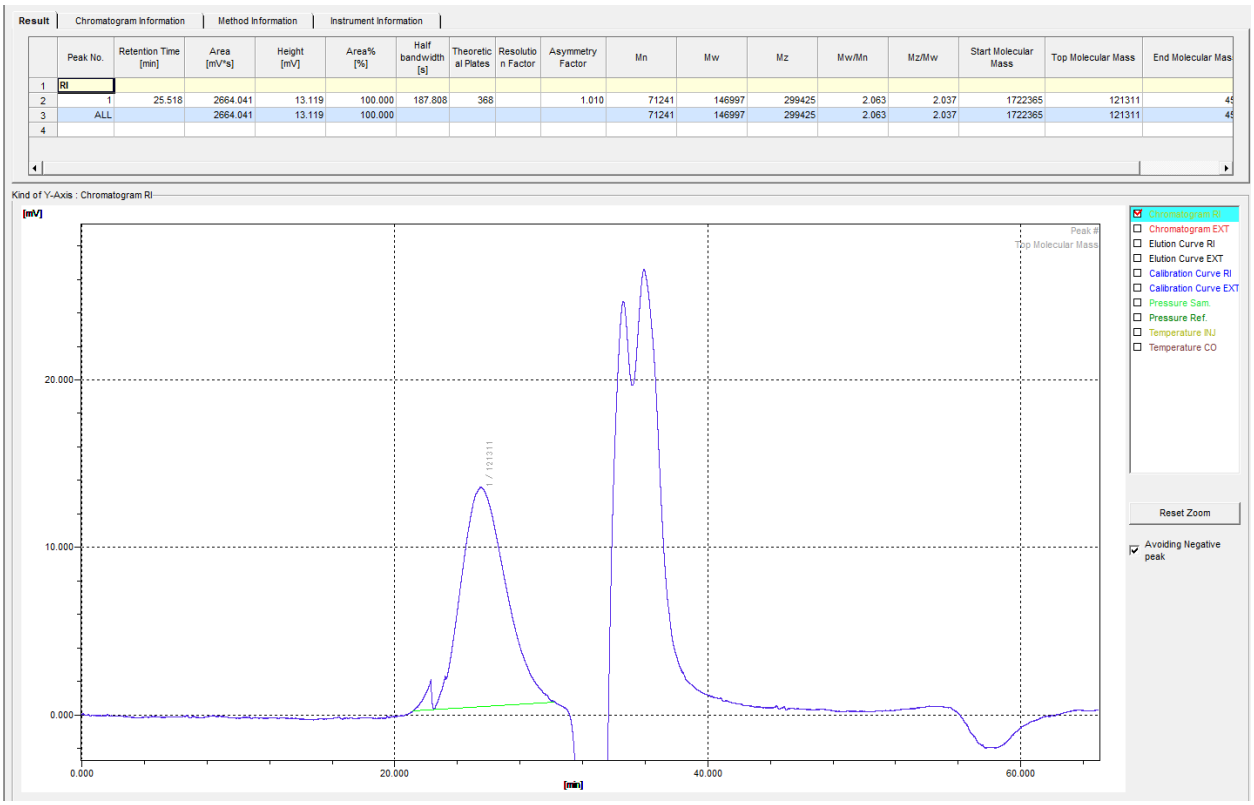

Figure S76. GPC of polymer in entry 8, Table 2.

4.2.3 GPC Traces from Table 3

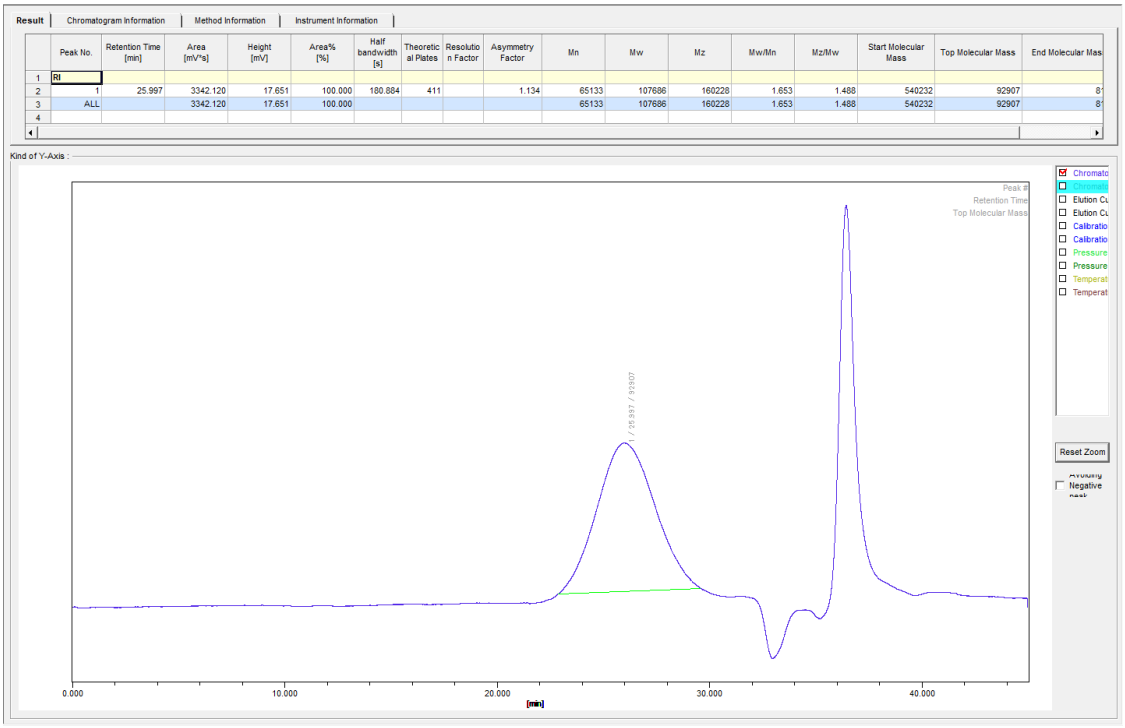

Figure S77. GPC of polymer in entry 1, Table 3.

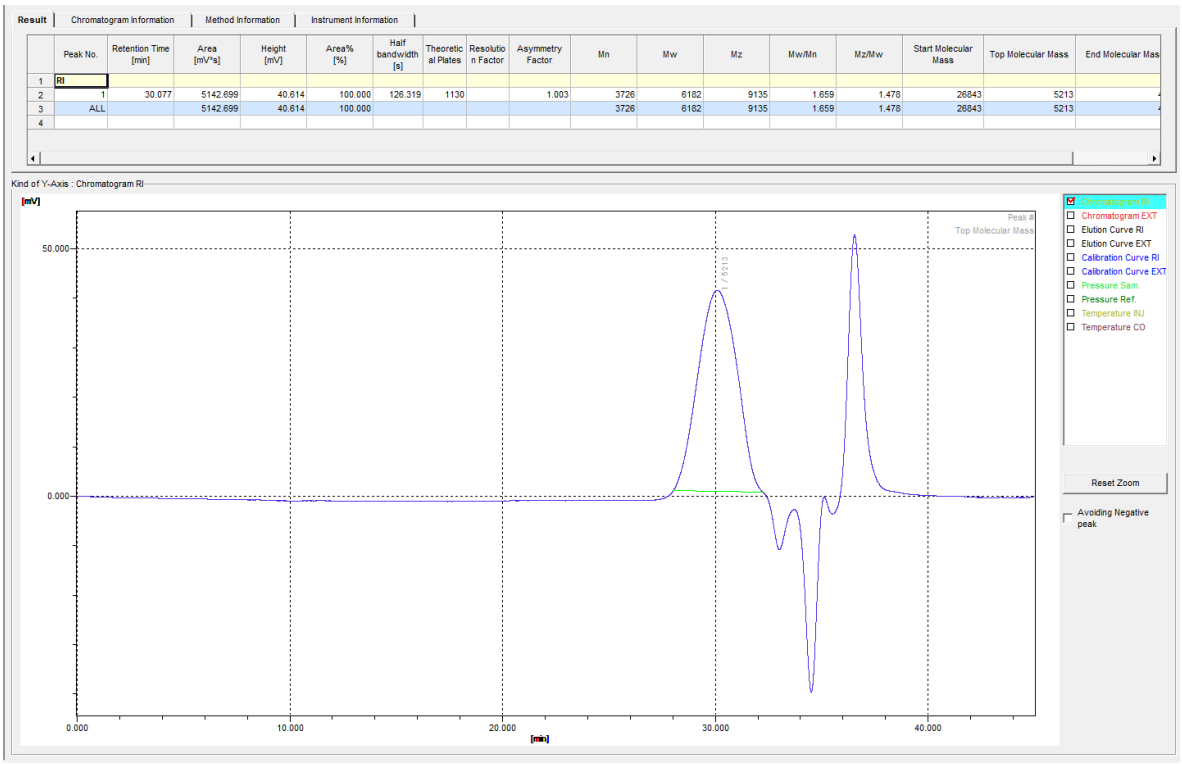

Figure S78. GPC of polymer in entry 3, Table 3.

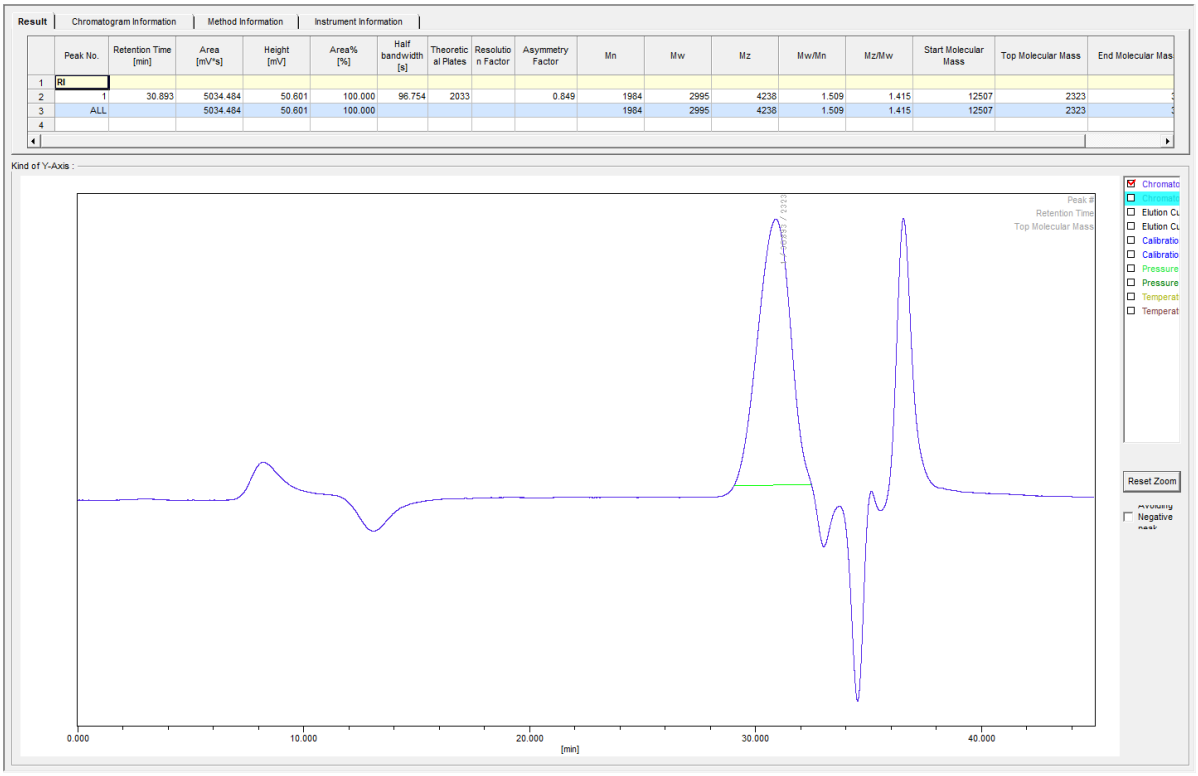

Figure S79. GPC of polymer in entry 4, Table 3.

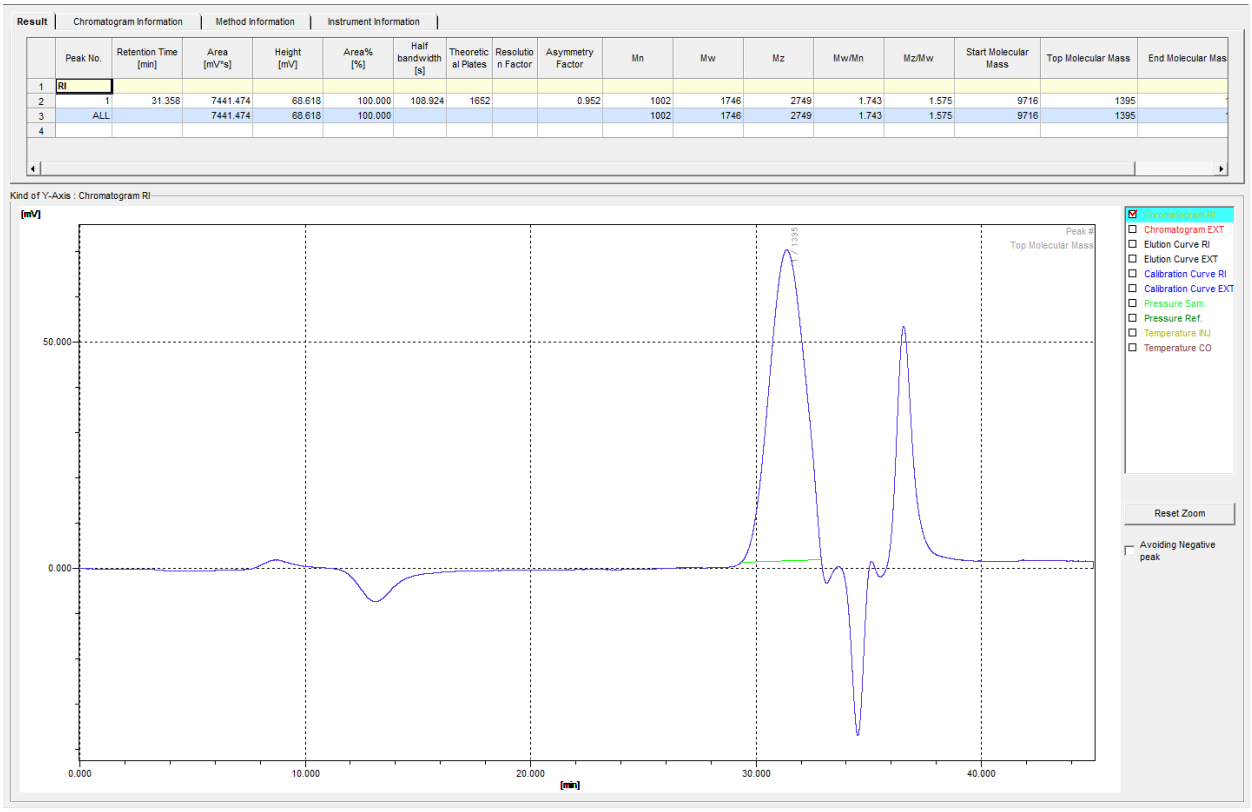

Figure S80. GPC of polymer in entry 5, Table 3.

4.2.4 GPC Traces from Table 4

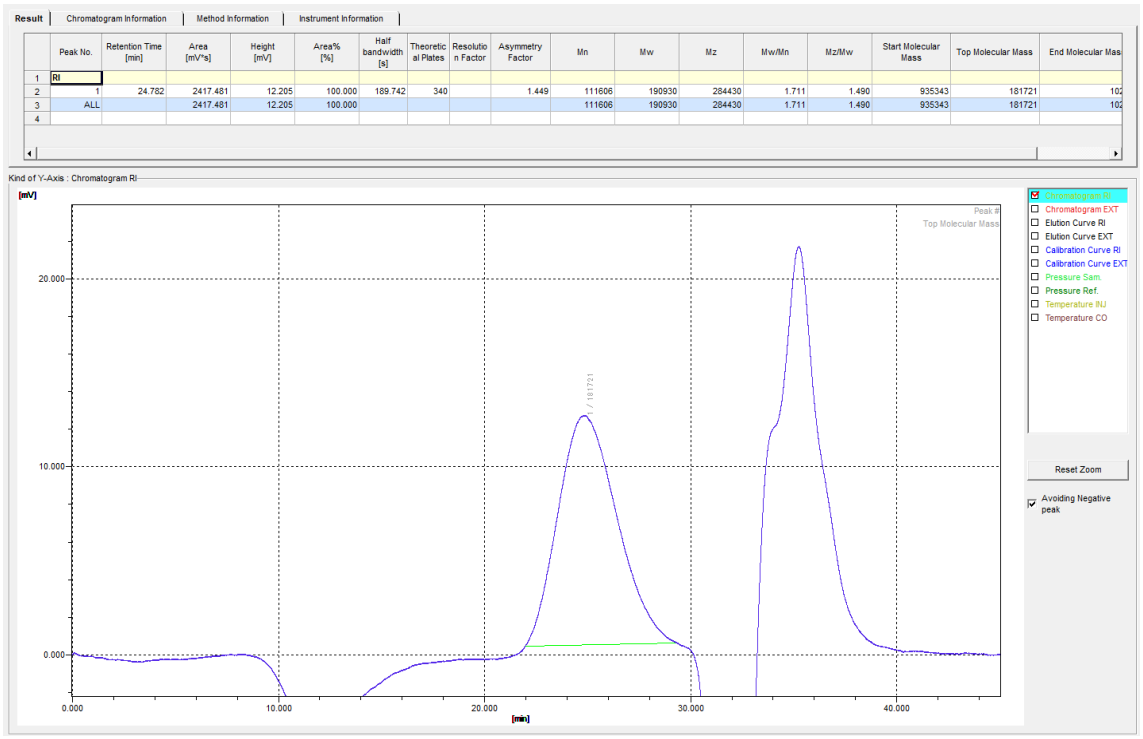

Figure S81. GPC of polymer in entry 1, Table 4.

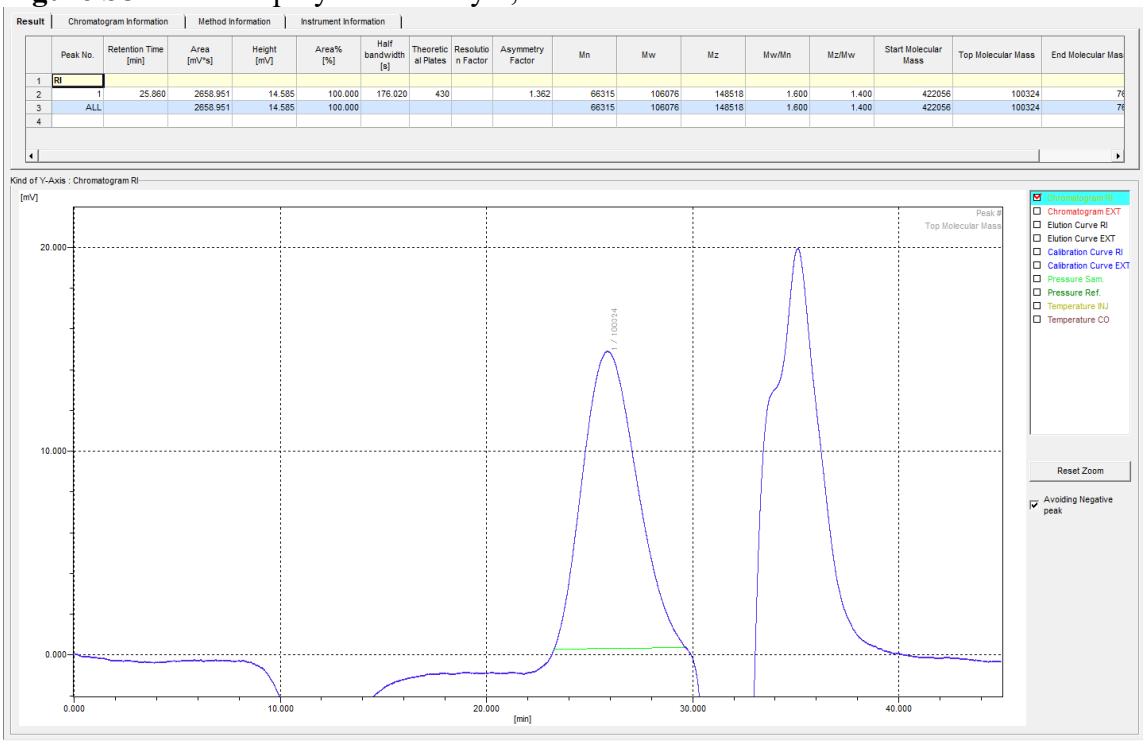

Peak No.	Retention Time [min]	Area [mV*s]	Height [mV]	Area% [%]	Half bandwidth [s]	Theoretical Plates	Resolution Factor	Asymmetry Factor	Mn	Mw	Mz	Mw/Mn	Mz/Mw	Start Molecular Mass	Top Molecular Mass	End Molecular Mass
RI																
1	25.860	2658.951	14.585	100.000	176.020	430		1.362	66315	106076	148518	1.600	1.400	422056	100324	76
ALL		2658.951	14.585	100.000					66315	106076	148518	1.600	1.400	422056	100324	76

Figure S82. GPC of polymer in entry 2, Table 4.

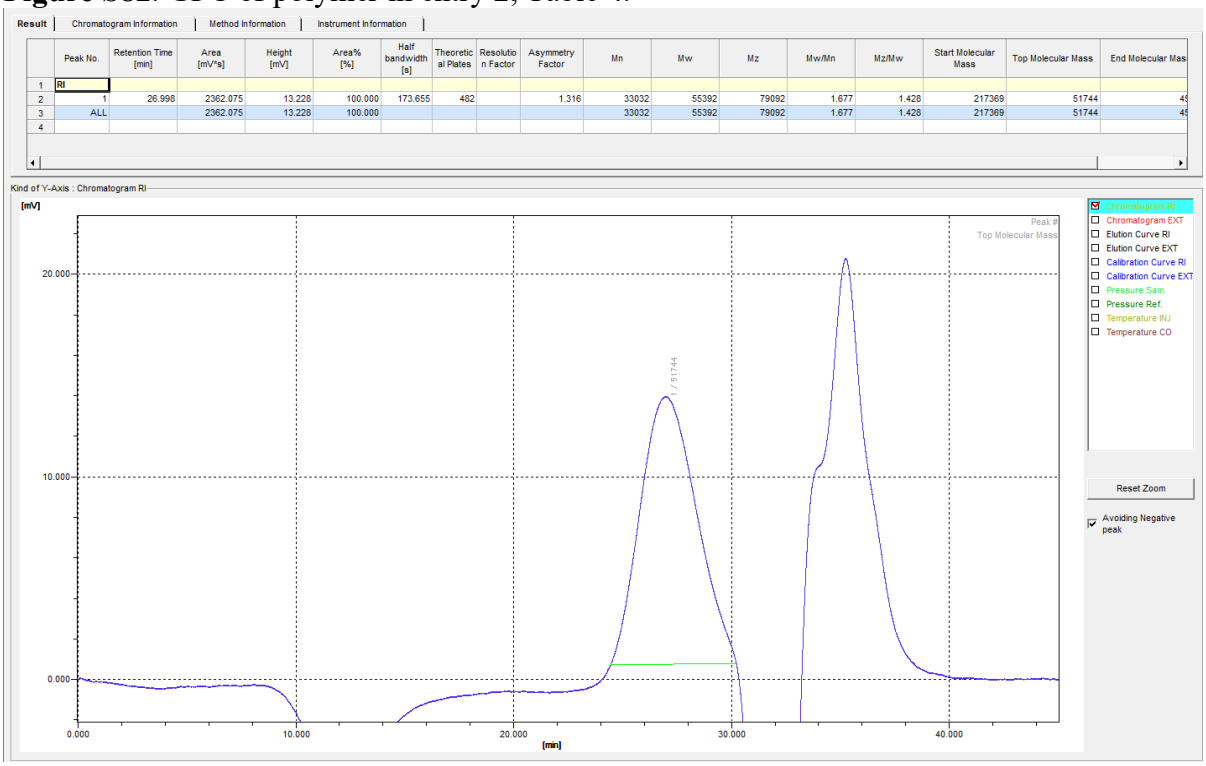

Peak No.	Retention Time [min]	Area [mV*s]	Height [mV]	Area% [%]	Half bandwidth [s]	Theoretical Plates	Resolution Factor	Asymmetry Factor	Mn	Mw	Mz	Mw/Mn	Mz/Mw	Start Molecular Mass	Top Molecular Mass	End Molecular Mass
RI																
1	26.998	2362.075	13.228	100.000	173.655	482		1.316	33032	55392	79092	1.677	1.428	217369	51744	45
ALL		2362.075	13.228	100.000					33032	55392	79092	1.677	1.428	217369	51744	45

Figure S83. GPC of polymer in entry 3, Table 4.

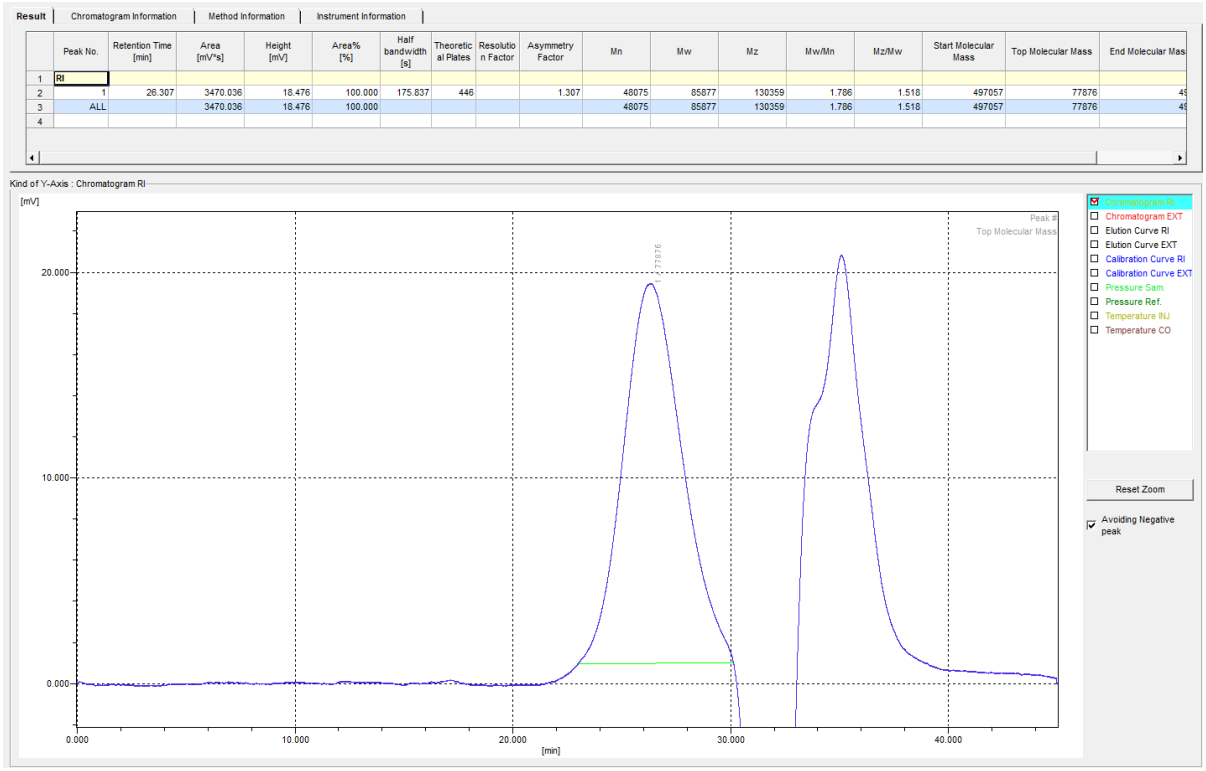

Figure S84. GPC of polymer in entry 4, Table 4.

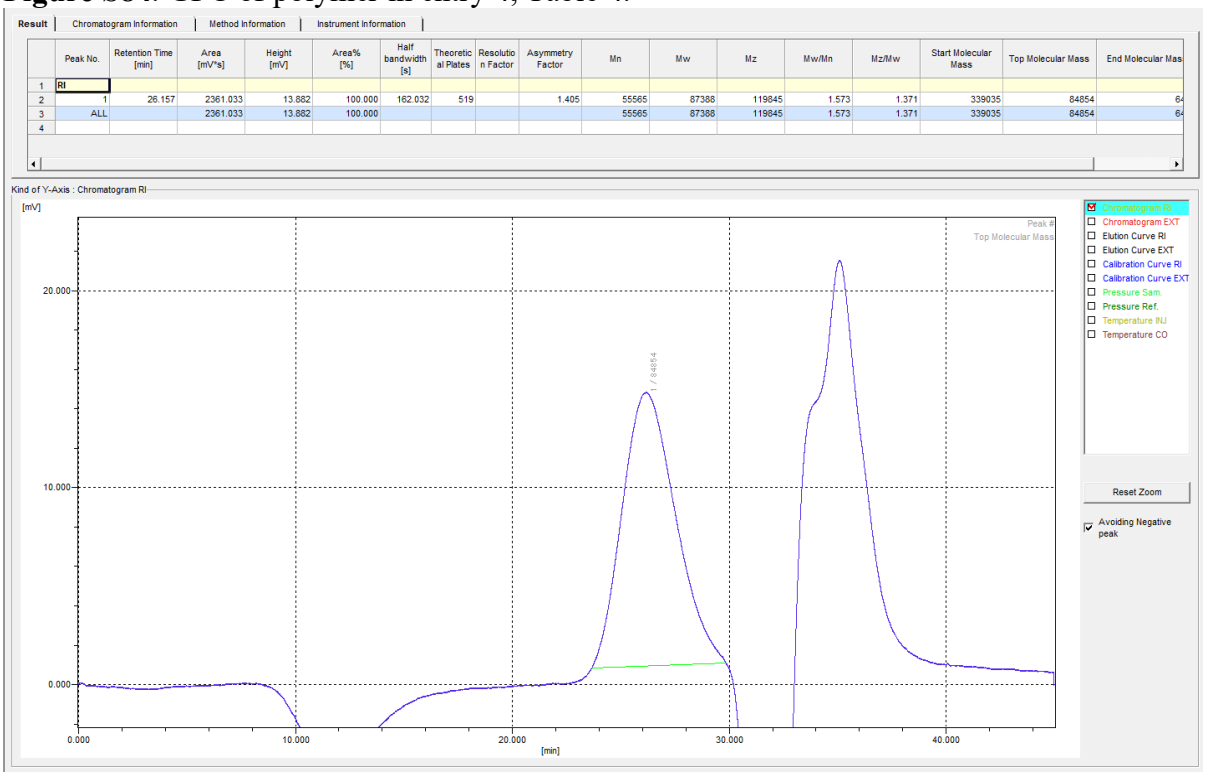

Figure S85. GPC of polymer in entry 5, Table 4.

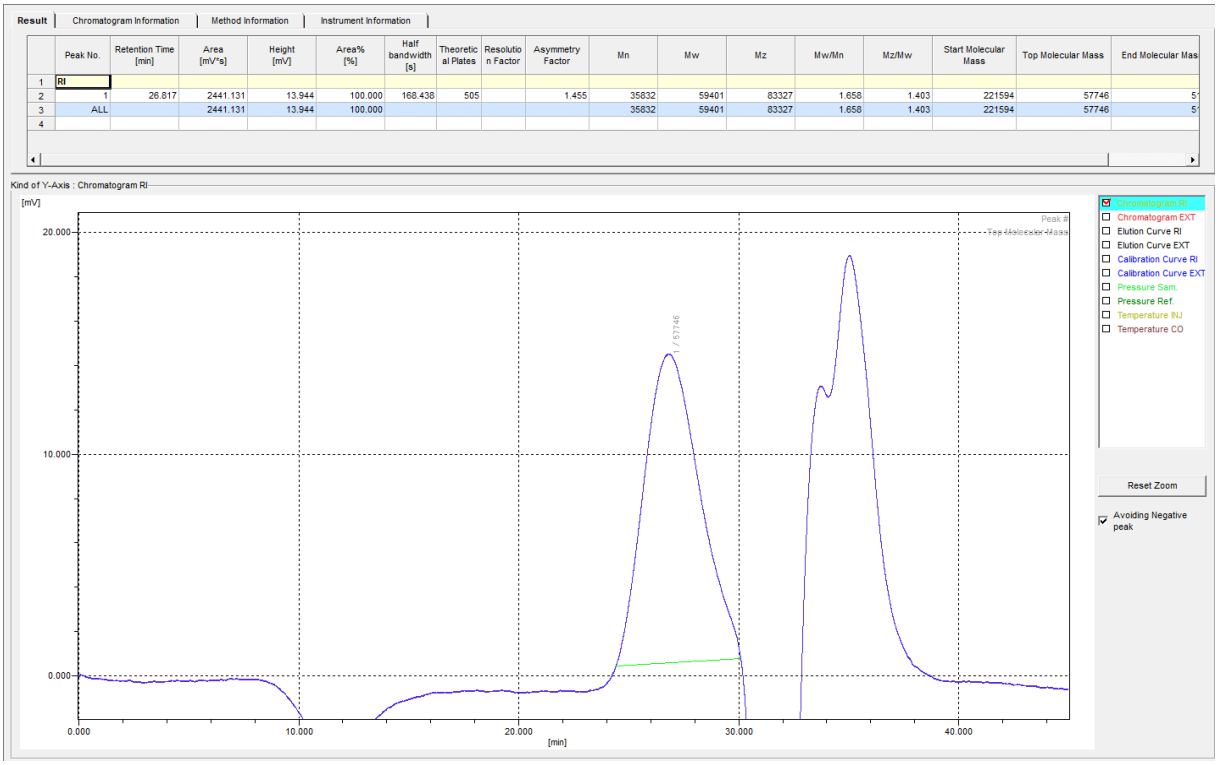

Figure S86. GPC of polymer in entry 6, Table 4.

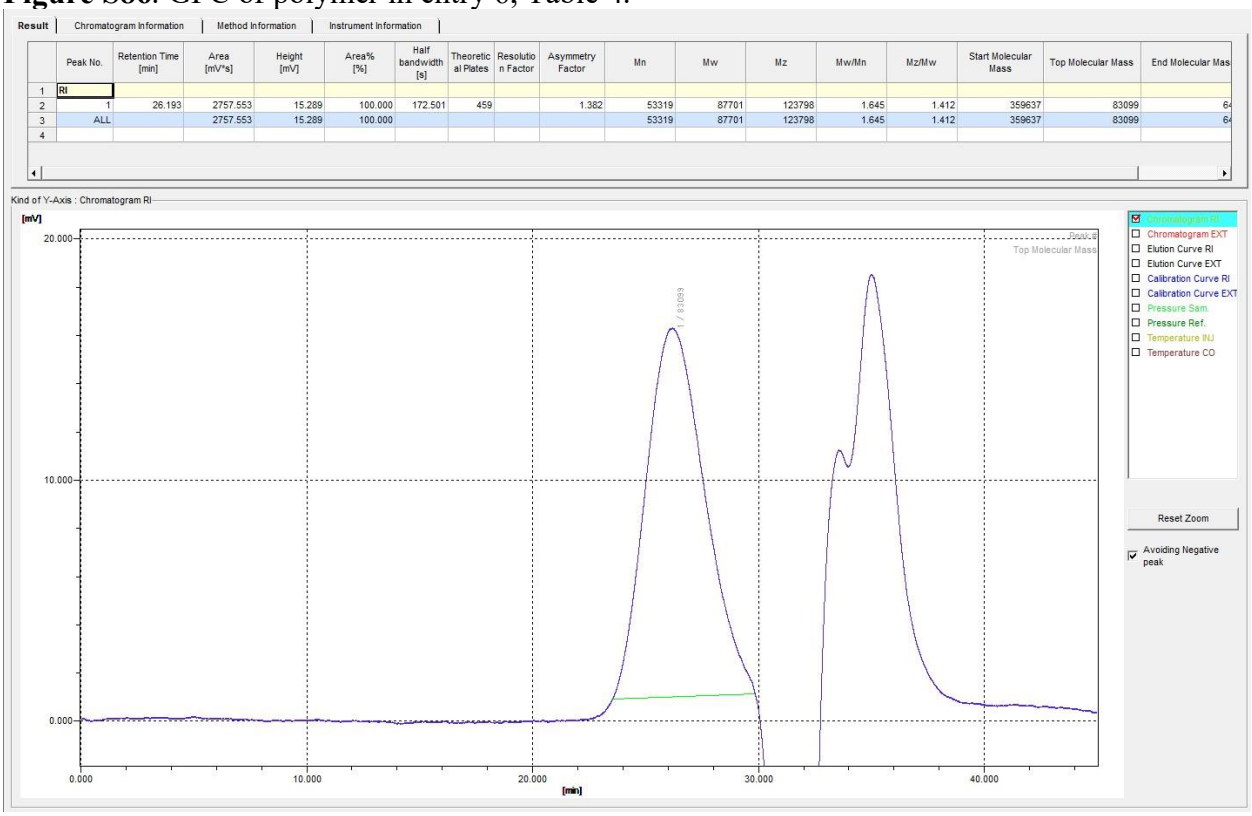

Figure S87. GPC of polymer in entry 7, Table 4.

4.2.5 GPC Traces from Table S1

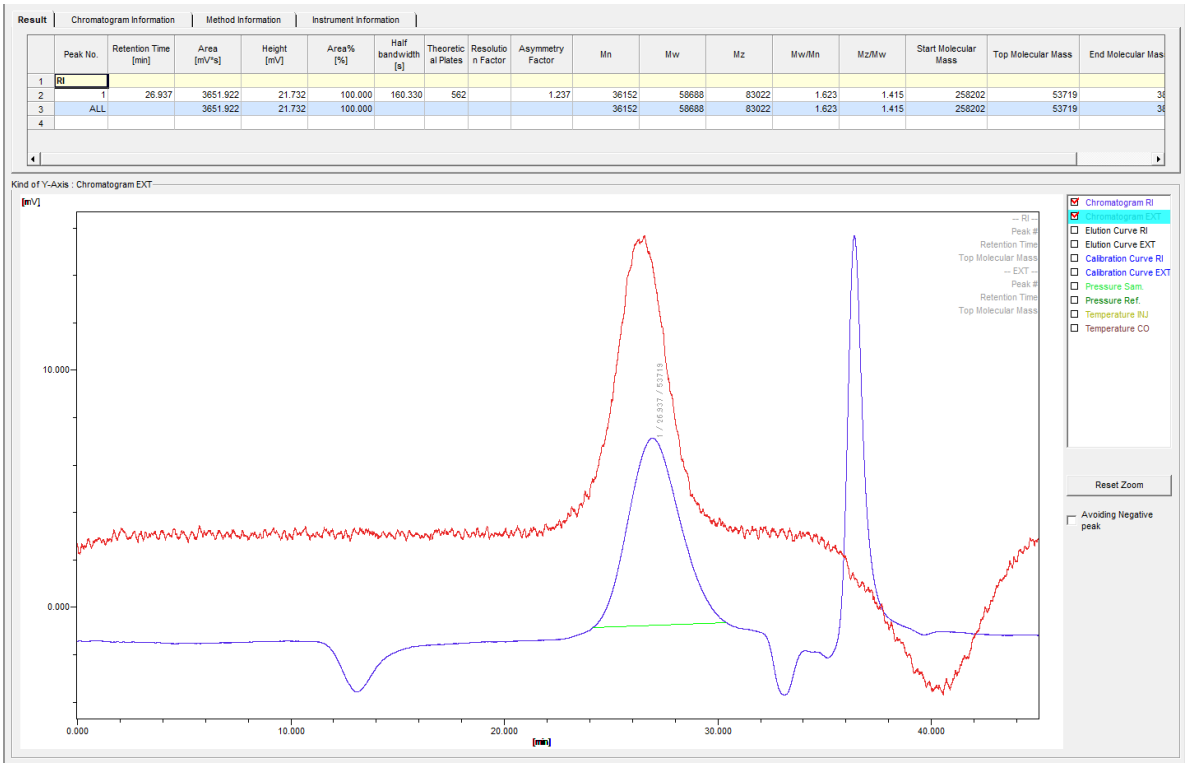

Figure S88. GPC of polymer in entry 1, Table S1.

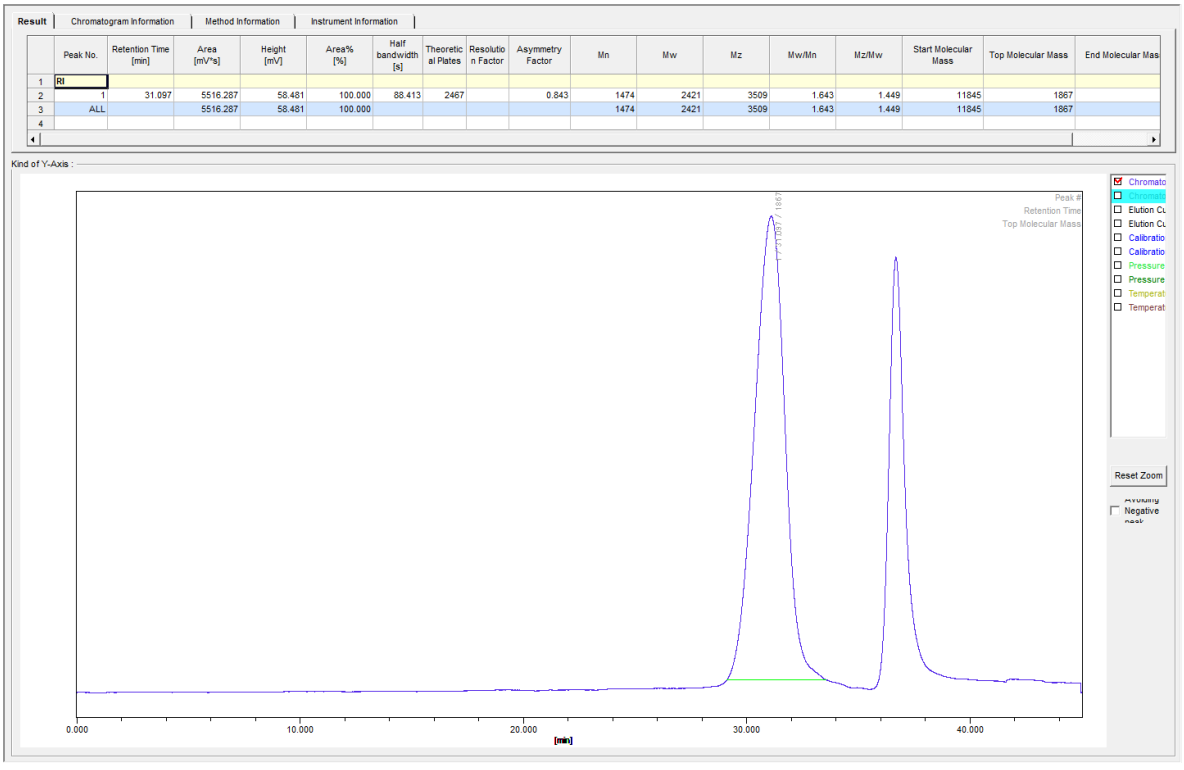

Figure S89. GPC of polymer in entry 2, Table S1.

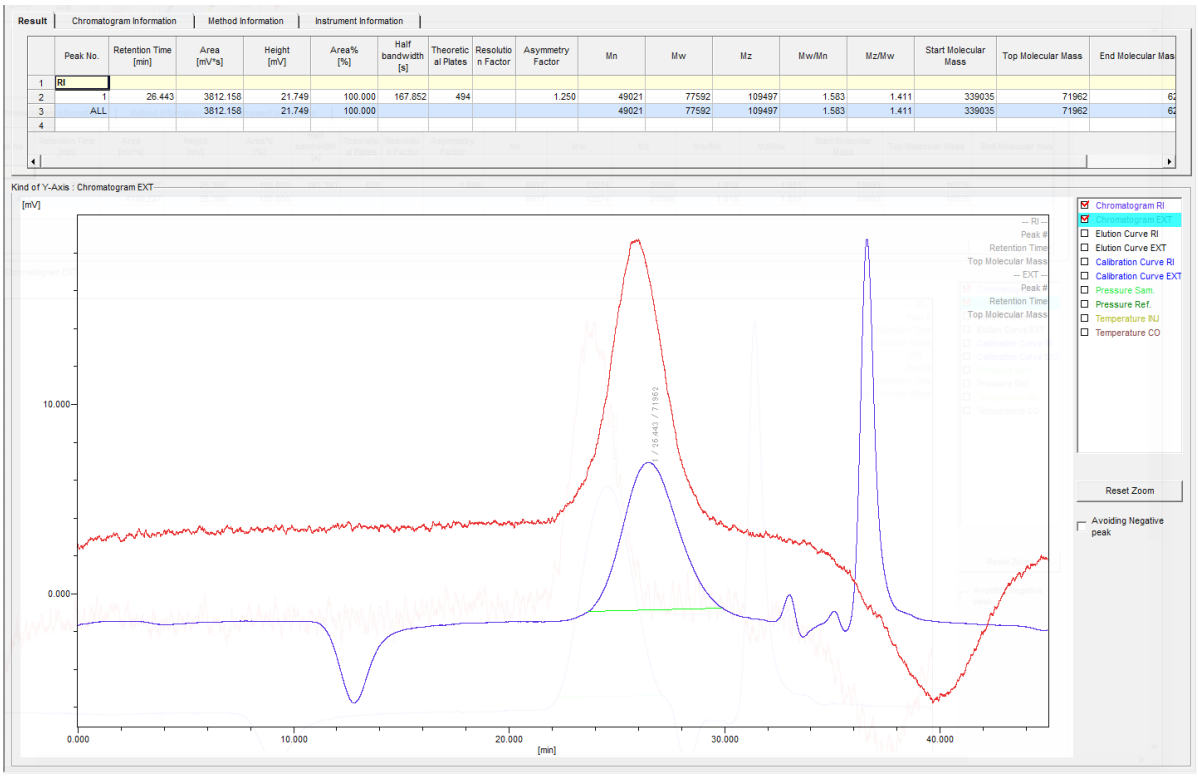

Figure S90. GPC of polymer in entry 3, Table S1

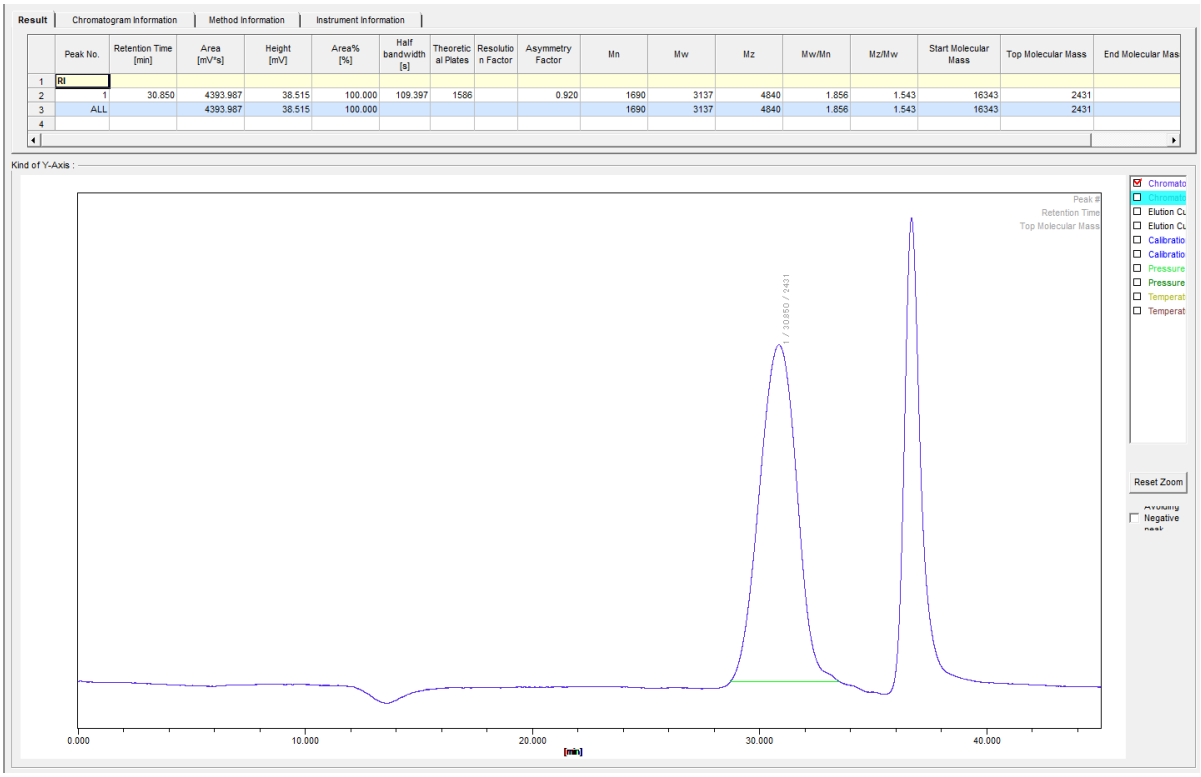

Figure S91. GPC of polymer in entry 4, Table S1.

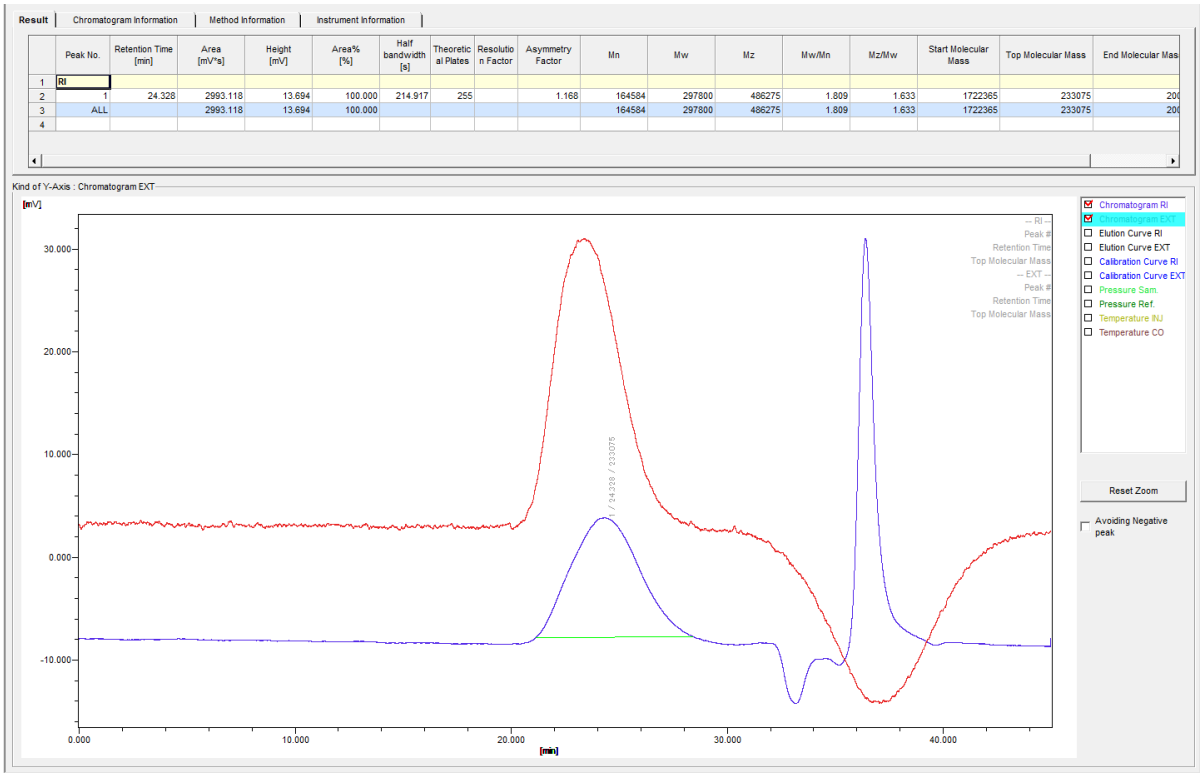

Figure S92. GPC of polymer in entry 5, Table S1.

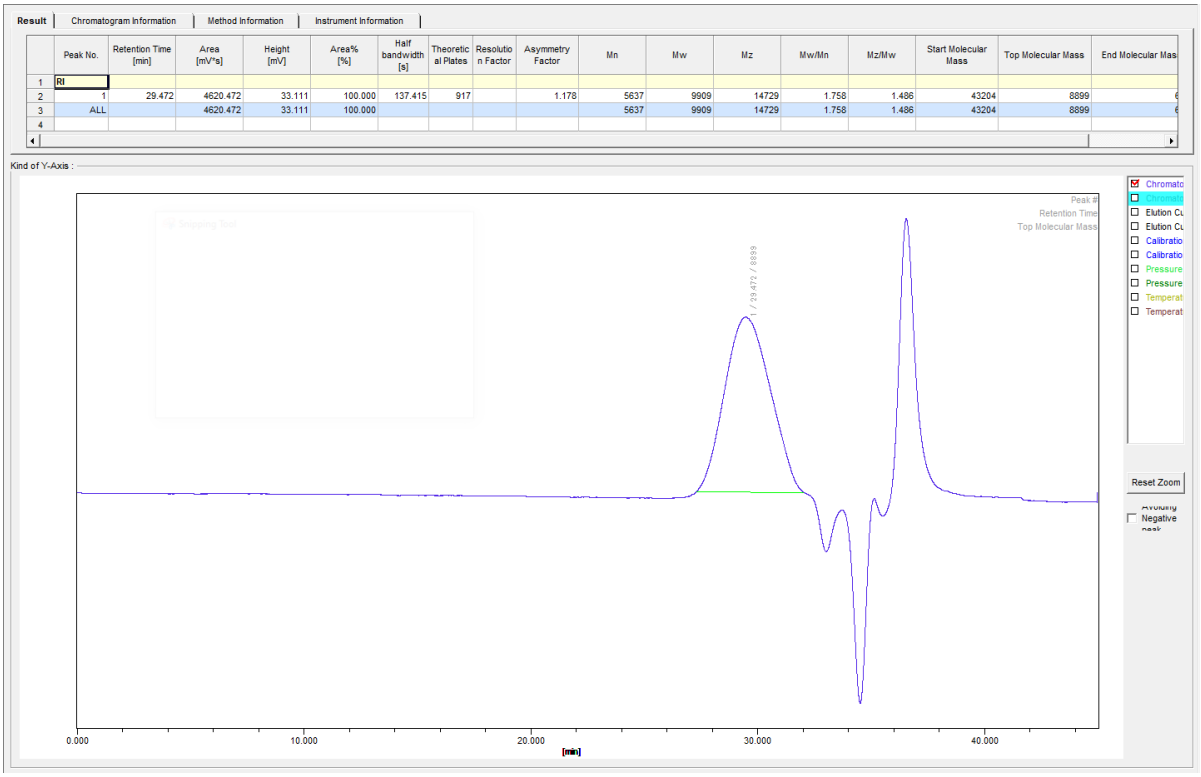

Figure S93. GPC of polymer in entry 6, Table S1.

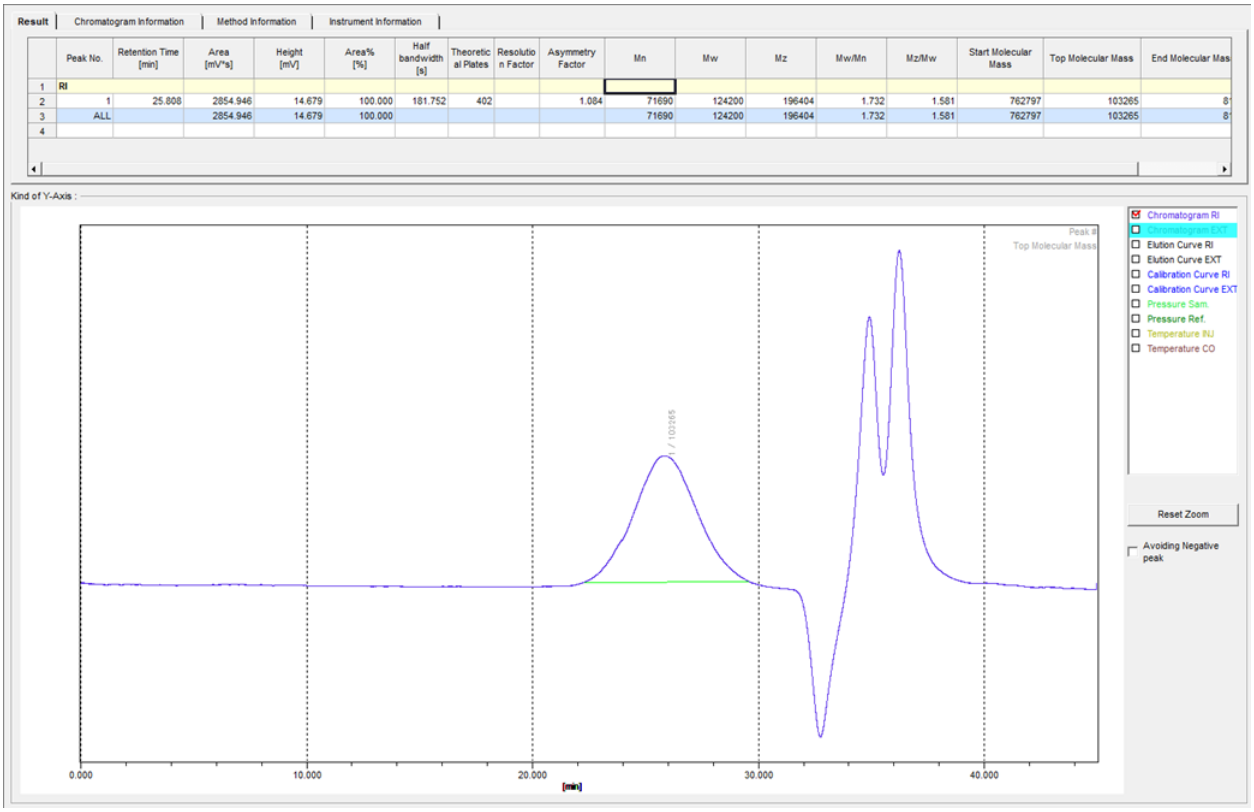

Figure S94. GPC of polymer in entry 7, Table S1.

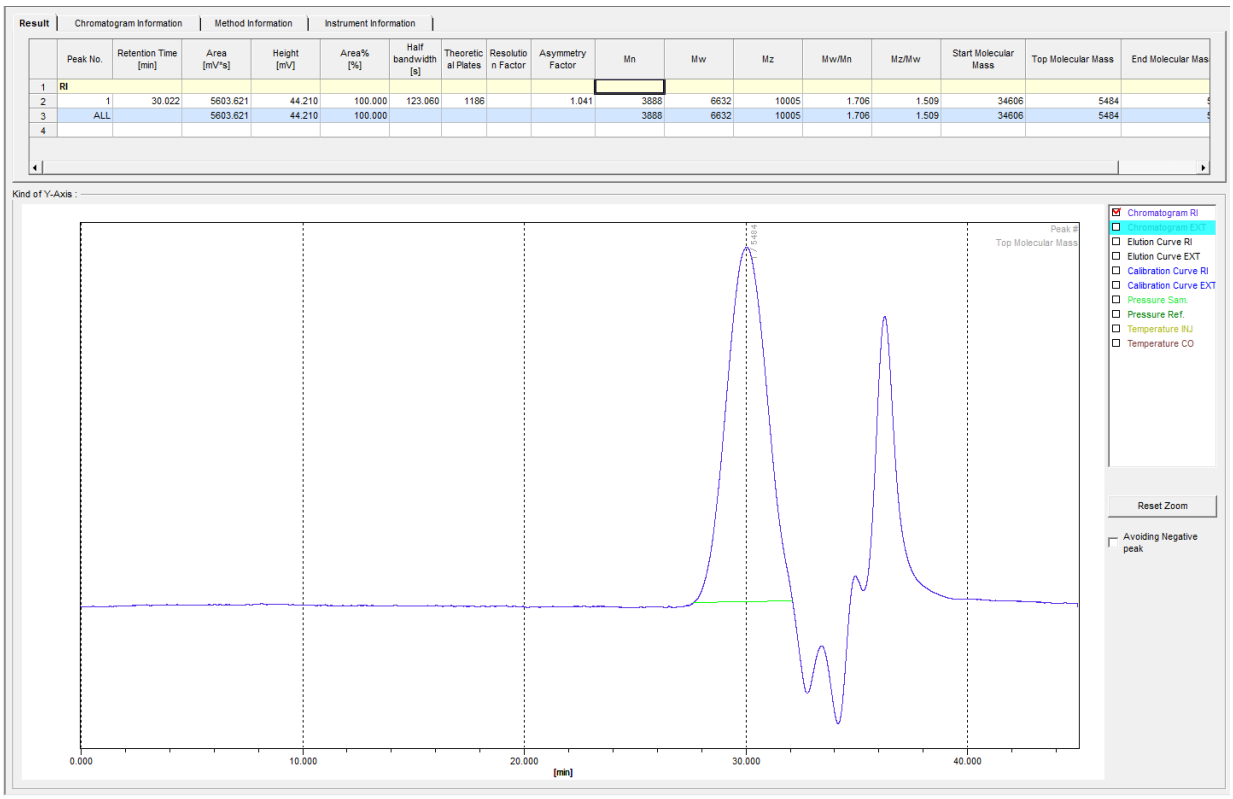

Figure S95. GPC of polymer in entry 8, Table S1.

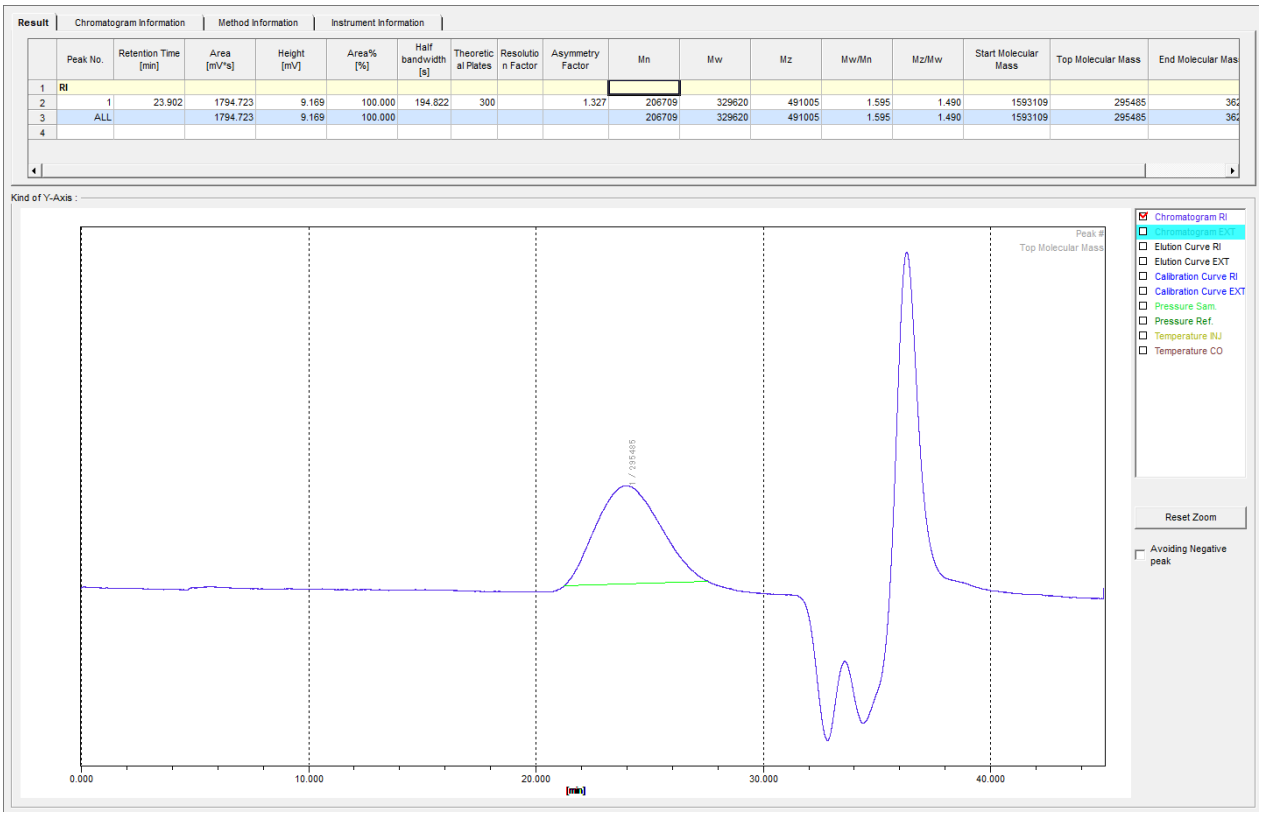

Figure S96. GPC of polymer in entry 9, Table S1.

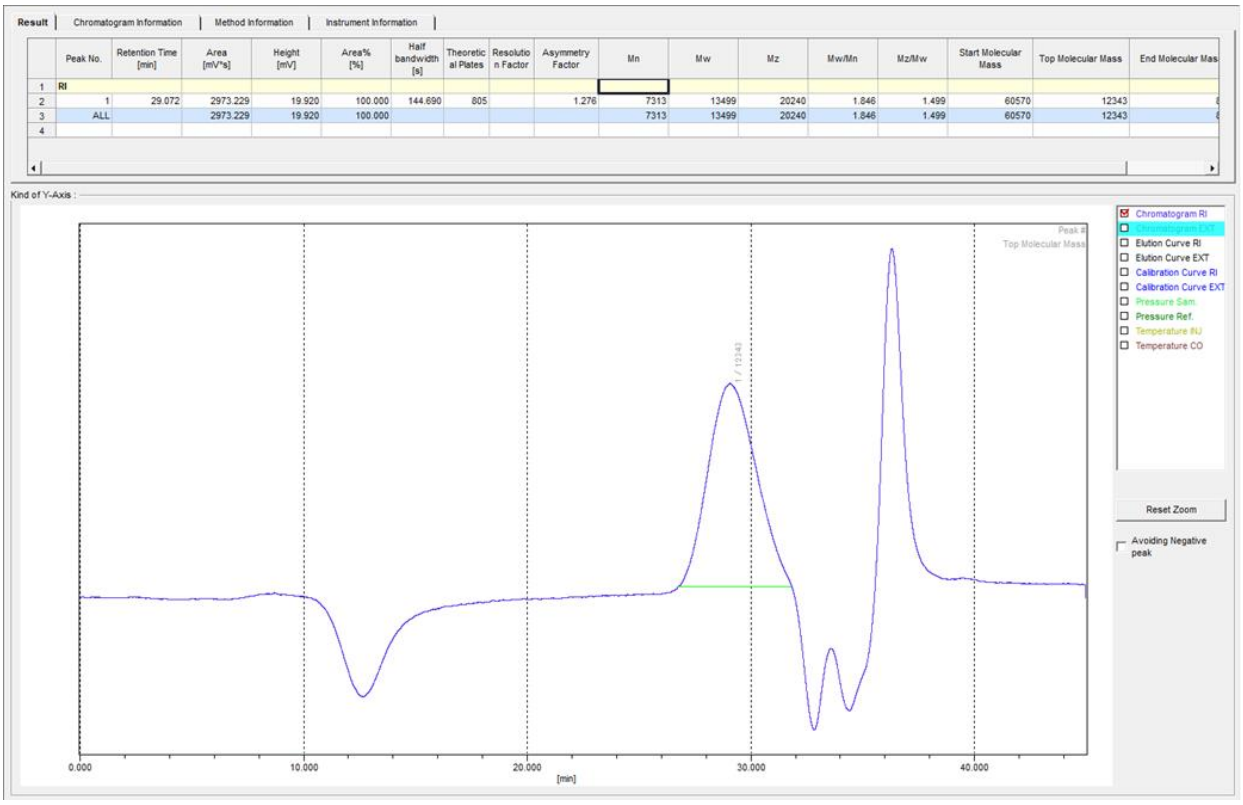

Figure S97. GPC of polymer in entry 10, Table S1.

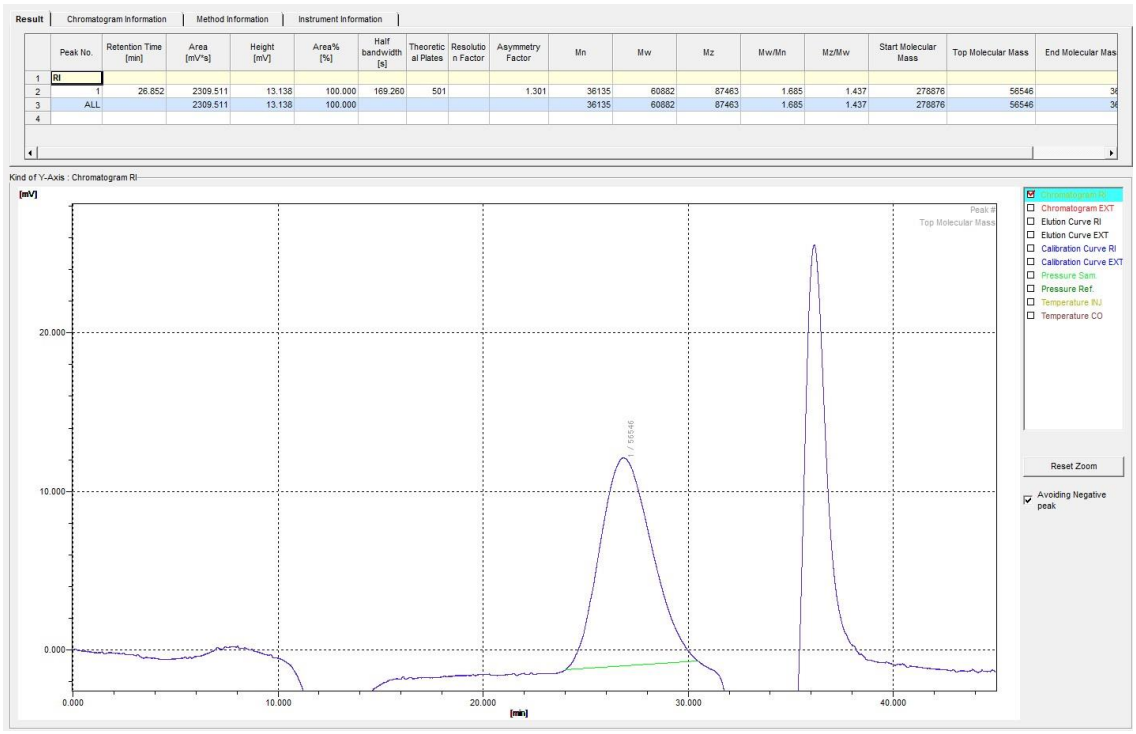

Figure S98. GPC of polymer in entry 11, Table S1.

4.3 Differential Scanning Calorimetry (DSC)

4.3.1 DSC Traces of Table 1

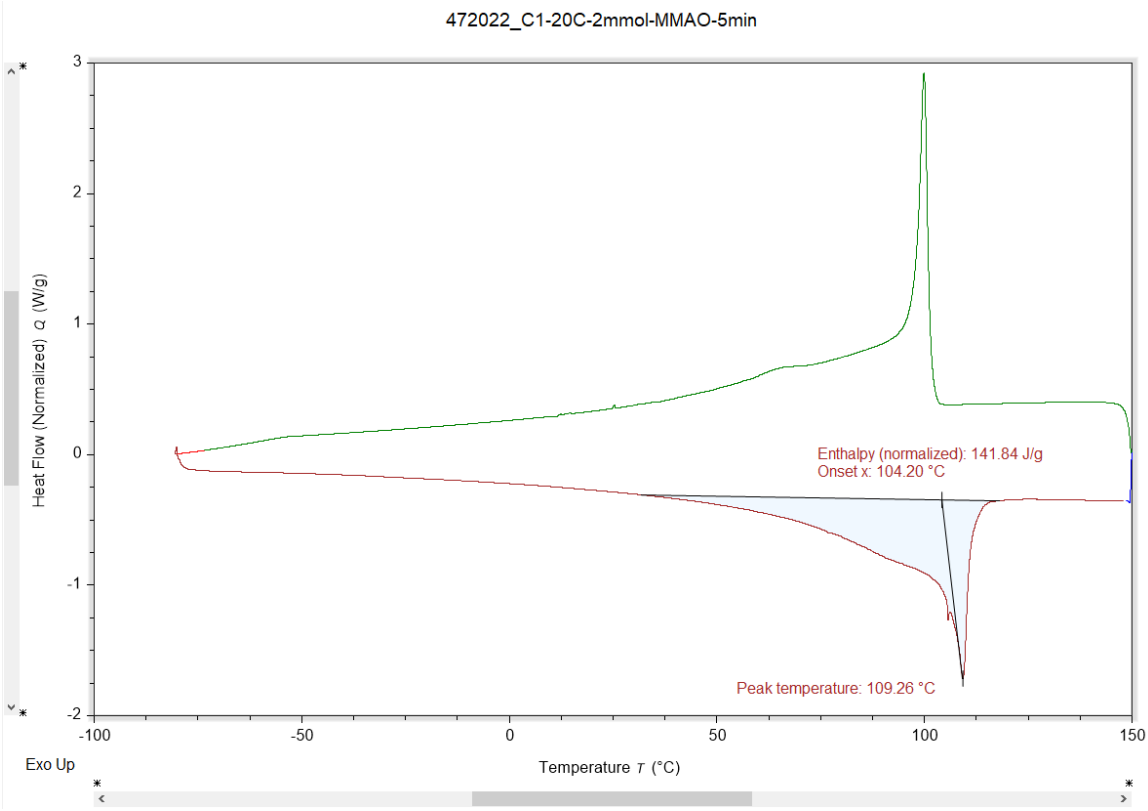

Figure S99. DSC of polymer in entry 1, Table 1.

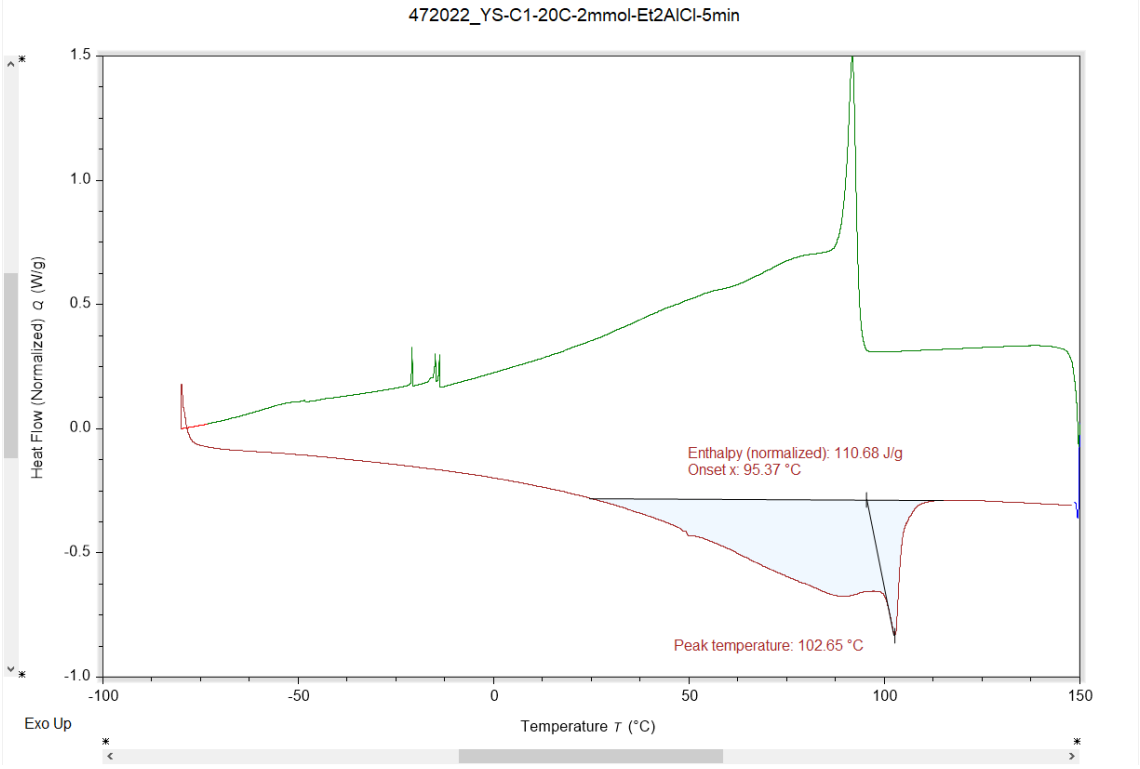

Figure S100. DSC of polymer in entry 2, Table 1.

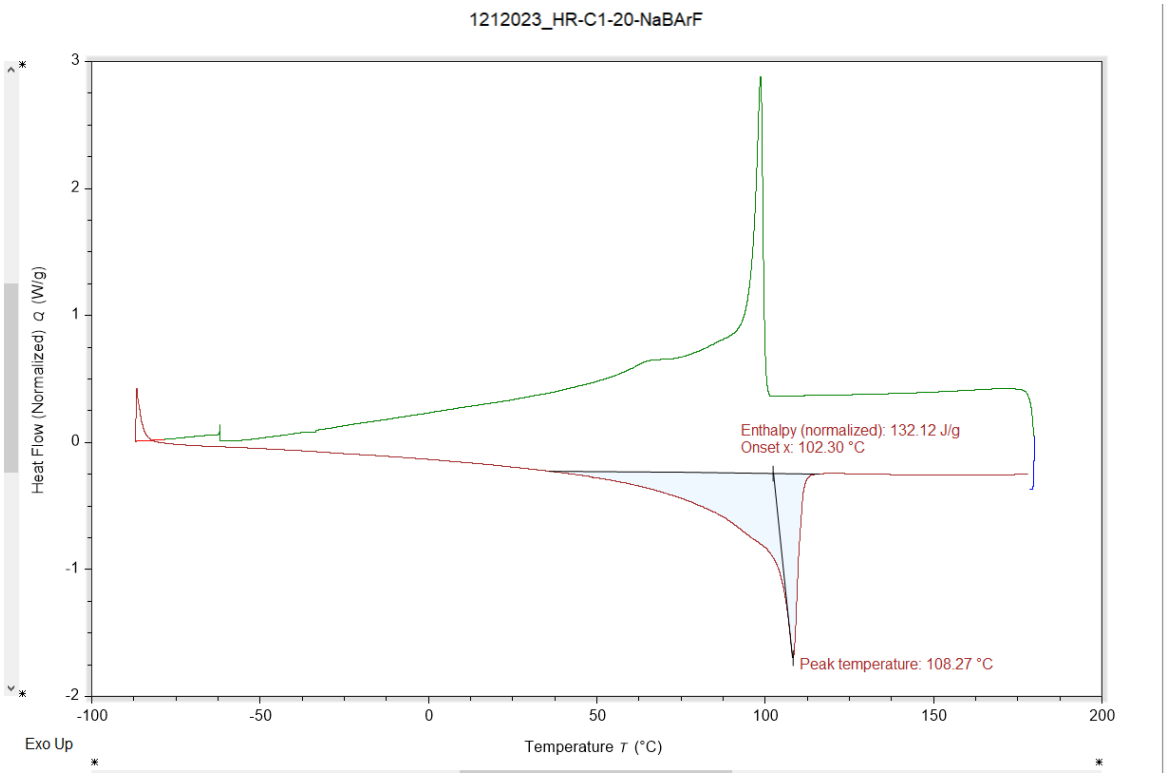

Figure S101. DSC of polymer in entry 3, Table 1.

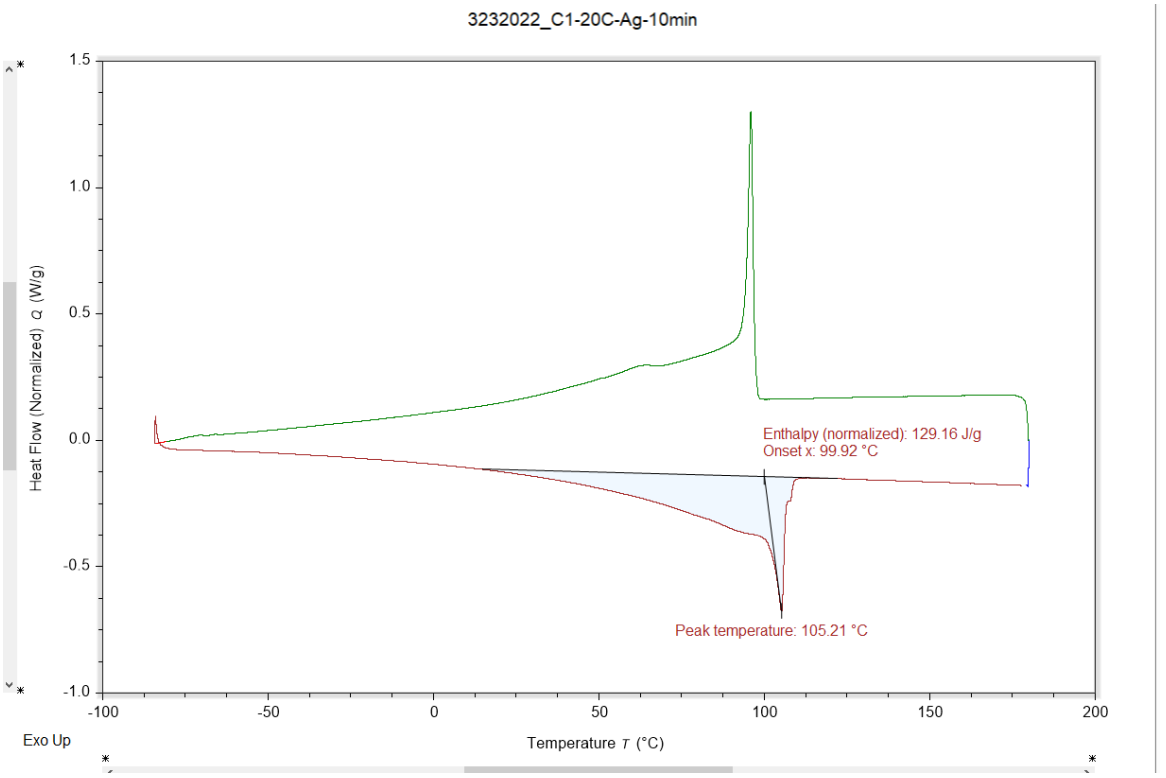

Figure S102. DSC of polymer in entry 4, Table 1.

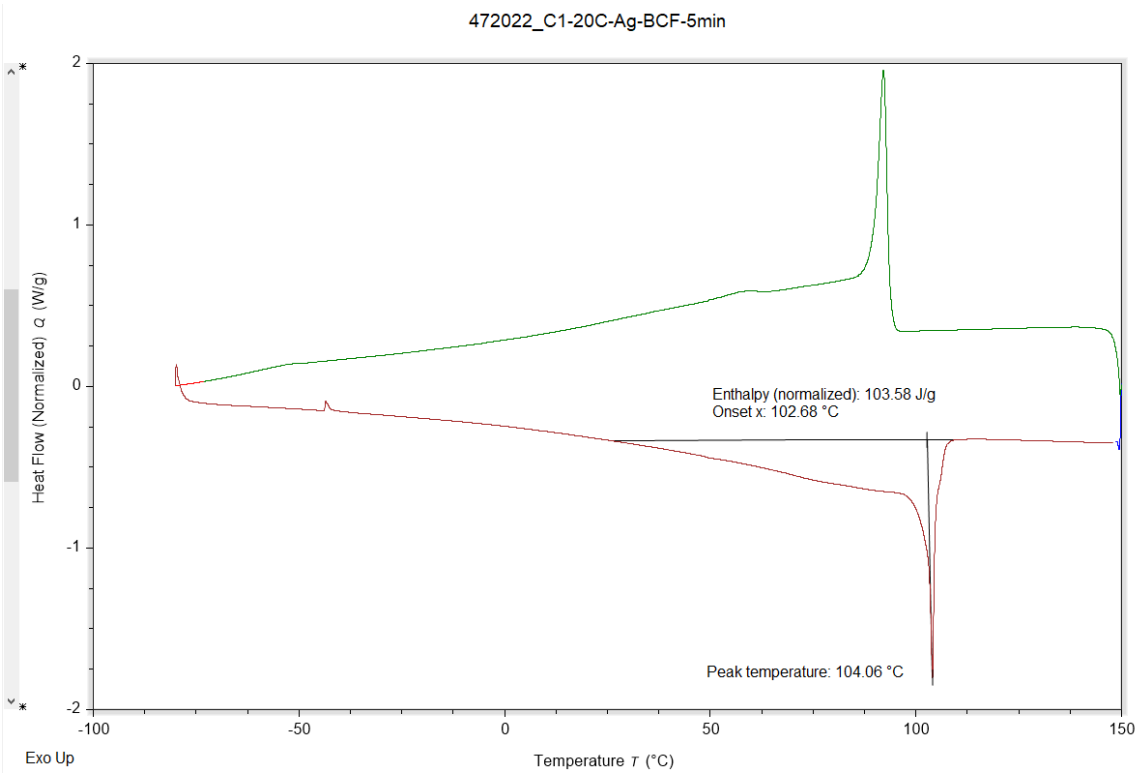

Figure S103. DSC of polymer in entry 5, Table 1.

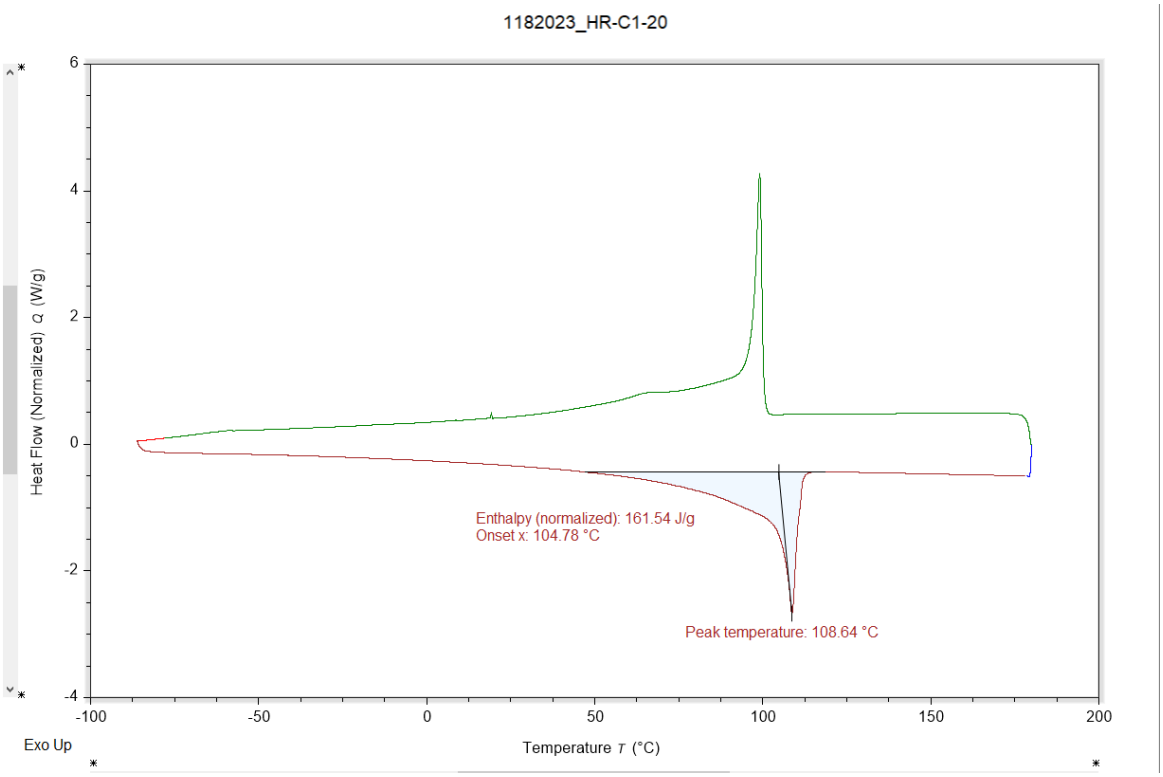

Figure S104. DSC of polymer in entry 6, Table 1.

4.3.2 DSC Traces of Table 2

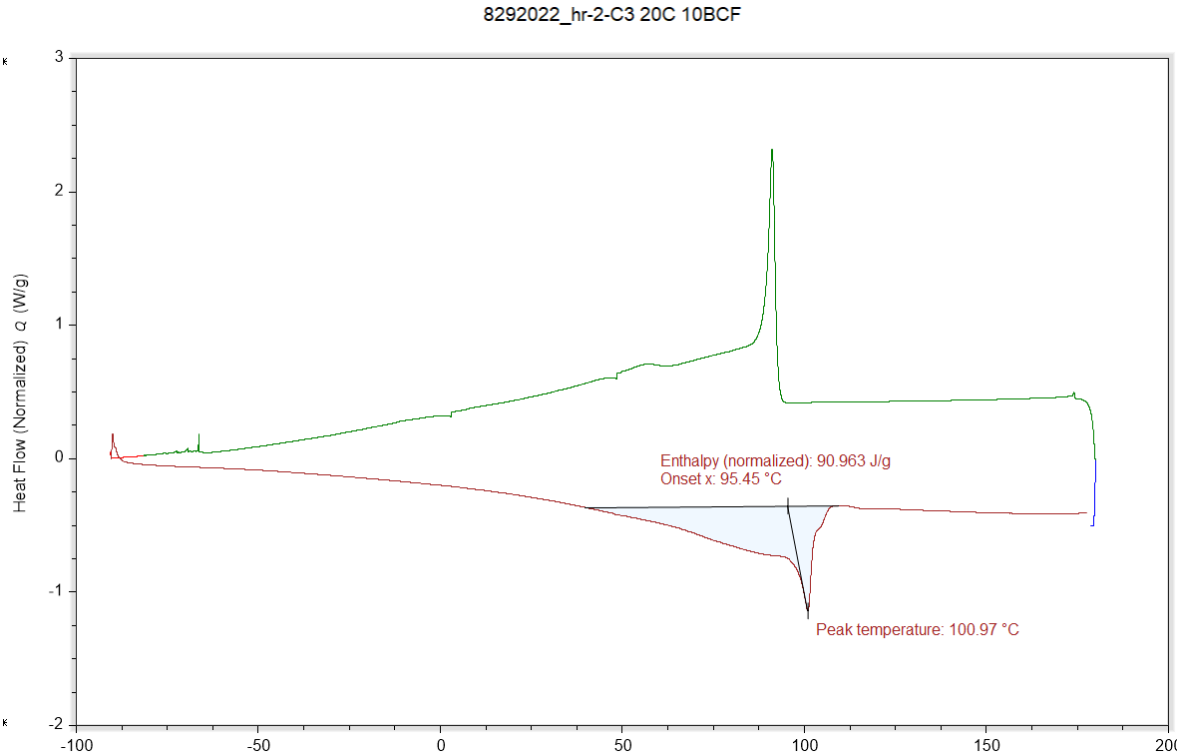

Figure S105. DSC of polymer in entry 2, Table 2

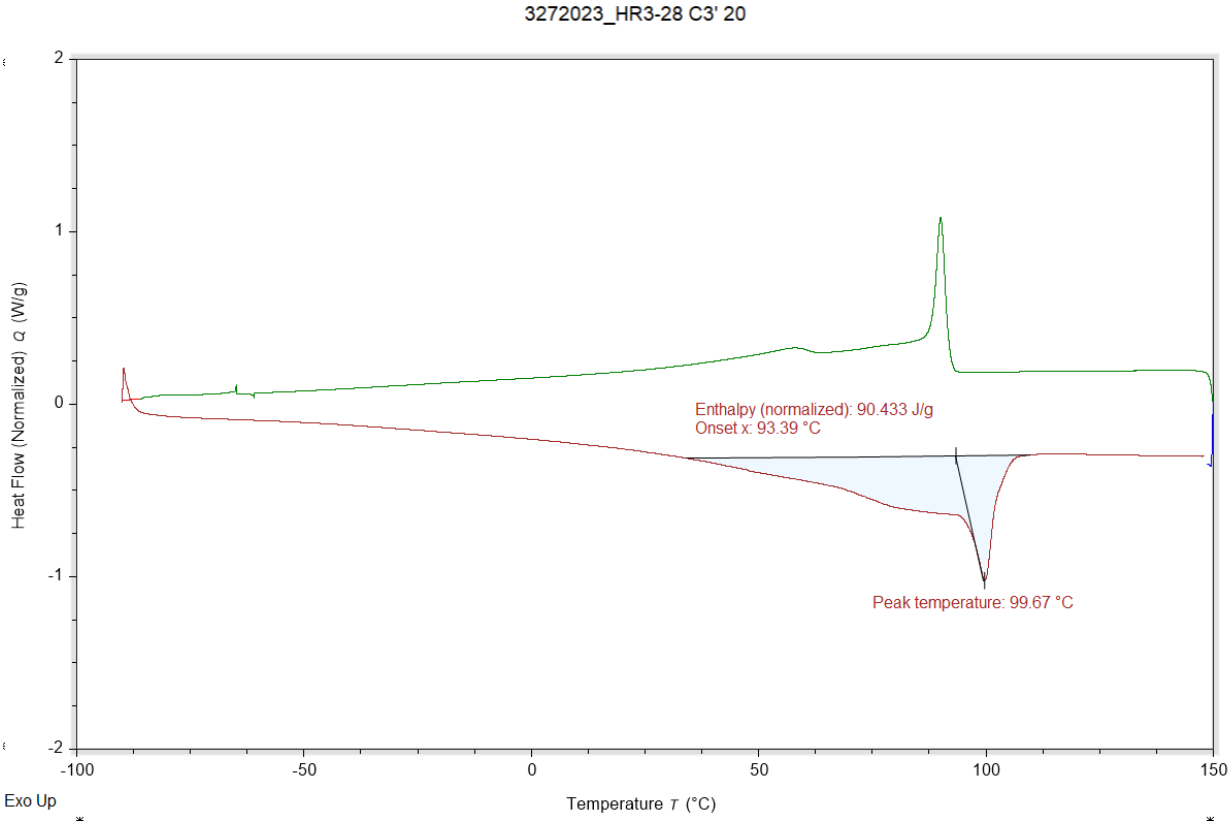

Figure S106. DSC of polymer in entry 3, Table 2.

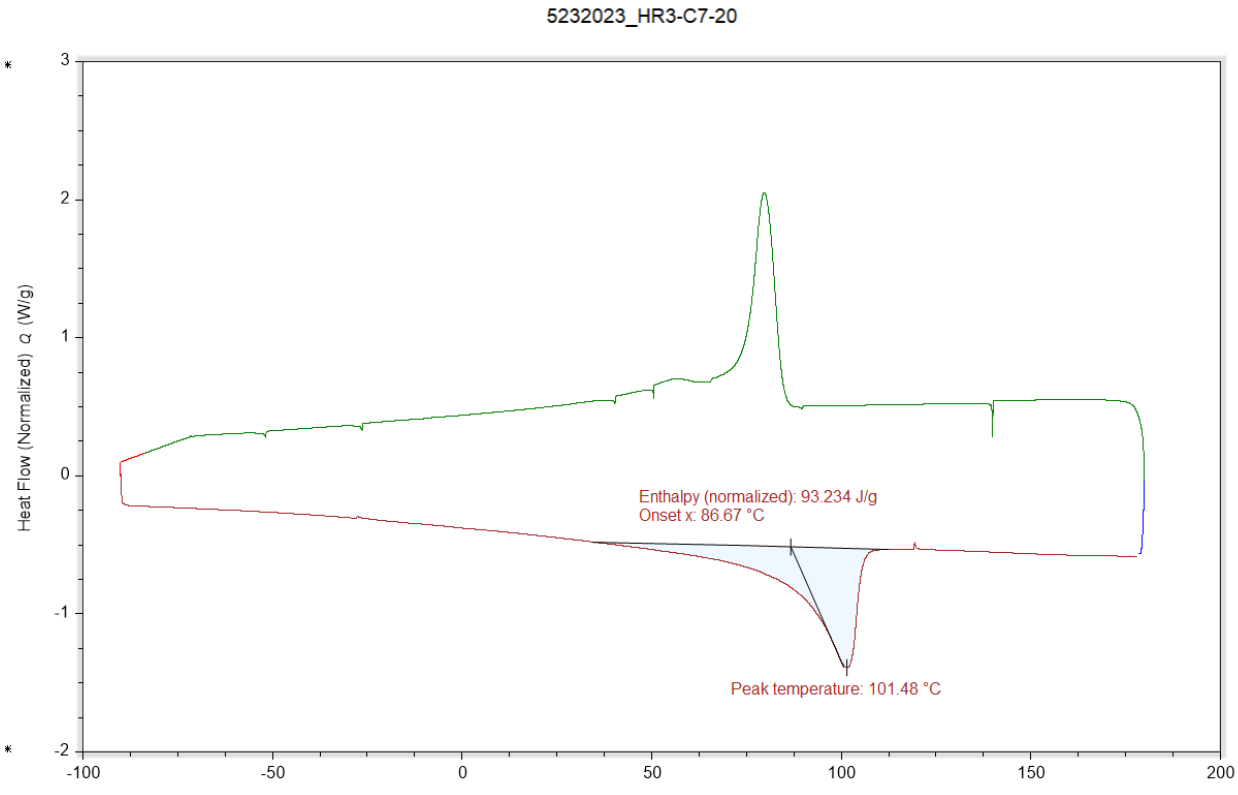

Figure S107. DSC of polymer in entry 4, Table 2.

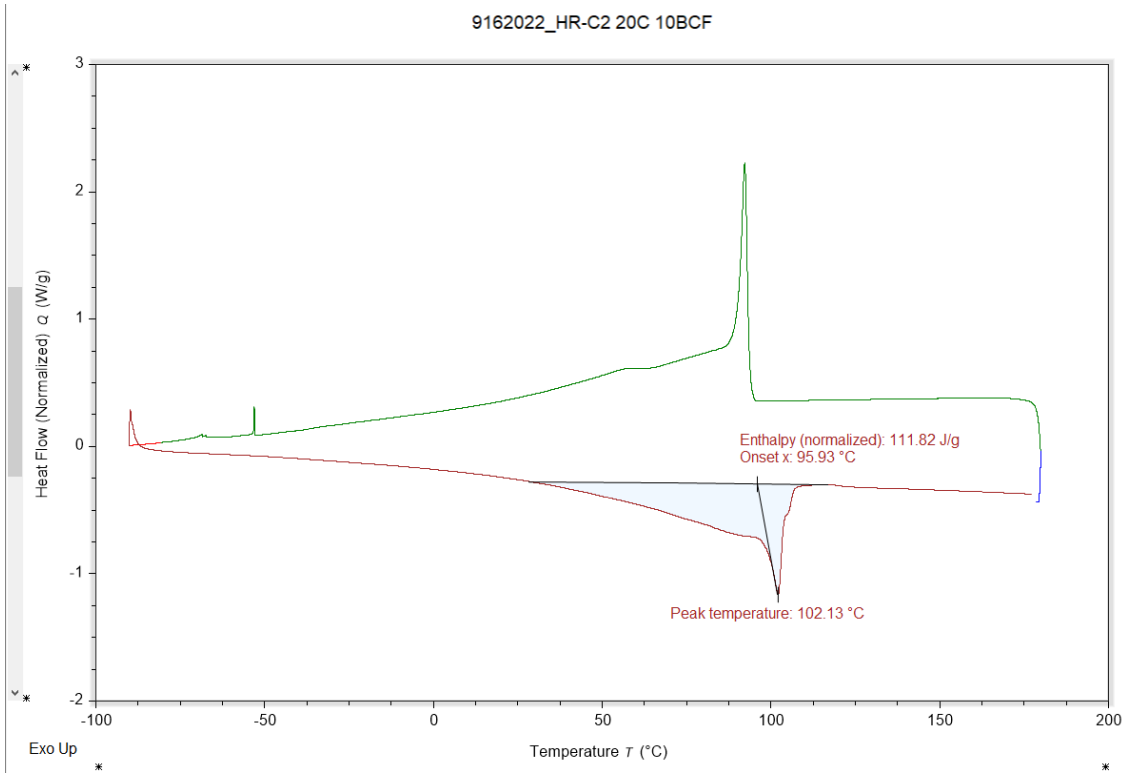

Figure S108. DSC of polymer in entry 5, Table 2.

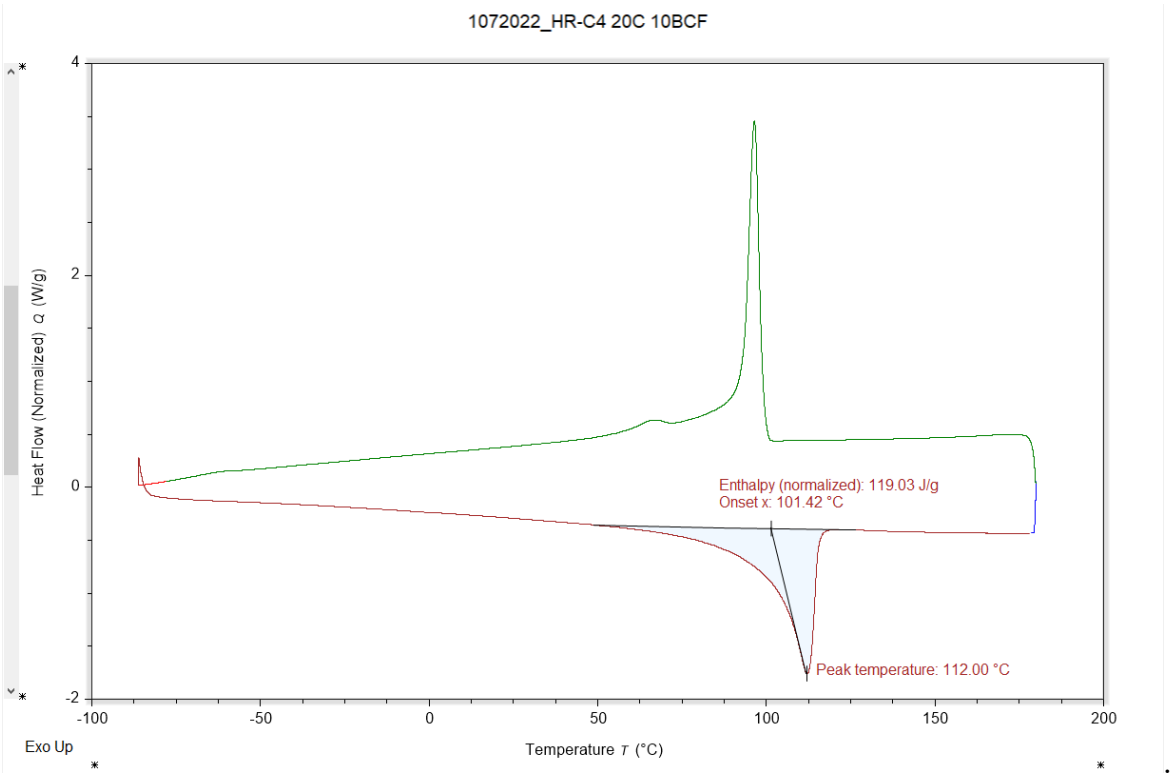

Figure S109. DSC of polymer in entry 6, Table 2.

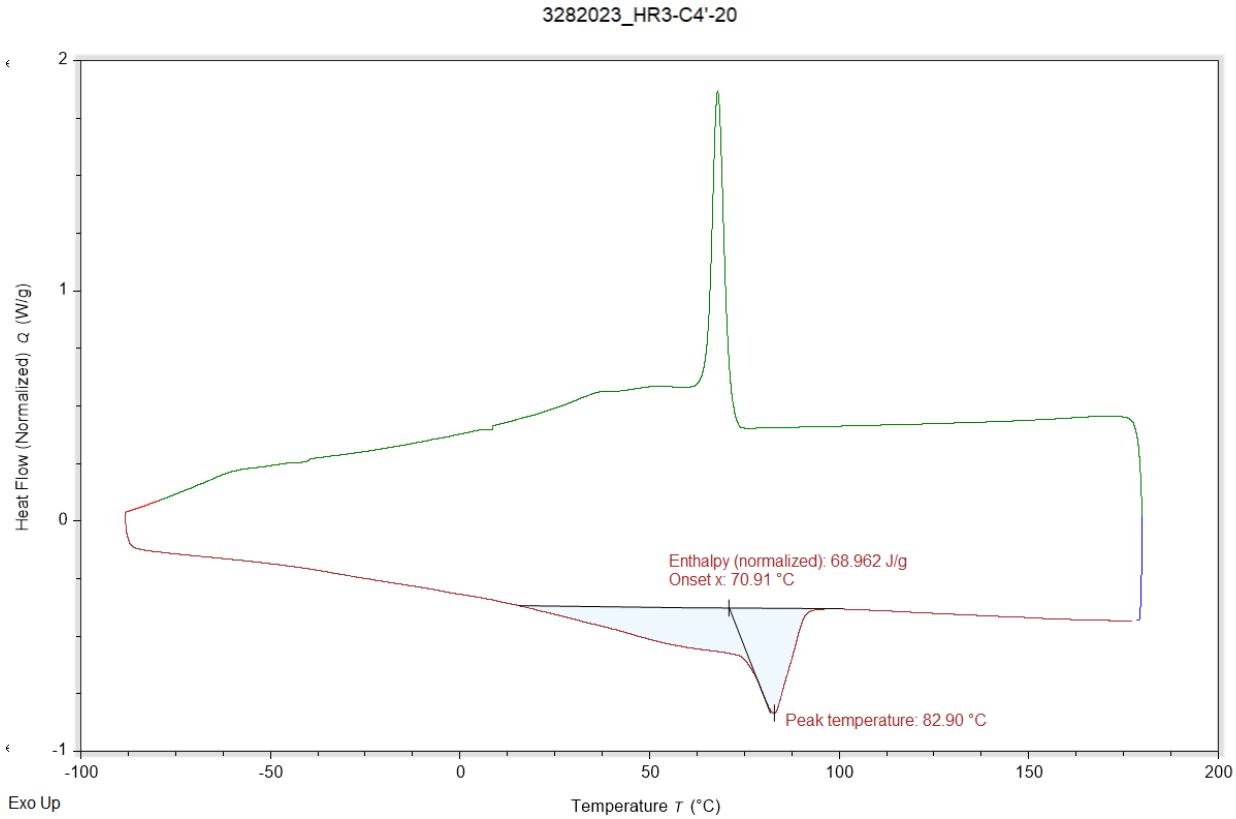

Figure S110. DSC of polymer in entry 7, Table 2.

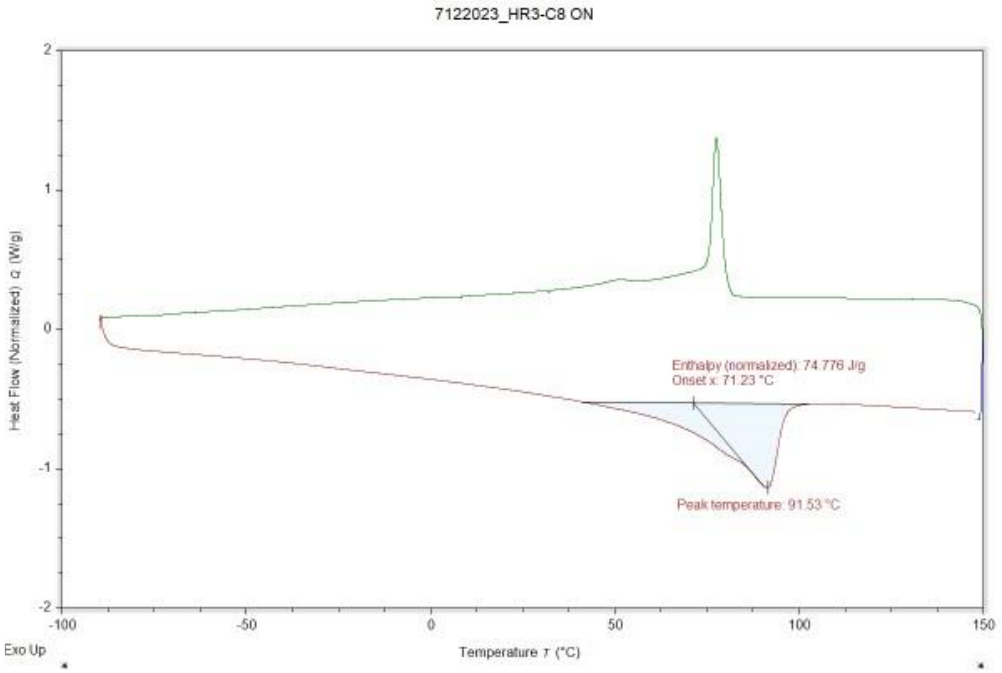

Figure S111. DSC of polymer in entry 8, Table 2.

4.3.3 DSC Traces of Table 3

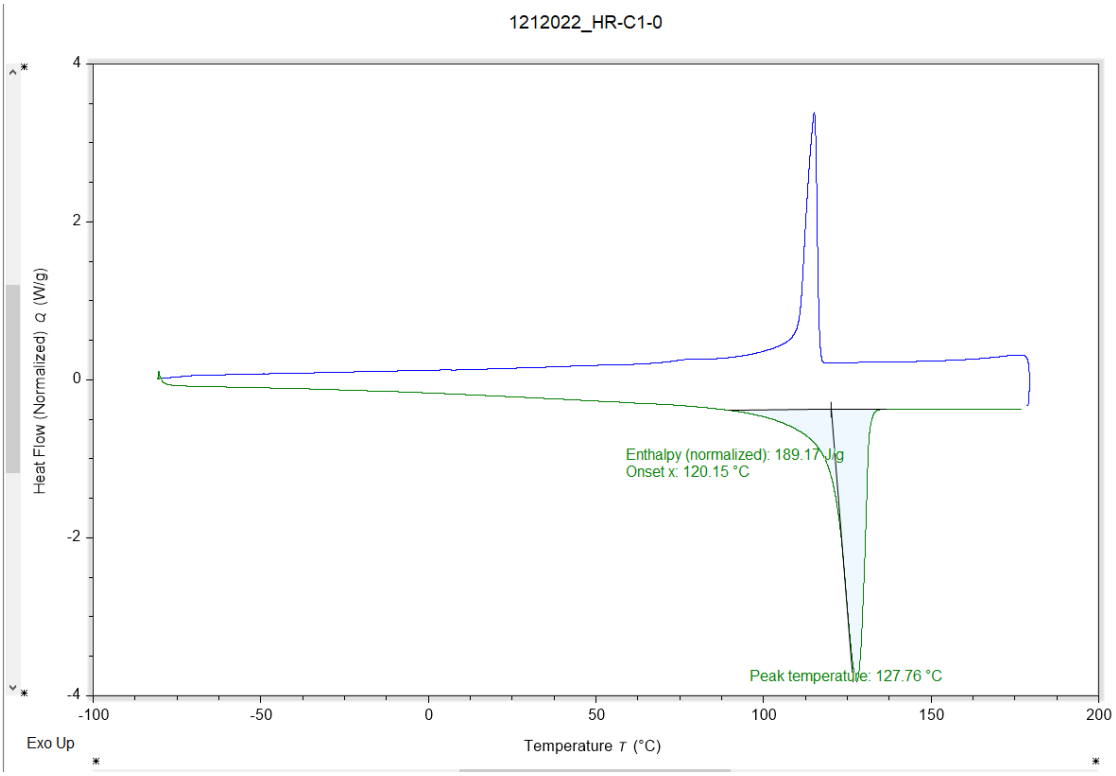

Figure S112. DSC of polymer in entry 1, Table 3.

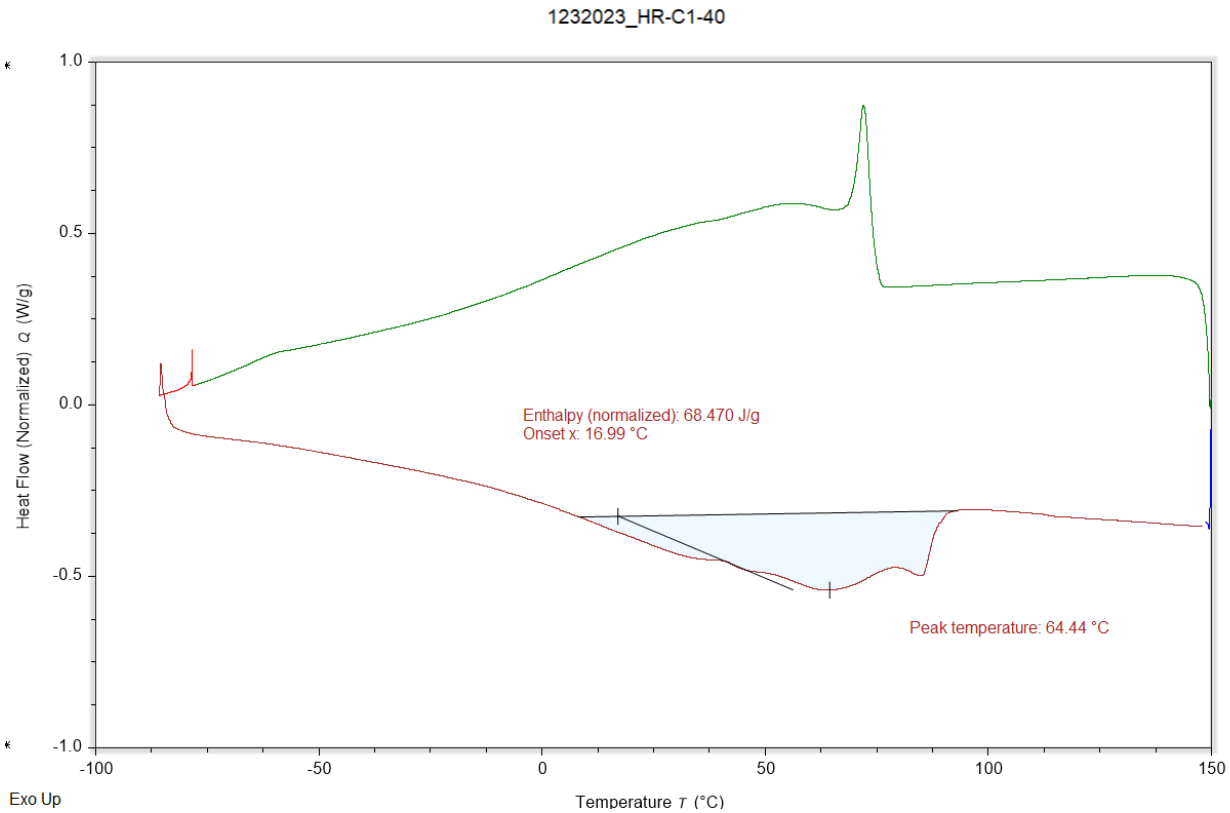

Figure S113. DSC of polymer in entry 3, Table 3.

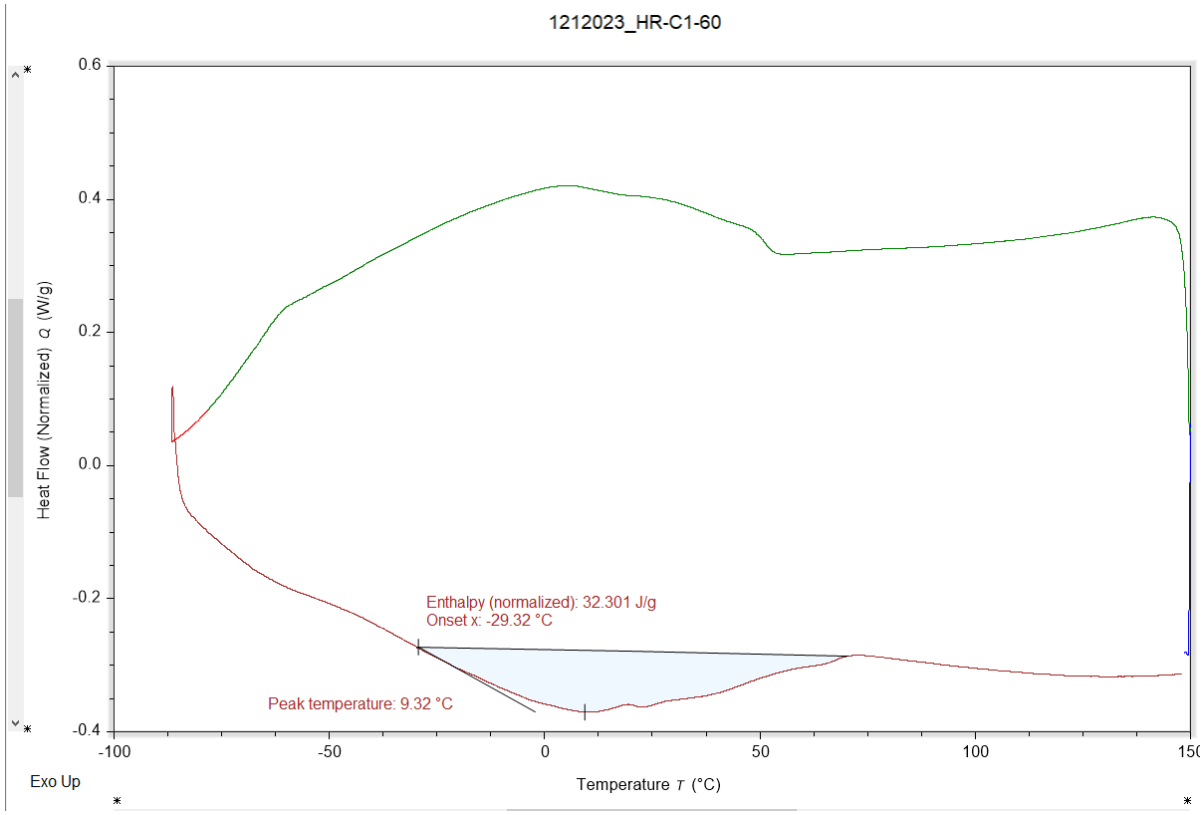

Figure S114. DSC of polymer in entry 4, Table 3.

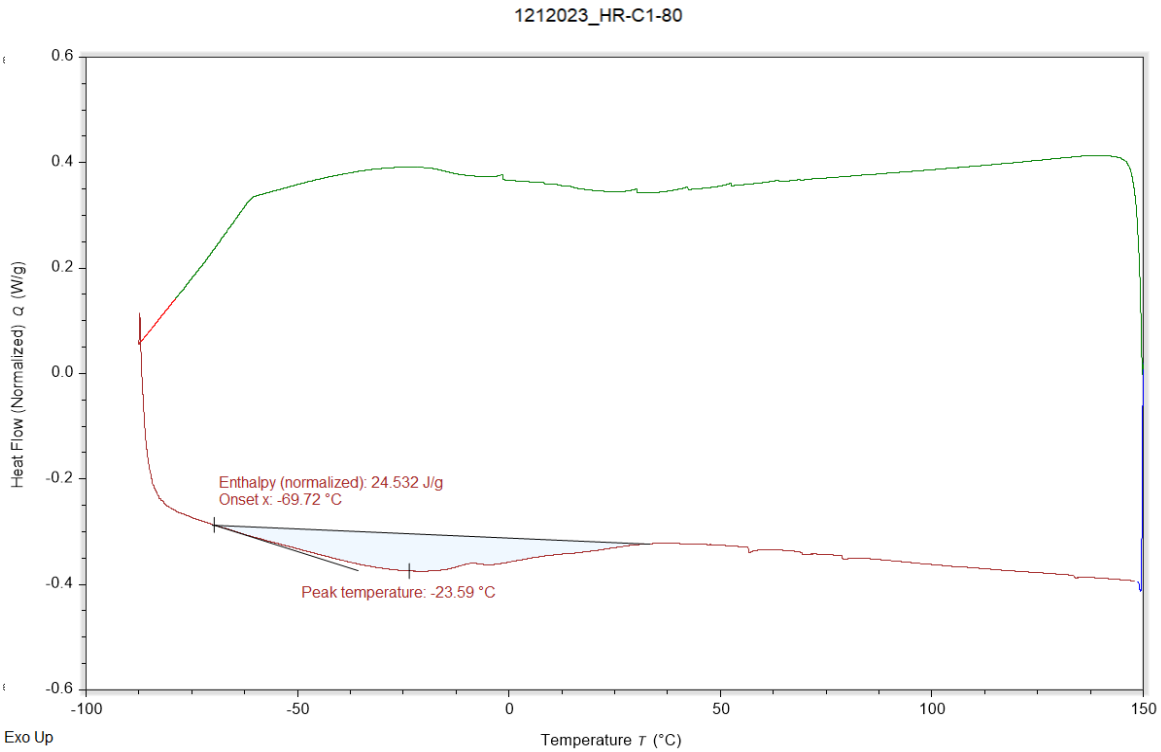

Figure S115. DSC of polymer in entry 5, Table 3.

4.3.4 DSC Traces of Table 4

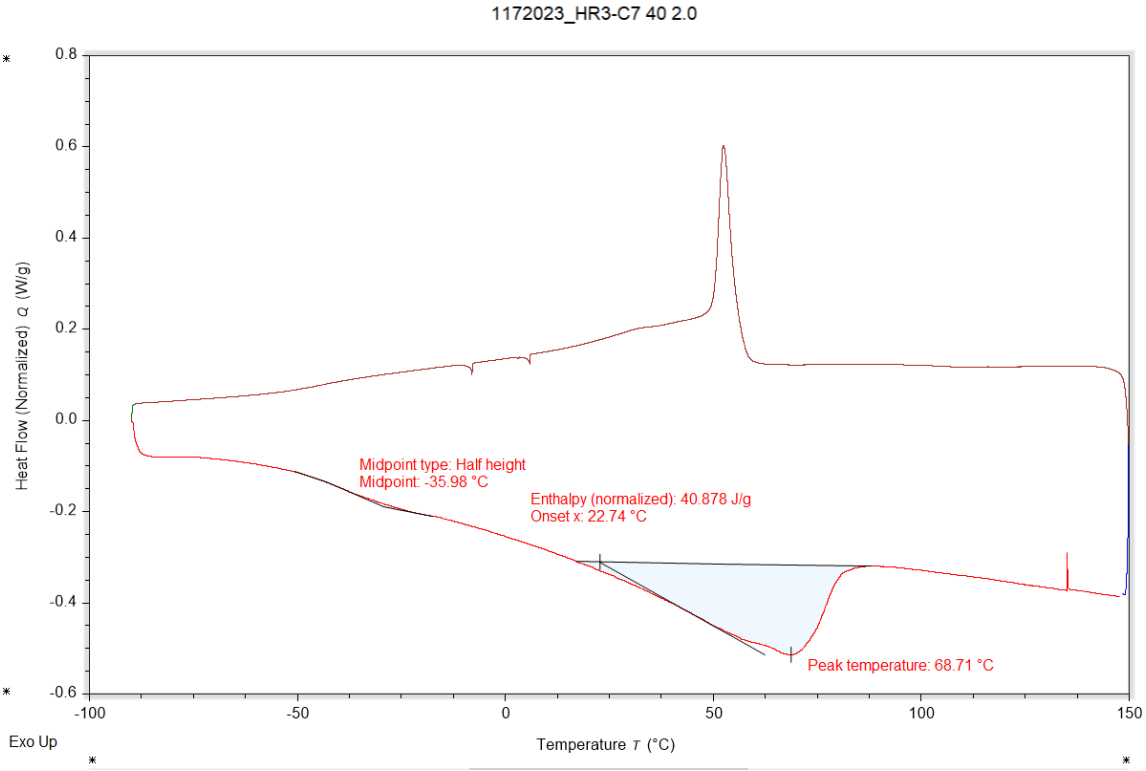

Figure S116. DSC of polymer in entry 1, Table 4.

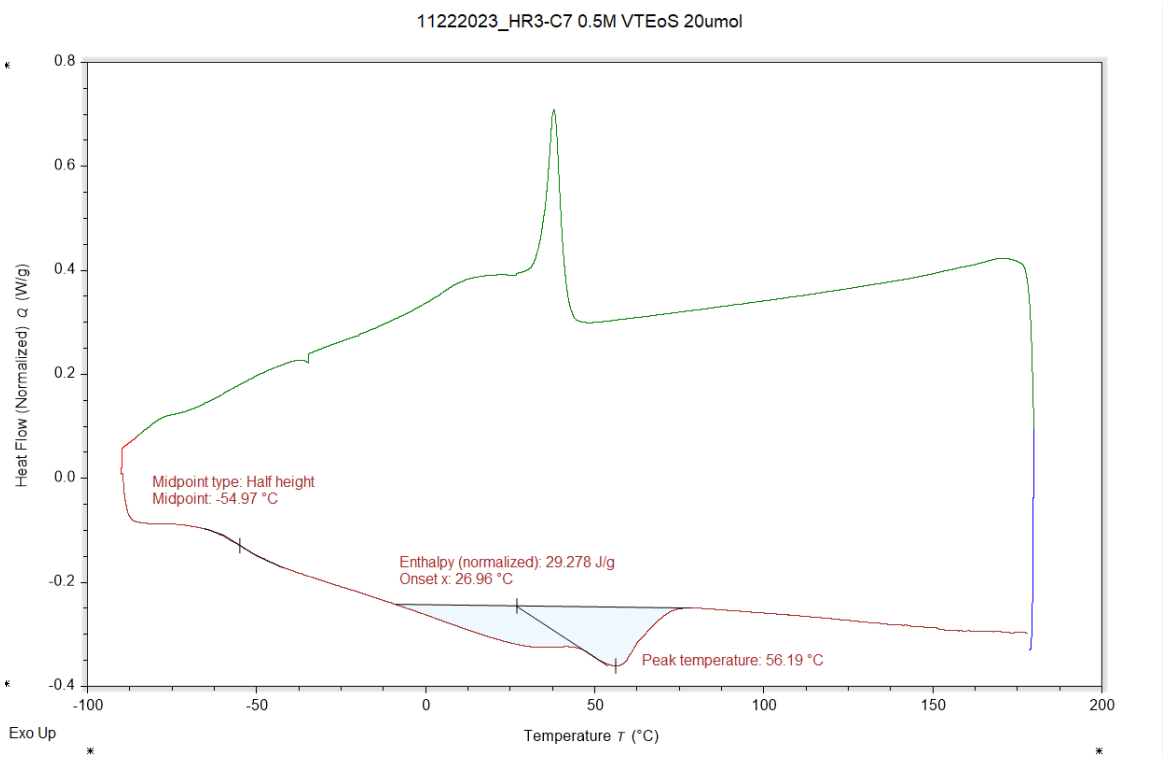

Figure S117. DSC of polymer in entry 2, Table 4.

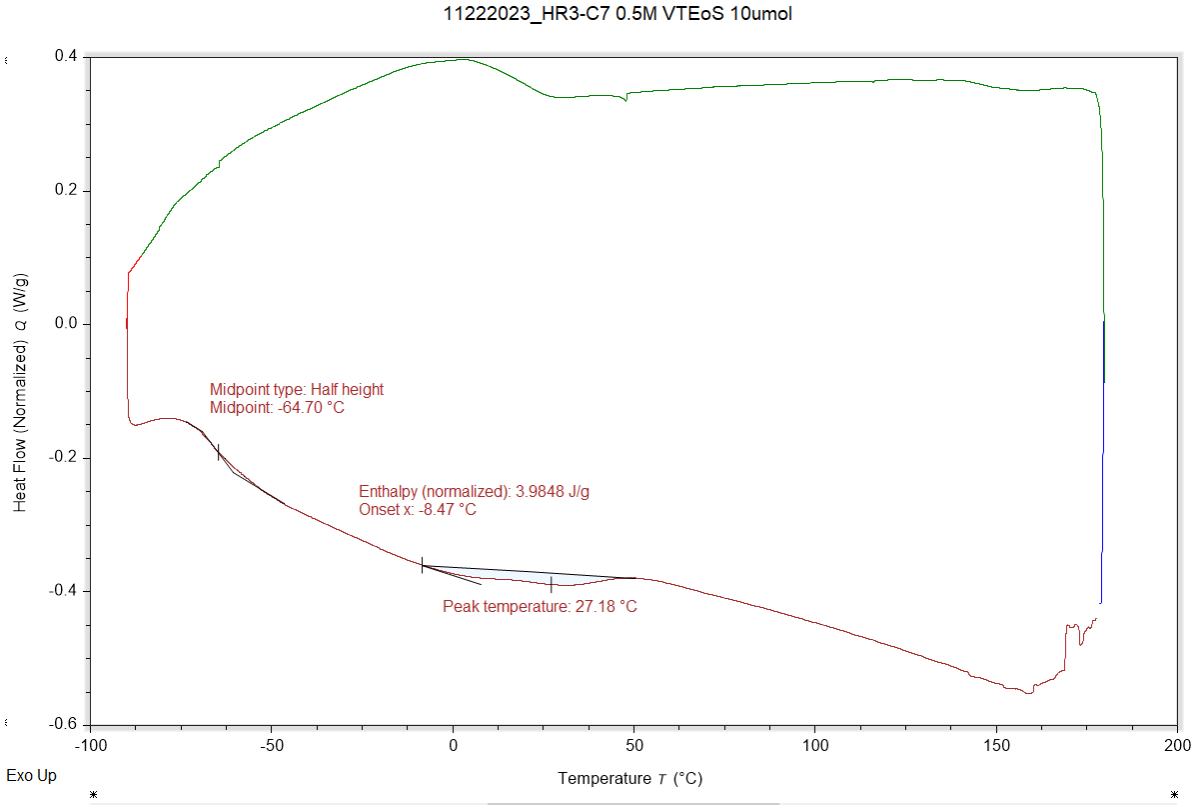

Figure S118. DSC of polymer in entry 3, Table 4.

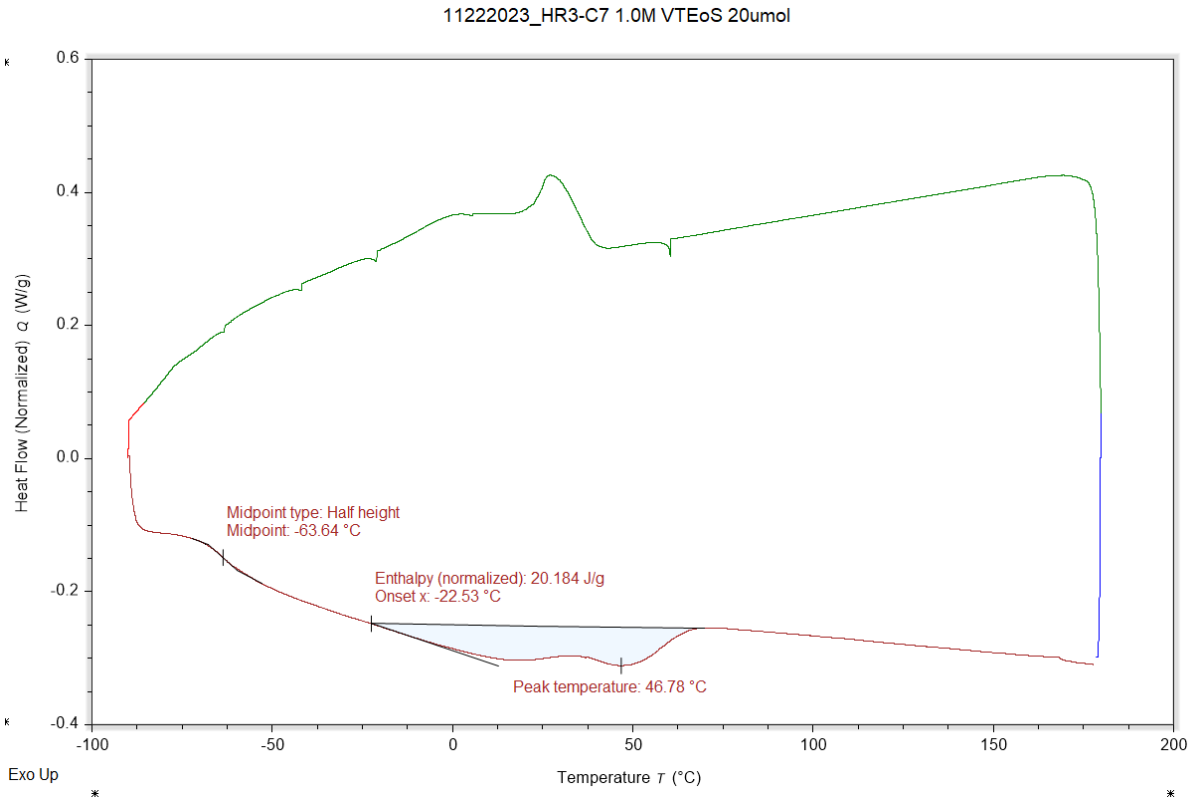

Figure S119. DSC of polymer in entry 4, Table 4.

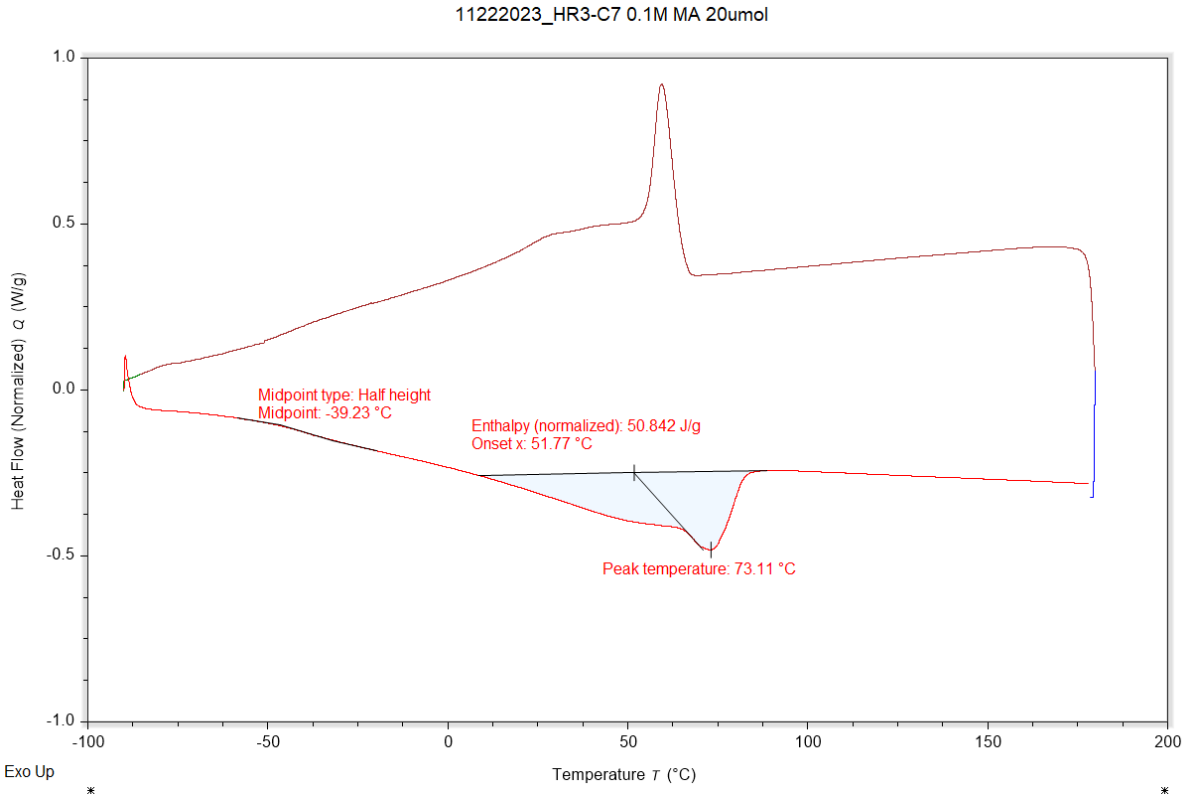

Figure S120. DSC of polymer in entry 5, Table 4.

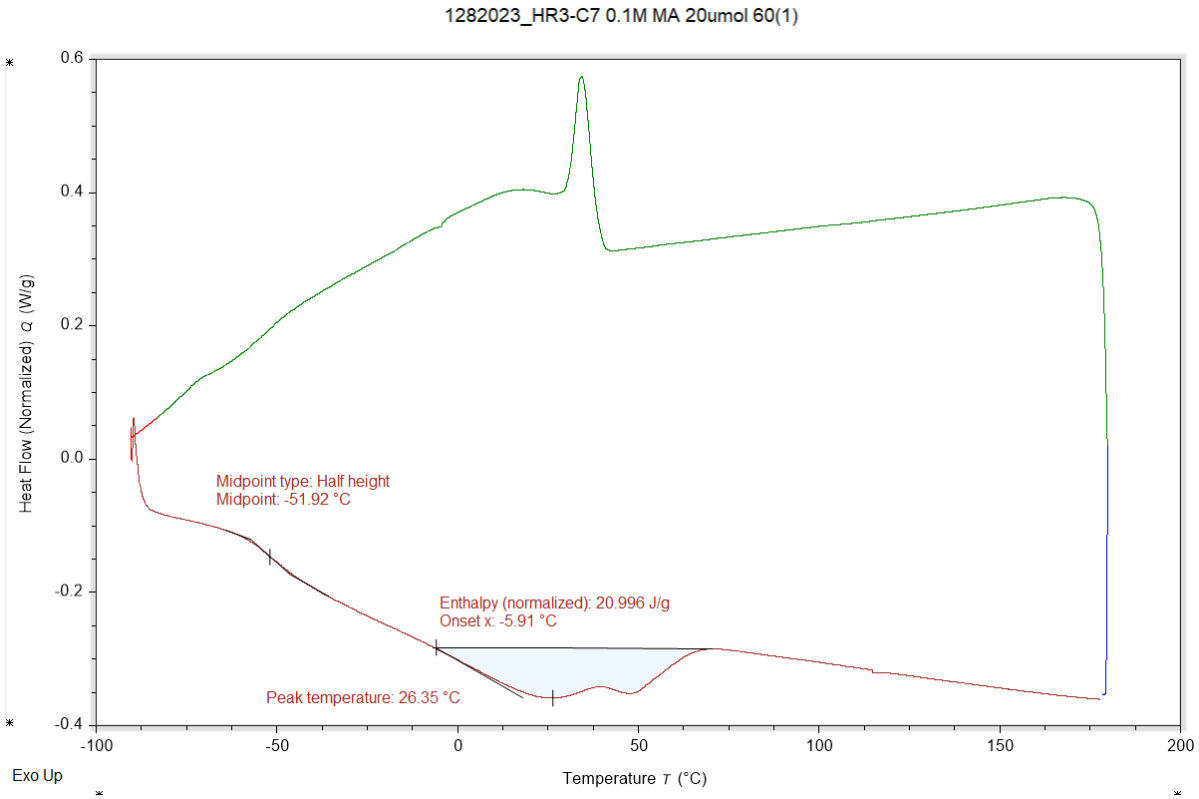

Figure S121. DSC of polymer in entry 6, Table 4.

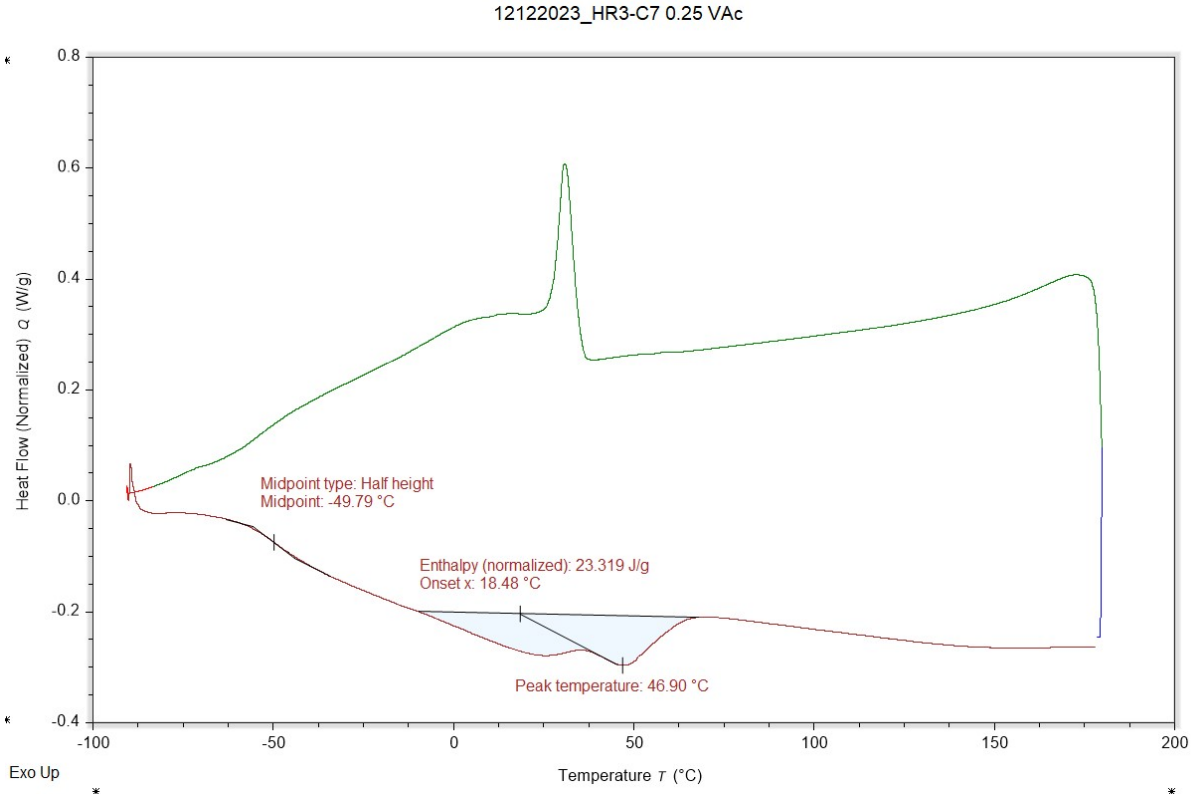

Figure S122. DSC of polymer in entry 7, Table 4.

4.3.5 DSC Traces of Table S1

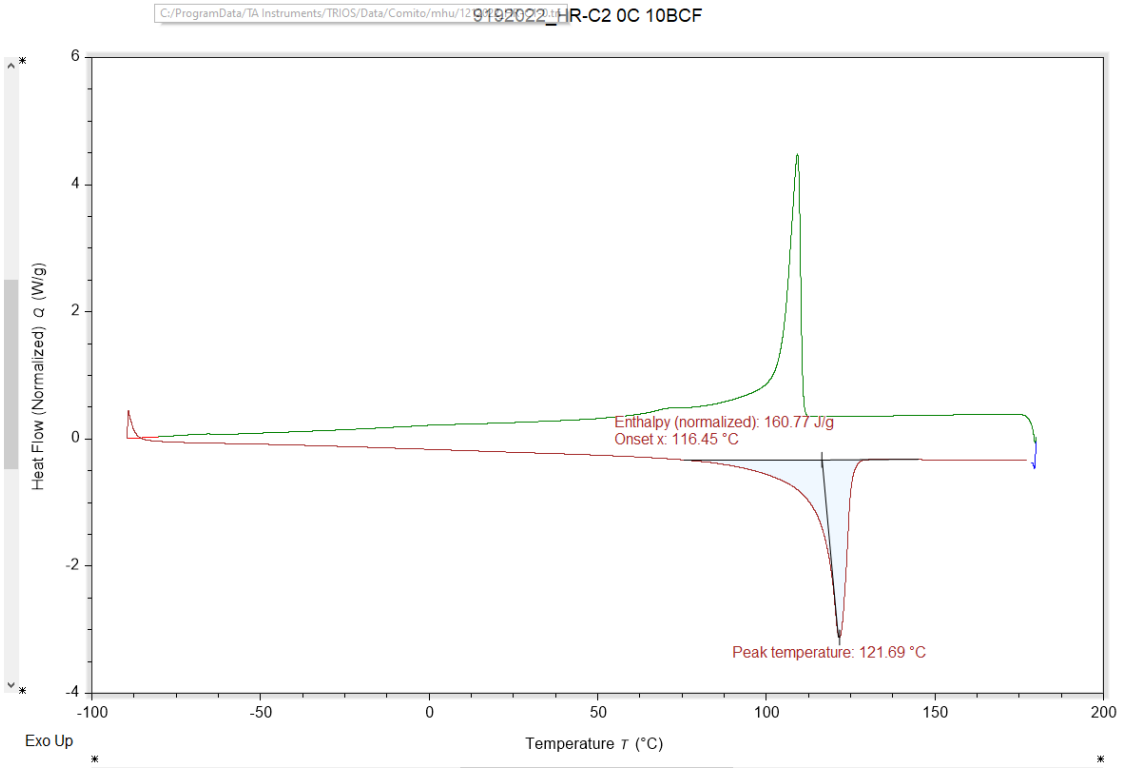

Figure S123. DSC of polymer in entry 1, Table S1.

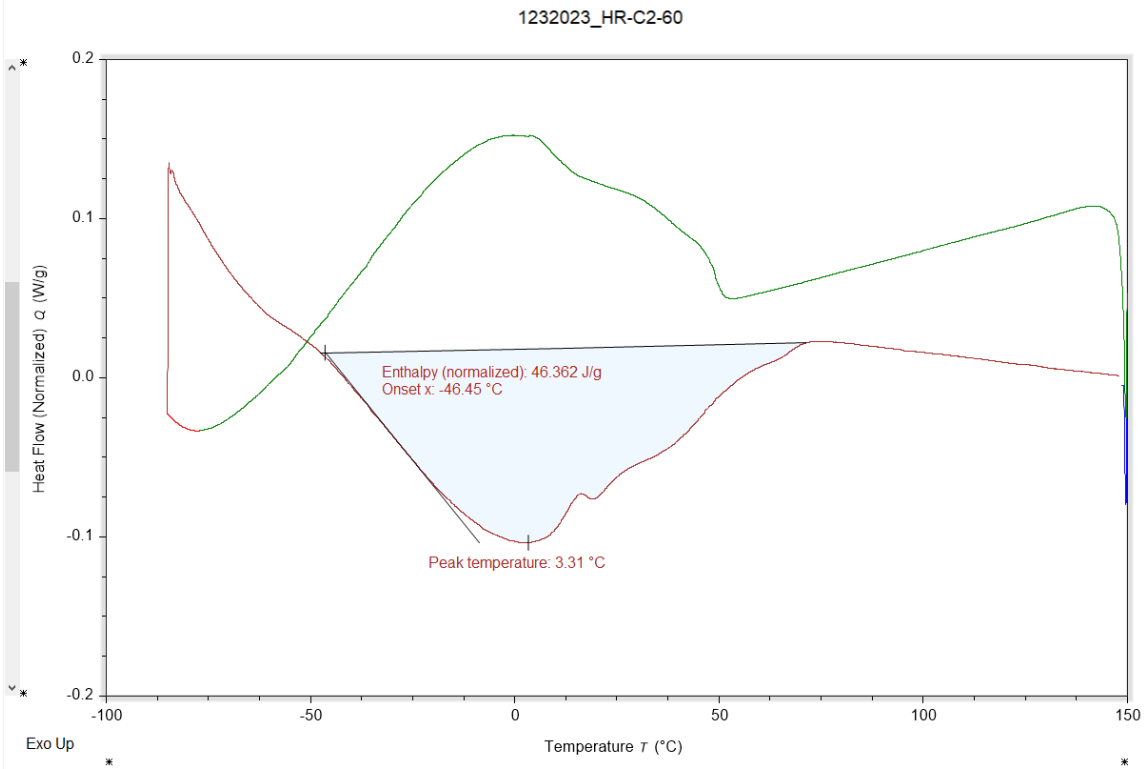

Figure S124. DSC of polymer in entry 2, Table S1.

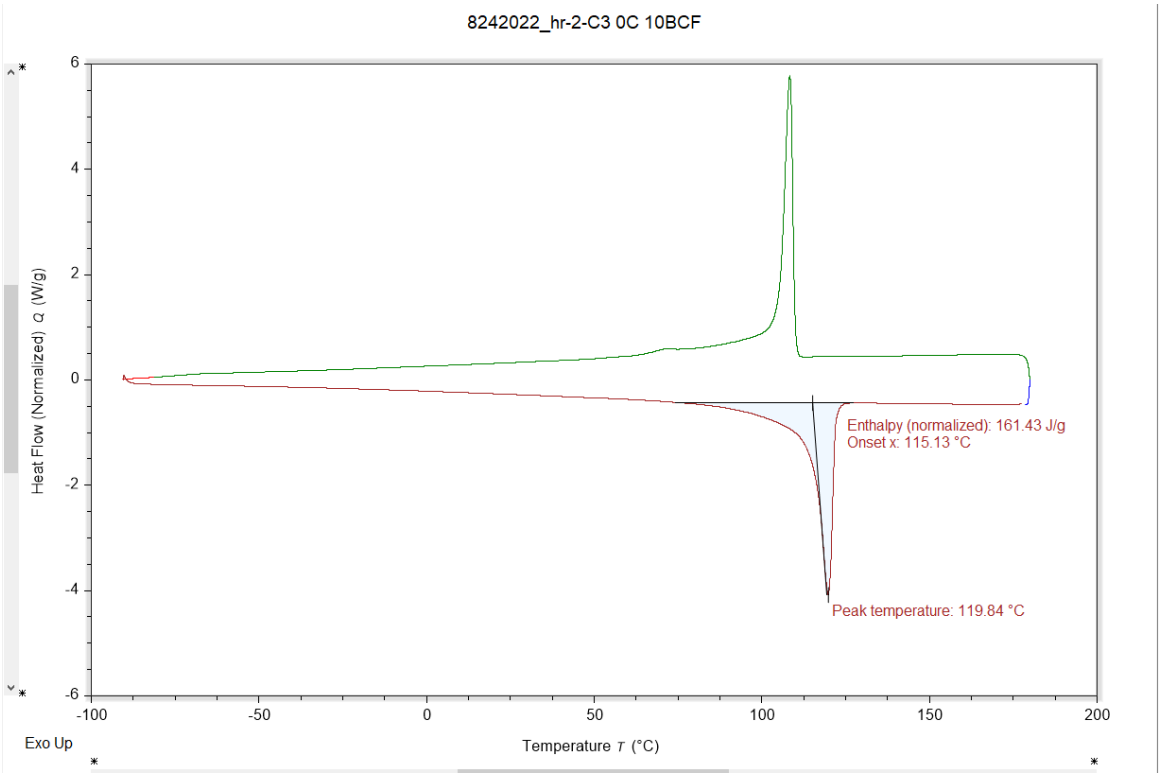

Figure S125. DSC of polymer in entry 3, Table S1.

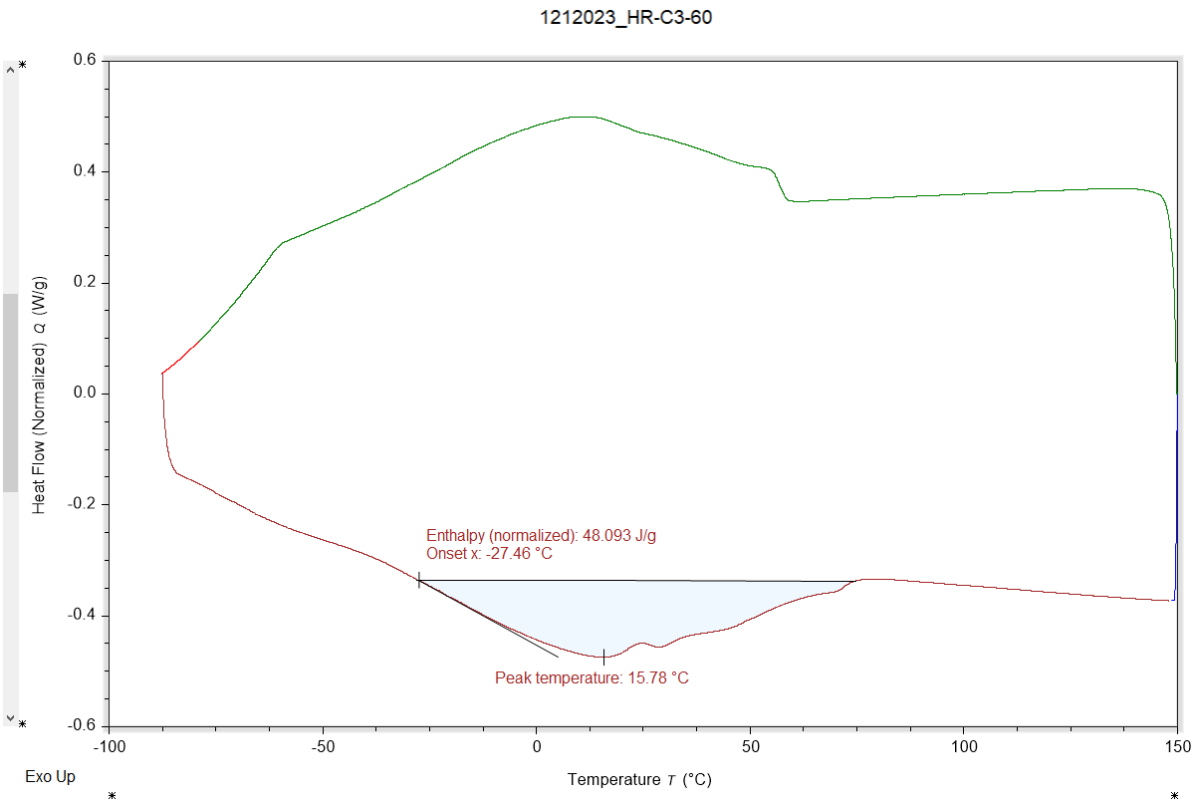

Figure S126. DSC of polymer in entry 4, Table S1.

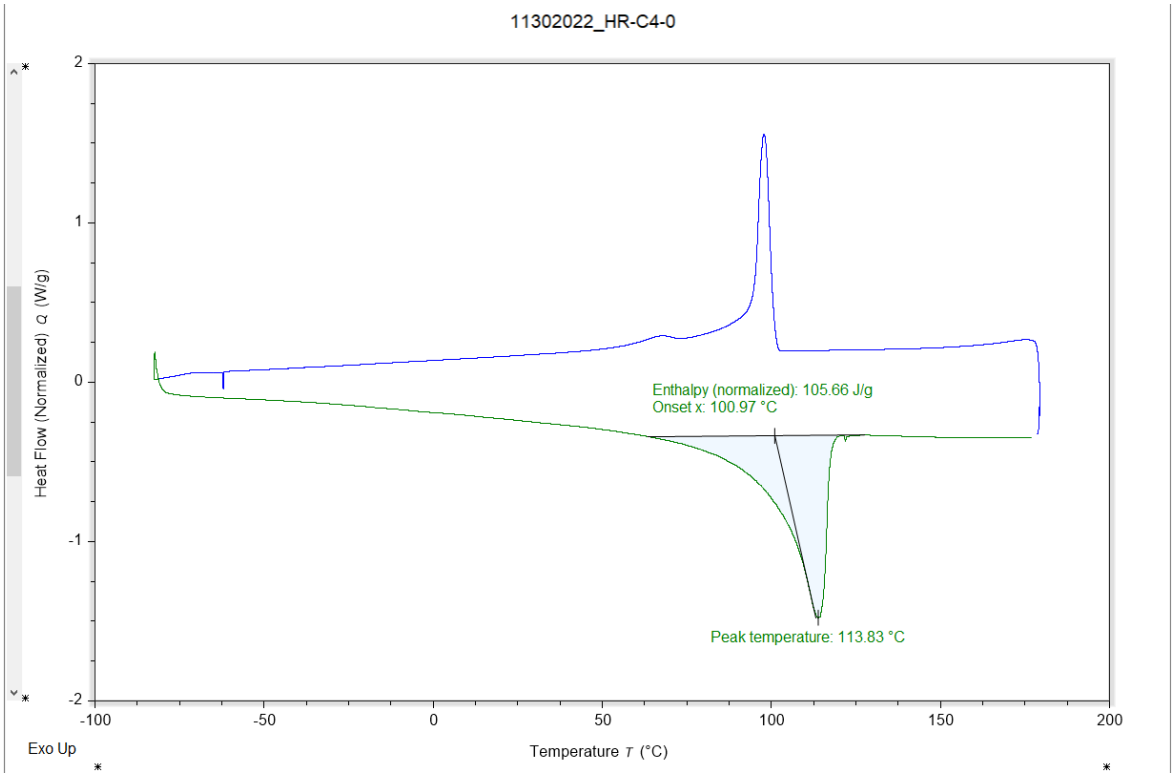

Figure S127. DSC of polymer in entry 5 Table S1.

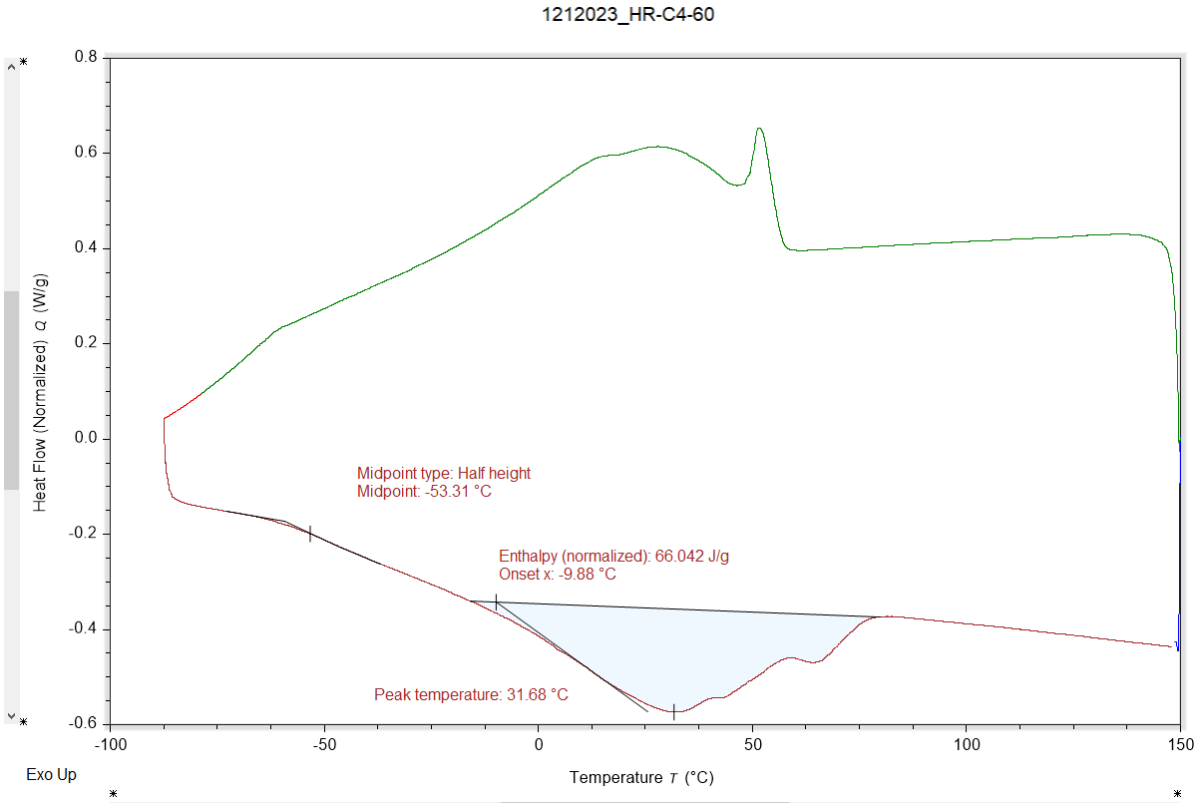

Figure S128. DSC of polymer in entry 6, Table S1.

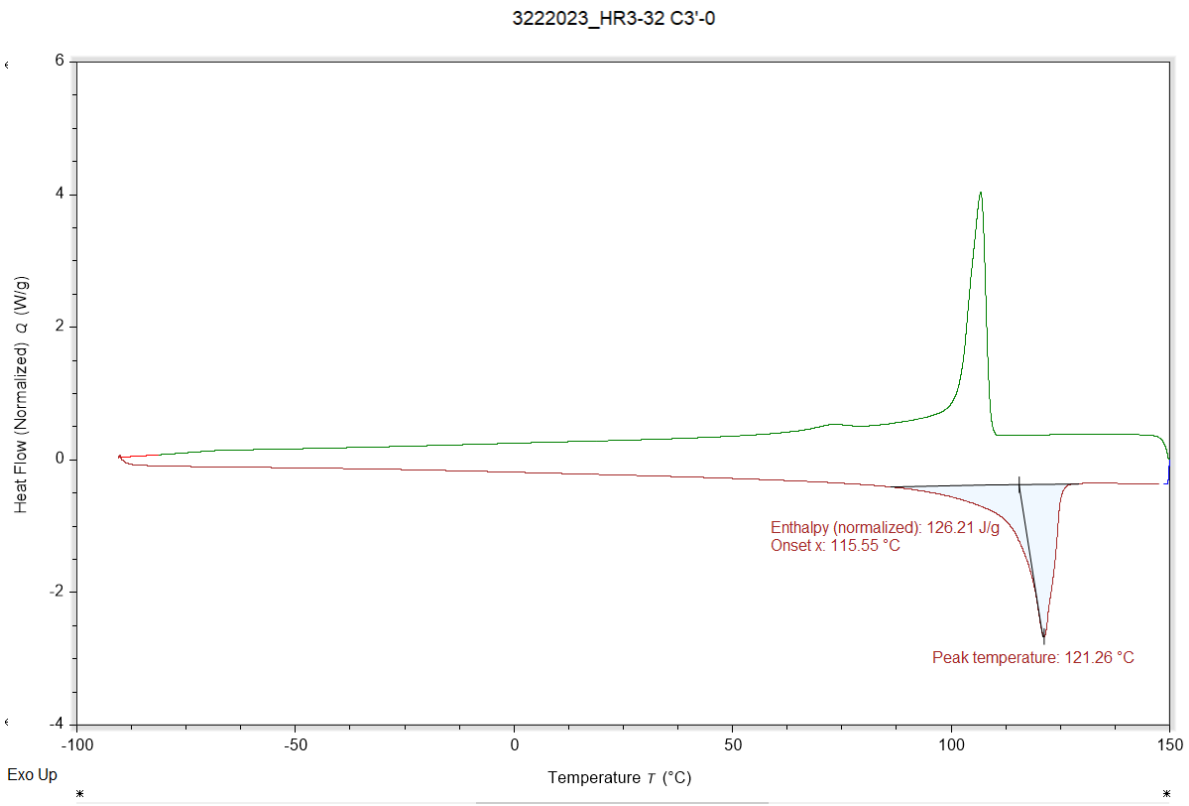

Figure S129. DSC of polymer in entry 7, Table S1.

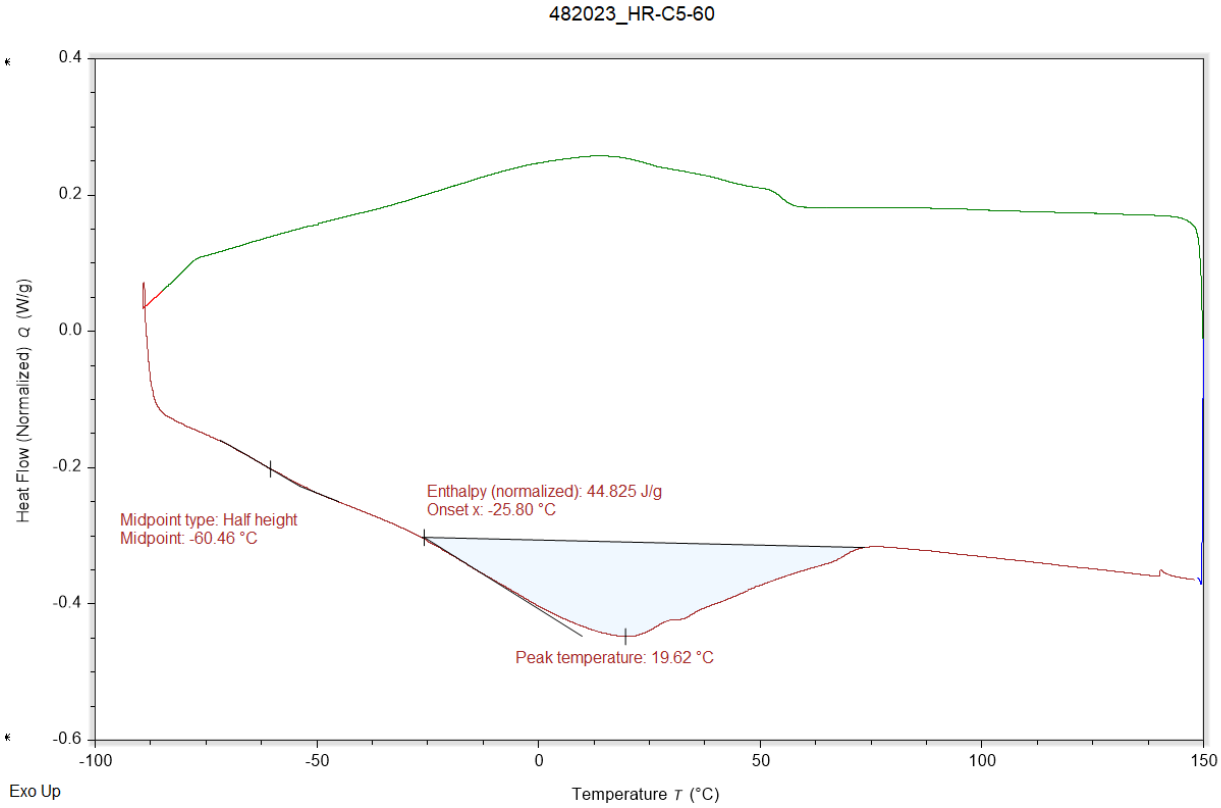

Figure S130. DSC of polymer in entry 8, Table S1.

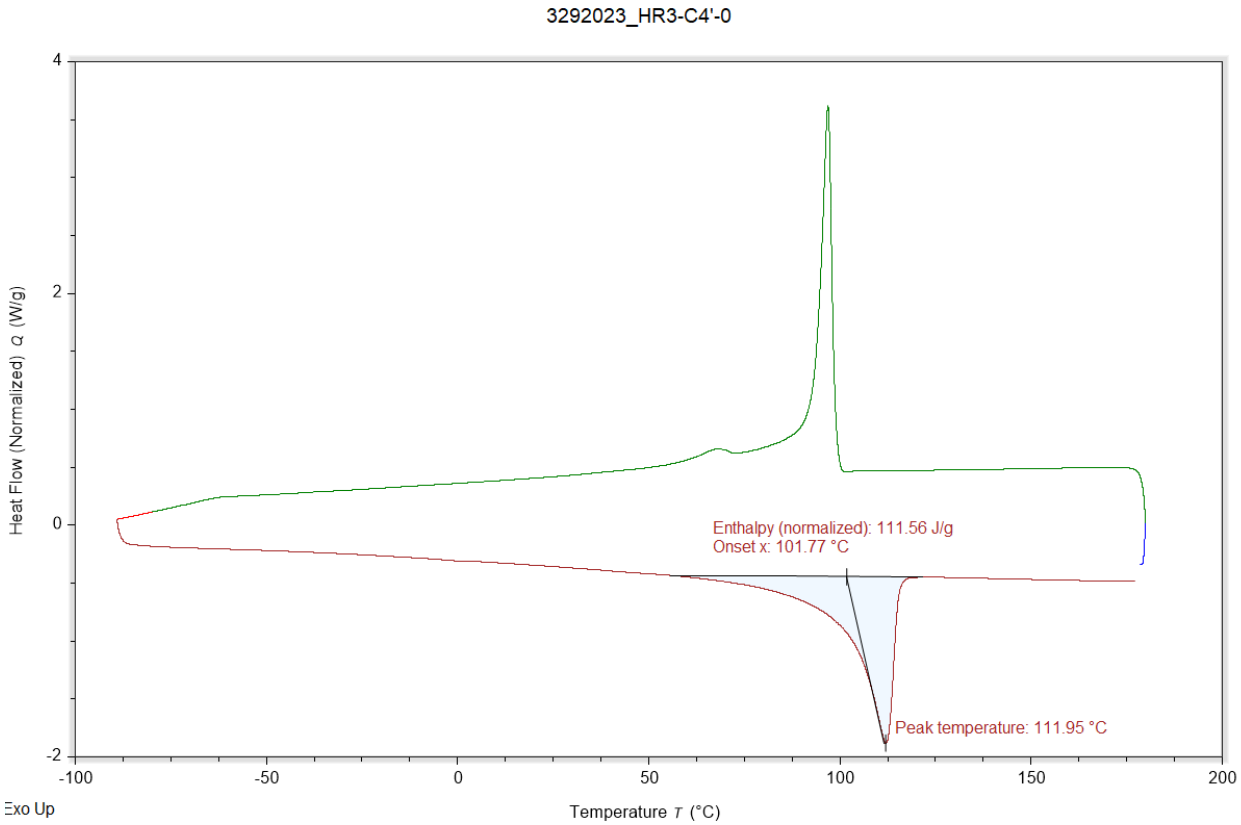

Figure S131. DSC of polymer in entry 9, Table S1.

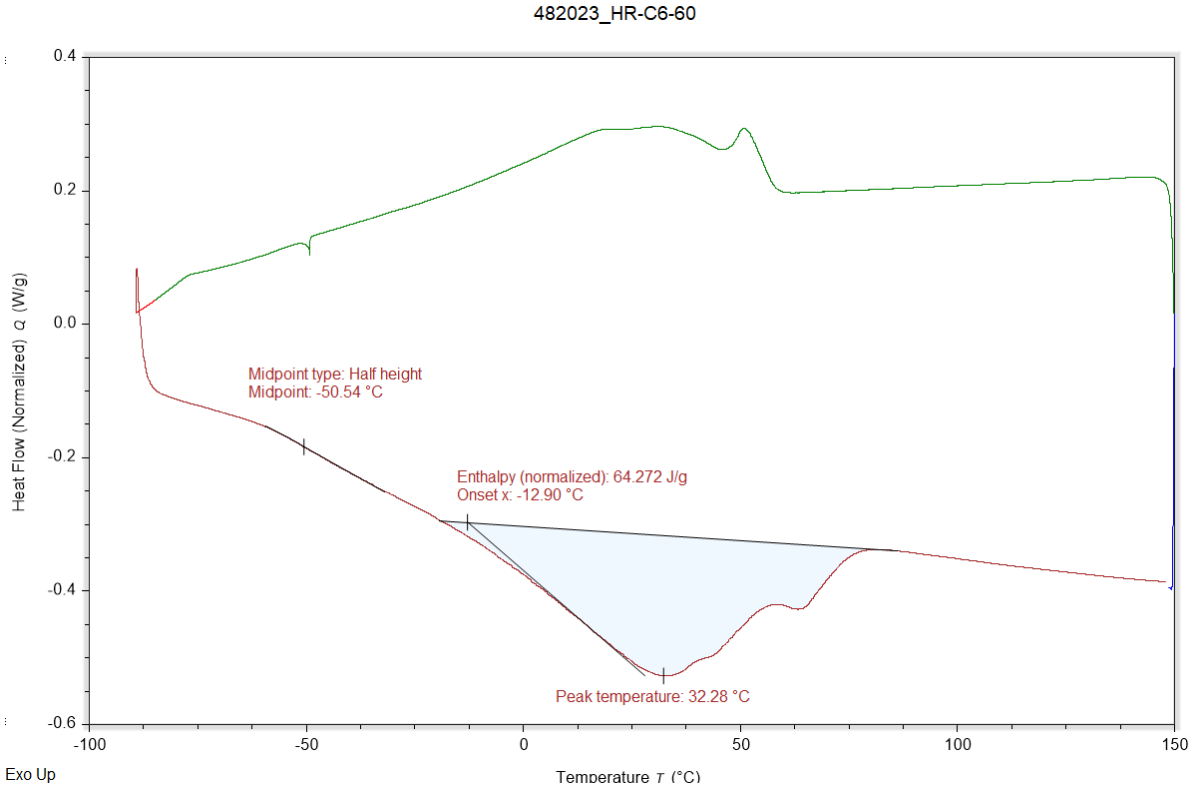

Figure S132. DSC of polymer in entry 10, Table S1.

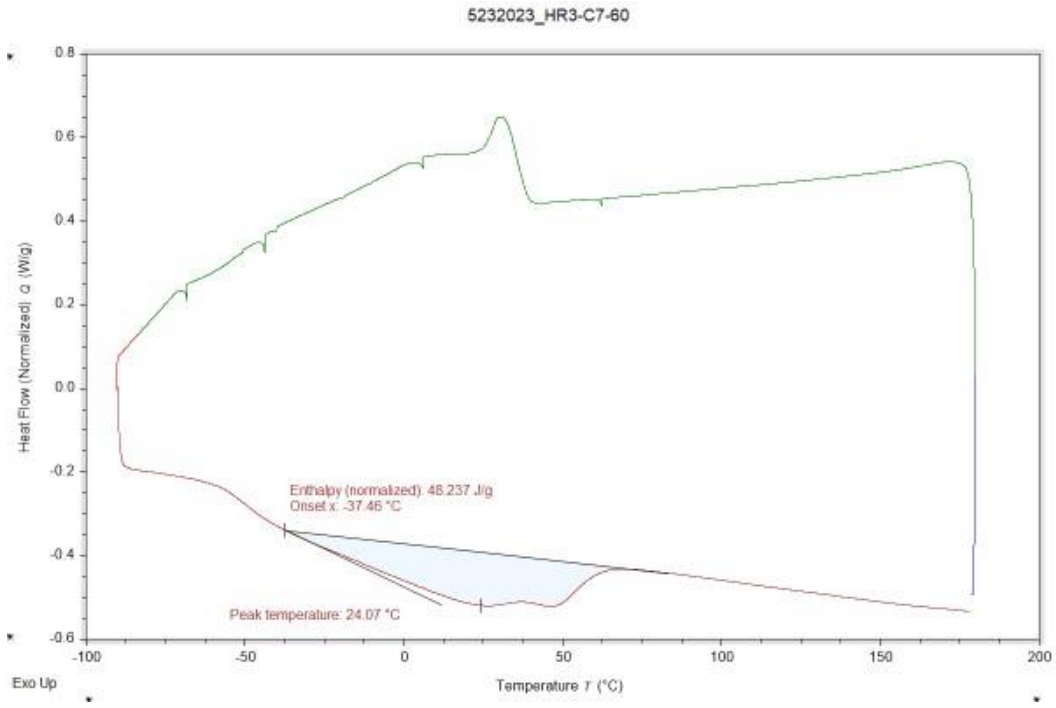

Figure S133. DSC of polymer in entry 11, Table S1.

5. X-ray Crystallographic Information of Complexes

The X-Ray measurements were made with a Bruker DUO platform diffractometer equipped with a 4K CCD APEX II detector and an Incoatec 30-Watt Cu microsource with compact multilayer optics. Data were collected using a narrow-frame algorithm with scan widths of 0.50\% in omega at 4 cm detector distance. The data were integrated using the Bruker SAINT program, with the intensities corrected for Lorentz factor, polarization, air absorption, and absorption due to variation in the path length through the detector faceplate. The data were scaled, and an absorption correction was applied using SADABS. The structure was solved with SHELXT 2018, and refined with SHELXL 2018 using full-matrix least-squares refinement. The non-H atoms were refined with anisotropic thermal parameters, and all of the H atoms were calculated in idealized positions and refined riding on their parent atoms.

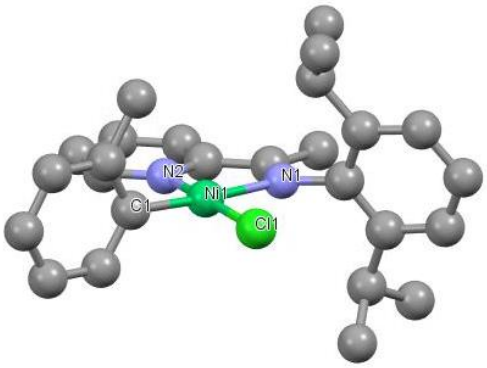

Figure S134. Molecular structure of Ni complex **C1** (CCDC number: 2320312). Hydrogen atoms are omitted for clarity. Thermal ellipsoids are shown in the 50% probability level. Select bond distances (Å) and angles (deg): Ni(1)–N(1) = 1.9911(12), Ni(1)–N(2) = 1.8969(13), Ni(1)–C(1) = 1.8974(15), Ni(1)–Cl(1) = 2.1562(7); N(2)–Ni(1)–N(1) = 82.22(5), N(2)–Ni(1)–C(1) = 95.24(6), C(1)–Ni(1)–Cl(1) = 87.52(5), N(1)–Ni(1)–Cl(1) = 95.18(4).

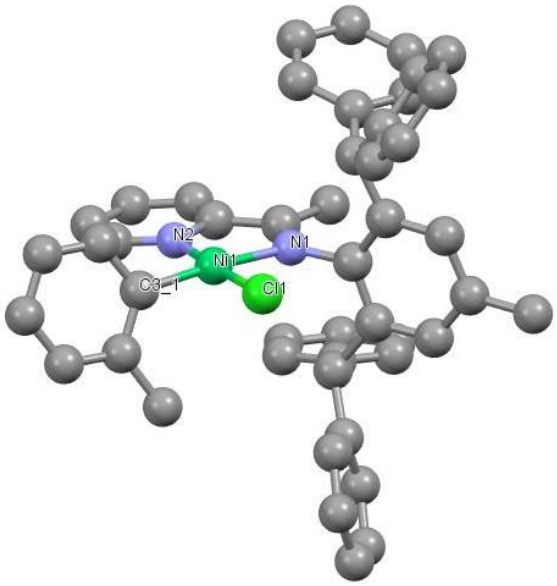

Figure S135. Molecular structure of Ni complex **C3** (CCDC number: 2320311). Hydrogen atoms are omitted for clarity. Thermal ellipsoids are shown in the 50% probability level. Select bond distances (Å) and angles (deg): Ni(1)–N(1) = 1.980(2), Ni(1)–N(2) = 1.905(2), Ni(1)–C(3_1) = 1.888(9), Ni(1)–Cl(1) = 2.1554(9); N(2)–Ni(1)–N(1) = 81.96(10), N(2)–Ni(1)–C(3_1) = 96.2(7), C(3_1)–Ni(1)–Cl(1) = 86.5(7), N(1)–Ni(1)–Cl(1) = 95.25 (7).

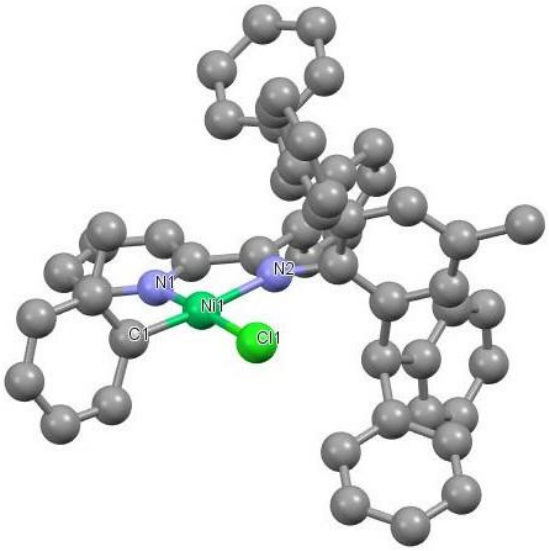

Figure S136. Molecular structure of Ni complex **C4** (CCDC number: 2320309). Hydrogen atoms are omitted for clarity. Thermal ellipsoids are shown in the 50% probability level. Select bond distances (Å) and angles (deg): Ni(1)–N(1) = 1.905(3), Ni(1)–N(2) = 2.013(3), Ni(1)–C(1) = 1.906(5), Ni(1)–Cl(1) = 2.136(10); N(2)–Ni(1)–N(1) = 82.63(12), N(1)–Ni(1)–C(1) = 94.65(15), C(1)–Ni(1)–Cl(1) = 86.95(12), N(2)–Ni(1)–Cl(1) = 96.07 (8).

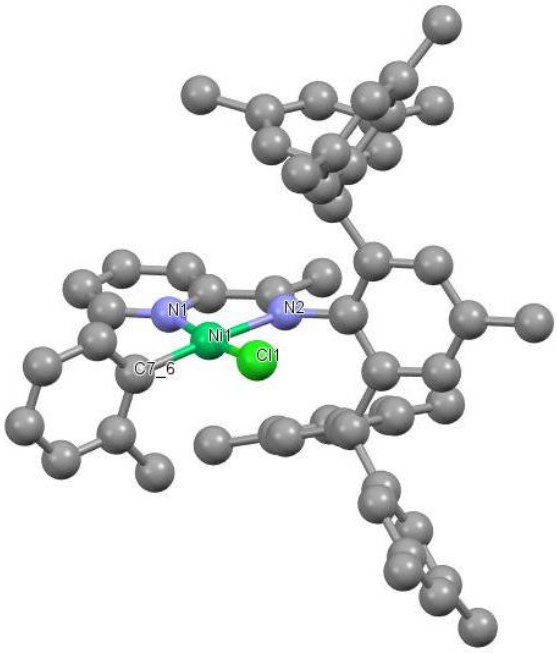

Figure S137. Molecular structure of Ni complex **C5** (CCDC number: 2320313). Hydrogen atoms are omitted for clarity. Thermal ellipsoids are shown in the 50% probability level. Select bond

distances (Å) and angles (deg): Ni(1)–N(1) = 1.8959(18), Ni(1)–N(2) = 1.9969(16), Ni(1)–C (7_6) = 1.908(3), Ni(1)–Cl(1) = 2.1469(6); N(1)–Ni(1)–N(2) = 82.08(7), N(1)–Ni(1)–C(7_6) = 94.24(10), C(7_6) – Ni(1) – Cl(1) = 88.56(8), N(2) – Ni(1) – Cl(1) = 95.61(5).

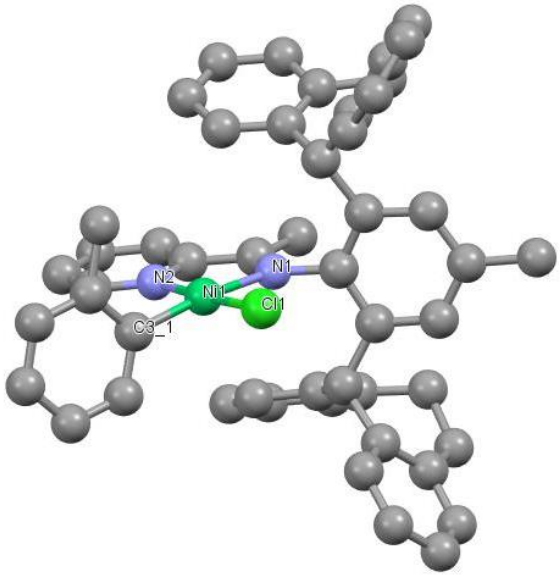

Figure S138. Molecular structure of Ni complex **C7** (CCDC number: 2320310). Hydrogen atoms are omitted for clarity. Thermal ellipsoids are shown in the 50% probability level. Select bond distances (Å) and angles (deg): Ni(1)–N(1) = 1.9852(14), Ni(1)–N(2) = 1.9098(14), Ni(1)–C(3_1) = 1.904(3), Ni(1)–Cl(1) = 2.1487(5); N(2)–Ni(1)–N(1) = 82.44(6), N(2)–Ni(1)–C(3_1) = 92.67(9), C(3_1)–Ni(1)–Cl(1) = 89.96(8), N(1)–Ni(1)–Cl(1) = 95.17(4).

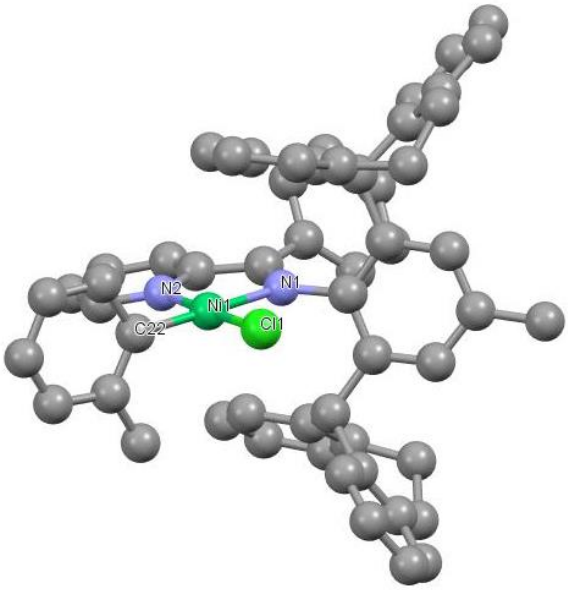

Figure S139. Molecular structure of Ni complex **C8** (CCDC number: 2320308). Hydrogen atoms are omitted for clarity. Thermal ellipsoids are shown in the 50% probability level. Select bond distances (Å) and angles (deg): Ni(1) – N(1) = 2.034 (4), Ni(1)–N(2) = 1.886(4), Ni(1)–C22(1) =

1.895(6), Ni(1)–Cl(1) = 2.1427(13); N(2)–Ni(1)–N(1) = 82.22(15), N(2)–Ni(1)–C22(1) = 92.62(19), C22(1)–Ni(1)–Cl(1) = 87.68(15), N(1)–Ni(1)–Cl(1) = 97.52(11).

6. Density Functional Theory (DFT) Figures

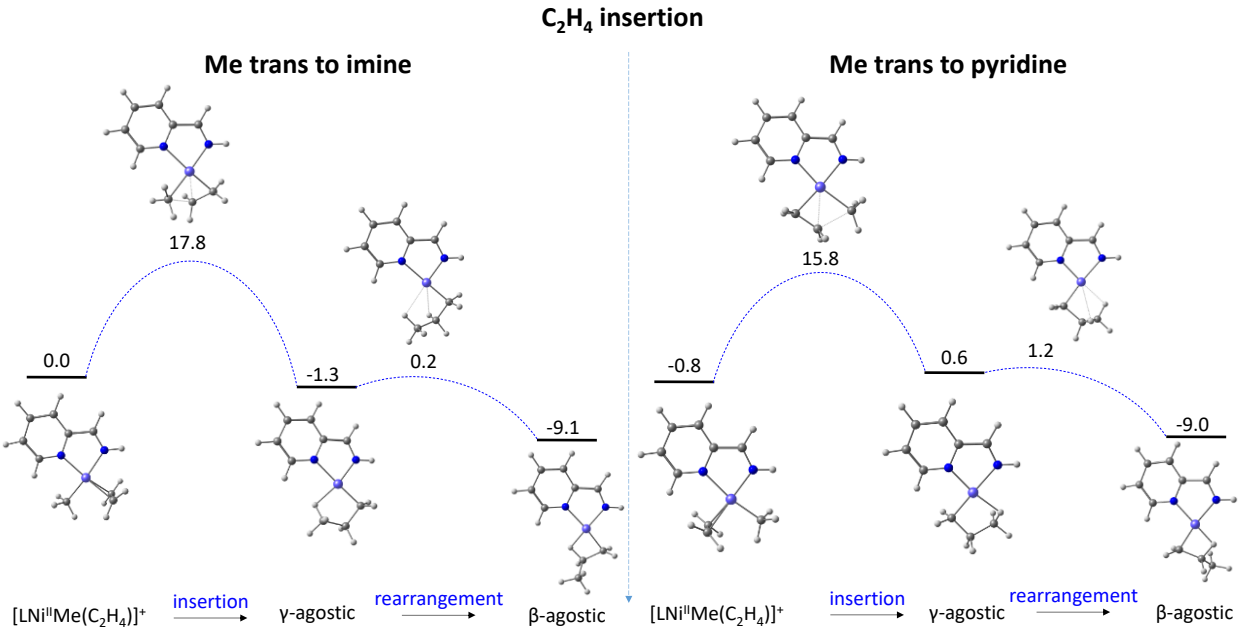

Figure S140. Gibbs energy profiles (values in kcal mol^{-1}) for the ethylene insertion into the Ni-CH_3 bond in the two $[Ni(NC_5H_4CHNH)(CH_3)(C_2H_4)]^+$ stereoisomers. The calculations considered both regioisomers, with the initial CH_3 group trans to either the pyridine ring or the imine function, and the initial ethylene insertion step was explored only for the free cation. The most stable conformation was obtained when the alkyl ligand is located trans to the pyridine, but the difference is quite small (0.8, 1.9 and 0.1 kcal mol^{-1} for Me, γ-agostic Pr and β-agostic Pr, respectively (Supplementary Figure S140). The ethylene insertion barrier is slightly lower when starting from the most stable Ni-Me isomer, leading to the less stable γ-agostic Ni-Pr insertion product. The rearrangement to the more stable β-agostic Ni-Pr isomer occurs with an exceptionally low barrier for both isomers.

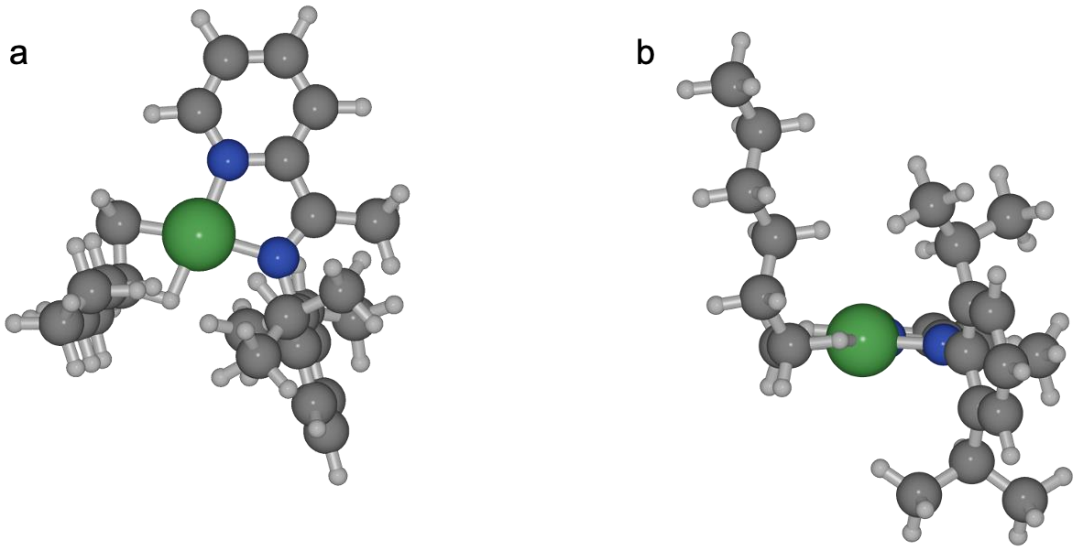

Figure S141. a) Top view of optimized β-CH agostic species **C1** with a propagating polymer chain consisting of 7 carbons. b) Side view illustrating out-of-plane polymer chain.[11]

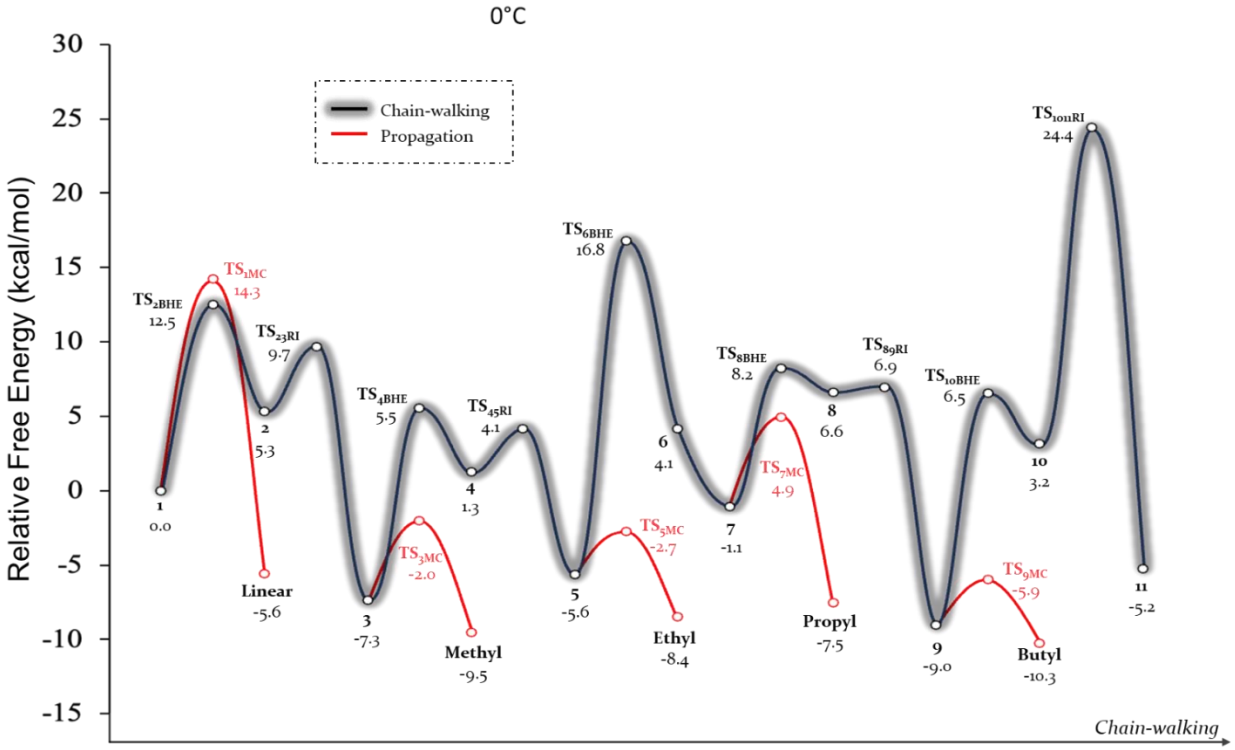

Figure S142. Free energy diagram for chain-walking and propagation for **C1** calculated from DFT simulations at 0 °C

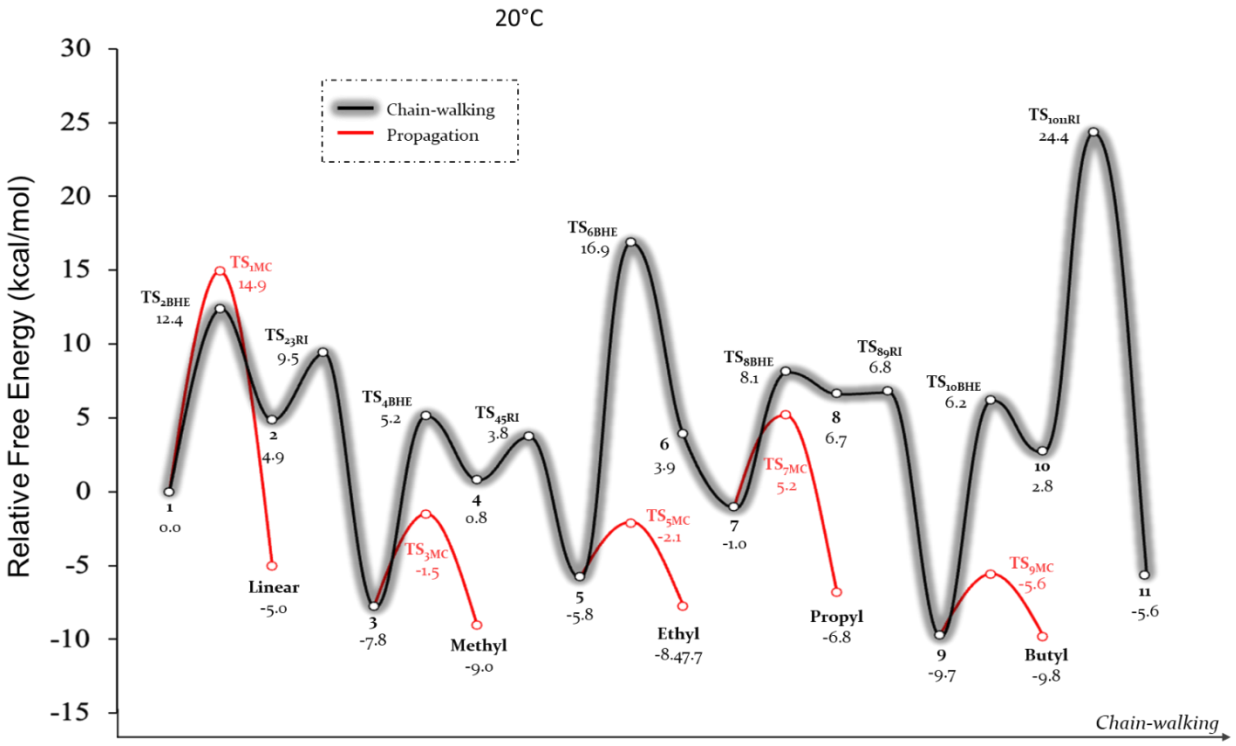

Figure S143. Free energy diagram for chain-walking and propagation for **C1** calculated from DFT simulations at 20 °C

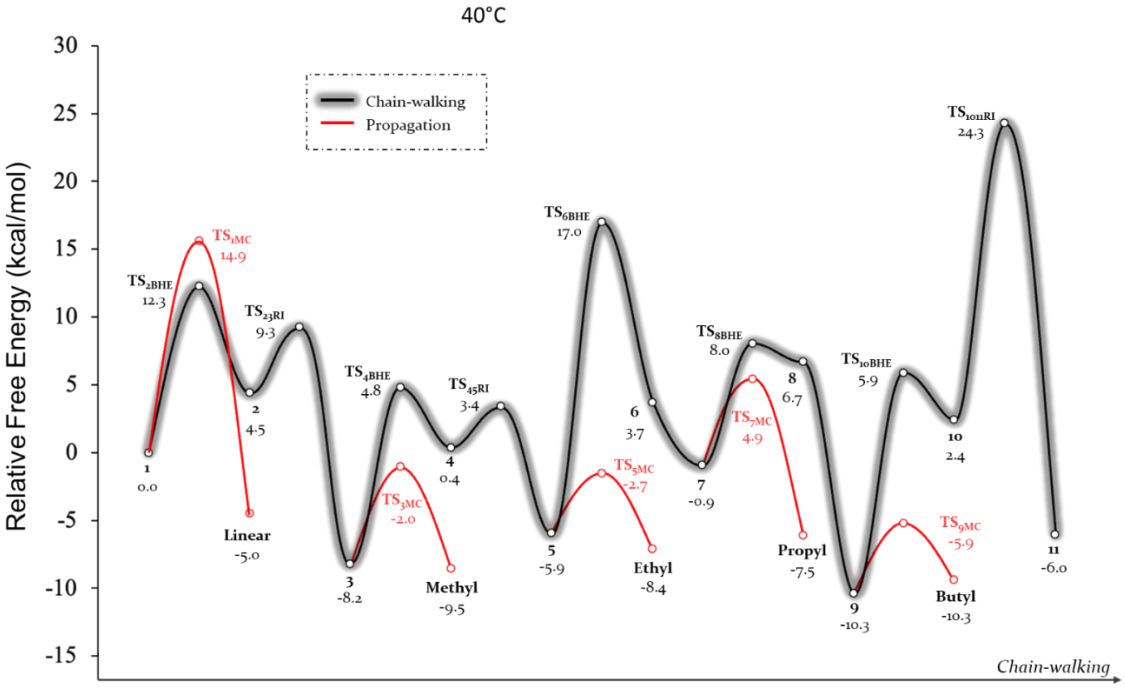

Figure S144. Free energy diagram for chain-walking and propagation for **C1** calculated from DFT simulations at 40 °C

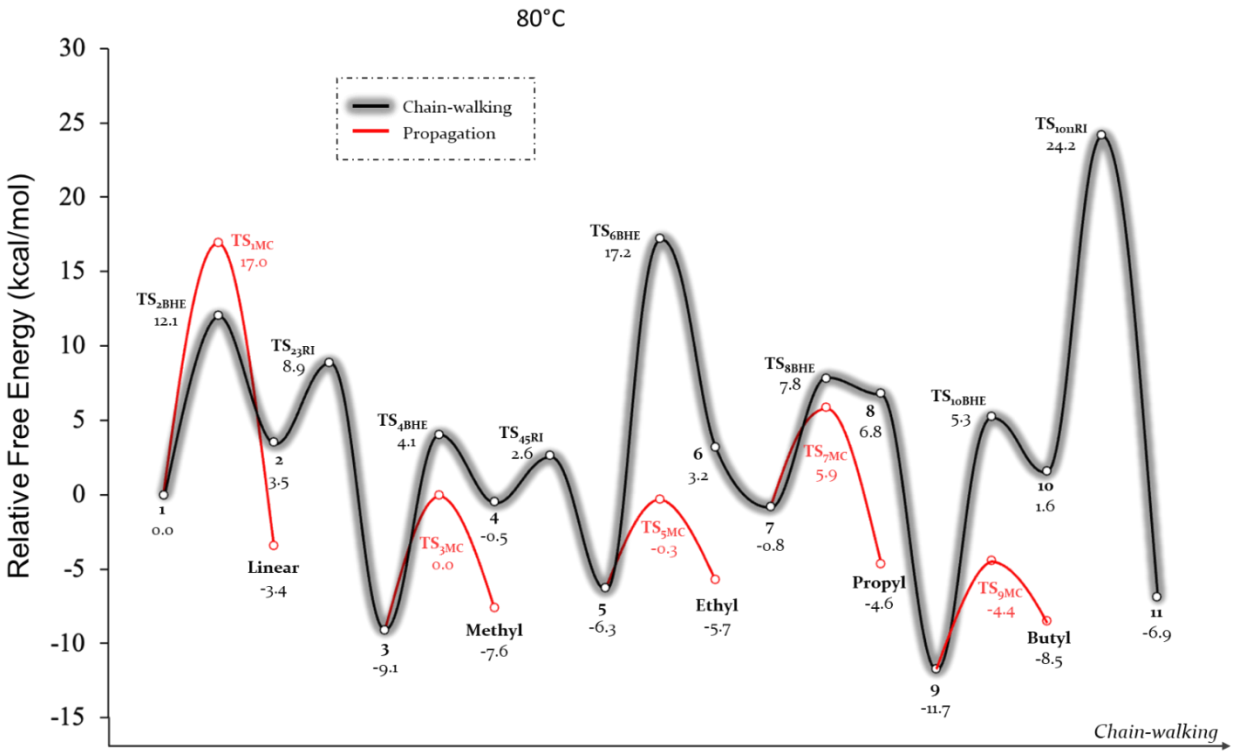

Figure S145. Free energy diagram for chain-walking and propagation for **C1** calculated from DFT simulations at 80 °C

7. References

1 Martínez-Martínez, A. J. & Weller, A. S. Solvent-free anhydrous Li+, Na+ and K+ salts of [B(3,5-(CF3)2C6H3)4]−, [BArF4]−. Improved synthesis and solid-state structures. *Dalton Trans.* **48**, 3551-3554, doi:10.1039/C9DT00235A (2019).

2 Hayashi, Y., Rohde, J. J. & Corey, E. J. A Novel Chiral Super-Lewis Acidic Catalyst for Enantioselective Synthesis. *J. Am. Chem. Soc.* **118**, 5502-5503, doi:10.1021/ja960766s (1996).

3 Berthon-Gelloz, G. *et al.* IPr* an easily accessible highly hindered N-heterocyclic carbene. *Dalton Trans.* **39**, 1444-1446, doi:10.1039/B921894G (2010).

4 Liu, Y.-S. & Harth, E. Distorted Sandwich α-Diimine PdII Catalyst: Linear Polyethylene and Synthesis of Ethylene/Acrylate Elastomers. *Angew. Chem. Int. Ed.* **60**, 24107-24115, doi:https://doi.org/10.1002/anie.202107039 (2021).

5 Peng, H. *et al.* Rotation-restricted strategy to synthesize high molecular weight polyethylene using iminopyridyl nickel and palladium catalyst. *Appl. Organomet. Chem.* **35**, e6140, doi:https://doi.org/10.1002/aoc.6140 (2021).

6 Sieh, D., Lacy, D. C., Peters, J. C. & Kubiak, C. P. Reduction of CO2 by Pyridine Monoimine Molybdenum Carbonyl Complexes: Cooperative Metal–Ligand Binding of CO2. *Chem. Eur. J.* **21**, 8497-8503, doi:https://doi.org/10.1002/chem.201500463 (2015).

7 Laine, T. V. *et al.* Pyridinylimine-based nickel(II) and palladium(II) complexes: preparation, structural characterization and use as alkene polymerization catalysts. *J.*

Organomet. Chem. **606**, 112-124, doi:https://doi.org/10.1016/S0022-328X(00)00291-6 (2000).

8 Sun, W.-H. *et al.* Ethylene polymerization by 2-iminopyridylnickel halide complexes: synthesis, characterization and catalytic influence of the benzhydryl group. *Dalton Trans.* **41**, 11999-12010, doi:10.1039/C2DT30989K (2012).

9 Mogheiseh, M., Zohuri, G. H. & Khoshsefat, M. Synthesis of LDPE Using Pyridineimine-Based Nickel (II) Bromide Complexes: Effect of Catalyst Bulkiness on Thermal, Structural, and Morphological Properties. *Macromol. React. Eng.* **12**, 1800006, doi:https://doi.org/10.1002/mren.201800006 (2018).

10 Li, S., Lu, Z., Fan, W. & Dai, S. Efficient incorporation of a polar comonomer for direct synthesis of hyperbranched polar functional ethylene oligomers. *New J. Chem.* **45**, 4024-4031, doi:10.1039/D0NJ05857B (2021).

11 D'Auria, I., Milione, S., Caruso, T., Balducci, G. & Pellecchia, C. Synthesis of hyperbranched low molecular weight polyethylene oils by an iminopyridine nickel(ii) catalyst. *Polym. Chem.* **8**, 6443-6454, doi:10.1039/C7PY01215B (2017).